PERFORMANCE ENHANCEMENT OF SOLAR STILL DESALINATION SYSTEMS USING REVOLVING TUBES: CFD SIMULATION AND EXPERIMENTAL INVESTIGATION

A Thesis submitted by

Ahmed Kasim Taha Alkaisi
M.Sc. B.Sc. Mechanical Engineering

For the award of

Doctor of Philosophy

2019

Abstract

Water and energy are indispensable resources for life and civilisation. The scarcity of both water and energy have emerged as amongst the most serious concerns of our time due to the dramatic growth in population, enhancement in our standards of living, and the rapid development of the agricultural and industrial sectors in many countries. Desalination seems to be one of the most promising solutions to solve the problem of water scarcity; however, it is not without costs, as the desalination process is energy-intensive. Conventional sources of energy, such as fossil fuels, are limited, depleted and pollute the environment. Therefore, the use of renewable sources of energy such as solar energy is essential and represents a better option. Solar desalination systems are environmentally friendly and offer a win-win solution to solve shortages of both water and energy. The simplest and the most straightforward solar desalination process is the natural evaporation-condensation process of the Solar Still Desalination (SD) system. An SD system simply consists of a water basin and a tilted transparent cover that is exposed to solar radiation. SD systems have a low capital cost; however, the low productivity of these systems make the cost of the water that they produce higher than that produced via other traditional desalination systems. On balance, the selection of SD systems for remote areas that have relatively low demand for water makes those systems a feasible option, due to the elimination of the high costs of water transfer if such systems are deployed locally. SD systems can work powered by solar energy, which makes them environmentally friendly and suitable for areas that have no access to electricity, such as remote villages and less developed regions of the world.

The main purpose of this study is to find a method to increase the productivity of SD systems to provide people in remote and less developed regions of the world with freshwater. The proposed technique is a simple amendment to the regular double-sloped SD system. The suggested modification was to add three parallel and symmetrical PVC tubes into the water basin of the SD system to be rotated by small DC motors. These tubes were wrapped in an absorbent black mat and were placed horizontally along the basin to be semi immersed in the water. The purpose of this modification is to stir the water in the basin and to generate a thin water layer around the tubes' circumference, which leads to an increase in the surface area for water

evaporation. This modification enhanced the water evaporation rate within the SD system, and thereby increased the productivity of this system.

In this study, two SD systems: the Normal SD (NSD) system and the Modified SD (MSD) system were designed and manufactured, simulated numerically and tested experimentally. The CFD simulation was done using ANSYS-Fluent software. The experimental investigations were carried out during spring and summer in Toowoomba, Australia. The effective operation and design parameters such as water depth, the tubes' diameter and the tubes' rotation speed were analysed and optimised using the sensitivity analysis. The dimensional analysis, uncertainty analysis, and the cost analysis for the present experimental setup of both the SD systems were conducted as well.

The daily productivity of the SD systems is equal to the distillate yield within a day and the daily efficiency is equal to this productivity divided by the daily insolation. The results show that the daily productivity and the daily efficiency of the MSD system were always higher than that of the NSD system. According to the experimental results, the maximum daily productivity and the maximum daily efficiency of the MSD system were $2.908\frac{l}{m^2 day}$ and 21.01%, respectively. While the maximum daily productivity and the maximum daily efficiency of the NSD system were $1.685\frac{l}{m^2 day}$ and 13.12%, respectively. The maximum enhancement in the daily productivity and the daily efficiency of the MSD system due to the modification were 74.8% and 63.4% higher than the NSD system, respectively. The results of the CFD simulation showed a very good agreement with the data of the experimental investigation, which means it is a successful tool for modelling SD systems. The cost analysis of the present experimental setup estimated that the price of the water produced by the MSD system and the NSD system is \$0.57 per litre and \$0.34 per litre, respectively.

Certification of Thesis

This Thesis is entirely the work of Ahmed Kasim Taha Alkaisi except where otherwise acknowledged. The work is original and has not previously been submitted for any other award, except where acknowledged.

Principal Supervisor: Dr Ahmad Sharifian-Barforoush

Associate Supervisor: Dr Ruth Mossad

Student and supervisors signatures of endorsement are held at the University.

Acknowledgements

First, thank God for giving me health, courage, knowledge and strength to accomplish this work.

With a deep sense of gratitude, I would like to express my deepest thanks and sincere gratitude to my supervisors Dr Ruth Mossad and Dr Ahmad Sharifian-Barforoush, for their invaluable help, advice, and encouragement. It has been a privilege to have worked with them. I am sure without their guidance; this work would not have taken this final shape.

I am indebted to all staff members at the University of Southern Queensland, special thanks to Mr Mohan Trada, Mr Brian Aston, Mr Oliver Kinder, and Mr Brett Richards for their assistance in the experimental setup of this project, and special thanks to Ms Libby Collett for proofreading this thesis.

I would like to thank my sponsor the Higher Committee for Education Development and the Ministry of Water Resources in Iraq for their financial support throughout this research.

At last, I offer my sincere thanks to my family, my friends, and all of the people that supported and encouraged me during the period of my study.

Ahmed Alkaisi

2019

Dedication

To my beloved mother with gratitude

To the memory of my dear father and my dear sister

Table of Contents

Nomenclature

The symbols used in this thesis have the following meanings unless otherwise stated in the text.

Symbol	Description	Units
A	*Area*	m^2
C	*Constant*	
c_p	*Heat capacity at constant pressure*	$kJ/kg.K$
E	*Energy*	kJ
$\vec{F}$	*Force vector*	N
G	*Solar insolation*	$MJ/m^2.day$
Gr	*Grashof number (ratio of buoyancy forces to viscous forces)*	*Dimensionless*
$\vec{g}$	*Gravitational acceleration*	m/s^2
h	*Heat transfer coefficient*	$W/m^2.K$
	Species enthalpy	kJ/kg
I	*Solar radiation intensity*	W/m^2
k	*Thermal conductivity*	$W/m.K$
	Kinetic energy of turbulence per unit mass	J/kg
L_v	*Latent heat of evaporation*	MJ/kg
l	*Length*	m
m	*Mass*	kg
$\dot{m}$	*Mass flow rate*	kg/s
Nu	*Nusselt number (ratio of convective to conductive heat transfer)*	*Dimensionless*
p	*Pressure*	$Pa = N/m^2$
Pr	*Prandtl number (ratio of momentum diffusivity to thermal diffusivity)*	*Dimensionless*
Q	*Heat*	W
$\dot{q}$	*Heat flux*	W/m^2
R	*Radius*	m
Ra	*Rayleigh number* (*strength of buoyancy in natural convection)*	*Dimensionless*
Re	*Reynolds number (ratio of inertial forces to viscous forces)*	*Dimensionless*
T	*Temperature*	K, ℃
t	*Time*	s
U	*Free-stream velocity*	m/s
V	*Volume*	m^3
$\vec{v}$	*Velocity vector*	m/s
W	*Work*	J

Greek symbols

Symbol	Description	Units
α	*Absorptivity*	*Dimensionless*
	Thermal diffusivity	m^2/s
β	*Thermal expansion coefficient*	K^{-1}
Δ	*Change in variable* $(final - initial)$	
ε	*Emissivity*	*Dimensionless*
	Turbulent dissipation rate	m^2/s^3
η	*Efficiency*	*Dimensionless*
μ	*Dynamic viscosity*	$kg/m.s$
ν	*Kinematic viscosity*	m^2/s
ρ	*Density*	kg/m^3
σ	*Reflectivity*	*Dimensionless*
	Surface tension	kg/m
τ	*Transmissivity*	*Dimensionless*
ω	*Rotational speed*	$rpm, rad/s$

Subscripts

Symbol	Description
a	*Ambient*
b	*Basin*
c	*Cover*
e, ev	*Evaporation*
eff	*Effective*
g	*Glass*
k	*Conduction*
l	*Liquid*
r	*Radiation*
s	*Storage, Solar, Surface*
t	*Total*
v	*Vapour*
w	*Water*
∞	*Freestream*

Abbreviations

Symbol	Description
3D	*Three-Dimensional*
AY	*Annual Average Yield*
CFD	*Computational Fluid Dynamics*
CPL	*Cost Per Litre*
FC	*Fixed Cost, Capital Cost*
MC	*Maintenance Cost*
MSD	*Modified Solar Still Desalination*
NSD	*Normal Solar Still Desalination*
PC	*Power Cost*
SD	*Solar Still Desalination*
SV	*Salvage Value, Resale Value*
TC	*Total Cost*

1 Chapter One: Introduction

Water means life. Freshwater is an essential element not only to human life but also to almost all human daily activities such as domestic uses and hygiene, livestock farming, crop irrigation, and most industrial processes. Without freshwater, humans cannot survive or exist.

1.1 Background

Despite the fact that water covers about 75% of the earth's surface area, freshwater represents only about 2.5% of the total amount of global water stores and the rest is saline water (Eakins & Sharman, 2010). Moreover, not all of the 2.5% is an accessible resource, as most of the freshwater is in the form of groundwater, permafrost, glaciers, and ice caps; and only about 0.007% is accessible surface freshwater such as that stored in lakes and rivers (Gleick, 1993). Figure 1.1 shows by percentages the distribution of water globally (Perlman, 2016).

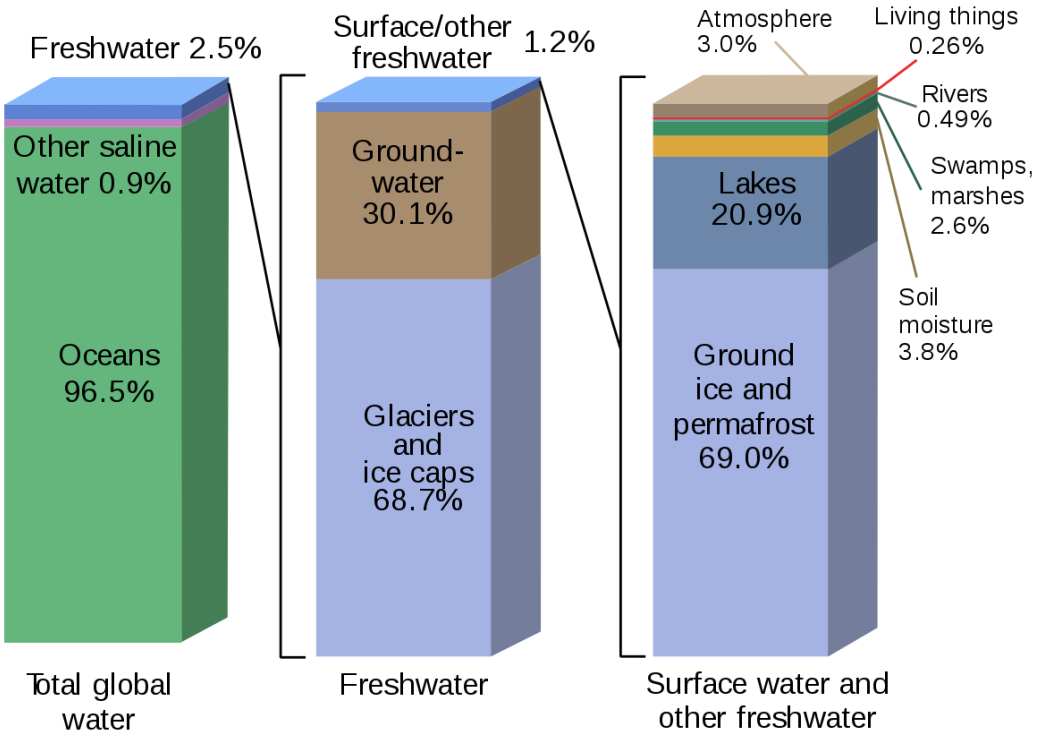

Figure 1. 1 Global water distribution (Perlman, 2016)

Water can be classified into four categories according to its salt contents (from fresh to salty) into; freshwater, brackish water, seawater, and brine. Freshwater is defined as water with a total dissolved salts/solids (TDS) level of fewer than 500 parts per million (ppm) or (mg/l), while brackish water has a TDS of up to 7000 ppm, seawater has a TDS of up to 35000 ppm and beyond salinity level, water is considered to be brine (Lethea, 2017). According to the World Health Organisation (2011), the best quality of drinking water has less than 300 ppm, but the permissible limit of salinity in potable water is up to 1000 ppm.

Water scarcity is the most crucial issue of our time. Water scarcity occurs when water supplies fall below 1000 cubic meters per capita per year and absolute scarcity occurs when the water supplies are below 500 cubic meters per capita per year (Rijsberman, 2006). Freshwater is an unsustainable resource due to overexploitation, contamination, weather changes, and global warming. Furthermore, the population explosion, the increase in living standards and their consequential results such as the growth in the industrial and the agricultural sectors have worsened the problem of the water scarcity. According to a recent report by the World Health Organization and UNICEF (2017), 844 million people do not have sufficient freshwater.

To overcome the water shortage problem, many plans and solutions have been applied such as building dams and reservoirs, recycling and reusing greywater (wastewater), harvesting rainwater, and seawater desalination. However, there are some negative impacts caused by the afore-mentioned solutions. The main disadvantages of the use of dams and reservoirs are that they use of large areas of land that could otherwise be used for agricultural, industrial or residential activities, as well as the high capital cost. Meanwhile there are public health issues that have held back the widespread use of recycled and reused wastewater. Seawater desalination is one of the most promising techniques in producing freshwater; however, seawater desalination is an energy-intensive process, which also creates environmental pollution. Employing renewable energy sources into the seawater desalination process can mitigate the environmental issues of desalination and can reduce the cost of producing freshwater significantly (Shatat et al, 2013).

1.2 Desalination Techniques

Desalination is defined simply as the process of producing freshwater from saline water. Desalination techniques can be categorized into three main groups: evaporation-condensation, filtration, and crystallisation. Figure 1.2 presents the different techniques of desalination under these three main groups.

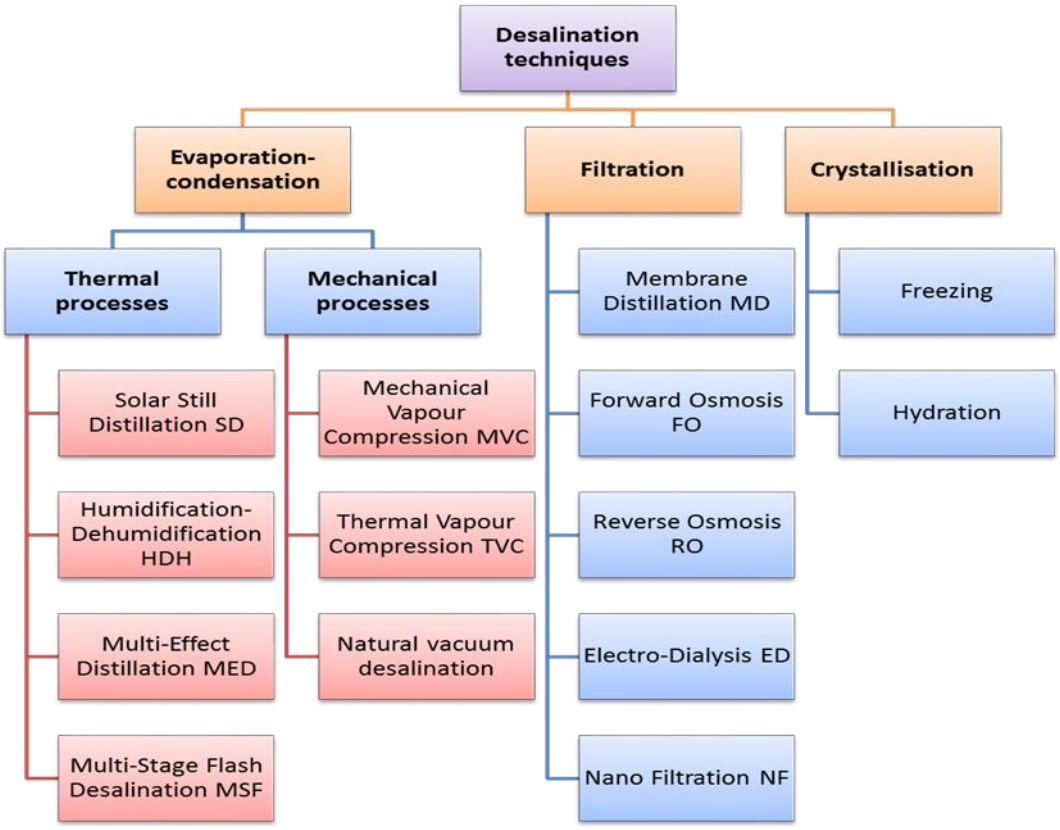

Figure 1. 2 Desalination techniques

1.2.1 Evaporation- Condensation Systems

In these systems, freshwater is obtained by evaporating the saline water then condensing the vapour to produce pure water. These systems produce freshwater with TDS up to 20 ppm, which is considered to be high-quality purification. The following are the most common evaporation-condensation techniques:

a) Multi-Effect Distillation (MED): In this process, the saline water is heated by solar energy or fossil fuels and sprayed in parallel vacuumed vessels to decrease the evaporation temperature. The latent heat rejected by the produced vapour in the condensation process is used to preheat the feed saline water. This method is commonly used in oil-rich countries because it requires heat from burning fuel or with the aid of solar energy more than electric power. Figure 1.3 shows a schematic diagram of a MED system with a solar water heater (Sharaf et al, 2011).

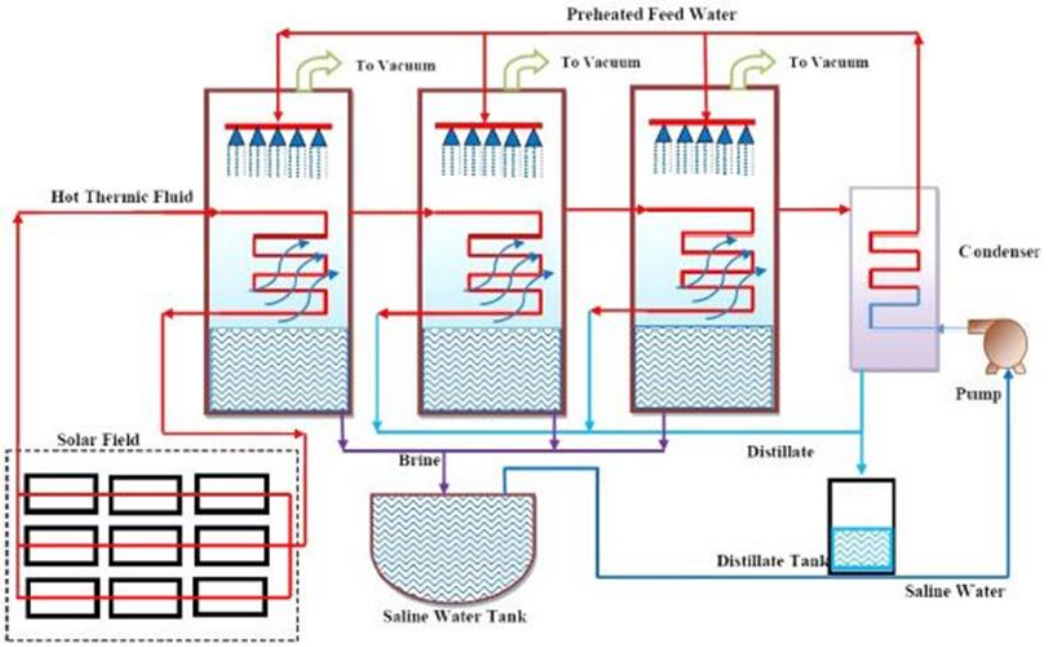

Figure 1. 3 Schematic diagram of the MED system (Sharaf et al, 2011)

b) Multi-Stage Flash Desalination (MSF): Saline water in the MSF system is heated by burning fuel or with the help of solar radiation under high pressure to increase the boiling temperature and then the water is pumped into low-pressure vessels to produce vapour. The formed vapour on the condenser tubes preheats the feed saline water. This system is also widely used in Middle-Eastern and oil-rich countries for the same reason mentioned in the previous paragraph (section a). Figure 1.4 shows a schematic diagram of the MSF system with a solar heater and heat storage (Moustafa et al, 1985).

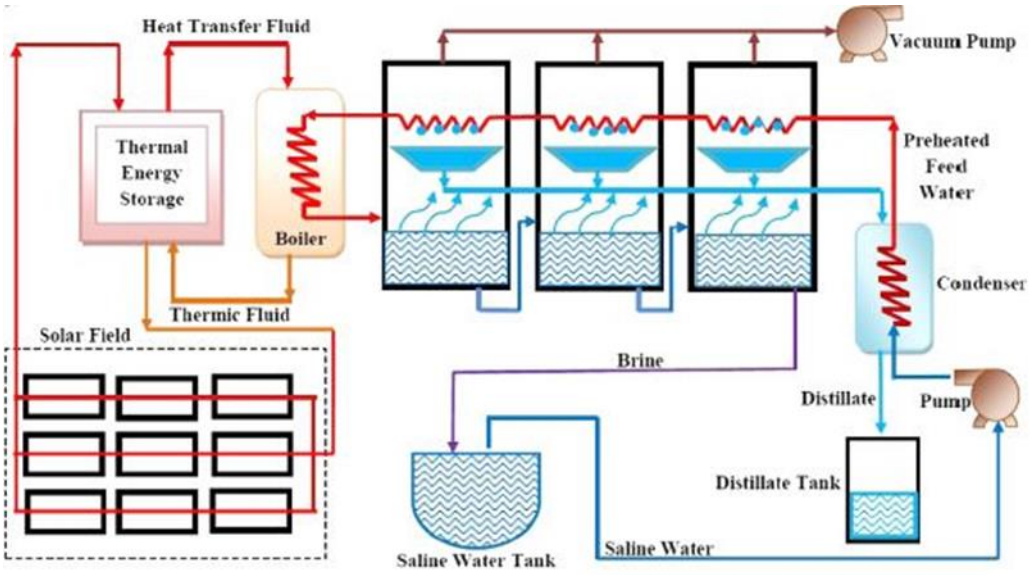

Figure 1. 4 Schematic diagram of the MSF system (Moustafa et al, 1985)

c) **Mechanical Vapour Compression (MVC):** In this system, a mechanical compressor is used to increase the vapour pressure and temperature. The compressed hot vapour is used to heat up the saline water to produce more vapour. The compressed vapour is then condensed under high temperature, and the latent heat of condensation is used to preheat the feed water. Figure 1.5 shows a schematic diagram of a single stage MVC system (Helal & Al-Malek, 2006).

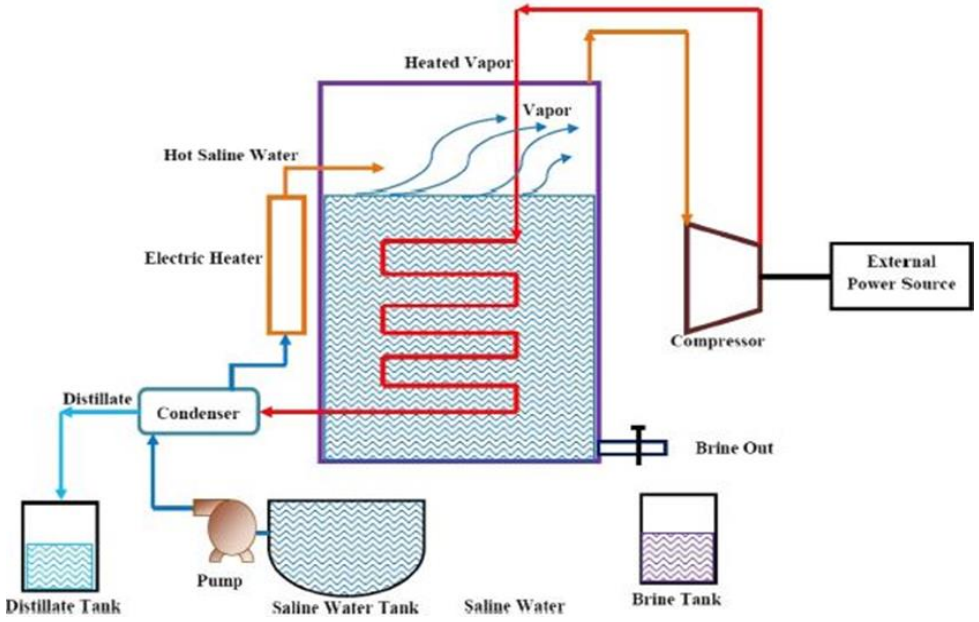

Figure 1. 5 Schematic diagram of the MVC system (Helal & Al-Malek, 2006)

d) Thermal Vapour Compression (TVC): In this system, a thermo-compressor is used to increase the steam pressure, which leads to enhancing the desalination performance due to increase in the condensation temperature and the vapour can be used as a heating medium to the feedwater. Figure 1.6 shows a schematic diagram of the TVC system combined with MED system (Yang et al, 2015).

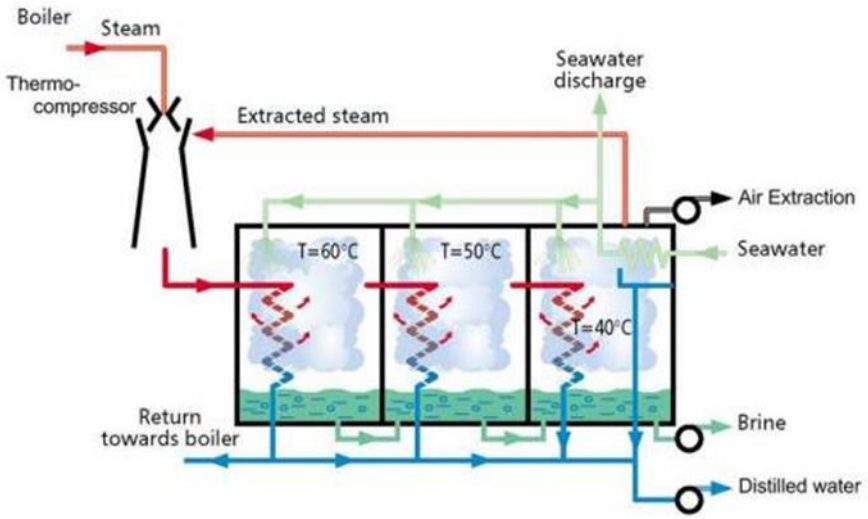

Figure 1. 6 Schematic diagram of the TVC system (Yang et al, 2015)

e) Natural Vacuum Desalination: The main idea of this system is to produce vapour at low water temperature. Whilst water can evaporate at low temperature under vacuum pressure, producing vacuum pressure requires a complex system and a huge amount of energy. In natural vacuum desalination systems, the saline water is pumped to a certain height and let it flow down under its weight and gravity, which produces a vacuum pressure that is required for the evaporation at low temperature. The main advantage of this process is the low power consumption. However, this method has limited productivity (Maroo & Goswami, 2009). Figure 1.7 shows a schematic diagram of a simple natural vacuum desalination system with a solar heater as a booster enhancement (Al-Kharabsheh & Yogi, 2003).

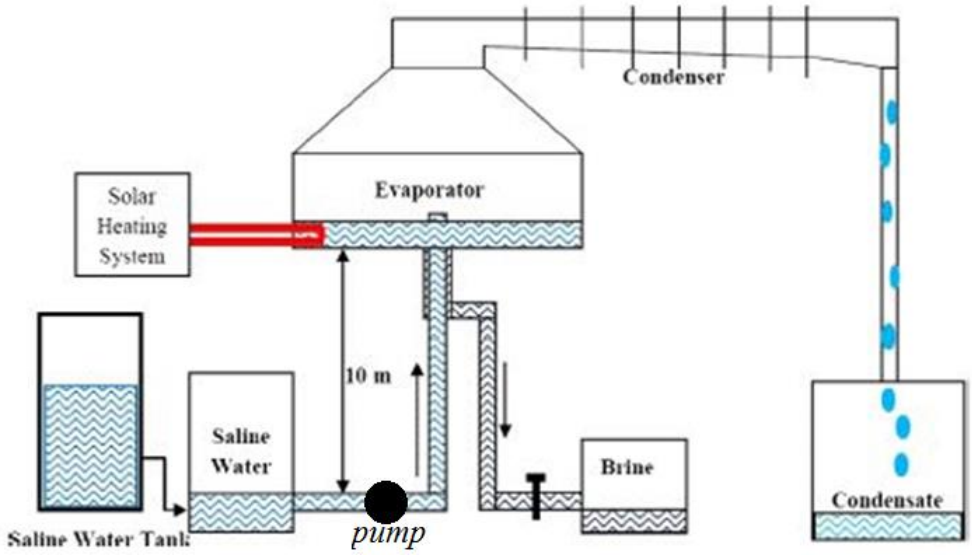

Figure 1. 7 Schematic diagram of the Natural vacuum desalination system (Al-Kharabsheh & Yogi, 2003)

f) Humidification-Dehumidification Desalination (HDH): As implied by the name, HDH is a system that combines two chambers, one for evaporation and one for condensation. There are four types of HDH systems; open water- open air, closed water- closed air, closed water- open air, and open water- closed air cycles (Parekh et al, 2004). The fact that hot air can carry more moisture is employed in the HDH systems. Therefore, heated air is circulated in the system using an external source of energy. In addition, the heat rejected from the vapour is used to heat up the feed saline water in sequence processes by employing a hot air circulation. Figure 1.8 shows a schematic diagram of a simple HDH system in four configurations with solar air and water heaters (Parekh et al, 2004).

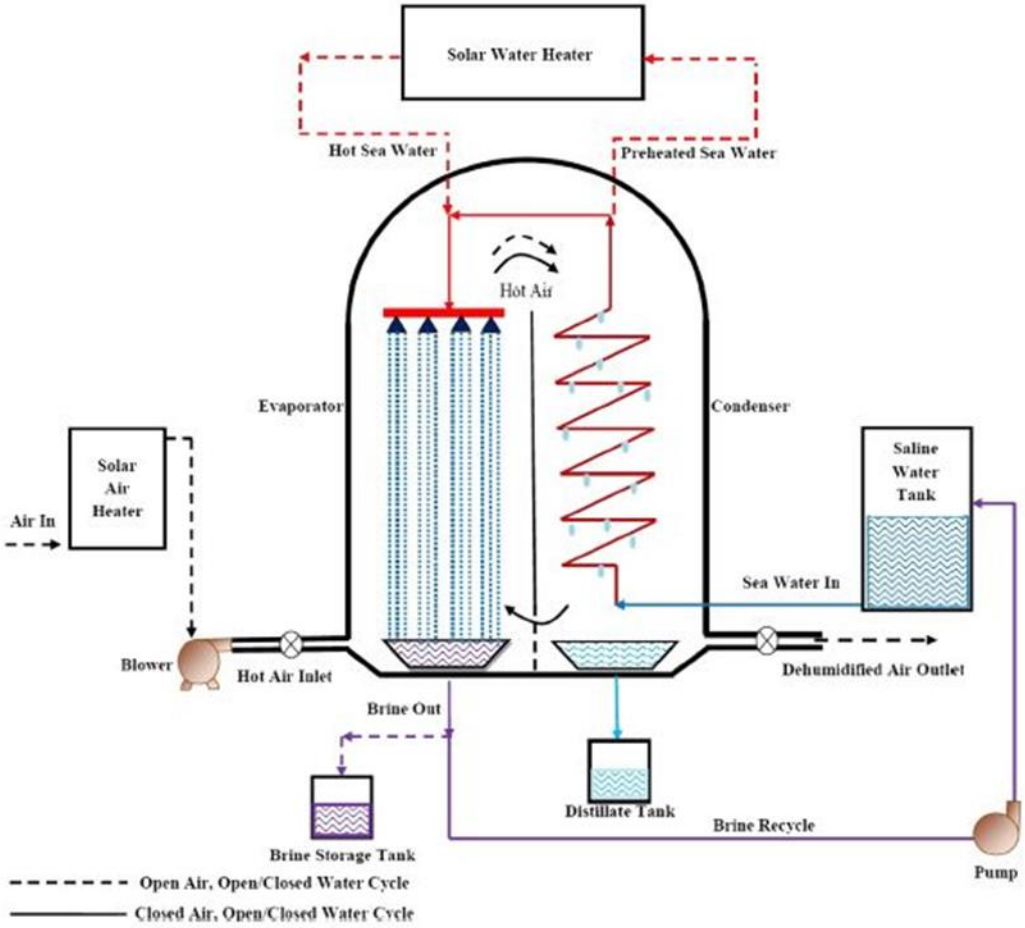

Figure 1. 8 Schematic diagram of the HDH system (Parekh et al, 2004)

1.2.2 Filtration Systems

In these systems, the saline water is pumped at high pressure through many stages of filters to purify the water from the suspended solids and dissolved salts. The total dissolved solids TDS of the water produced depends on the system type, size, pressure and the number of filtration stages. Most of these systems produce freshwater with TDS up to 500 ppm, which is an acceptable limit for human consumption. The following are the most common filtration techniques:

a) **Reverse Osmosis (RO):** RO is a widespread common technique used around the world, especially in the western developed countries, due to the fact that it consumes energy more efficiently compared with thermal systems. RO system is a pressure-driven desalination process in which the feedwater is pumped to

a pressure that is higher than the osmotic pressure of the membranes. The cross-flow membrane unit allows water molecules to pass through, leaving behind the bigger particles of the salt and other solids. The water processed in multi-stages until reaching a desirable TDS, usually in the range of 500 ppm to 700 ppm. The feed water is usually pre-treated to remove all impurities, and the freshwater produced is post-treated to be potable water. Figure 1.9 shows the basic elements of the RO system (Australian Water Association, 2009).

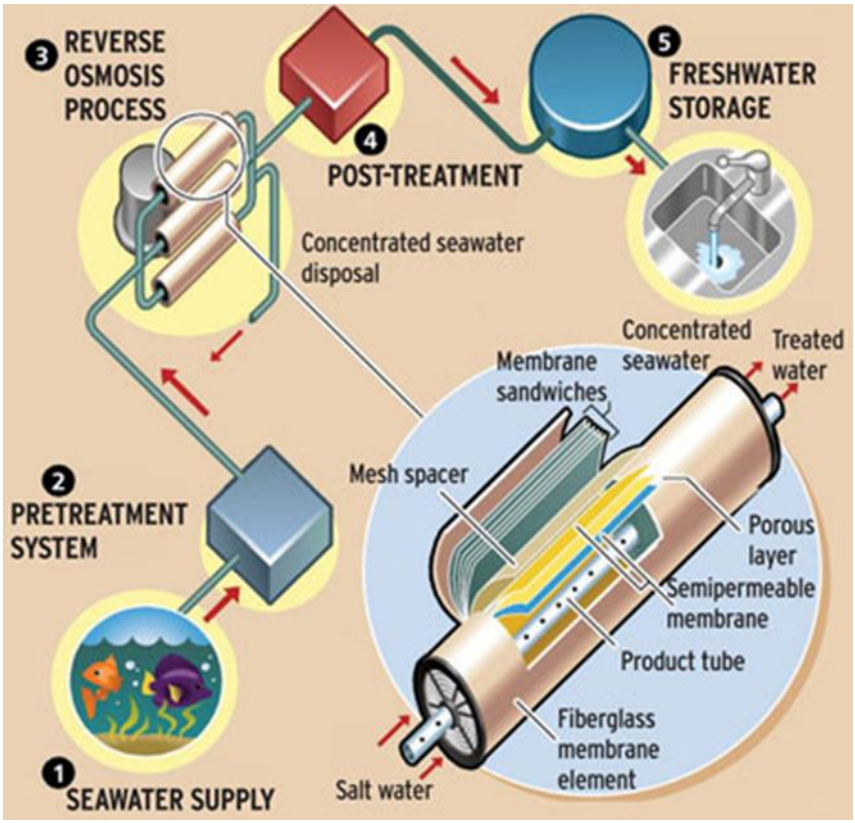

Figure 1. 9 Schematic diagram of the RO system (Australian Water Association, 2009)

b) Forward Osmosis (FO): FO is a new technique that allows the saline water to move naturally using osmotic pressure instead of applying a hydraulic pressure as in the RO systems. The seawater moves through a semipermeable membrane into a highly concentrated solution of ammonia salts leaving the sea salts on another side. This technique consumes less power than RO; however, this method requires more research and development (Akther, 2015).

c) **Electro-Dialysis (ED):** The seawater is composed of negative ions called anions and positive ions called cations. When DC polarity is applied across the cathode and anode the feed water converts it into two streams; concentrated brine and freshwater. The negative ions pass through the anion exchange membrane and positive ions pass through the cation exchange membranes and these ions get accumulated in a certain compartment and are cleared out as a brine, while freshwater passes through the other passages (Sadrzadeh & Mohammadi, 2008).

d) **Nano Filtration (NF):** Nano-filtration is a recently developed membrane filtration technique that relies on the permeability of membranes to distinguish between the physical size and the type of the particles in mixtures or in solutions. NF works under low pressure and is mainly used for water post-treatment and food processing (Hirunpinyopas, 2017).

e) **Membrane Distillation (MD):** MD is a separation process in which only vapours are allowed to pass through a porous hydrophobic membrane. It is a new desalination technique that is still under development. It combines both the evaporation-condensation and filtration processes (Wang & Chung, 2015).

1.2.3 Crystallisation Systems

In these methods, a salt separation occurs due to molecular crystallisation. Freshwater can be produced by removing the formed salts or the concentrated brine. The following are the most common methods:

a) **Freezing:** In this process, a pure water ice crystal grows on the saline water surface leaving concentrated brine. The freshwater is achieved by separating the ice from the concentrated brine. The main advantages of this system are that the energy required for freezing is less than that required for evaporation. In addition, ice has a less corrosive effect on the system materials than vapour. The disadvantages of this method are the inherent complexities of the refrigeration systems and the ice separation mechanisms. In addition, this

process requires freshwater to wash the produced ice before melting (Qiblawey & Banat, 2008).

b) Hydration: This is an old fashioned chemical-based desalination process employing a gas hydrate such as methane, carbon dioxide or nitrogen to remove the dissolved minerals from the seawater such as Na, K, Mg2, Ca, B, Cl, and SO4 (Kang et al, 2014).

1.3 Solar Still Desalination Systems

The Solar Still Desalination (SD) system is a simple device that has a low cost and low maintenance. The SD simply consists of a blackened basin covered with an inclined transparent cover. The working principle of the SD system is simple and it relies on the phenomenon of evaporation and condensation as well as gravity. The blackened basin and the brackish water in it absorb the solar energy that transmits through the transparent cover, which produces water vapour due to the increase in the water temperature. The water vapour condenses on the tilted cover, producing freshwater that trickles down into the discharge channel. Figure 1.10 shows a schematic diagram of a conventional SD system (Sharshir et al, 2016).

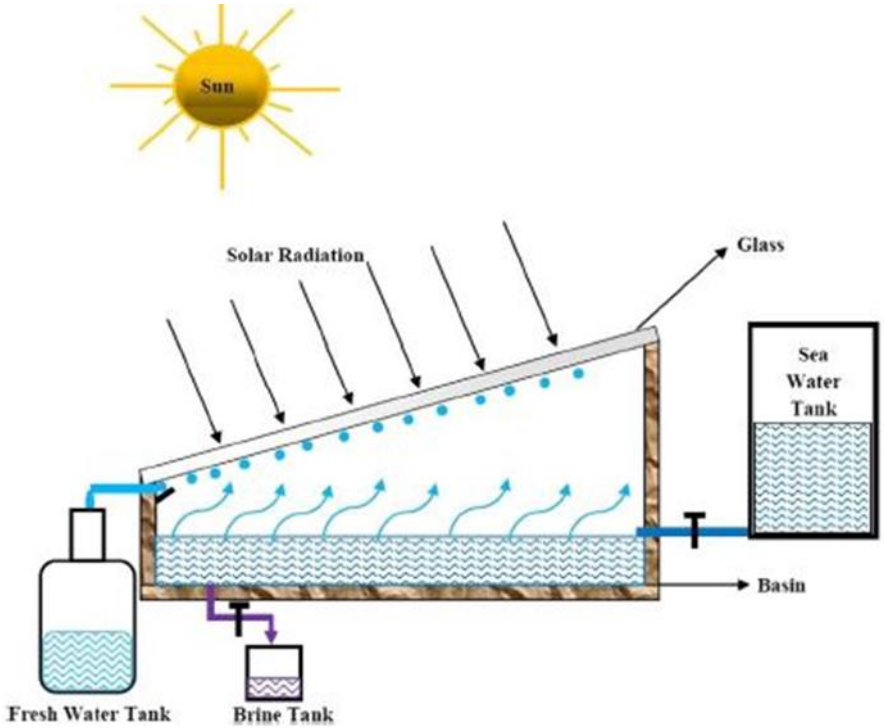

Figure 1. 10 A schematic diagram of the conventional single-slope SD system (Sharshir et al, 2016)

The SD systems can be divided - according to its operation method - into passive and active types. The passive SD systems typically depend only on solar energy and do not require any mechanical parts or the use of any other sources of energy, while the active SD systems require an external source of energy to run special mechanical equipment such as pumps and fans. The SD system also can be sorted according to the cover shape into single-slope, double-slope, pyramidal, conical, hemispherical or tubular cover SD system or according to the basin to single basin, stepped basin, or multi-basin SD system. Most SD systems have the advantages of being cheap, simple, and do not require special skills or maintenance. It can be run by inexperienced people, and it is environmentally friendly. The only drawback of the SD systems is the low productivity per unit area which is about (2-3) litres per meter square per day (Qiblawey & Banat, 2008).

1.4 Cost of Desalination

Over the last few decades, systematic research and development have reduced the cost of desalination technology due to more efficient designs, lower power requirement, and higher water productivity. According to the International Desalination Association (IDA), more than 86.8 million cubic meters per day are produced by 18,426 desalination plants that are installed in over 150 countries to provide more than 300 million people with fresh water daily (Baawain et al, 2015). Figure 1.11 shows the desalination capacity of some countries with production size over 70,000 cubic meters per day (Peluffo & Neger, 2013).

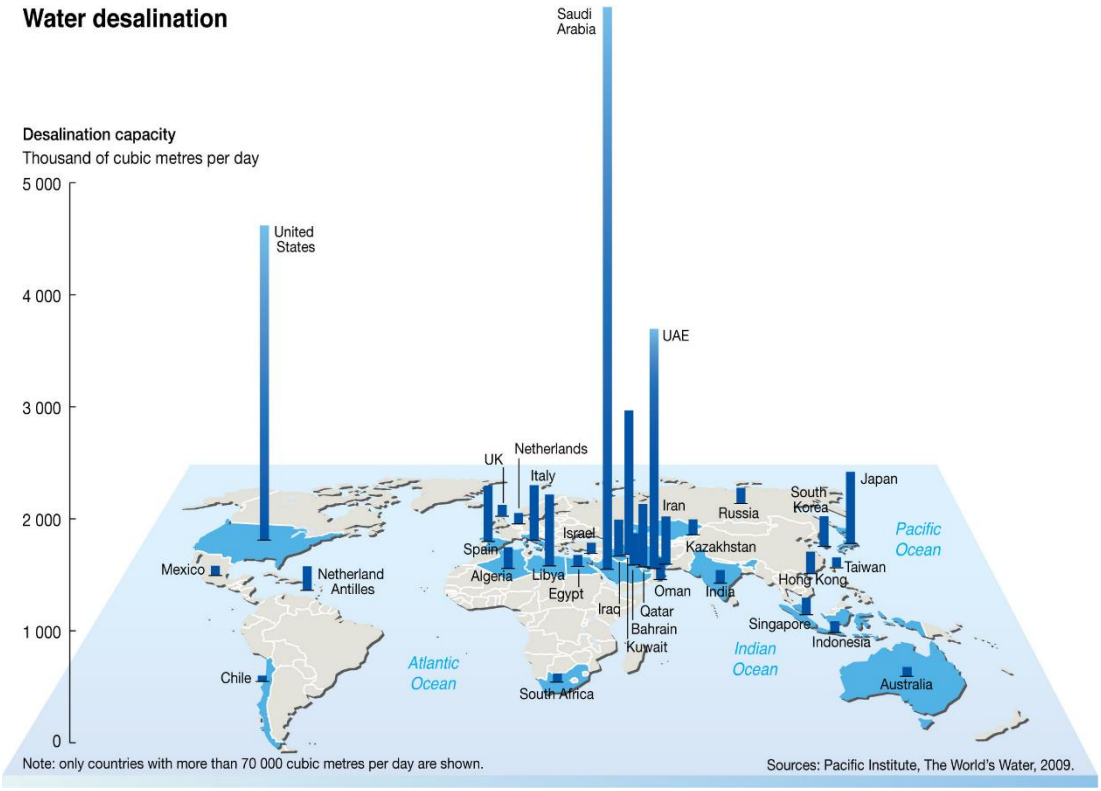

Figure 1. 11 The global desalination capacity (Peluffo & Neger, 2013)

The contribution of each desalination technique to the world water production is as follows; about 62% is the RO systems production, about 24% is the MED and MSF systems production, and about 14% desalinated water is produced by other desalination techniques as shown in the figure 1.12 (Ghaffour et al, 2015). The RO systems are the most applicable in the western countries because they are electrically driven and more energy-efficient than other desalination systems while, the MED and MSF systems are the most common desalination techniques in the oil-rich countries because these systems depend on the heat produced from burning fuel which is abundant in these countries.

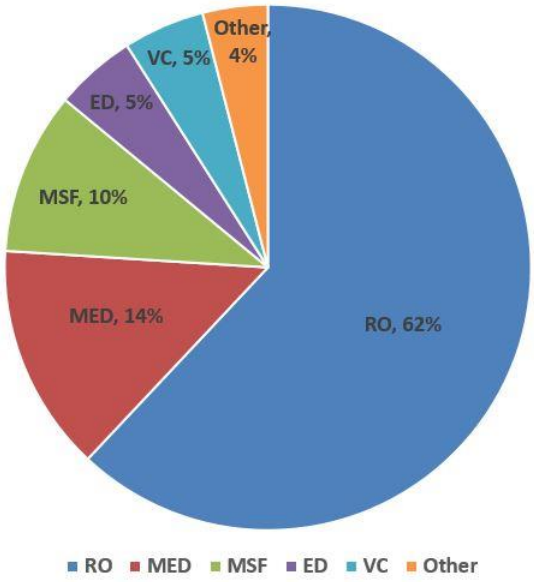

Figure 1. 12 The contribution of each desalination technique by percentages (Ghaffour et al, 2015)

The impact of the desalination on the environment is the production of greenhouse gases, and these gases are regarded as being the main cause of global warming. Desalination using the above methods is power-intensive process in which, to produce 1,000 cubic meters per day of freshwater requires about 10,000 tons of oil per year (Shatat et al, 2013). Therefore, it is not easy to estimate the exact cost of the desalination process or the cost of freshwater produced by the desalination techniques due to the hidden environmental factor as well as fluctuating oil prices. However, the availability and the cost of the energy and the feedwater, the workforce wages, the maintenance cost, the land cost, and the government subsidy are the main factors, which play a significant role in estimating the cost of the water produced by the desalination technology.

In general, the total cost of desalination can be divided into three main categories; about 45-50% is the capital investment repayment, about 33-49% is the cost of the electrical and/or thermal energy, and about 6-17% is the operational and maintenance cost. Figure 1.13 shows the percentage of the total annual cost of the main desalination techniques (Huttner, 2013).

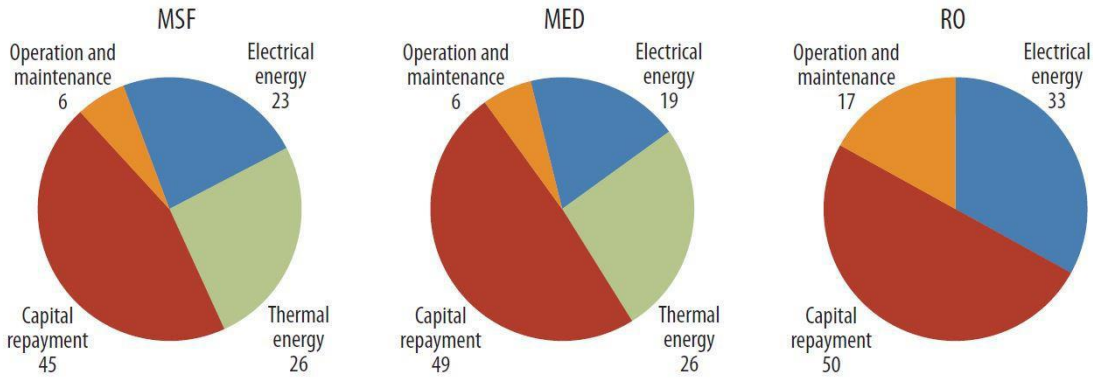

Figure 1. 13 The total annual cost percentage of the main desalination systems (Huttner, 2013)

The cost of the water produced by desalination systems can be lowered significantly by increasing the size/scale of production; which means that the bigger desalination plants are more economical and feasible than the smaller ones. However, in the remote areas, a small desalination plant is feasible due to the high cost of water transport (Gude et al, 2010). Table 1.1 lists the cost of freshwater produced by some desalination systems.

Table 1. 1 The cost of the water produced by the main desalination technologies

Desalination systems	***Capacity (m^3/day)***	***Energy source***	***Cost (USD/m^3)***	***Reference***
SD	*1*	*Solar*	*12*	*(Banat & Jwaied, 2008)*
SD	*5*	*Solar*	*3*	*(Goosen et al, 2000)*
RO	*10*	*Electrical*	*14*	*(Banat & Jwaied, 2008)*
RO	*250*	*Electrical*	*3.2*	*(Slesarenko, 2001)*
RO	*500*	*Electrical*	*2.6*	*(Rayan et al, 2001)*
RO	*2000*	*Electrical*	*2.2*	*(Lamei et al, 2008)*
ED	*10*	*Electrical*	*5*	*(Banat & Jwaied, 2008)*
MED	*100*	*Thermal*	*5.5*	*(Karagiannis & Soldatos, 2008)*
MSF	*20,000*	*Thermal*	*2*	*(Banat & Jwaied, 2008)*
MVC	*375*	*Thermal and electrical*	*3.8*	*(El-Mudir et al, 2004)*

1.5 Present Study

The SD system is the most appropriate technique for remote and rural areas, whose populations are suffering from water and energy stress. SD systems are simple, could be portable, provide a reasonable amount of potable water, and the most important feature of these systems is that they could solely run on solar energy, hence they are environmentally friendly. The only disadvantage of the SD systems is their low productivity, which makes it a costly and unfeasible choice for areas experiencing high demand for water. However, in scenarios with a small scale of water demand such as on small islands, ships, villages, or even for household use, the use of the SD system is a competitive option due to the high cost of other methods of acquiring water such as water transportation or connection to the electricity grids.

The low productivity of the SD systems has motivated researchers to try to improve the performance of those systems. Numerous researchers had proposed several modifications and improvements to the SD systems to enhance the systems' performance and to increase the water production of those systems. However, most of these modifications and improvements to the SD systems led to an increase in costs and/or complexities of those systems, and/or a failure to achieve significant augmentation in water productivity. Therefore, further research is required to produce an SD system with higher productivity, whilst maintaining simplicity and low cost. Some examples of the previous efforts to enhance the performance of the SD systems (all mentioned in details in chapter two) are: increasing the temperature of the feedwater using heat exchangers and heaters (Kumar et al, 2014); storing the solar energy using thermal storages (Kabeel & Abdelgaied, 2017); increasing the solar gain using reflectors (Estahbanati et al, 2016); increasing the condensation rate using vacuum fans and separated condensers (El-Samadony et al, 2015); decreasing the temperature of the cover using film cooling (Sharshir et al, 2017); and increasing the surface area of the water using fins (Srivastava & Agrawal, 2013).

The main aim or purpose of this research is finding ways to improve the productivity of the SD systems - using a simple and low-cost technique - to make them available to a wide range of beneficiaries, especially to those living in remote and arid/semi-arid areas, and poorer/less-developed regions. From previous research that was found in the literature review, extending the surface area of the water seems to be

promising. Since the evaporation occurs on the free surface of the water that is in contact with the ambient air, increasing the water surface area will lead to an increase in the evaporation rate, which will enhance the productivity of the SD systems. Another finding from the literature review that - as implied by the name of the Solar "Still" Desalination system - the water in these systems is usually "still" or "stagnant"; and most previous studies of the SD systems deal with water that is stagnant in the basins of these systems.

The research gap is how combining two ideas for enhancements will affect the performance of the system; for instance, extending the water surface area and generating water movement within the basin of the SD system. The research question then is: what are the effects of stirring the water and increasing the surface area of the water on the SD system's performance and productivity? To achieve this goal, revolving tubes have been introduced into the water basin of the SD system to produce water circulation around the tubes' circumference and to extend the surface area the water. Three symmetrical PVC tubes were proposed to be semi-immersed into the water basin of the SD system. These tubes placed horizontally in a parallel arrangement and coupled with small DC motors to generate the rotational movement. These tubes have the advantages of stirring the water, extending the surface area of the water, and absorbing solar radiation as well. This amendment or modification to the SD system will hopefully increase the water evaporation rate, and thereby, enhance the SD system performance and productivity.

In this study, two SD systems will be run at the same time under the same weather conditions in Toowoomba, Australia during two seasons, spring and summer. The first system is a regular or normal double-sloped SD system that is denoted by (NSD) and the second system is the modified SD system with the proposed revolving tubes that is denoted by (MSD). Both the SD systems will have the same dimensions and are made of the same construction materials, except for the modification of the revolving tubes in the MSD system. Figures 1.14 and 1.15 show sketches of the two SD systems; the MSD and the NSD under study.

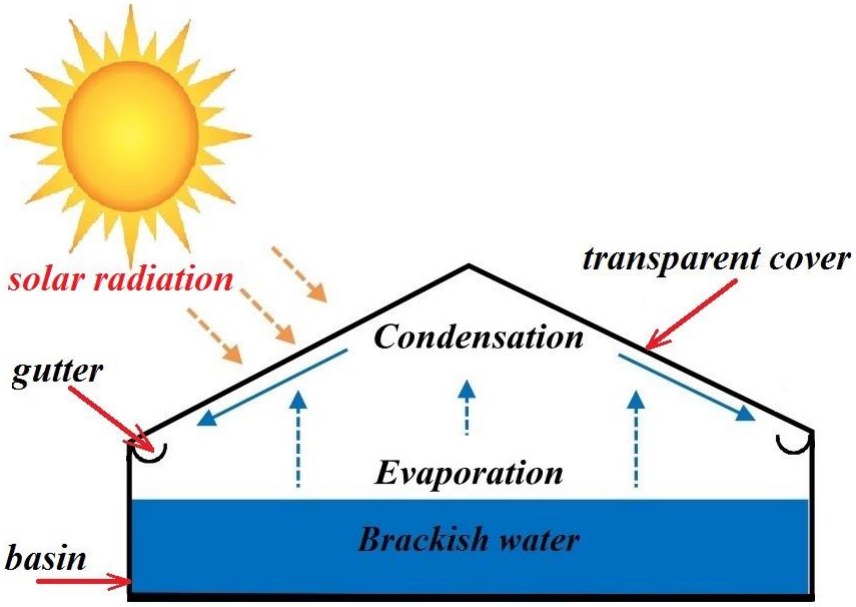

Figure 1. 14 A schematic diagram of the NSD system under study

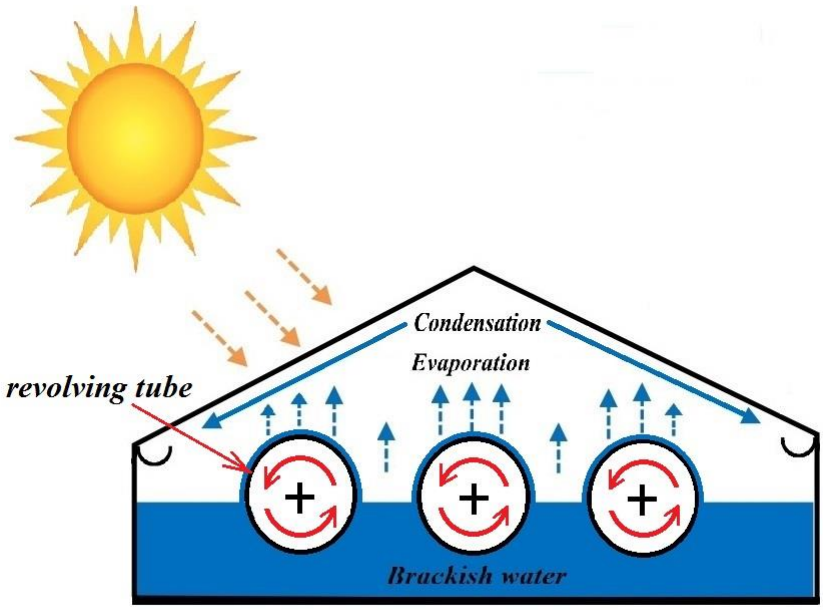

Figure 1. 15 A schematic diagram of the MSD system under study

The methodology of this research is conducting numerical simulation and experimental investigations for both SD systems. The numerical simulation will be done by developing a CFD model with the aid of ANSYS-Fluent software. The experimental investigations will be done by manufacturing two physical small-scale models to meet with the research budget. Comparisons will be done between these two SD systems. The sensitivity analysis (optimisation) to the design parameters such as water depth, tube diameter, tube rotation speed, the dimensional analysis, the uncertainty analysis of the measured values, and the cost analysis of both the SD systems will be conducted as well.

The significance of this research is its contribution to engineering and health sectors. Water, energy, and the environment are amongst the most vital factors affecting our life and wellbeing. We all need clean and safe water, sustainable and green energy, and an environment that is free of contaminants to survive and thrive. Traditional desalination techniques that use fossil fuels produce greenhouse gases that pollute the environment and worsen the problem of global warming. Moreover, fossil fuels are finite and will soon run out. Using solar energy in desalination has become essential to mitigate the effect of using fossil fuels. Solar desalination provides a clean and sustainable solution to the problems of both energy and water scarcity. The availability of fresh and safe water without the need for using traditional energy sources has great significance and high levels of impact on the economy, society, environment, health, and human life. Another significance of this research is the provision of a device at low cost, that is simple to maintain, easy to run, and environmentally friendly for water desalination purposes that will be available to a wide range of people, especially for those living in remote and arid areas and poor people living in less-developed countries with few resources. This system can sustain communities in those areas and has the potential to revive abandoned remote lands. Other important outcomes of this study are to provide researchers with knowledge of the effect of combining these enhancement ideas and provide the designers with a simple optimisation to some important parameters of designing SD systems. If the suggested modification to the SD system achieves a good enhancement in producing freshwater, it can be manufactured in larger scales to provide a wide range of beneficiaries with reasonably priced freshwater.

1.6 Thesis Objectives

The objectives of the present research are as follows:

1. Designing the NSD system, which is a conventional double-slope SD system depending on the current knowledge that is available in the literature; then design the MSD system including the proposed modification of three revolving tubes in its basin.
2. Developing a CFD model to simulate numerically the NSD system and the MSD system using ANSYS-Fluent software.
3. Manufacturing moderate-sized NSD and MSD systems.
4. Conducting experimental investigations for both the SD systems over two seasons; spring and summer in Toowoomba, Australia.
5. Estimating the uncertainty analysis of the measured values.
6. Validating the results of the CFD simulation using the experimental data.
7. Implementing a sensitivity analysis (optimisation) of the operation and design parameters for both the SD systems using the developed CFD model.
8. Conducting a dimensional analysis of the parameters that affect the productivity of the SD systems.
9. Performing a cost analysis of the present experimental setup of both the SD systems.
10. Presenting and discussing the results, reaching conclusions, and suggesting recommendations for future work.

1.7 Thesis Outline

The following is a brief description of the structure or an overview of this thesis;

1. **Chapter One: Introduction:** Gives a brief background of the current water status and the water desalination techniques. States the research problem and suggests a possible solution. Presents the research aim, the research gap, the research question, the research methodology, and the significance of the study. Outlines the objectives of this project.
2. **Chapter Two: Literature Review:** Presents the existing knowledge and the current efforts undertaken by the researchers in developing the SD systems. Reaches conclusions that will help in identifying the research gap and developing the aim of the present research.
3. **Chapter Three: CFD Simulation:** Presents the theoretical background and the correlations that were used to estimate the productivity and the efficiency of the SD system. The chapter presents the governing partial differential equations and highlight the assumptions used to facilitate the solution. It describes the steps that were taken to conduct the numerical simulation such as creating the geometry and generating the computational grid. Then it presents the numerical models that were used in this study and the solution method.
4. **Chapter Four: Experimental Investigation:** Describes the experimental setup of both the SD systems that were used in this project and presents the instrumentation, observation, and data collection.
5. **Chapter Five: Results and Discussion:** Presents and discusses the results of the CFD simulation and the recorded data from the experimental investigations and makes a comparison between both SD systems under study. Validates the CFD results with the experimental data.
6. **Chapter Six: Analyses:** Presents the important analyses that were done in this study, the sensitivity analysis (optimisation) of the operation and design conditions, the dimensional analysis to the parameters that affect the productivity, the uncertainty analysis, and the cost analysis of both the SD systems under study.
7. **Chapter Seven: Conclusions and Recommendations:** Presents a summary of the thesis, reaches conclusions and provides suggestions for future work.

2 Chapter Two: Literature Review

This chapter presents recent efforts done by researchers to enhance the performance of the Solar Still Desalination (SD) systems and the recent developments applied to SD systems found in the literature. This chapter is divided into the following sections; firstly it presents the conventional SD systems, then the enhancements that were introduced to the SD systems, then the previous numerical simulation of the SD systems, then the water productivity and its cost by the SD systems, and finally the conclusions drawn from the literature review.

2.1 Conventional SD Systems

The conventional SD system refers to the regular and prevalent Solar Still Desalination system without modifications or enhancements. Some researchers have studied the conventional SD systems to understand the working principle of the SD system and the effect of the weather, designs, and operations factors on SD systems' performance.

Al-Hinai et al (2002) studied the effect of some weather conditions and design parameters on the productivity of a double-slope SD system using a mathematical model. They used a simple energy balance approach to estimate the heat transfer coefficient of evaporation, and hence the productivity of the SD system. They found that higher hourly productivity can be achieved with a higher solar intensity, a higher ambient temperature, a higher wind velocity, a greater cover's slope-angle during winter and a steeper cover's slope-angle during summer, a thicker basin's insulation, a higher feedwater temperature, and shallower water. The results showed that the average annual productivity was (4.15 kg/m^2.day) and the average cost was ($16.3 USD/$m^3$). Figure 2.1 shows a schematic diagram of the SD system.

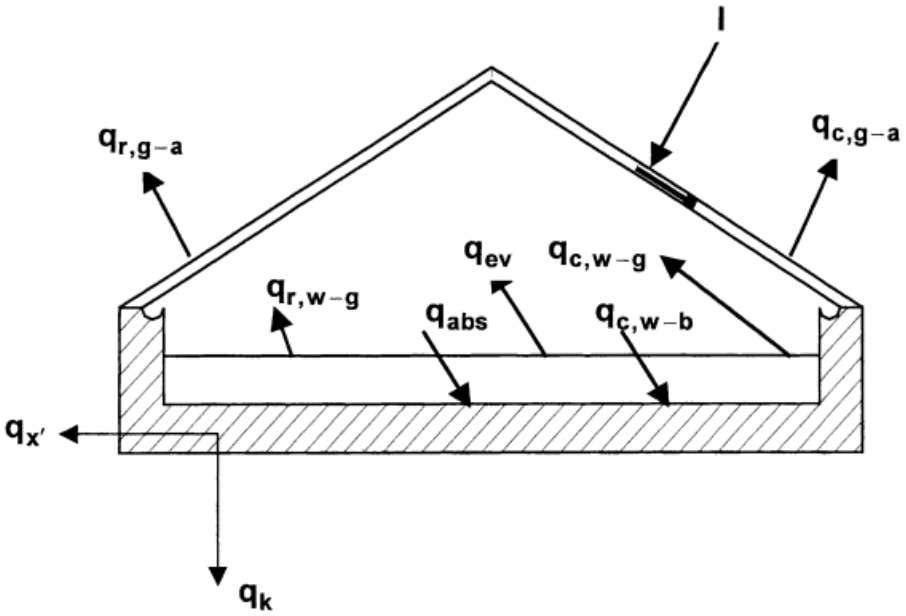

Figure 2. 1 The schematic diagram of the SD system and the heat balance. Where: I= solar incidence, q= heat transfer, and the subscript: abs= absorbed, c= convection, ev = evaporation, k= conduction, r = radiation, x=stored, while w-b= the direction from water to basin, w-g= from water to glass, and g-a= from glass to ambient (Al-Hinai et al, 2002)

Jamil and Akhtar (2017) investigated experimentally the effect of the gap between the basin and the cover of a single-slope SD system. The fixed design parameters were; (0.7m× 1.4m) of the basin's dimensions, (28°) of the cover's slope-angle (which is the same latitude angle of the location), and (10 mm) of the water depth. They controlled the height of the gap between the basin and the cover using polystyrene sheets within five stages and it was from 0.266m to 0.366m. They concluded that a smaller cavity (the gap between the basin and the cover) increases the SD system productivity. According to the results, the average daily productivity ranged from 1.341 L/m^2 to 4.186 L/m^2, the average daily efficiency ranged from 11.25% to 39.59%, and the average cost of the produced water ranged from ($0.074 USD/L) to ($0.024 USD/L). Figure 2.2 shows a schematic diagram of the experimental setup.

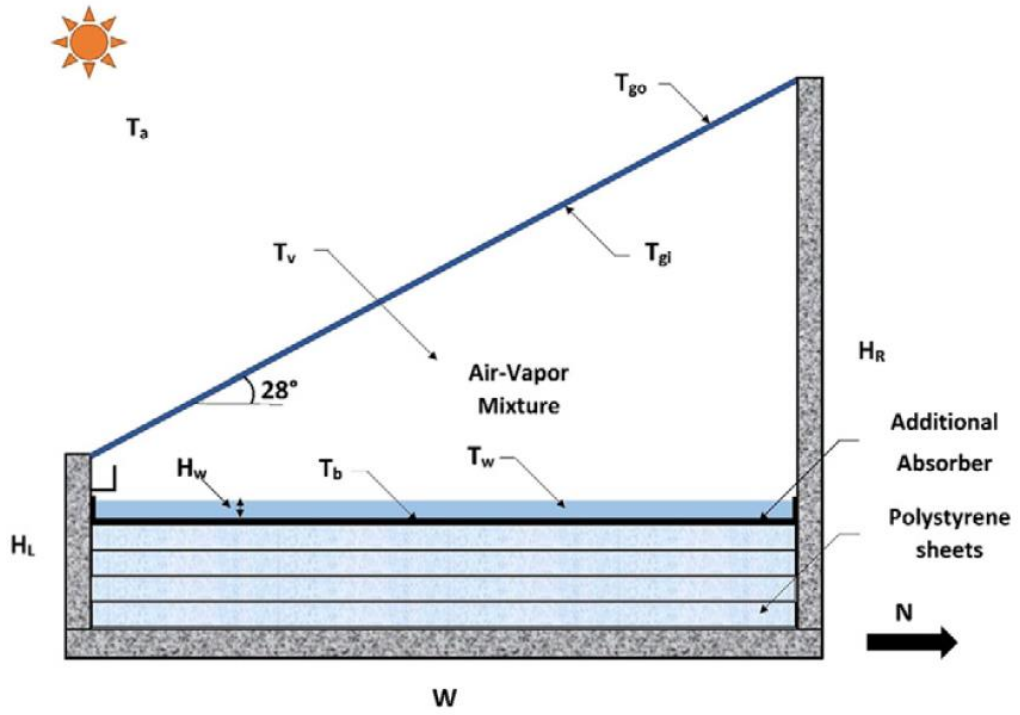

Figure 2. 2 The schematic diagram of the experimental setup where the polystyrene sheets used to adjust the height between the basin and the cover, T= temperature, and the subscript b= basin, w= water, v = vapour, gi= glass inner, go= glass outer (Jamil & Akhtar, 2017)

2.2 Modified SD Systems

Numerous researchers have introduced many types of enhancements or modifications to the conventional SD system. Improving water productivity (the distillate yield) of the SD systems was the main purpose of these enhancements. This section presents the literature, which is divided according to the type of enhancement to the SD system as follows;

2.2.1 SD Systems with External Heat Sources

One enhancement to the SD systems is by combining a further heat source to the conventional SD system. Some researchers attempted to increase the SD systems' productivity by accelerating the evaporation rate. For this purpose, they combined the basin of the SD system with a sort of heat exchanger to heat up the brackish water in the basin or to heat up the feed water pre-accessing the SD system. The external heat

source could be a solar collector, solar pond, or any other waste heat source such as the rejected heat of an engine's exhaust system.

Badran and Al-Tahaineh (2005) investigated experimentally the effect of coupling a flat plate solar collector with a single-slope SD system to heat up the brackish water into the SD basin. They found that productivity of the SD system increased by (36%) due to this modification. Figure 2.3 shows a schematic diagram of the experimental setup and Figure 2.4 shows the variation of the hourly productivity of the conventional and the enhanced SD systems.

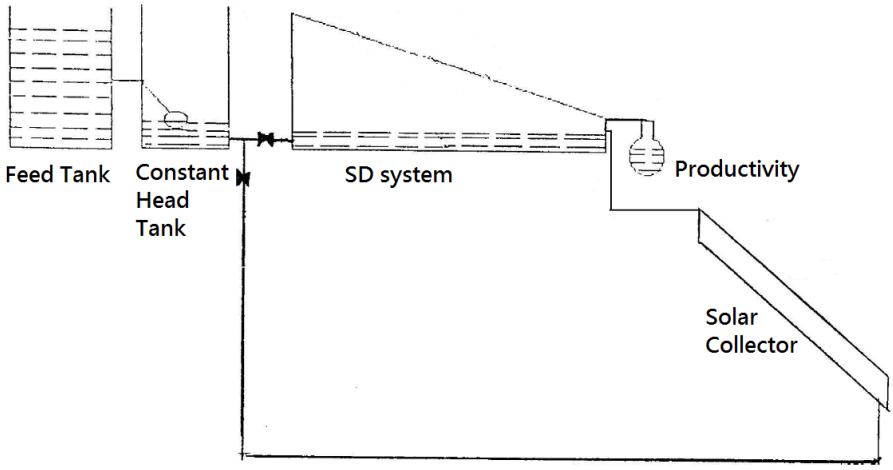

Figure 2. 3 The schematic diagram of the experimental setup (Badran & Al-Tahaineh, 2005)

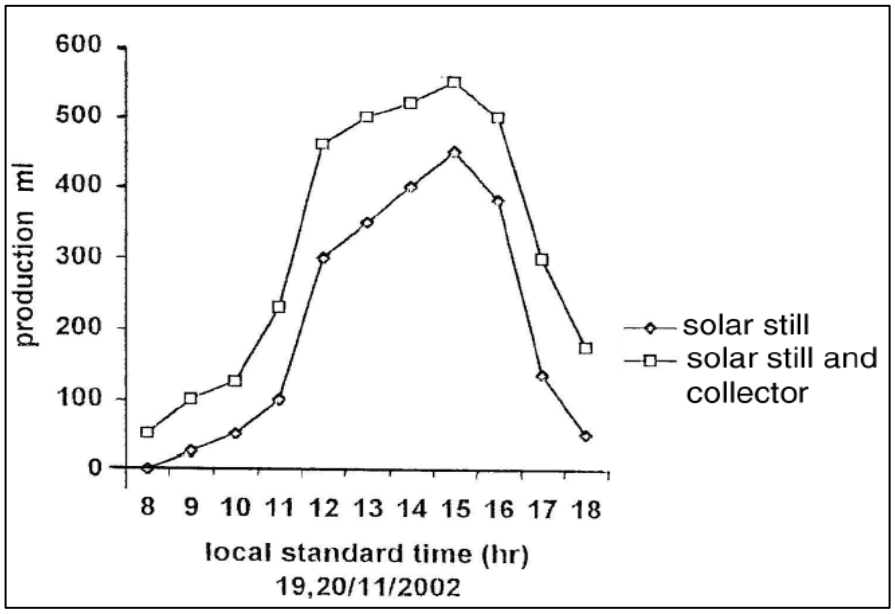

Figure 2. 4 The hourly productivity of the conventional and the enhanced SD systems (Badran & Al-Tahaineh, 2005)

Abdel-Rehim and Lasheen (2007) combined the SD system with a solar parabolic trough with a focal pipe and a simple heat exchanger with oil as working fluid to heat up the brackish water in the SD basin. They found that the productivity of the SD system increased by an average of (18%) due to the modification. Figure 2.5 shows a schematic diagram of the experimental setup and Figure 2.6 shows the variation of the accumulative productivity of the conventional and the modified SD systems.

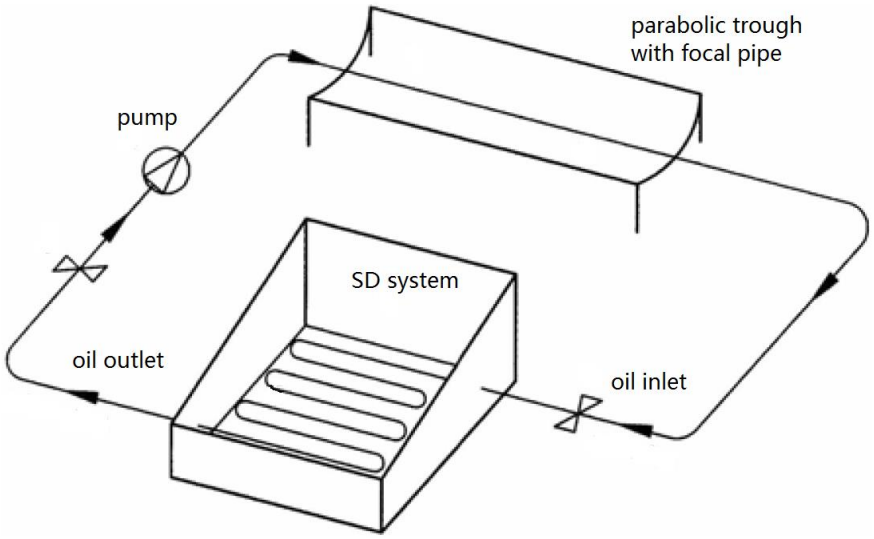

Figure 2. 5 The schematic diagram of the experimental setup (Abdel-Rehim & Lasheen, 2007)

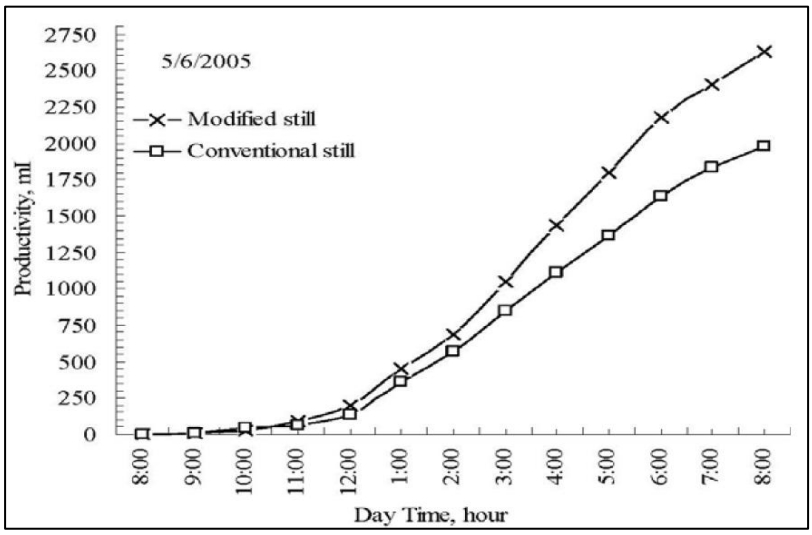

Figure 2. 6 The hourly accumulative productivity of the conventional SD system (without heater) and modified SD system (with heater) in mL on 5/6/2005 (Abdel-Rehim & Lasheen, 2007)

El-Sebaii et al (2008) studied the effect of coupling the SD system with a shallow solar pond by a tube heat exchanger to heat up the brackish water before it gets into the SD basin. They found that productivity and efficiency of the modified SD system were higher by (52.36%) and (43.8%), respectively. The daily productivity of the modified SD system ranged from (1.904 kg/m^2) in winter to (6.570 kg/m^2) in summer. Figure 2.7 shows a schematic diagram of the experimental setup.

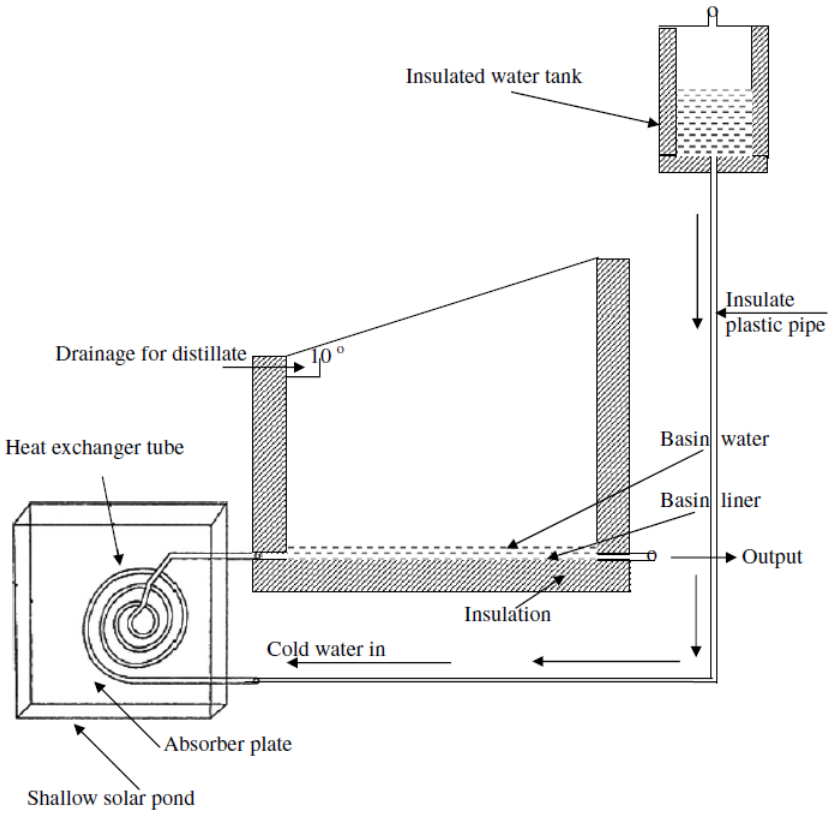

Figure 2. 7 The schematic diagram of the experimental setup (El-Sebaii et al, 2008)

Kumar et al (2014) integrated a single-slope SD system with an evacuated tube solar collector to heat up the brackish water as it goes into the SD basin. They found that during a typical summer day, the maximum daily yield was (3.47 kg/m^2) which is higher than a conventional SD system by about (20%). The result also showed that the maximum efficiency was (33.8%), which is higher approximately (26%) than the SD system without this enhancement. They also concluded that the optimum water depth into the basin is (0.03 m). Figure 2.8 shows a schematic diagram of the experimental setup.

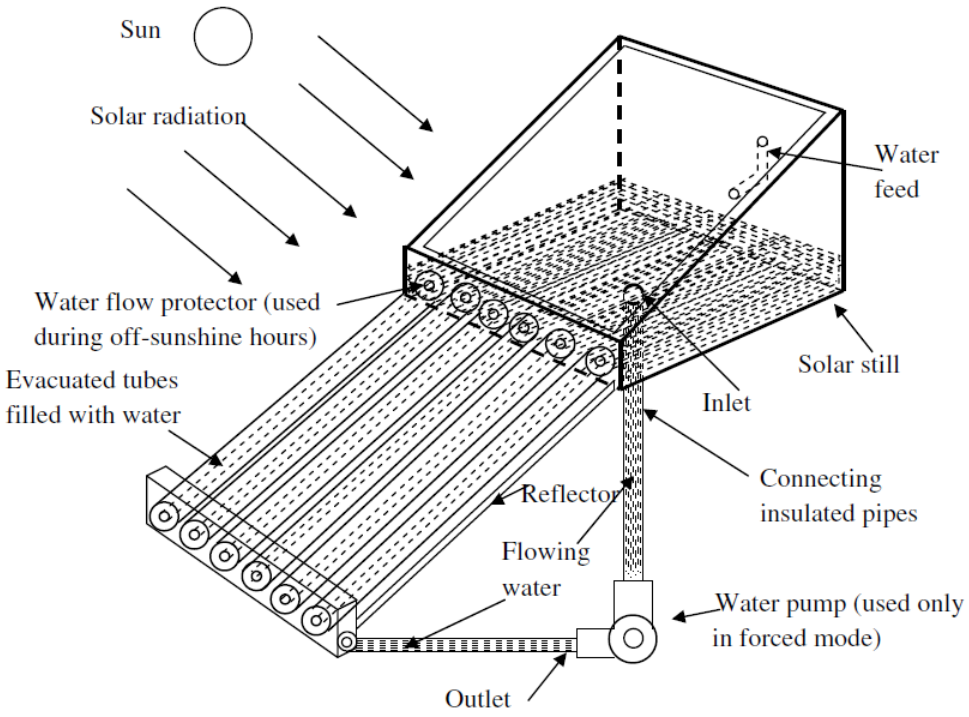

Figure 2. 8 The schematic diagram of the experimental setup (Kumar et al, 2014)

2.2.2 SD Systems with Thermal Energy Storages

Another improvement to the SD systems is made by adding heat storage to the SD system. Some researchers tried to store the heat of solar energy during the daytime sunlight hours to produce more freshwater during the night and the cloudy weather, i.e. during the absence of sunlight. For this purpose, they used many types of materials such as rubber, rocks, marbles, etc. as sensible heat storage or Phase Change Materials (PCM) such as paraffin wax as latent heat storage.

El-Sebaii et al (2009) investigated theoretically only the effect of adding a PCM to a single-slope SD system. Using 3.3 cm thickness of stearic acid PCM underneath the SD absorber surface on a typical summer day, they found that the maximum daily productivity was (9.005 kg/m^2) and (4.998 kg/m^2) of the SD system with, and without PCM, respectively. The improvement in daily productivity was about 80% due to the enhancement of adding the PCM. Figure 2.9 shows a schematic diagram of the SD system with the PCM.

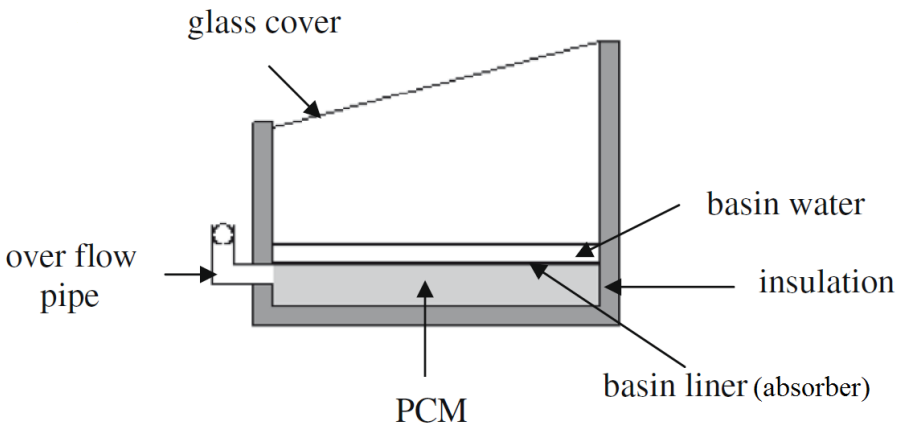

Figure 2. 9 The schematic diagram of the experimental setup (El-Sebaii et al, 2009)

Shalaby et al (2016) studied experimentally the effect of using Paraffin wax PCM under a v-corrugated solar absorber of a single- slope SD system. They found that using the paraffin wax PCM as latent heat storage decreases the productivity of the SD system during the daylight by (7.4%) while increases the productivity by (72.7%) overnight. The total daily productivity of the SD system was about (11.7%) higher when using PCM than without PCM. Figure 2.10 shows a schematic diagram of the experimental setup.

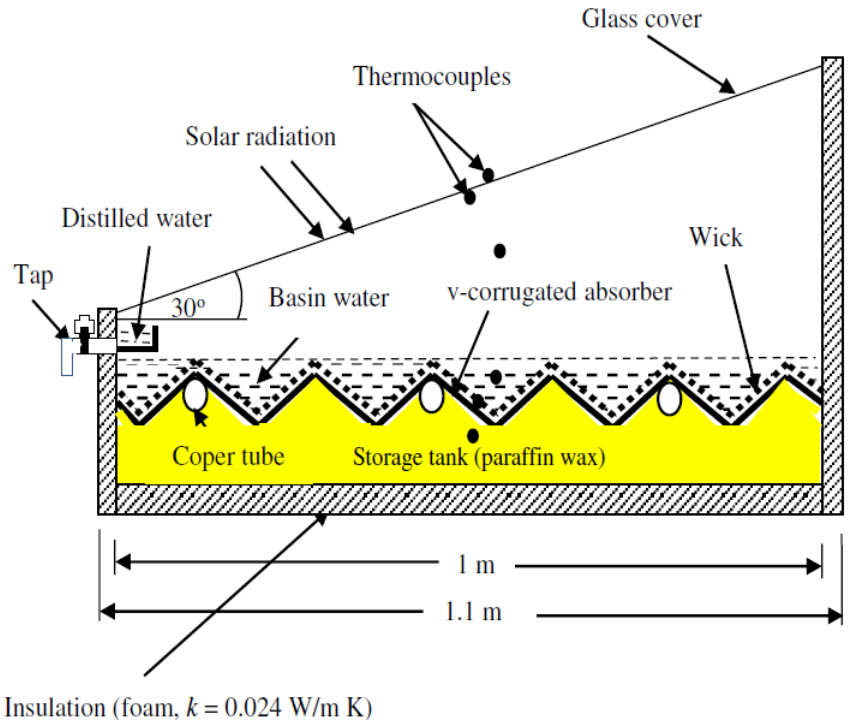

Figure 2. 10 The schematic diagram of the experimental setup (Shalaby et al, 2016)

Dashtban and Tabrizi (2011) studied experimentally a weir-type cascade SD system with paraffin wax PCM underneath the solar absorber surface. They found that daily productivity of the SD system increased by (31%) when using PCM. The daily yield was (6.7 kg/m^2) and (5.1 kg/m^2) for the SD system with and without PCM, respectively. The overall thermal efficiency was 64% and 47% of the SD system with and without PCM, respectively. Figure 2.11 shows a schematic diagram of the experimental setup.

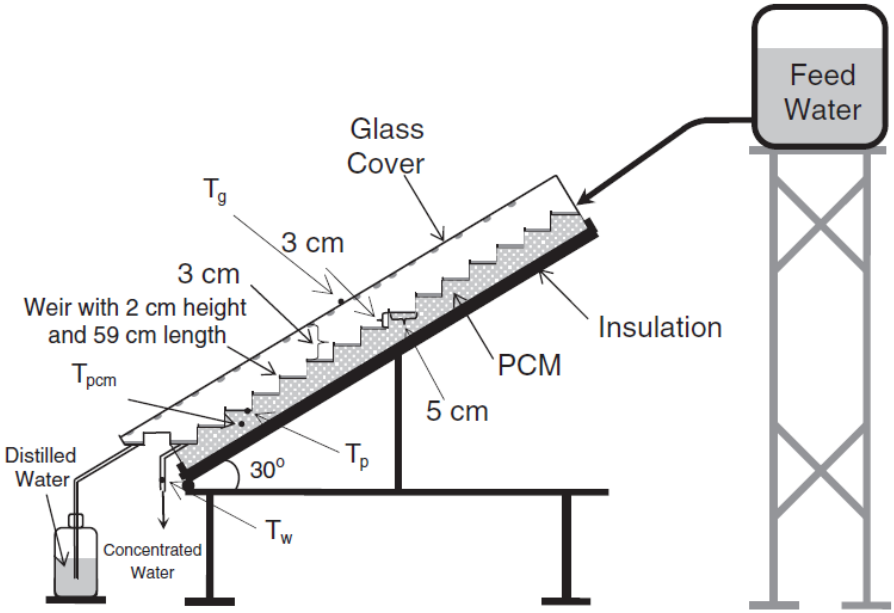

Figure 2. 11 The schematic diagram of the experimental setup (Dashtban & Tabrizi, 2011)

Kabeel and Abdelgaied (2016) improved the daily productivity of the SD system from (4.51 l/m^2) to (7.54 l/m^2) by using PCM (Paraffin wax) layer beneath the absorber surface of the SD system. The productivity of the SD system with PCM was higher by (67.18%) than the SD system without PCM. Kabeel and Abdelgaied (2017) also performed experimental tests to a modified SD system with two enhancements, a PCM as a latent heat energy storage and an oil heat exchanger to heat the feed water. They found that the maximum freshwater productivity was (4.48 l/m^2.day) and (10.77 l/m^2.day) of the conventional and the modified SD systems, respectively. The result also showed that the maximum daily efficiency was 25.73% and 46% for the conventional and the enhanced SD system respectively. The enhancement in the

productivity and efficiency were about (140.4%) and (44%) due to the modifications, respectively. Figure 2.12 shows a schematic diagram of the experimental setup.

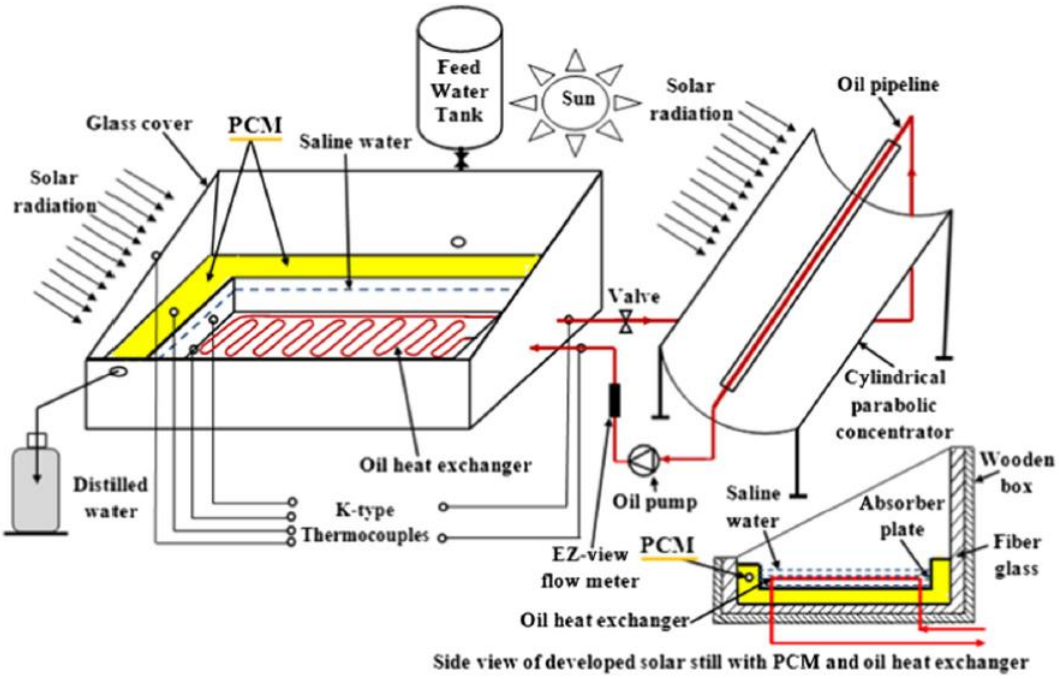

Figure 2. 12 The schematic diagram of the experimental setup (Kabeel & Abdelgaied, 2017)

Murugavel et al (2010) investigated the effect of using different materials as sensible heat storages on the SD system performance. They tested adding different types of materials such as; quartzite rock, red brick pieces, cement concrete pieces, washed stones, and iron scraps into the water basin of a double-slope SD system. The dimensions of the basin were 2.08m×0.84m and the water depth in the basin was (0.5 - 0.75 cm). The results showed that the maximum enhancement in daily productivity was 6.2% using 0.75 inches sized quartzite rock as sensible heat storage. Figure 2.13 shows the variation in the hourly productivity of the SD system using different materials into its water basin and Figure 2.14 shows the materials that were used in this study.

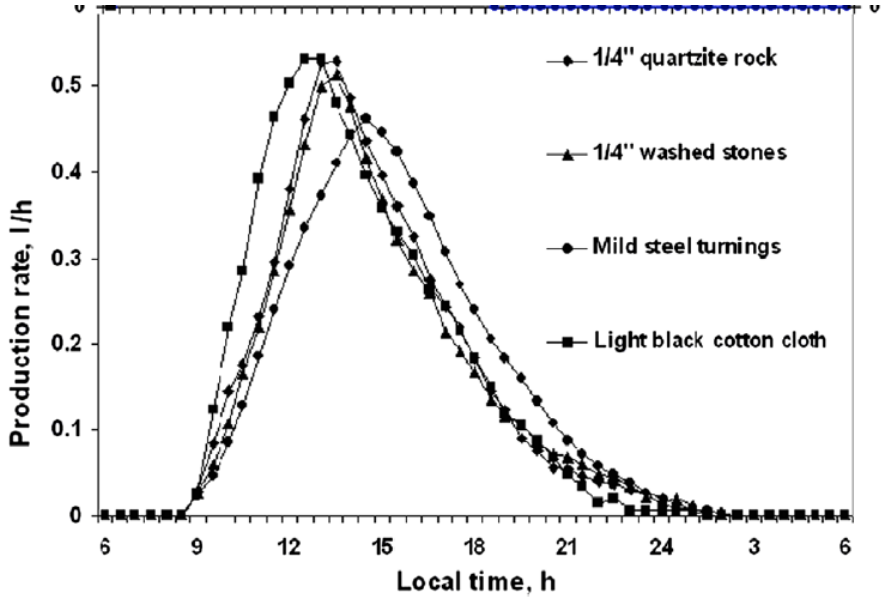

Figure 2. 13 The variation in the hourly productivity of the SD system using different materials into its water basin as sensible heat storage (Murugavel et al, 2010)

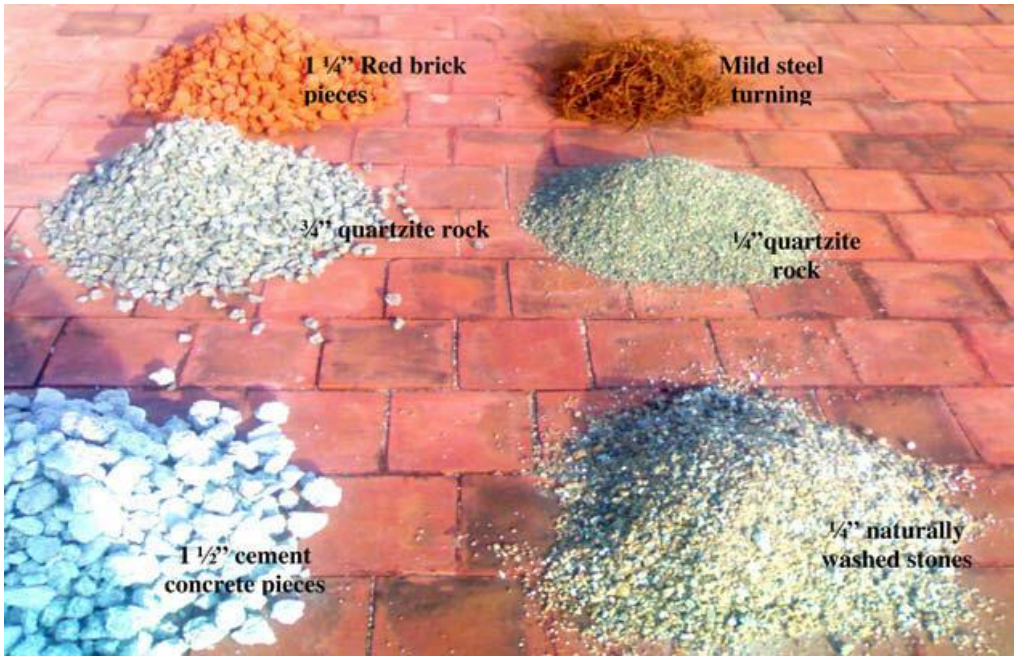

Figure 2. 14 The material used in the experimental investigation (Murugavel et al, 2010)

2.2.3 SD Systems with Reflective Surfaces

Another improvement to the SD systems is by adding internal and/or external sunlight reflectors. Some researchers tried to increase the solar radiation gain by attaching reflector surfaces inside the basin and/or over the cover of the SD system. Increasing the solar radiation gain means increasing the water temperature, which leads to accelerating the evaporation rate, hence increase the productivity of the SD system.

Tanaka and Nakatake (2006) studied theoretically the effects of adding internal and external reflectors on the SD system performance. They concluded that the annual distillate productivity increases by an average of (48%) higher than the SD system without reflectors. Figure 2.15 shows the schematic diagram of the modified SD system.

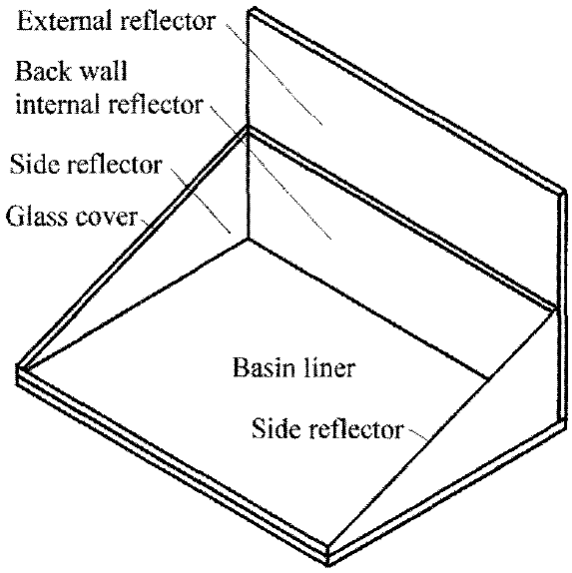

Figure 2. 15 The schematic diagram of the experimental setup (Tanaka & Nakatake, 2006)

Khalifa and Ibrahim (2009) studied experimentally the effect of the internal reflectors, the external reflector, and the inclination angle of the external reflector during all seasons on the SD system productivity. They found that the average enhancement in the annual productivity was (19.9%) with internal reflectors only and (34.4%, 34.5%, 34.8%, and 24.7%) for combined internal and external reflectors at (0°, 10°, 20°, and 30°) slope angle of the external reflector, respectively higher than the SD system

without reflectors. They also concluded that the effect of the reflectors was negative during summer. Figure 2.16 shows the schematic diagram of the experimental setup.

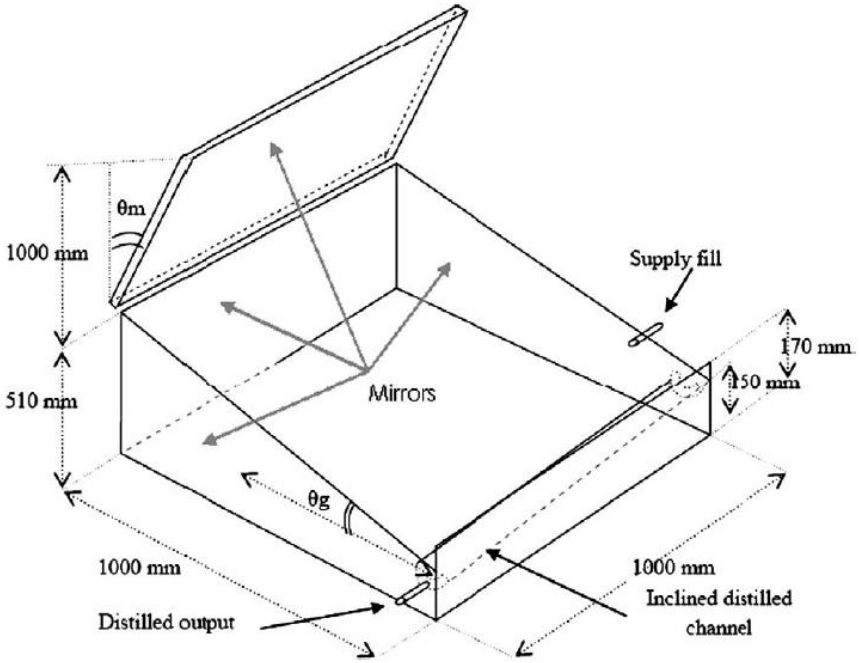

Figure 2. 16 The schematic diagram of the experimental setup (Khalifa & Ibrahim, 2009)

Estahbanati et al (2016) compared theoretically and experimentally the distillate productivity of the SD system with and without internal reflectors. The results showed that average (annual, winter, and summer) enhancement in the productivity of the SD system with reflectors on all inner walls were (34%, 65%, and 22%) higher than the SD system without reflectors, respectively. They also concluded that the internal reflectors are more beneficial during winter than in summer.

Omara et al (2014) investigated the performance of a stepped basin SD system with and without internal and external reflectors and compared it to a conventional SD system. The results showed that the daily productivity of the stepped basin SD system was higher than the conventional SD system by (57%, 75%, and up to 125%) when it was without reflectors, with internal reflectors only, and with internal and external reflectors, respectively. The daily efficiency of the conventional SD system, stepped without reflectors SD system, and stepped with reflectors SD system were 34%, 53%, and 56%, respectively. Figure 2.17 shows the schematic diagram of the experimental

setup and Figure 2.18 shows the variation in productivity between the conventional and modified SD systems.

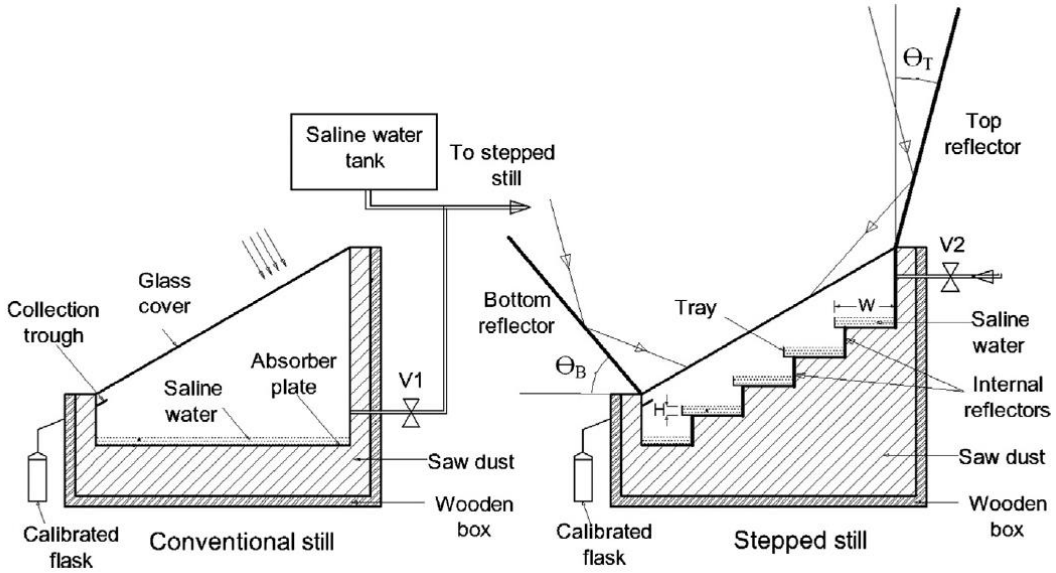

Figure 2. 17 The schematic diagram of the experimental setup (Omara et al, 2014)

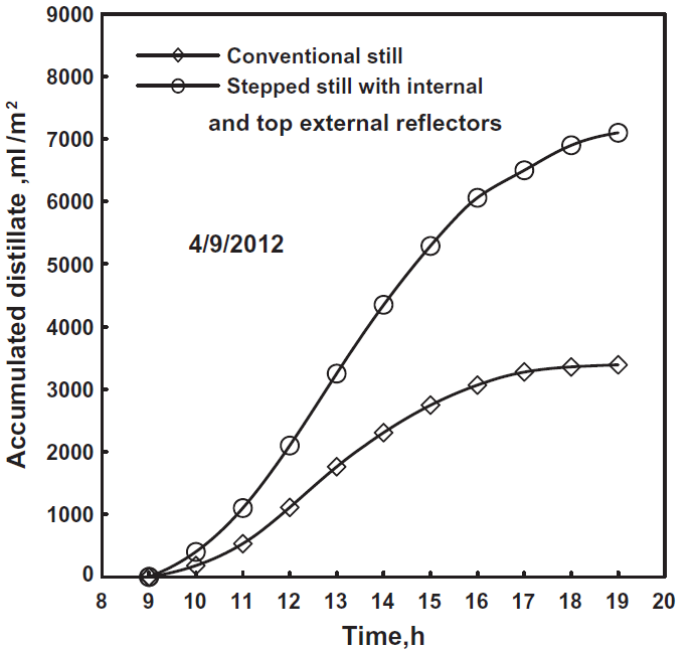

Figure 2. 18 The accumulative productivity of the conventional and enhanced SD systems (Omara et al, 2014)

2.2.4 SD Systems with External Condensers

Another improvement to the SD system is by adding an external condenser to the conventional SD system to increase the yield of the SD system. The idea is to cool down the produced vapour, which leads to speed up the condensation rate hence increase the productivity of the SD system. Combining the SD system with an external condenser will increase the thermal efficiency of the SD system as well. However, this modification to the SD systems requires more land area in addition to the increase in the system capital and operation cost, complexity and further maintenance requirements.

Abu-Qudais and Othman (1996) compared the performance of two SD systems, with and without an external condenser. They found that the thermal efficiency of the SD system is higher by (47%) when using the external condenser modification. Figure 2.19 shows a schematic diagram of the experimental setup.

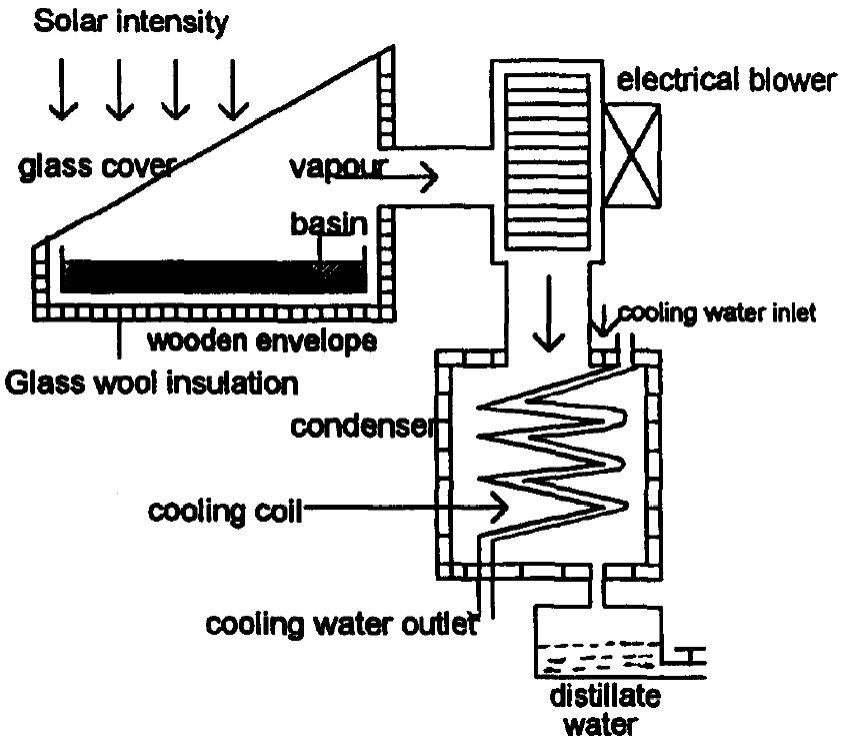

Figure 2. 19 The schematic diagram of the experimental setup (Abu-Qudais & Othman, 1996)

El-Bahi and Inan (1999a) examined experimentally attaching an outside passive condenser and external reflector to a single-slope SD system with (4°) minimum cover's slope angle. They found that the maximum daily productivity of the modified SD system was about (7 l/m^2). The daily yield and the efficiency of the enhanced SD system were improved by about (70%) and (75%), respectively. Figure 2.20 shows a schematic diagram of the experimental setup.

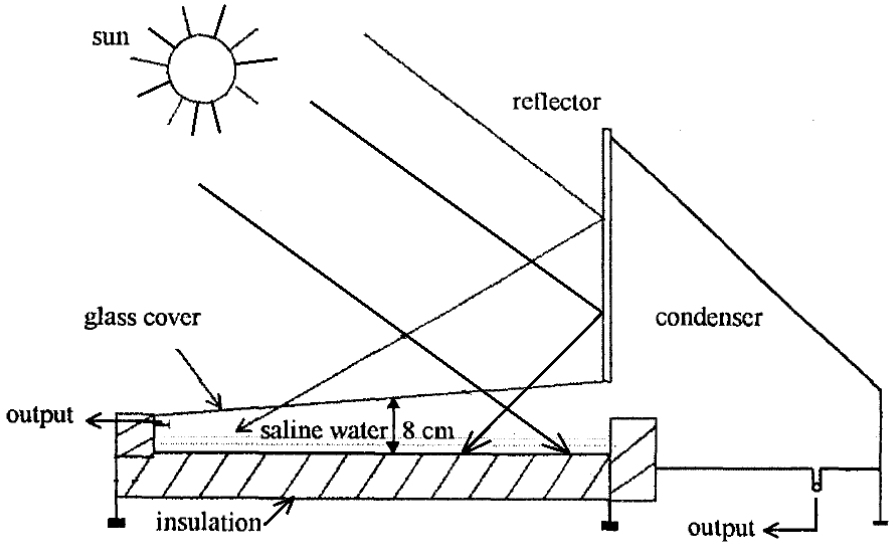

Figure 2. 20 The schematic diagram of the experimental setup (El-Bahi & Inan, 1999)

Monowe et al (2011) proposed a new design of the SD system for domestic purposes with two enhancements: an external reflector and external condenser. The results showed that the efficiency of the proposed SD system was up to (77%) when using the latent heat of condensation to preheat the feed brackish water (in the condenser). The daily water productivity was up to (8 l/m^2). Figure 2.21 shows a schematic diagram of the experimental setup.

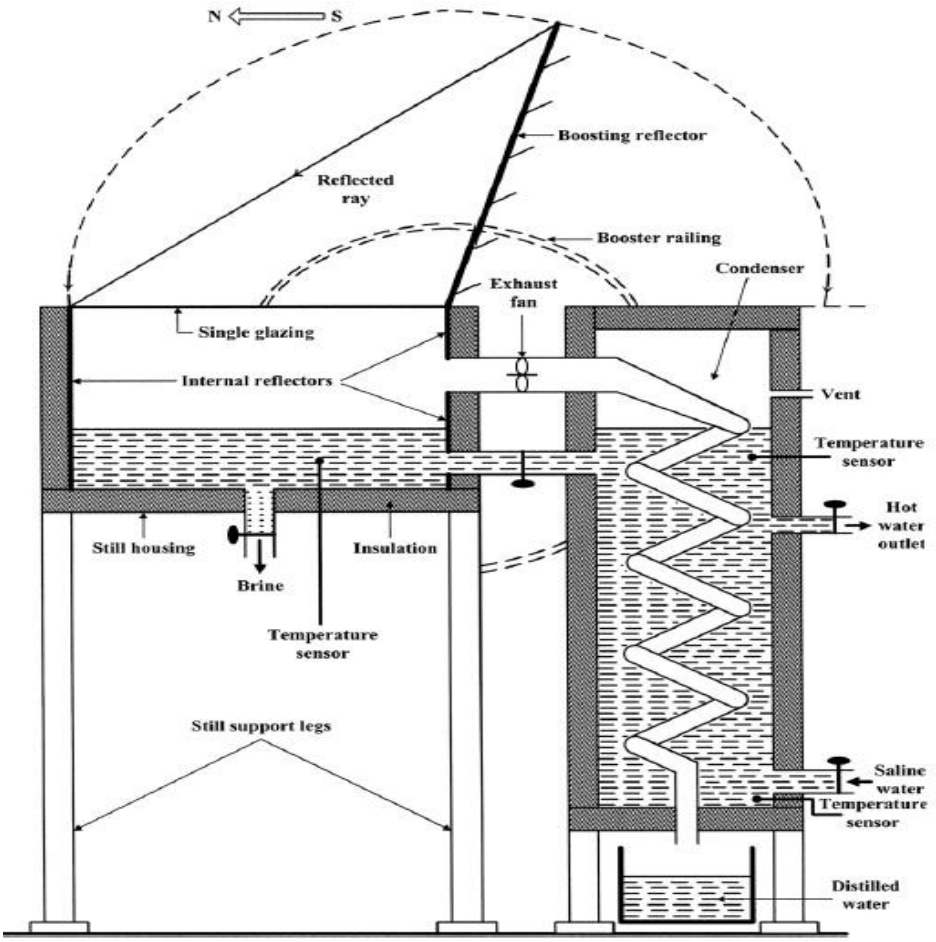

Figure 2. 21 The schematic diagram of the experimental setup (Monowe et al, 2011)

Kabeel et al (2014a) investigated three enhancements to the conventional single-slope SD system. The enhancements included adding an external condenser, adding Nanoparticles into the water, and adding a vacuum fan. The results showed that the daily productivity of the enhanced SD system compared to the conventional SD system improved by (53.2%) when using the external condenser only, by (76%) when using the external condenser and the nanoparticles into the water, and up to (116%) when using the external condenser, the nanoparticles, and the vacuum fan. The advantage of the vacuum fan is to extract and accelerate the humid-air flow from the SD system to the condenser. Figure 2.22 shows a schematic diagram of the experimental setup.

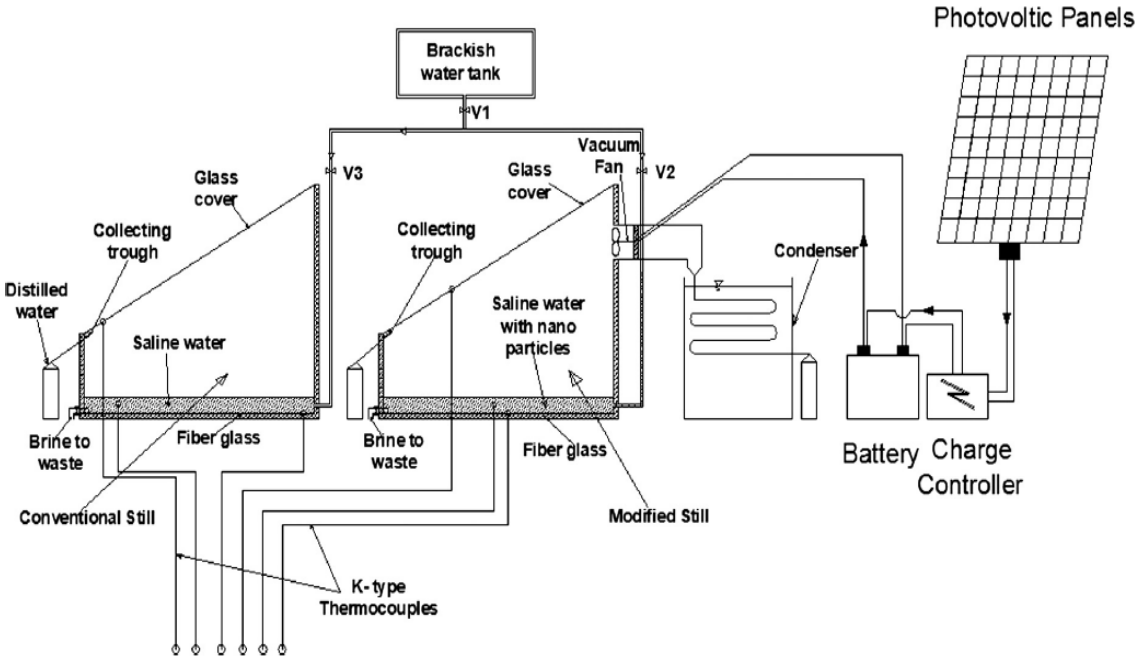

Figure 2. 22 The schematic diagram of the experimental setup (Kabeel et al, 2014)

El-Samadony et al (2015) modified a stepped SD system by adding an external condenser and internal and external reflector surfaces. They compared the modified model with a conventional single-slope SD system and they found that the productivity was higher by (66%) when using external condenser only and by (165%) when using the external condenser and the internal and external reflectors. Figure 2.23 shows a schematic diagram of the experimental setup and Figure 2.24 shows the variation of the accumulative productivity between the conventional and the modified SD systems.

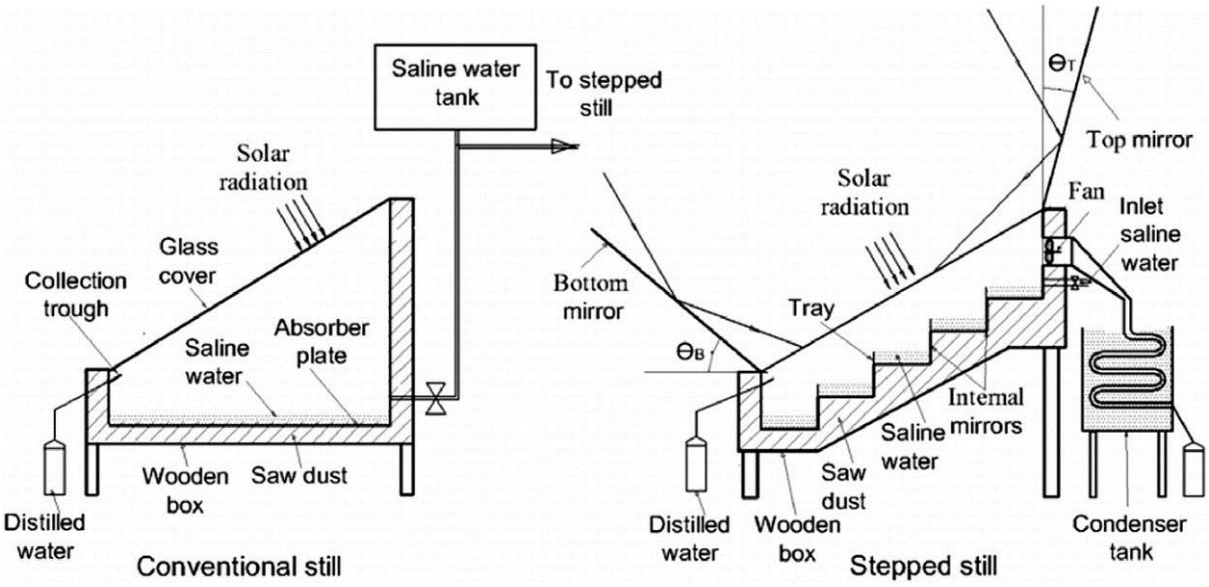

Figure 2. 23 The schematic diagram of the experimental setup (El-Samadony et al, 2015)

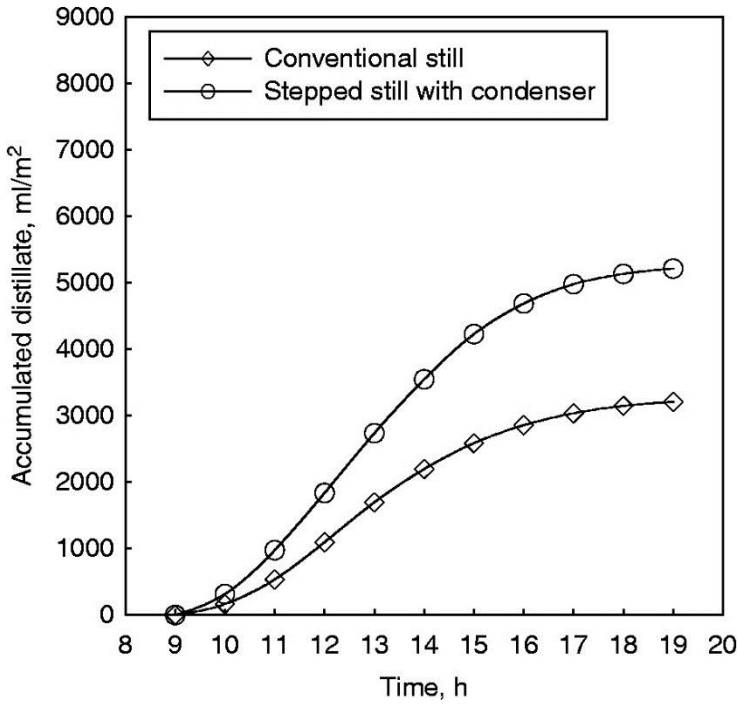

Figure 2. 24 The accumulative productivity of the conventional and the enhanced SD systems (El-Samadony et al, 2015)

Ibrahim et al (2015) investigated the effect of attaching an external condenser to a single-slope SD system working under vacuum pressure. The result showed that the productivity of the enhanced model was higher by (16.2%) than the conventional SD system. The daily efficiency was (29% and 37.6%) for the conventional and the

enhanced SD systems, respectively. Figure 2.25 shows a schematic diagram of the experimental setup.

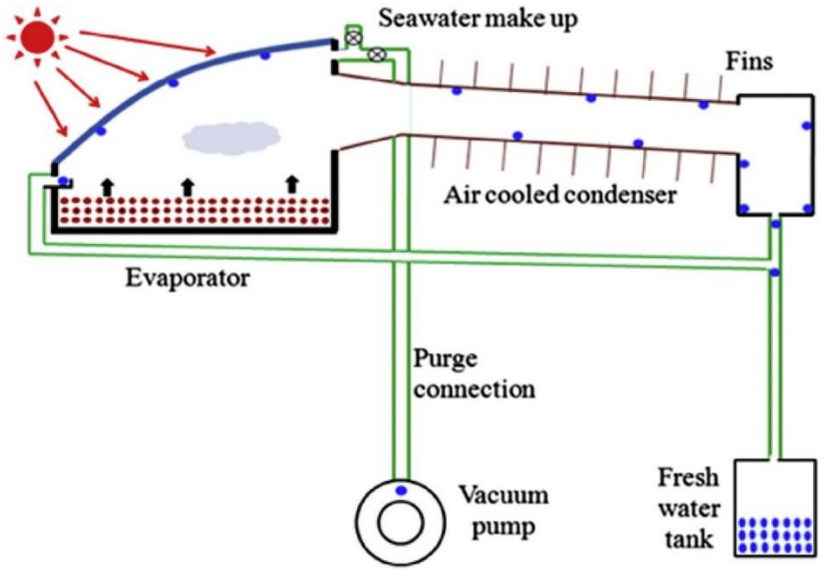

Figure 2. 25 The schematic diagram of the experimental setup (Ibrahim et al, 2015)

2.2.5 SD Systems with Cover Cooling

Another enhancement to the SD systems is by cooling down the cover of the SD system to increase the condensation rate. Some researchers increased the distillate yield of the SD system by lowering the temperature of the SD system cover using many techniques.

Gupta et al (2016) investigated experimentally the effect of attaching a water sprinkler with a constant discharge of (0.0001 kg/s) over the glass cover of a single-slope SD system. The dimensions of the SD system were; the basin= (1×1×0.1 m), the water depth= (5 cm), and the cover slope angle= (23°) which is equal to the latitude angle of the experiment location. The results showed an increase in daily productivity and the efficiency of the enhanced SD system by (20%) and (21%), respectively. The daily productivity was (2.940 l/m^2) and (3.541 l/m^2) for the conventional and the enhanced SD systems, respectively.

Somwanshi and Tiwari (2014) used cool water from a tank of an air cooler to flow over the cover of a single-slope SD system. According to the experimental data, the productivity and the efficiency of the SD system improved by (56.5%) and (9.9%), respectively. The results showed that the optimum flow rate of the cooling water over the cover of the SD system was (0.075 kg/s). Figure 2.26 shows the schematic diagram of the experimental setup.

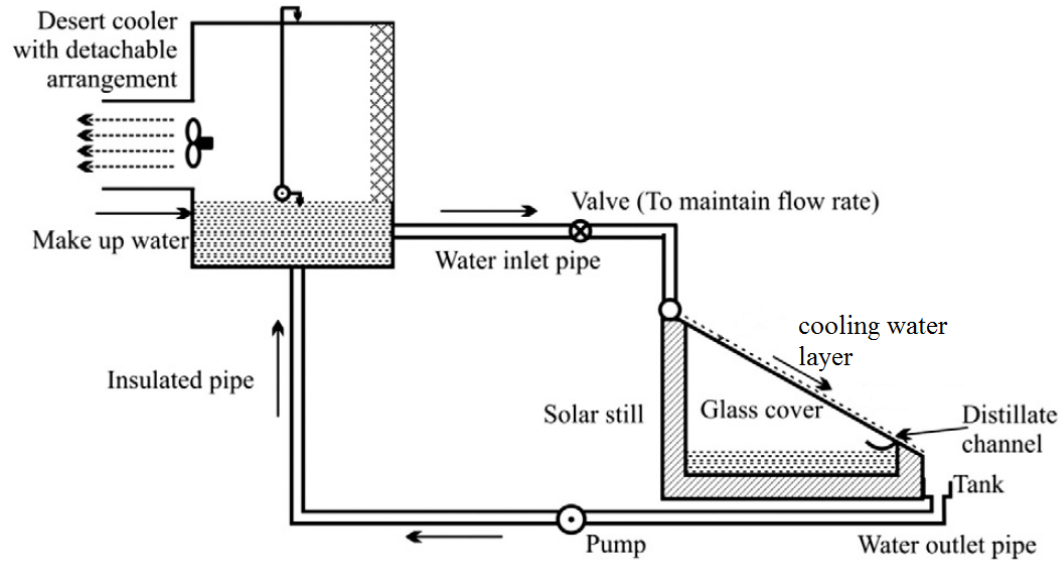

Figure 2. 26 The schematic diagram of the experimental setup (Somwanshi & Tiwari, 2014)

Sharshir et al (2017) investigated and compared the effects of four modifications on the performance of a single-slope SD system. The modifications were namely (A, B, C, and D) included: (A) adding nanoparticles (flake graphite) into the water, (B) adding nanoparticles plus PCM, (C) adding nanoparticles with cover cooling, and (D) adding nanoparticles plus PCM with cover cooling. The purpose of adding the nanoparticles into water is to increase the solar radiation absorbance and the thermal conductivity of the water, the PCM is to store latent heat thermal energy, and the cover film cooling is to decrease the cover temperature. The results showed improvement in the productivity of the SD system by (50.28% for the model A), (65% for the model B), (56.15% for the model C), and by (73.8% for the model D). Figure 2.27 shows the schematic diagram of the experimental setup.

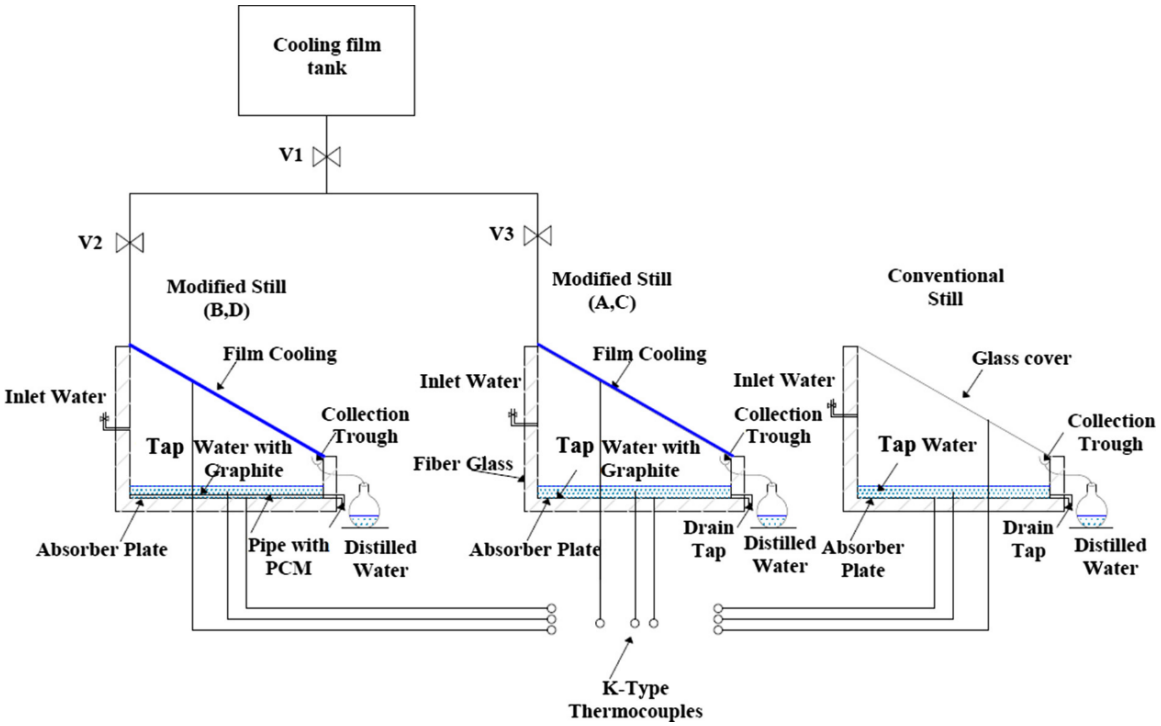

Figure 2. 27 The schematic diagram of the experimental setup (Sharshir et al, 2017)

Rahbar and Esfahani (2012) introduced a heat-pipe heat exchanger as surface cooler to the SD system. They tested their system experimentally for five days and they concluded that the maximum daily efficiency was 70% and the system has a potential for further developments. Figure 2.28 shows the schematic diagram of the experimental setup and Figure 2.29 shows the productivity and efficiency of the modified SD system.

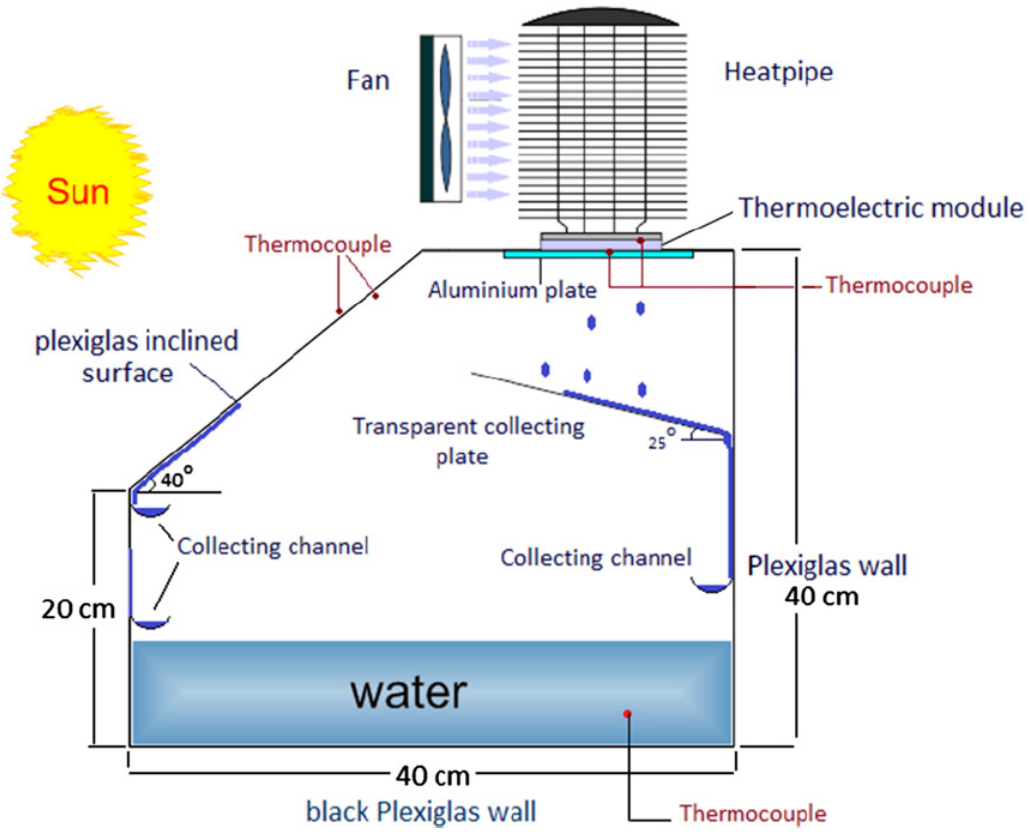

Figure 2. 28 The schematic diagram of the experimental setup (Rahbar & Esfahani, 2012)

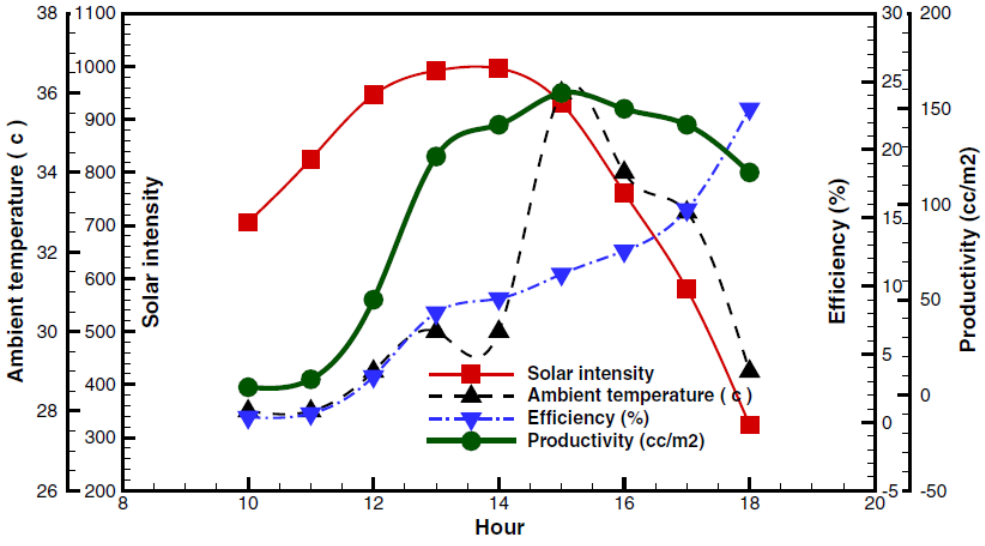

Figure 2. 29 The hourly variation of climatic conditions, productivity, and instantaneous efficiency in a typical day (8/2/2010) (Rahbar & Esfahani, 2012)

2.2.6 SD Systems with Extended Surfaces

Another improvement to the SD systems is by adding further surfaces in the water basin to increase the surface area of the evaporation hence enhance the evaporation rate. The idea behind this modification is also to increase the amount of the absorbed solar energy in addition to increasing the surface area of the evaporation, which leads to improving the SD system productivity. For this purpose, researchers used many kinds of extended surfaces such as; different kinds of fins, corrugated plates, perforated plates, wicks, wire meshes etc.

Omara et al (2011) studied experimentally the effect of adding fins and corrugated plate to the water basin of a single-slope SD system. The dimensions of the SD system were (0.5 m×2 m) and the water depth was (50 mm). The result showed that adding fins and corrugated plate into the basin of the SD system improved productivity by (40%) and (21%), respectively. Figure 2.30 shows the schematic diagram of the experimental setup and Figure 2.31 shows the accumulative yields for the different configurations of the SD system.

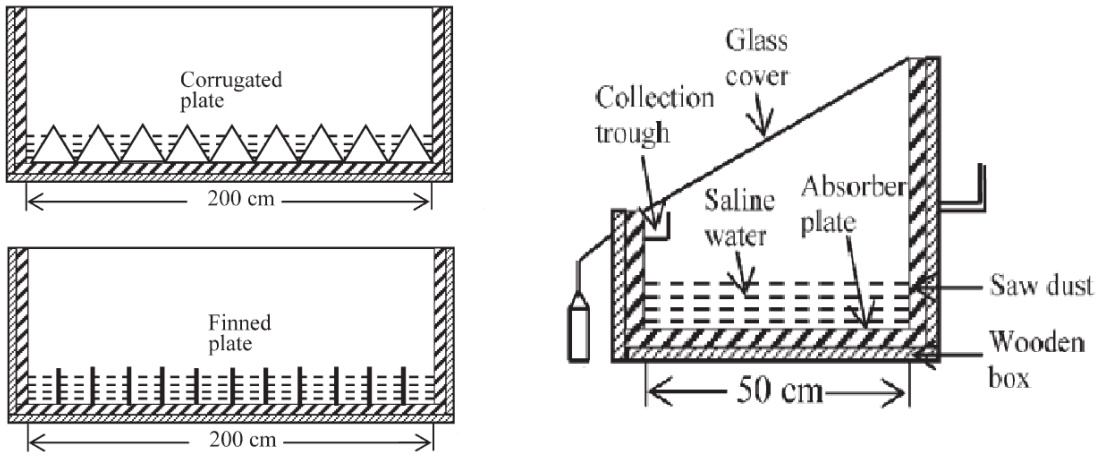

Figure 2. 30 The schematic diagram of the experimental setup (Omara et al, 2011)

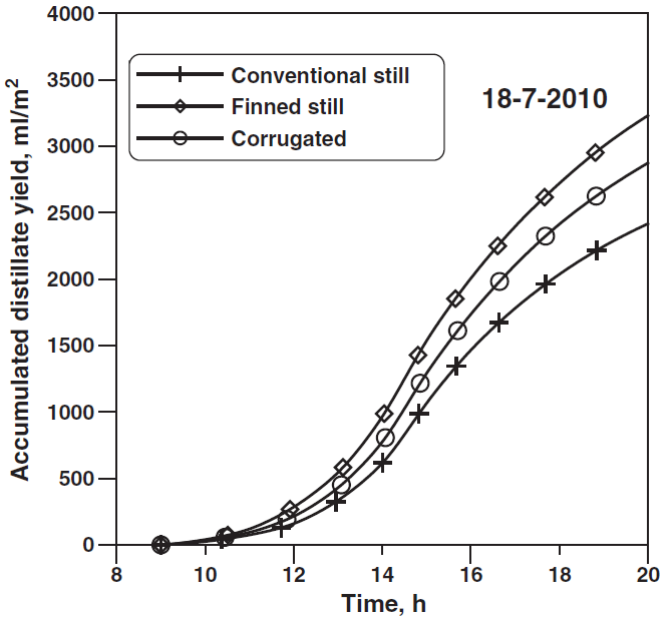

Figure 2. 31 The accumulative productivity of the conventional and enhanced SD systems (Omara et al, 2011)

Nafey et al (2002) studied experimentally the effect of adding a floating perforated black aluminium plate into the water basin of the SD system at different water depth (3, 4, 5, and 6 cm). The results showed that this enhancement was more effective with higher water depth. The distillate yield of the enhanced SD system was greater than the conventional SD system by up to (15%) at a water depth of (3 cm), and up to (40%) at a water depth of (6 cm).

Srivastava and Agrawal (2013a) used a floating water absorber porous material (blackened jute cloth) to increase the evaporation surface area. The results showed that the distillate yield of the SD system increased due to this enhancement by about (68%) and (35%) during clear days and cloudy days, respectively. They also investigated the effect of adding external reflectors and they achieved up to (79%) increase in productivity due to both enhancements; i.e. the floating absorber and the external reflectors. The results also showed that the depth of the water in the basin of the SD system had a slight effect on productivity when using the floating absorber. Figure 2.32 shows the schematic diagram of the experimental setup and Figure 2.33 shows the effect of the water depth in the basin of the SD system.

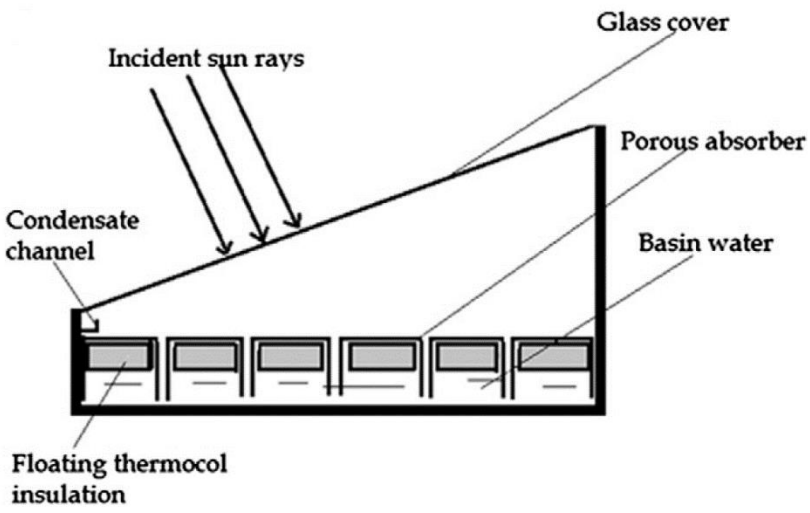

Figure 2. 32 The schematic diagram of the experimental setup (Srivastava & Agrawal, 2013a)

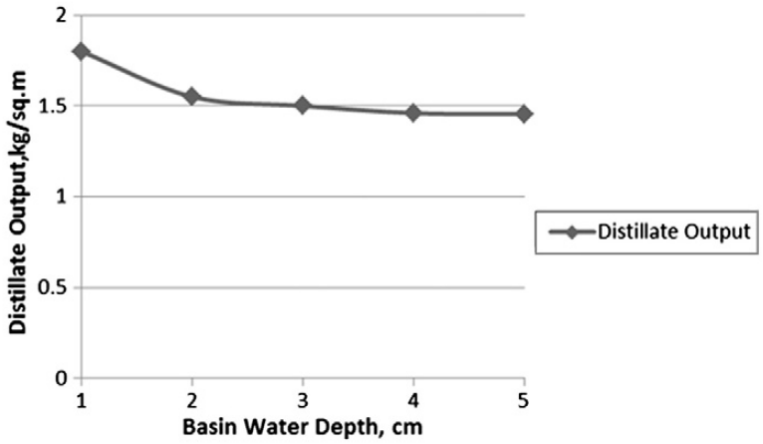

Figure 2. 33 The effect of the water depth in the basin of the enhanced SD system (Srivastava & Agrawal, 2013a)

Srivastava and Agrawal (2013b) also studied the effect of adding porous fins that extended from the base of the water basin to over the water surface on the SD performance. The porous fins made of blackened cotton rag. The results showed that the daily productivity of the enhanced SD system was higher by (15%) during May (summer) and by (48%) during February (winter) compared to the conventional SD system. The maximum achieved productivity was (7.5 kg/m^2) during May. Figure 2.34 shows the schematic diagram of the experimental setup and Figure 2.35 shows the accumulated productivity of the conventional and modified SD system during a typical day of winter and summer seasons.

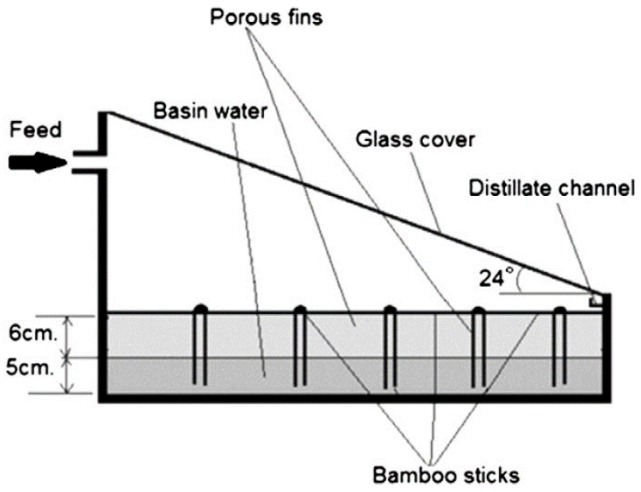

Figure 2. 34 The schematic diagram of the experimental setup (Srivastava & Agrawal, 2013b)

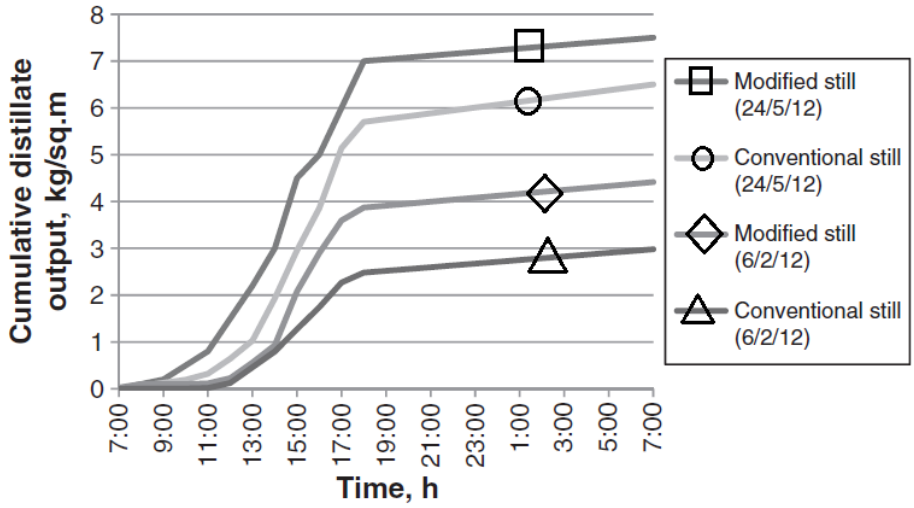

Figure 2. 35 The accumulative productivity of the modified and the conventional SD systems during summer (May) and winter (February) 2012 (Srivastava & Agrawal, 2013b)

Abu-Hijleh and Rababa'h (2003) investigated the effect of adding black coal, yellow sponge cubes, black sponge cubes, and black steel cubes into the water basin of the SD system. The results showed an increase in the SD system productivity about (18% - 73%) and the black sponge cubes was the most effective. The tested SD system dimensions were; the basin = (0.5×0.5 m), the cover slope angle = (23°), and the water depth (50 mm). Figure 2.36 shows the schematic diagram of the experimental setup.

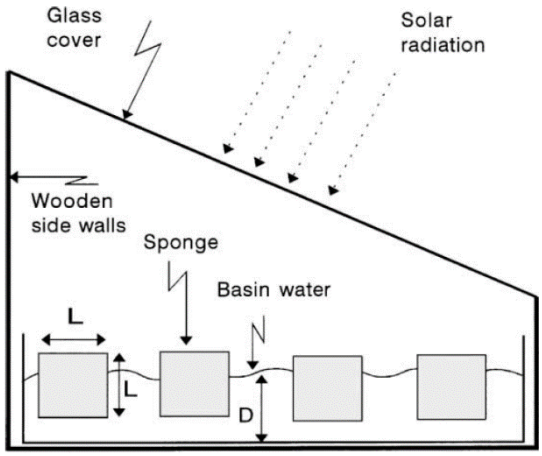

Figure 2. 36 The schematic diagram of the experimental setup (Abu-Hijleh & Rababa'h, 2003)

Sakthivel et al (2010) studied the effect of using jute cloth to extend the evaporation surface area. According to the results, the maximum improvement in the daily productivity of the modified SD system compared to the conventional SD system was (20%), and the maximum daily efficiency of the modified SD system was (52%), which was higher than the conventional SD system by (8%). Figure 3.37 shows the schematic diagram of the experimental setup.

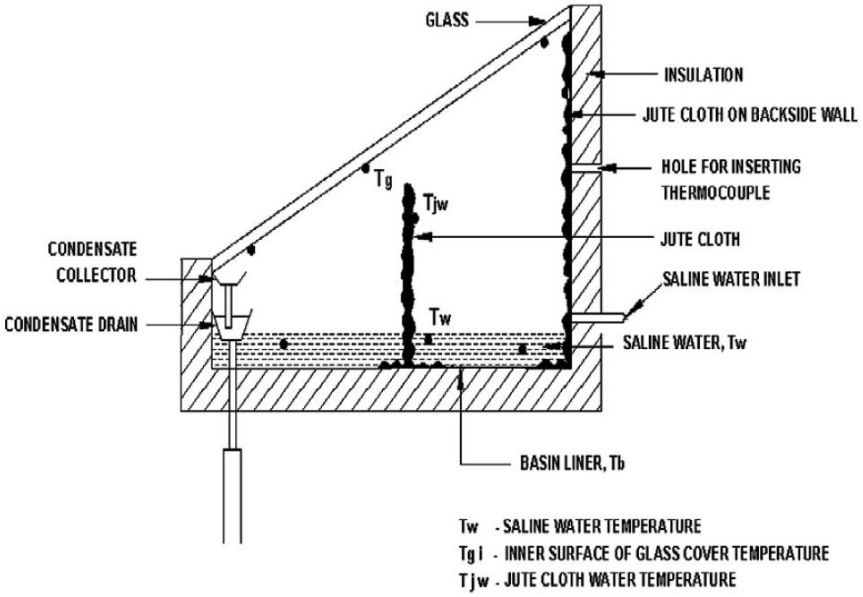

Figure 2. 37 The schematic diagram of the experimental setup (Sakthivel et al, 2010)

2.2.7 Other Improvements to the SD Systems

Abdallah and Badran (2008) employed a sun tracking system to enhance SD system productivity. They used a simple single-slope single basin SD system with the dimensions of (1m×1.2 m) and (32°) of the cover tilt angle. The results showed that the sun tracking system improved the daily productivity of the SD system by about (22%) higher than the fixed SD system. Figure 2.38 shows the difference in the hourly productivity of both the SD systems.

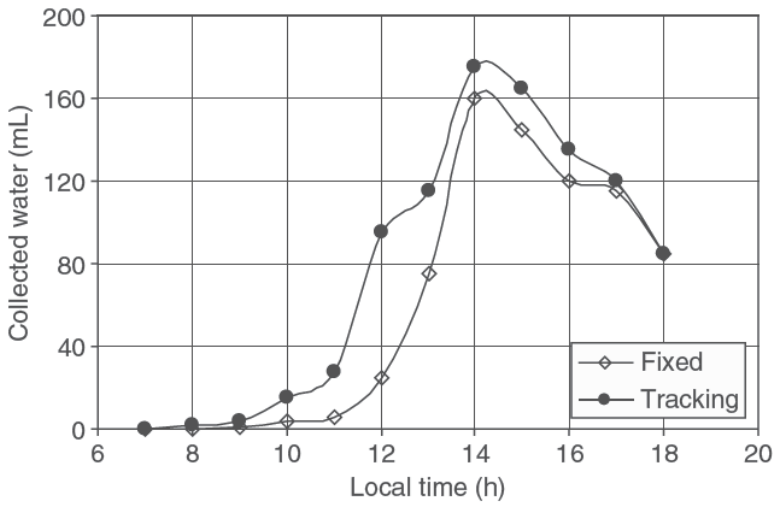

Figure 2. 38 The variation in the hourly productivity between the fixed and sun tracked SD systems (Abdallah & Badran, 2008)

Kianifar et al (2012) investigated the effect of adding fan inside a pyramid-shaped cover SD system. They found that during the summer season, the productivity of the SD system increased by (20%) due to using the fan, while the fan had an unnoticeable effect during the winter season. Figure 2.39 shows the schematic diagram of the experimental setup.

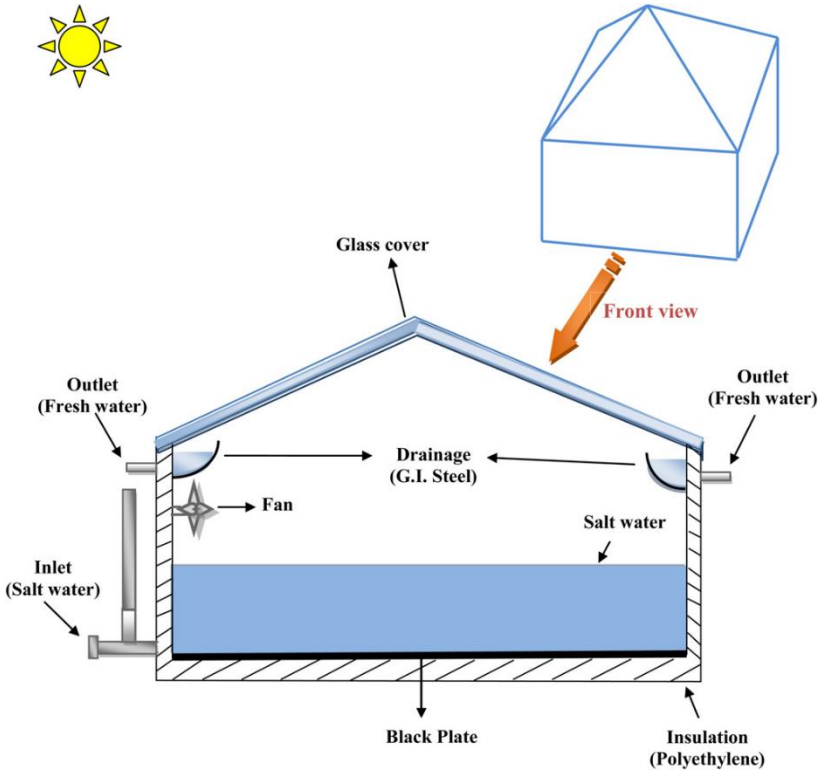

Figure 2. 39 The schematic diagram of the experimental setup (Kianifar et al, 2012)

Dev et al (2011a & 2011b) introduced an inverted absorber SD system and compared its performance to a conventional SD system. The results showed that the maximum daily productivity was (6.3 kg/m^2) and (4.15 kg/m^2) for the inverted SD system and the conventional SD system, respectively. The results also showed that the maximum daily efficiency was (34.6%) and (48%) for the inverted SD system and the normal SD system, respectively. They also studied the effect of the water depth, and they found that the optimal water depth was (3 cm). Figure 2.40 shows the schematic diagram of the experimental setup.

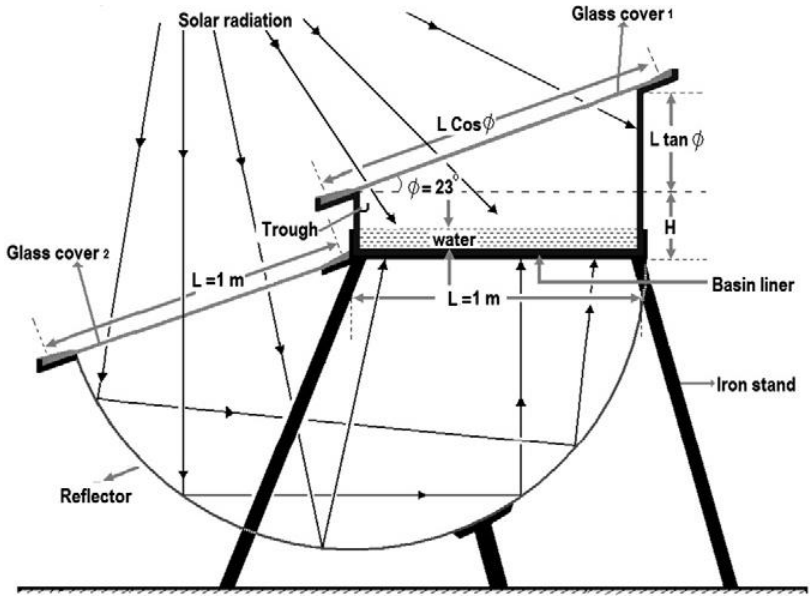

Figure 2. 40 The schematic diagram of the experimental setup (Dev et al, 2011b)

El-Agouz (2014) tested a single-slope stepped basin SD system with water circulation using a water pump. The results showed that the productivity of the modified SD system was higher than the conventional SD system by up to (48%), and the daily efficiency was higher by about (20%). Figure 2.41 shows the schematic diagram of the experimental setup.

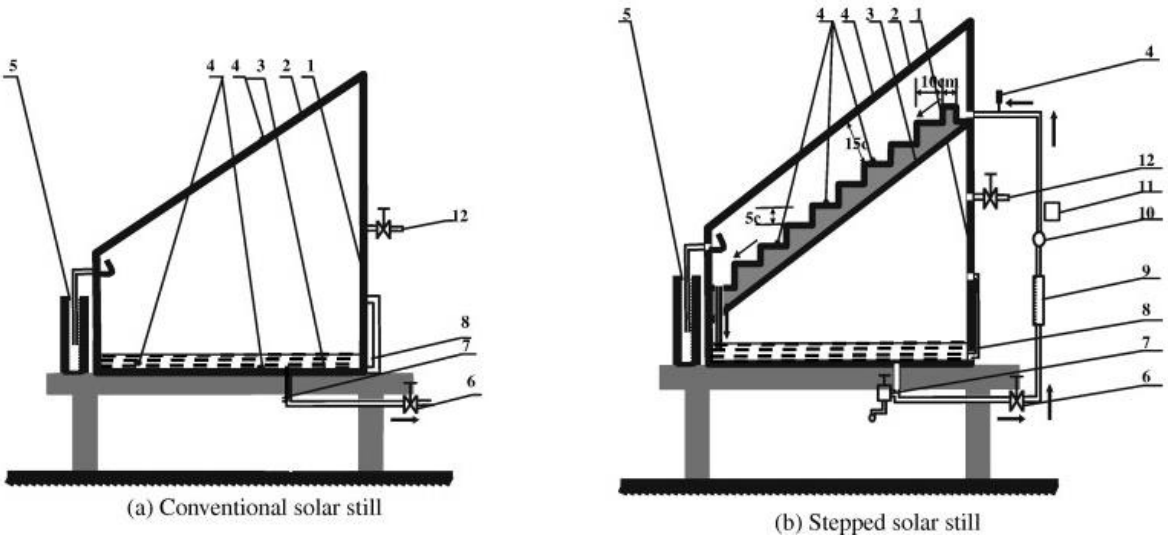

Figure 2. 41 The schematic diagram of the experimental setup. (1) Solar still frame, (2) glass cover, (3) absorber plate, (4) digital thermometer, (5) water vessel, (6, 12) control valve, (7) water drain, (8) graduate level, (9) flow meter, (10) water pump and (11) control timer (El-Agouz, 2014)

Al-Sulttani et al (2017) tested a Double-slope SD system with rubber scrapers on the cover inner-surface. The rubber scrapers are similar to windshield wiper blades. The purpose of the rubber scrapers is to collect the condensed water on the inner surface of the cover of the SD system allowing more light (solar energy) to be transmitted and preventing the condensed water from re-evaporating. The results showed that the average daily productivity was (4.24 l/m^2) and the productivity enhancement was about (63%) due to using the rubber scrapers enhancement. Figure 2.42 shows the schematic diagram of the experimental setup and Figure 2.43 shows the accumulated productivity of the conventional and the modified SD systems.

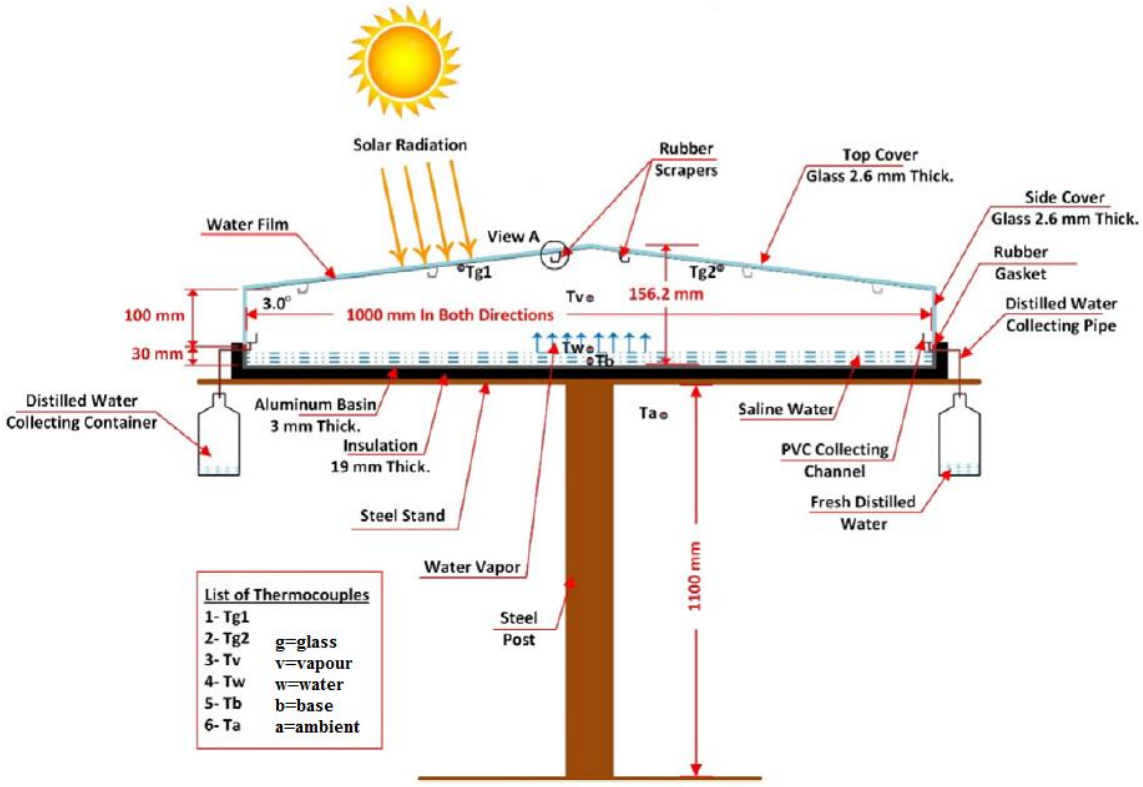

Figure 2. 42 The schematic diagram of the experimental setup (Al-Sulttani et al, 2017)

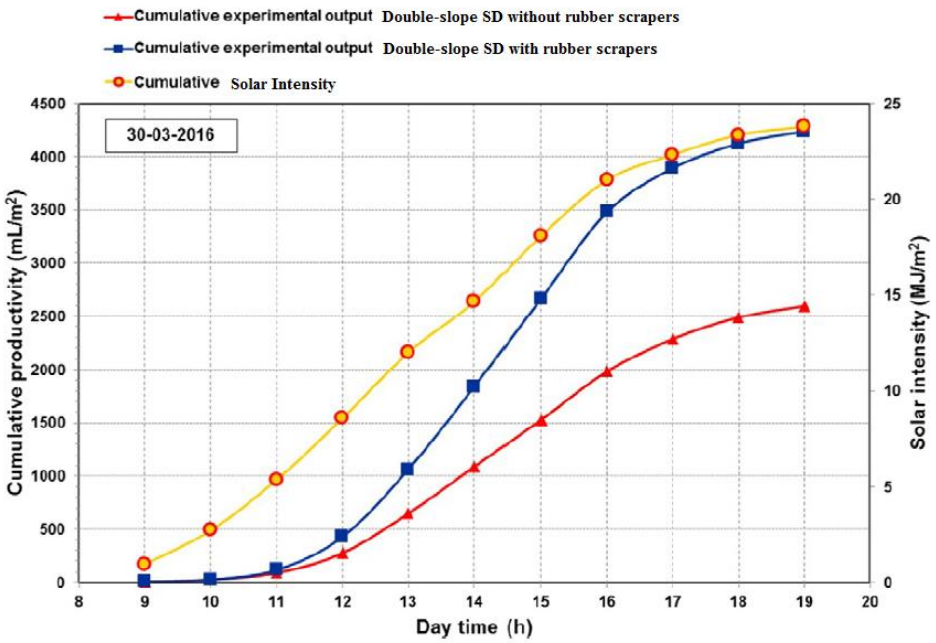

Figure 2. 43 The accumulative productivity of the conventional and modified SD systems (Al-Sulttani et al, 2017)

2.3 SD Systems Simulation

Due to the complexity of the evaporation-condensation phenomena involved in the SD systems, most previous work on the SD systems were experimental investigations. Only a few researchers had conducted a numerical simulation of the SD systems.

Setoodeh et al (2011) used CFD software (ANSYS CFX 11) to simulate the evaporation-condensation processes in a single-slope SD system to estimate the evaporation flow rate. For that purpose, they employed the volume of fluid (VOF) multiphase model with two phases; the water-liquid phase and the water-vapour phase. They did not include a turbulence model as they assumed a low evaporation rate. In addition, they assumed a steady-state condition, and they employed a quasi-steady analysis with constant temperature boundary conditions. They concluded that CFD is a powerful tool for the purpose of simulation and parametric analysis of SD systems. Figure 2.44 shows the contour of the water distribution on the cover of the SD system.

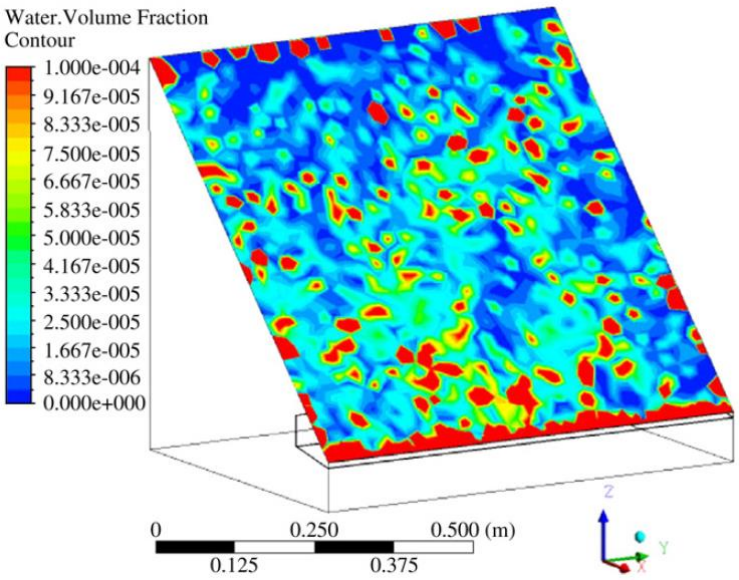

Figure 2. 44 The contour of the water volume fraction on the cover of the SD system (Setoodeh et al, 2011)

Rashidi et al (2018) employed a two-phase flow model using (ANSYS fluent) solver to simulate the evaporation-condensation problem occur in the SD system. They used the VOF multiphase model in two-dimensional (2D) geometry under steady state condition. The boundary conditions were; no heat flux from the walls, and constant temperature of 30° and 40° for the glass cover and the absorber plate, respectively. They did not include the solar radiation effect nor the turbulence flow. Figure 2.45 shows the contour of the water volume fraction in the SD system.

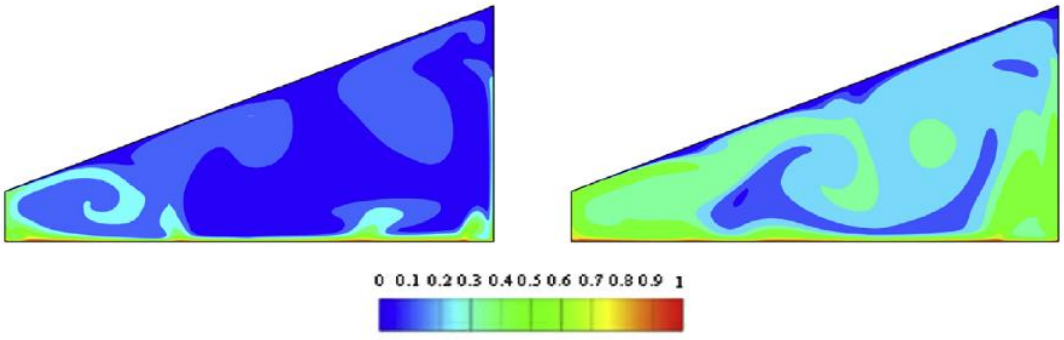

Figure 2. 45 The contour of the water volume fraction in the SD system (Rashidi et al, 2018)

Rahbar and Esfahani (2013) examined the capability of a two-dimensional simulation using ANSYS Fluent CFD software to estimate the SD system productivity. They compared the results of the CFD simulation with a well-known correlation (Dunkle's model) for the estimation of the daily yield of the SD system. They concluded that the CFD simulation was a successful tool to estimate the productivity of the SD system and in a good agreement with the available experimental results. They used steady-state, laminar flow, and assumed that the vapour is an incompressible ideal gas. For the boundary conditions, they assumed adiabatic walls and constant temperature for the cover and the bottom. Figure 3.46 shows the vapour mass fraction contour lines.

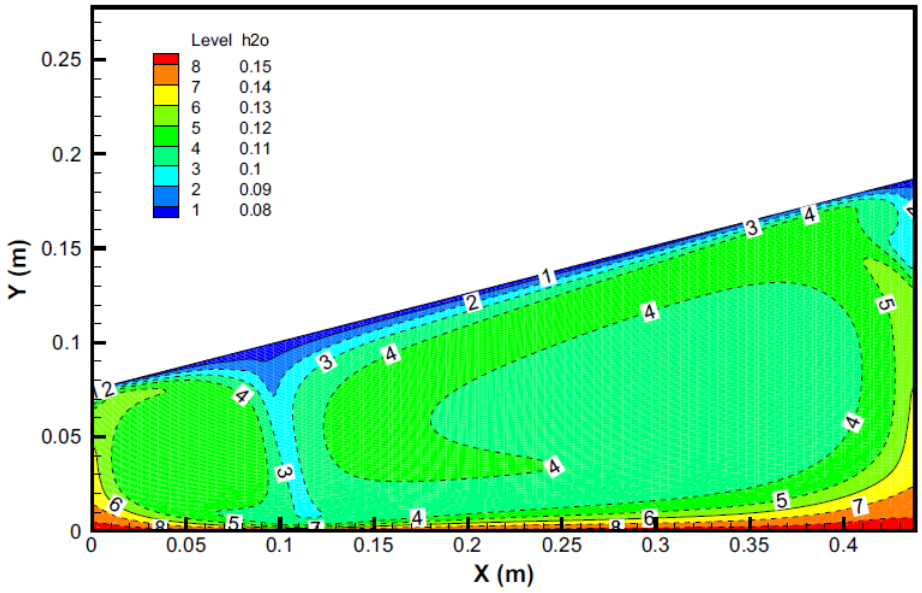

Figure 2. 46 The vapour mass fraction contour lines of the SD system (Rahbar & Esfahani, 2013)

Rahbar et al (2015) also investigated the distillate yield of a tubular SD system using CFD simulation. They employed two-dimensional analysis in (ANSYS fluent 14) CFD software. They assumed laminar flow, steady-state, and constant properties for the water and the vapour. The boundary conditions assumed to be constant temperature for the water and the vapour and adiabatic walls. They concluded that the accuracy of the results of the CFD simulation was about ±15% compared to the previous experimental work.

2.4 SD Systems Productivity and Cost

The main drawback of the SD system is the low productivity per unit area. The cost of the water produced by the SD system is not competitive with other traditional desalination methods; however, the use of the SD system is still feasible in some cases including in remote areas, on voyages, in small villages with low populations and in less developed. Due to the low levels of productivity, the cost of the distillate yield of the SD system is usually measured by USD per litre. The cost of the water produced by the SD systems depends on many factors, including the capital cost of the SD system, the average annual yield produced by the SD system, and the life span of the SD system. These parameters are also controlled by other factors such as the materials cost, quality and availability of the feedwater, the fabrication cost, the labour wages, and the common weather conditions in the region of use. Table 2.1 lists the average daily productivity, the capital cost, and the cost of the water produced by different types of SD systems that are found in the literature. The presented cost depends on the researchers' assumptions and estimations, the time of the study, and the country of the study and it may not reflect the actual cost. From the literature review, it is not easy to estimate accurately the water production or price of the water produced by SD systems without conducting experimental investigations.

Table 2. 1 The average daily productivity and cost of the SD systems found in the literature

Type of SD system and enhancements	***Country,***	***Average daily productivity (l/m2)***	***Capital cost ($USD)***	***Production cost ($USD/l)***
Single-slope cover, single basin with flat plate collector (Eltawil & Omara, 2014)	Egypt	6	427	0.053
Single-slope cover, single basin with evacuated tube collector (Mamouri et al, 2014)	Iran	6.3	160	0.019
Single-slope cover, single basin with evacuated tube collector (Kumar et al, 2014)	India	3.8	381	0.075
Single-slope cover, triple basin, evacuated with flat plate collector (Ahmed et al, 2009)	Malaysia	9	1100	0.09
Single-slope cover, single basin with shallow solar pond (El-Sebaii et al, 2008)	Egypt	4.5	320	0.052
Single-slope cover, single basin with sponge and solar pond (Velmurugan & Srithar, 2007)	India	3.2	350	0.08
Single-slope cover, single basin with solar concentrator (Abdel-Rehim & Lasheen, 2007)	Egypt	3.8	300	0.058
Single-slope cover, single basin with solar collector (Badran & Al-Tahaineh, 2005)	Jordan	3.1	480	0.115

Type of SD system and enhancements	***Country,***	***Average daily productivity (l/m2)***	***Capital cost ($USD)***	***Production cost ($USD/l)***
Single-slope cover, single basin with fins and solar pond (Appadurai & Velmurugan, 2015)	India	3	310	0.076
Single-slope cover, single basin with fins (Velmurugan et al, 2008a)	India	2.8	200	0.054
Single-slope cover, single basin with fins and wick (Velmurugan et al, 2008b)	India	2.8	250	0.065
Single-slope cover, single basin with PCM and wick (Shalaby et al, 2016)	Egypt	3.3	238	0.095
Single-slope cover, single basin with PCM (Kabeel & Abdelgaied, 2016)	Egypt	3.5	165	0.032
Single-slope cover, single basin with PCM (Ansari et al, 2013)	Morocco	3	245	0.06
Single-slope cover, Stepped basin with pebbles (Velmurugan et al, 2009)	India	3.3	160	0.072
Single-slope cover, Stepped basin with reflectors (Omara et al, 2014)	Egypt	5.1	240	0.031
Single-slope cover, single basin, vacuum with external condenser (Ibrahim et al, 2015)	Egypt	2.5	195	0.041
Single-slope cover, single basin, nanoparticles with external condenser and vacuum fan (Kabeel et al, 2014b)	Egypt	6	268	0.022
Double-glass cover, single basin with separate condenser (El-Bahi & Inan, 1999b)	Turkey	4.3	350	0.06
Single-slope cover, single basin with cover cooling (Rahbar & Esfahani, 2012)	Iran	4.1	181	0.27
Hemispherical cover with cover cooling (Arunkumar et al, 2012)	India	4.2	165	0.041
Single-slope cover, single basin with fins and corrugated plate (Omara et al, 2011)	Egypt	3.5	122	0.03
Pyramidal cover, concave basin with wick (Kabeel, 2009)	Egypt	4.1	145.5	0.065
Triangular cover (Ahsan et al, 2014)	Malaysia	4.1	35	0.017
Tubular cover (Ahsan et al, 2012)	Japan	5	355	0.105
Hemispherical cover (Ismail, 2009)	Canada	4	958	0.18
Pyramidal cover (Fath et al, 2003)	Egypt	2.9	99.5	0.016
Single-slope cover, stepped basin with water circulation (El-Agouz, 2014)	Egypt	5.2	300	0.035
Single-slope cover, single basin with inverted absorber (Dev et al, 2011b)	Oman	4	165	0.031
Single-slope cover, single basin with sun tracking (Abdallah & Badran, 2008)	Jordan	1.25	282	0.167
Single-slope cover, Stepped basin with sun tracking (Abdallah et al, 2008)	Jordan	3.7	350	0.071

2.5 Conclusions Drawn From the Literature

After conducting an intense literature review of numerous previous studies on the Solar Still Desalination (SD) Systems, the following conclusions were drawn:

1. Due to the complexity of the evaporation-condensation phenomena involved in the SD systems, most previous research on the SD systems were experimental investigations, very few studies were theoretical or mathematical models based upon experimental correlations, and far fewer studies used numerical methods such as CFD simulation. In this study, both CFD simulation and experimental investigations will be conducted to compare the results and to evaluate the performance of the SD systems. The present study will test the reliability of the numerical simulation and the possibility of using it for the purpose of optimisation. The experimental investigation is essential to estimate the cost of the SD systems and the price of the water produced by those systems. The experimental investigation is also important and necessary to validate the computational results.
2. Since the productivity of the SD systems is low, the purpose of most of the previous research was to increase the distillate yield or the productivity of the SD systems. Improving the SD systems' productivity was achieved by many means as follows:
    i. **Increase the evaporation rate:** this was done using four methods; by increasing the brackish water temperature using heaters, solar collectors, and heat exchangers, or by extending the surface area of the evaporation using fins and wicks, or by increasing the solar gain using reflector surfaces, or by storing the solar heat using storage materials.
    ii. **Increase the condensation rate:** this was done using two approaches; by decreasing the cover temperature using film cooling, or by using an external condenser.
    iii. **Enhance the thermo-optical properties of brackish water:** by adding dyes and/or nanoparticles to improve the thermal conductivity and the solar radiation absorption of the brackish water
    iv. Some researchers combined two or more enhancements to the SD system or introduced new designs such as multi-stage SD systems.

3. According to the literature review, extending the evaporation surface enhancement to improve the productivity of the SD systems seems to be a promising enhancement and it will be employed in this research. Since the evaporation occurs from the water surface, extending the surface area of the evaporation enhances the productivity of the SD system.
4. According to the literature review, most previous studies were for SD systems with stagnant or still water in their basins. In the current study, a rotational movement will be introduced to the water in the basin of the SD system.
5. **The research gap:** According to the literature survey, an important research gap is to find a novel, simple, and inexpensive technique to enhance the productivity of the SD systems with retaining the simplicity of those systems and the low cost of the water production. From the previous points (3 and 4), the research gap is to study the effects of combining two enhancements; generating a water movement in the basin and increasing the surface area of the water evaporation. For this purpose, semi-immersed revolving tubes that are wrapped in an absorbent substance will be introduced to the water basin of the SD system.
6. According to the literature review, it is not easy to estimate accurately the size of the water production or the price of the water produced by the SD systems without conducting experimental investigations.
7. To design the NSD system and then the MSD system, the following parameters were found to be useful to consider to achieve the best design possible for the preliminary investigations:
    i. **The cover slope angle:** According to references Khalifa (2011); Sarray et al (2017); and Velmurugan and Srithar (2011), the cover tilt angle was preferred to be equal to the latitude of the geographical location. The previous research used slope angle from 10° to 40°. In the current study, a tilt of 27.5° will be considered.
    ii. **The cover thickness:** According to references Dimri et al (2008); Panchal and Shah (2012); and Sarray et al (2017), less cover thickness was preferable to decrease the heat stored in the cover; however, the cover should be durable and capable to resist the weather conditions. In this study, 3 mm thick cover will be considered.

iii. **The water depth:** According to Khalifa and Hamood (2009); Panchal and Patel (2017); Sarray et al (2017); and Tiwari and Tiwari (2006), less depth increased the day productivity; however, higher depth enhanced the nightly productivity. The previous research used water depth from 10 mm to 70 mm. In this study, a depth of 40 mm will be considered.

iv. **The basin material:** According to Malaiyappan and Elumalai (2016), the aluminium sheet was superior to other materials due to its good thermo-physical properties and using it led to enhanced productivity. In this study, a 3 mm aluminium sheet will be used for the basin of the SD systems.

v. **The cover type:** According to Edalatpour et al (2016); Rajaseenivasan and Murugavel (2013); and Tiwari and Sahota (2017), the double-slope cover was preferable than the single-slope cover and will be considered in this study.

3 Chapter Three: CFD Simulation

The working principle of the Solar Still Desalination (SD) System is an Evaporation-Condensation process under the aid of solar radiation. The saline water is heated using solar energy to produce water vapour that is condensed to produce freshwater. The Evaporation-Condensation process is a transient heat transfer, mass transfer, and phase change phenomenon. In this chapter, modelling and simulating the proposed MSD and NSD systems and the theoretical background are described.

3.1 Theoretical Background

The purpose of using the SD system is to produce freshwater from salty water as happens in the hydrologic cycle or the natural water cycle, where seawater evaporates due to the solar radiation producing clouds that give freshwater through the rain. Engineers apply the same principle in the distillers or the SD systems design.

The brackish water in the water basin of the SD system heats up by absorbing the transmitted solar radiation through the transparent cover. The brackish water evaporates due to the increase in its temperature; the vapour condenses on the inner surface of the cover due to the temperature difference between the vapour temperature and the cover temperature producing freshwater, and the condensed freshwater trickles down into a discharge channel due to the gravity and the cover tilt angle.

The performance of the SD system depends on how much solar energy gets absorbed by the system and used efficiently in the water evaporation process. According to Malik et al. (1982), the evaporation process in the SD systems uses only about one-third of the total daily solar exposure. The rest of the solar energy is wasted due to the solar reflection and heat losses to the environment (Tiwari, 2002). Figure 3.1 shows the main heat transfer modes in the SD system adopted from (Sahota & Tiwari, 2016).

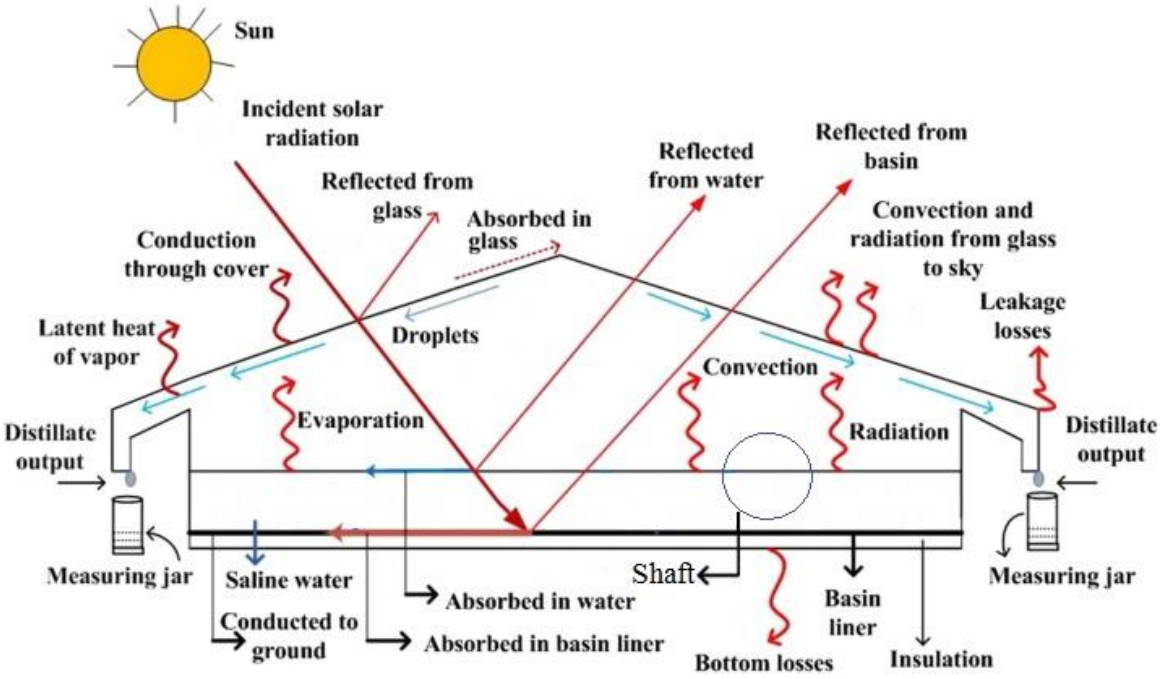

Figure 3. 1 The main heat transfer in the SD system adopted from (Sahota & Tiwari, 2016)

The energy balance on the water in the basin of the SD system, can be written as;

$$A_s\, G\tau_c\alpha_w + W_s = A_s[\dot{q}_{ev} + \dot{q}_{r_{w-c}} + \dot{q}_{c_{w-c}} + \dot{q}_{k_{w-b}}] + m_w\, \dot{q}_{s_w} \qquad (3.1)$$

Where;

A_s is the surface area of the SD system in (m^2)

G is the solar radiation or the insolation in $(kW/m^2 \equiv kJ/m^2.day)$

τ_c, α_w are the transmittance of the cover and the absorbance of the water, respectively

W_s is the shaft work (for the modified model) in $(kW \equiv kJ/day)$

$\dot{q}_{ev}$ is the evaporation heat transfer flux in $(kW/m^2 \equiv kJ/m^2.day)$

$\dot{q}_{r_{w-c}}$, $\dot{q}_{c_{w-c}}$ are the radiation and convection heat transfer flux (from the water to space above the water surface) in $(kW/m^2 \equiv kJ/m^2.day)$, respectively

$\dot{q}_{k_{w-b}}$ is the conduction heat transfer flux (from the water through the base) in $(kW/m^2 \equiv kJ/m^2.day)$

$\dot{q}_{s_w}$ is the heat stored in the water in $(kJ/kg.day)$.

m_w is the water mass in the basin in (kg)

Figure 3.2 shows the thermal network of the SD system

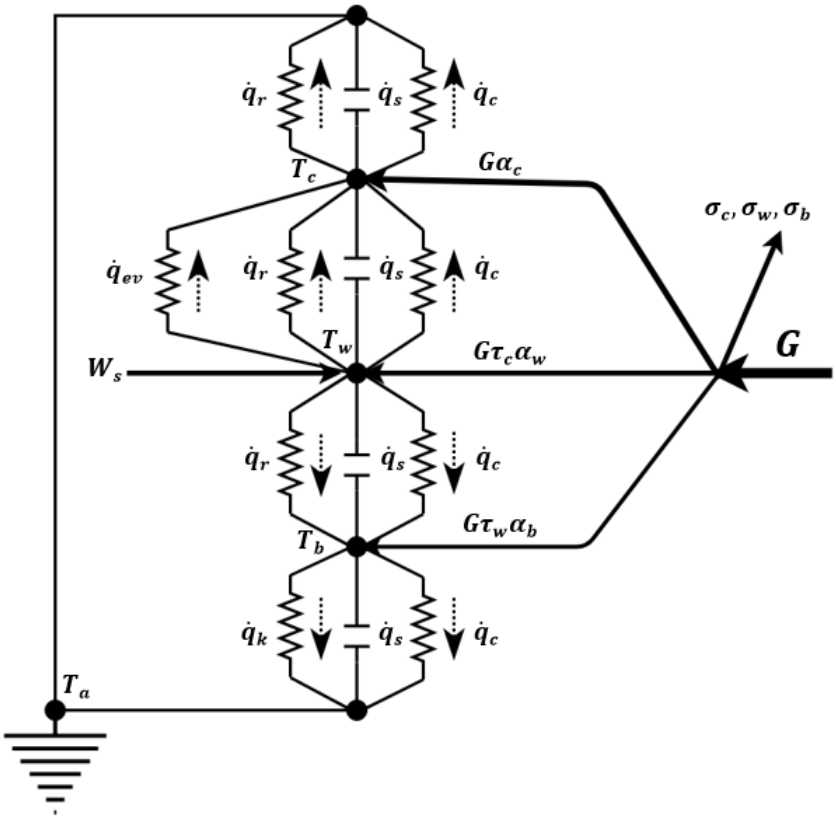

Figure 3. 2 The schematic diagram of the thermal network of the SD system

Where G is solar radiation, $\dot{q}_{ev}, \dot{q}_c, \dot{q}_r, \dot{q}_k, \dot{q}_s$ are the heat transfer by evaporation, convection, radiation, conduction, and the heat stored, respectively. T_w, T_c, T_b, T_a are the temperature of the water, cover, basin, and ambient, respectively. σ, τ, α are the reflectance, absorptance, and transmittance, respectively,

In the SD systems, evaporation rate reflects in somehow the condensation rate as well. The condensation rate represents the distillate yield of freshwater produced by the SD system, which is also referred to as the hourly or daily productivity of the SD system. The distilled yield of the SD system per unit time per unit area $(kg/m^2.day)$ can be expressed as;

$$\dot{m}_e = \frac{\dot{q}_{ev}}{L_v} \qquad (3.2)$$

Where $\dot{q}_{ev}$ is the evaporation heat transfer and L_v is the latent heat of evaporation in (kJ/kg)

The instantaneous thermal efficiency (η_i) of the SD system at any time is defined as the ratio of evaporation heat transfer $(\dot{q}_{ev})$ to the total solar radiation applied on the system (G);

$$\eta_i = \frac{\dot{q}_{ev}}{G} = \frac{\dot{m}_e L_v}{G} \quad (3.3)$$

This efficiency is usually integrated over some extended period to indicate long-term performance, i.e. day or month (Duffie & Beckman, 2013).

As can be noticed to estimate the productivity of the SD system from equation (3.2) and to estimate the efficiency of the SD system from equation (3.3), the challenging part is how to estimate the value of the evaporation heat transfer ($\dot{q}_{ev}$). Dunkle (1961) proposed the first empirical correlations to estimate the evaporation heat transfer coefficient (h_{ev}) from which we can estimate the evaporation heat transfer. Dunkle model has been extensively used by researchers since then until now for a rough estimation of the SD system yield (Al-Sulttani et al, 2017). However, Dunkle model has some limitations such as; it is based on low operating temperature (approximately 50℃), and low cover tilt angle (approximately 10°), and it is independent of the dimensions and the internal cavity of the SD system (Rahbar & Esfahani, 2013). These limitations lead to underestimating or overestimating the distilled yield by about $\pm 30\%$ when applied to the SD systems with a different temperature range and/or different design parameters (Dwivedi & Tiwari, 2009). Dunkle used the experimental data and the linear regression analysis to estimate the evaporation heat transfer ($\dot{q}_{ev}$) as follows,

$$\dot{q}_{ev} = h_{ev} A_s (T_w - T_c) \quad (3.4)$$

Where T_w and T_c are the temperature of the water (w) and the cover (c), respectively, A_s is the surface area of the water in the SD system, and h_{ev} is the evaporation heat transfer coefficient which can be expressed as (Al-Sulttani et al, 2017),

$$h_{ev} = 0.01623 \; h_c \frac{P_w - P_c}{T_w - T_c} \quad (3.5)$$

By substituting equation (3.5) in equation (3.4);

$$\dot{q}_{ev} = 0.01623 \; h_c A_s (P_w - P_c) \quad (3.6)$$

Where P_w and P_c are the saturation pressure at the water temperature T_w and cover temperature T_c, respectively, and (h_c) is the convection heat transfer coefficient, which can be found from the following relation;

$$Nu = \frac{h_c \; l}{k} = C(Ra)^n \quad (3.7)$$

Where (Nu) is the Nusselt number, which is a dimensionless number, it reflects the ratio of convective (h_c) to conductive (k) heat transfer, and (l) is the characteristic length or the vertical length from the water surface to the cover,

Parameters (C) and (n) are dimensionless constants which can be found from the experimental data regression analysis (in Dunkle model $C = 0.075$ and $n = {}^{1}/_{3}$). These values can be modified accordingly to the experimental data to better fit with the design parameters and the weather conditions,

(Ra) is the Rayleigh number, which is a dimensionless number used in the calculation of natural convection, defined as the product of Grashof Number (Gr) and Prandtl Number (Pr), and can be expressed as;

$$Ra = Gr\ Pr = \frac{Bouyancy\ force}{Viscous\ force} \cdot \frac{Viscous\ diffusion}{Thermal\ diffusion} = \frac{g\ \beta\ l^3\ \Delta T}{\nu\ \alpha} \qquad (3.8)$$

Where (g) is the acceleration due to gravity, (β) is the coefficient of thermal expansion of the vapour, ΔT is temperature difference, (ν) is the kinematic viscosity, and (α) is the thermal diffusivity of the vapour.

The convection heat transfer coefficient in the SI unit can be expressed in terms of temperatures as follows (Al-Sulttani et al, 2017);

$$h_c = 0.884\ \left[(T_w - T_c) + \left(\frac{(P_w - P_c)}{268900 - P_w}\right) T_w\right]^{\frac{1}{3}} \qquad (3.9)$$

Where

$$P_w = e^{\left(25.317 - \frac{5144}{T_w}\right)} \qquad (3.10)$$

$$P_c = e^{\left(25.317 - \frac{5144}{T_c}\right)} \qquad (3.11)$$

From the previous description, the evaporation-condensation problem implicated in the SD system problem is a complex phenomenon and cannot be solved theoretically. It can only be solved through empirical correlations verified by experimental tests or through numerical simulation as will be described in the following sections.

3.2 CFD Software

Computational Fluid Dynamics (CFD) is a branch of fluid mechanics that uses numerical analysis to solve and analyse problems that involve fluid flows. CFD has become an indispensable tool for engineering. Advances in CFD algorithms have increasingly enabled the simulation of complex flow phenomena. Furthermore, advances in high-performance computing (HPC) have significantly reduced the running time for complex simulations (Löhner, 2008).

To perform a numerical simulation, CFD software is required. The ANSYS-Fluent solver is well-known general-purpose CFD software based on the Finite Volume Method (FVM) and includes numerous codes that have been written in C computer language. The FVM is a numerical method to solve partial differential equations in the form of algebraic equations. The advantages of the FVM over other numerical methods are: it does not require a structured mesh; boundary conditions can be applied noninvasively because the values of the conserved variables are located within the volume element, not at nodes or surfaces; and it is powerful on non-uniform grids and in calculations where the mesh moves or track interfaces (Versteeg & Malalasekera, 2007). ANSYS-Fluent is a very powerful tool that can model and simulate a wide range of different engineering problems. ANSYS-Fluent solves the governing partial differential equations for the conservation of mass, momentum, and other scalars such as energy and turbulence equations in integral form and provides comprehensive modelling capabilities of steady-state or transient analyses for a wide range of compressible, incompressible, laminar, and turbulent fluid flow problems. Another very useful group of models included in ANSYS-Fluent is the multiphase flow models, which can be used for the analysis of gas-liquid, or solid-fluid flows problems (Fluent, 2017).

The following sections describe systematically the process of the numerical simulation using the ANSYS- Fluent software.

3.3 Models Design and Mesh

The first step of any CFD simulation is to determine the domain under study. Three-Dimensional (3D) geometry of the SD system has been sketched. This was done by using SpaceClaim DesignModeler SCDM version 18.1. Then, the geometry was imported into ANSYS 19.1 software. The proposed design of the SD system has a double-sloped glass cover with 27.5^{o} tilt angle from the two sides, the water basin dimensions are 800×600×100 mm, and the water depth is assumed to be 40 mm. Two SD systems have been created, the NSD system and the MSD system. The Two SD systems have the same design and dimensions except for the modification in the MSD system, which includes three symmetrical and parallel revolving tubes laying horizontally into the water basin. The tubes diameter is 90 mm, and their centre is 60 mm above the basin base in which the tubes are semi-immersed into the water. The centre to centre distance between the tubes is 200 mm. The SD systems have two channels on both sides to collect the condensed water trickling down from the slopped cover due to the gravitational force. The SD system also has one inlet tube to get the brackish water into the basin and to compensate for the evaporated amount of the water during the evaporation process. The inlet tube and the outlets' tubes have the same cross-sectional area, which is 707 mm^2. Figure 3.3 represents the 3D model of both NSD and MSD systems under study.

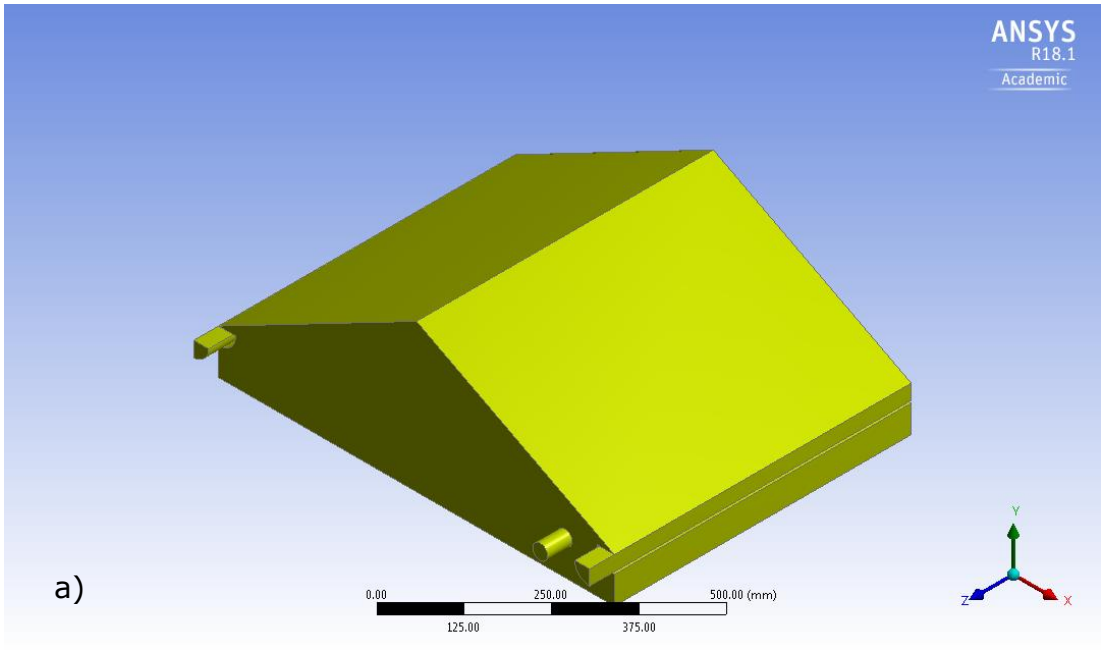

a)

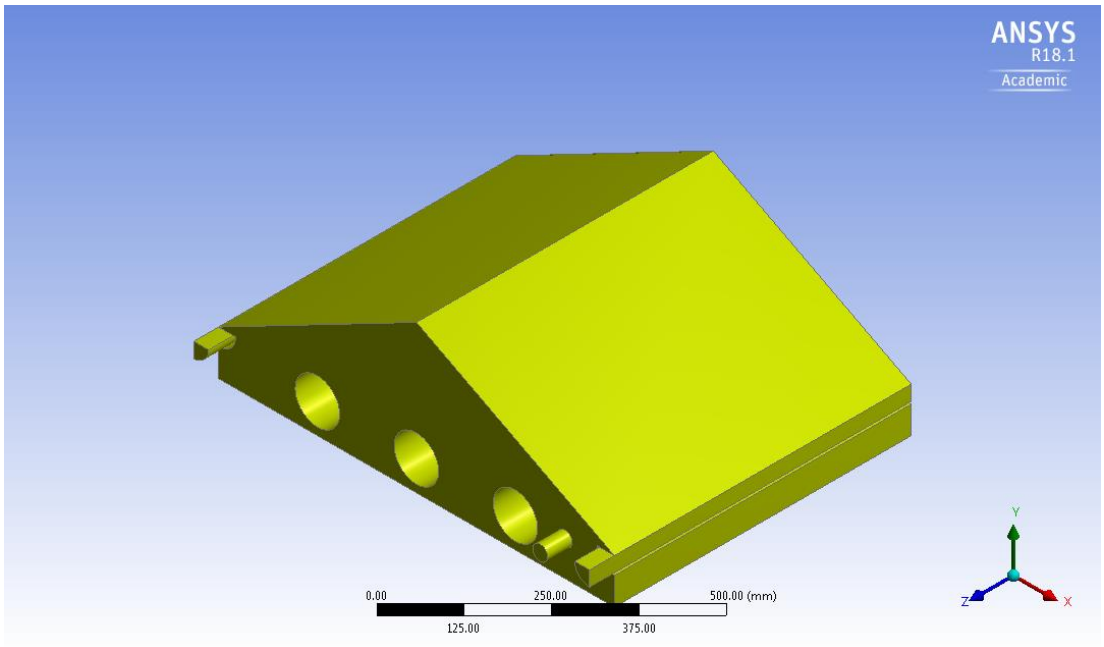

Figure 3. 3 The three-dimensional models of the a) NSD system b) MSD system

The next step is to generate a computational grid or mesh in the domain. The mesh is one of the most important steps of any CFD simulation. A good mesh can solve significantly faster and provide results that are more accurate. For 3D geometries, ANSYS-Fluent offers two main meshing methods, Tetrahedrons and Hexahedrons, depending on the element type (cell shape). As shown in Figure 3.4, the tetrahedral element has four faces and four nodes, and the hexahedral element has six faces and eight nodes. The Tetrahedrons meshing method has many advantages over the Hexahedrons meshing method such as; easy to mesh complex geometries, easy to achieve better mesh qualities, and much fewer nodes for the equivalent number of elements in the case of hexahedral which means less computational effort, faster solution, and results that are more accurate.

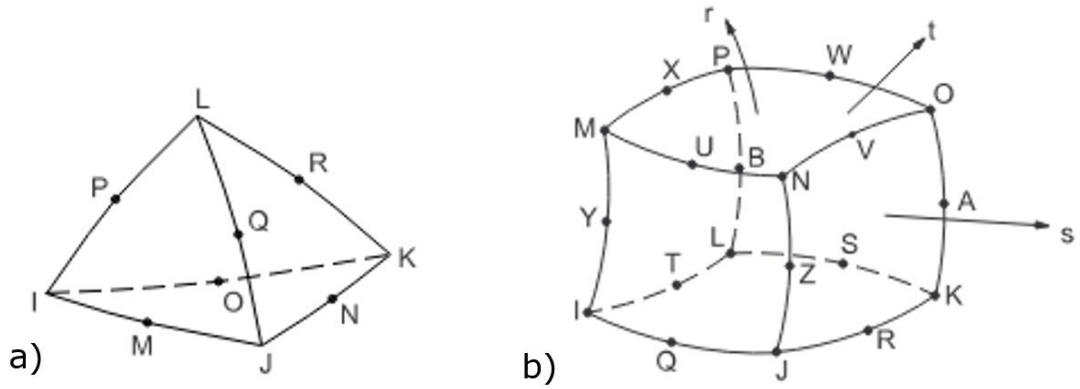

Figure 3. 4 The mesh element types a) Tetrahedral element b) Hexahedral element

The unstructured mesh has been created for the geometries using ANSYS Workbench and Fluent solver. The Tetrahedrons meshing method has been used to both geometries resulting in 138172 Elements (cell) and 27559 Nodes to the NSD system and 160446 Elements and 32590 Nodes to the MSD system.

The quality of the mesh plays a significant role in the accuracy and stability of the numerical computation. The main attributes associated with mesh quality are orthogonal quality and skewness (Fluent, 2017). The orthogonal quality represents a normalization of the cell faces and the skewness determines how much the cell faces are distorted from the standard shape. Figure 3.5 presents the criteria of the mesh quality for the skewness and the orthogonality (Fatchurrohman & Chia, 2017).

Skewness mesh metrics spectrum:

Excellent	Very good	Good	Acceptable	Bad	Unacceptable
0-0.25	0.25-0.50	0.50-0.80	0.80-0.94	0.95-0.97	0.98-1.00

Orthogonal Quality mesh metrics spectrum:

Unacceptable	Bad	Acceptable	Good	Very good	Excellent
0-0.001	0.001-0.14	0.15-0.20	0.20-0.69	0.70-0.95	0.95-1.00

Figure 3. 5 The mesh quality criteria (Fatchurrohman & Chia, 2017)

The mesh quality for both geometries is very good according to the mesh quality definition given above. The average mesh orthogonal quality was about 0.86, where the scale is (0 to 1), and 1 refers to the highest (perfect) quality. The average mesh

skewness is 0.23, where the scale is (0 to 1), and 1 refers to a high skewed (poor) mesh. Figure 3.6.shows the mesh for both SD systems.

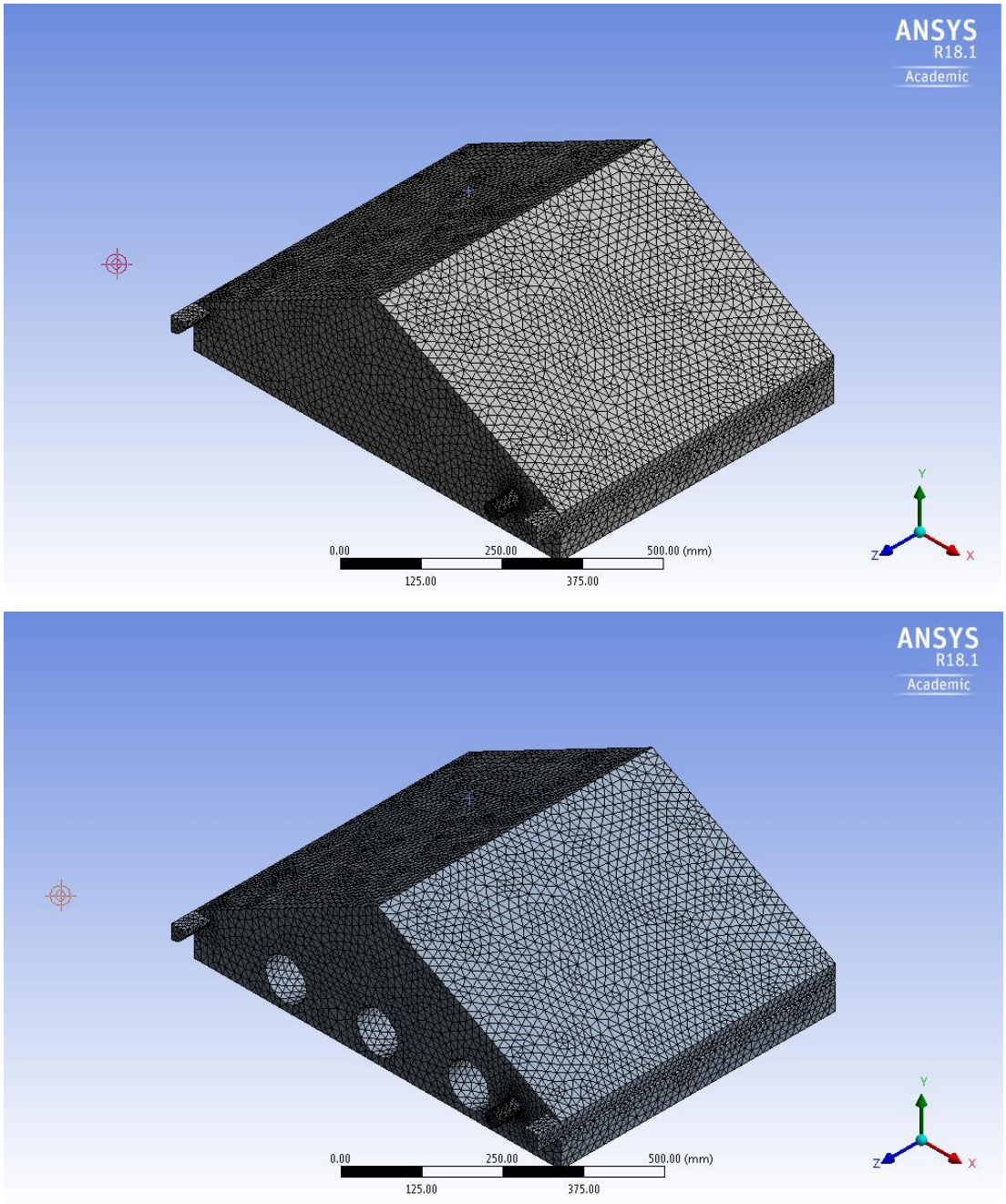

Figure 3. 6 The models mesh structure

3.4 Multiphase Flows

This study comprises of multiphase flow, mainly two phases, water liquid and water vapour. Currently there are two approaches for the numerical calculation of multiphase

flows: the Euler-Lagrange approach and the Euler-Euler approach. The Euler-Lagrange approach is used for the solid-fluid flow problems while the Euler-Euler approach is used for the fluid-fluid flow problems, such as liquid- vapour in our case. In the Euler-Euler approach, the different phases are treated mathematically as interpenetrating continua (Fluent, 2017). In ANSYS-Fluent, three different Euler-Euler multiphase models are available: the volume of fluid (VOF) model, the mixture model, and the Eulerian model.

The VOF model is a surface-tracking technique which is to be applied to a fixed mesh and is used to solve a time-dependent problem to calculate the mass transfer from the liquid phase to the vapour phase and vice versa. The VOF formulation relies on the fact that two or more fluids (or phases) are not interpenetrating (Fluent, 2017). A variable called the phase Volume Fraction (α) in the computational cell is introduced for each phase exists in the problem. The Volume Fraction is assumed to be a continuous function in space and time (Minocha et al, 2016).

The Volume Fractions of all phases sum to unity in each control volume. In our case the Volume Fraction of the liquid phase (α_l) and vapour phase (α_v) are presented as follows;

$$\alpha_l + \alpha_v = 1 \tag{3.12}$$

The fields for all variables and properties are shared by all the phases and represent volume-averaged values, as long as the Volume Fraction of each of the phases is known at each cell. Thus the variables and properties in any given cell are either purely representative of one of the phases, or representative of a mixture of the phases, depending upon the Volume Fraction values. In other words, if the fluid's Volume Fraction in the cell is denoted by α_q , then the following three conditions are possible:

- $\alpha_q = 0$: The cell is empty (of the q^{th} fluid).
- $\alpha_q = 1$: The cell is full (of the q^{th} fluid).
- $0 < \alpha_q < 1$: The cell contains the interface between the q^{th} fluid and one or more other fluids.

Based on the local value of α_q , the appropriate properties and variables will be assigned to each control volume (cell) within the domain.

The properties appearing in the transport equations are determined by the presence of the component phases in each control volume. In a two-phase system, if the phases are represented by the subscripts 1 and 2, and if the volume fraction of the second of these is being tracked, the density in each cell is given by

$$\rho = \alpha_2\rho_2 + (1 - \alpha_2)\rho_1 \quad (3.13)$$

In general, for an n-phase system, the volume-fraction-averaged density takes on the following form:

$$\rho = \sum \alpha_q \rho_q \quad (3.14)$$

All other thermal properties such as viscosity, thermal conductivity, and specific heat are computed in this way.

The VOF model has been proposed by many researchers to simulate the evaporation-condensation problem such as Rashidi et al (2018); Sharshir et al (2016); and Sun and Chen (2014). In the VOF model, The Eulerian Wall Film (EWF) model can be used to predict the creation and the flow of thin liquid films on the surface of walls. The VOF model can also include the effects of surface tension along with the interface between each pair of phases and specify a wall adhesion angle in conjunction with the surface tension model. The VOF method has inherent mass conservation, more easily capturing interface with heat transfer of phase change (Welch & Wilson, 2000).

3.5 Assumptions

To facilitate the simulation of the complex transient multiphase (the evaporation-condensation) problem, the following assumptions were proposed:

1. The cover of the SD system is airtight; i.e. there is no vapour leak from the SD system
2. The basin of the SD system is fully insulated; there are no heat losses from the SD system basin
3. It is a two-phase problem; there are only two phases (water-liquid and vapour-air mixture) present in the SD system
4. The thermal properties of the liquid (the brackish water) and the thermal properties of solid materials (the aluminium basin, the plexiglass cover, and

the revolving PVC tubes) remain at nearly constant values due to the low temperature rise

3.6 Governing Equations

The continuity, momentum, and energy conservation equations of a time-dependent problem with a multiphase flow are presented in the following sections. The problem also contains turbulent flows and mass transfer equations.

3.6.1 Continuity Equation

According to ANSYS Fluent theory guide (2019), the continuity or mass conservation equation is;

$$\frac{\partial \rho}{\partial t} + \nabla \cdot (\rho \vec{v}) = S_m \quad (3.15)$$

Where ρ is the fluid density, t is the time, $\vec{v}$ is the overall velocity vector, and S_m is mass source term to reflect the presence of the evaporation and condensation processes. The source S_m e.g. is the mass subtracted from the continuous phase (the water-liquid phase) and added to the dispersed second phase (the water-vapour phase) in the evaporation process (Fluent, 2017).

3.6.2 Momentum Equation

A single set of momentum equations is solved throughout the domain, and the resulting velocities field is shared among the phases. The momentum equation (Fluent, 2017), shown below, is dependent on the Volume Fractions of all phases through the properties ρ and μ.

$$\frac{\partial}{\partial t}(\rho \vec{v}) + \nabla \cdot (\rho \vec{v} \vec{v}) = -\nabla p + \nabla \cdot [\mu(\nabla \vec{v} + \nabla \vec{v}^{\mathrm{T}})] + \rho \vec{g} + \vec{F} \quad (3.16)$$

Where μ is the dynamic viscosity, p is the static pressure, $\rho \vec{g}$ is the gravitational body force, and $\vec{F}$ is any external body forces.

3.6.3 Energy Equation

The energy equation is also shared among the phases (Fluent, 2017) and can be described as;

$$\frac{\partial}{\partial t}(\rho E) + \nabla \cdot \left(\vec{v}(\rho E + p)\right) = \nabla \cdot \left(k_{eff} \nabla T \right) + S_h \quad (3.17)$$

Where E is the total Energy, k_{eff} is the effective conductivity, T is the Temperature, the first term on the right-hand side represents energy transfer due to conduction and convection, and S_h is a source term contains contributions from radiation as well as any other volumetric heat sources.

In the VOF model, the energy E is treated as a mass-averaged variable as follows;

$$E = \frac{\sum_{q=1}^{n} \alpha_q \rho_q E_q}{\sum_{q=1}^{n} \alpha_q \rho_q} \quad (3.18)$$

Where E_q for each phase is based on the specific heat of that phase and the shared temperature;

$$E_q = h - \frac{p}{\rho} + \frac{v^2}{2} \quad (3.19)$$

Where h is the enthalpy and for incompressible flow;

$$h = \sum_j Y_j h_j + \frac{p}{\rho} \quad (3.20)$$

Where Y_j is the mass fraction of species j;

$$h_j = \int_{T_{ref}}^{T} c_{p,j} \, dT \quad (3.21)$$

Where c_p is the heat capacity at constant pressure, and T_{ref} is a reference temperature.

3.6.4 Radiation Equation

ANSYS-Fluent provides a solar load model that allows the effect of solar radiation to be included. The radiative transfer equation for an absorbing, emitting, and scattering medium is (Fluent, 2017);

$$\frac{dI(\vec{r},\vec{s})}{ds} + (a + \sigma_s) I(\vec{r},\vec{s}) = an^2 \frac{\sigma T^4}{\pi} + \frac{\sigma_s}{4\pi} \int_0^{4\pi} I(\vec{r},\hat{s}) \Phi(\vec{s},\hat{s}) d\hat{\Omega} \quad (3.22)$$

Where,

- $\vec{r}$ = position vector
- $\vec{s}$ = direction vector
- $\vec{s}'$ = scattering direction vector
- s = path length
- a = absorption coefficient
- n = refractive index
- σ_s = scattering coefficient
- σ = Stefan-Boltzmann constant = $5.66 \times 10^{-8} W/m^2 K^{-4}$
- I = radiation intensity, which depends on the position $\vec{r}$ and direction $\vec{s}$
- T = surface temperature in K
- Φ = phase function
- $\acute{\Omega}$ = solid angle

$(a + \sigma_s)$ is the optical thickness or opacity of the medium. The refractive index (n), which is defined as the ratio of the speed of light in the medium to the speed of light in vacuum, is important when considering radiation in a semi-transparent media. Figure 3.7 illustrates the process of Radiative Heat Transfer.

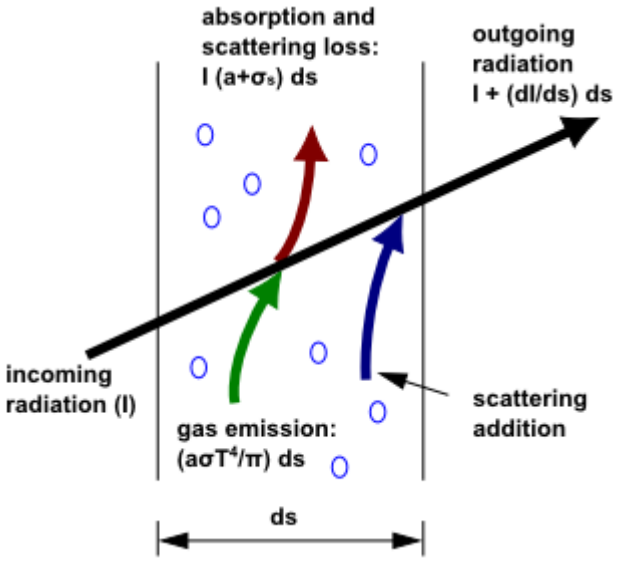

Figure 3. 7 Radiative Heat Transfer

3.6.5 Convection Equation

Since there is heat added to the system and the temperature of the air-vapour mixture changes, the fluid density varies. The force of gravity acting on the mixture causes density variations, which leads to a buoyancy-driven flow termed natural convection. The importance of buoyancy forces in the natural convection can be measured by the ratio of the Grashof (Gr) and the Reynolds (Re) numbers:

$$\frac{Gr}{Re^2} = \frac{g\beta\Delta TL}{v^2} \tag{3.23}$$

When this ratio approaches or exceeds unity, a strong buoyancy contribution to the flow is expected. Conversely, if it is very small, buoyancy forces may be ignored.

In pure natural convection, the strength of the buoyancy-induced flow is measured by the Rayleigh number (Ra), which is a dimensionless parameter indicates the instability of the fluid layers due to temperature and density differences described as follows;

$$Ra = \frac{g\beta\Delta TL^3\rho}{\mu\alpha} \tag{3.24}$$

Where β is the thermal expansion coefficient expressed as:

$$\beta = -\frac{1}{\rho}\left(\frac{\partial\rho}{\partial T}\right)_p \tag{3.25}$$

and α is the thermal diffusivity defined as:

$$\alpha = \frac{k}{\rho c_p} \tag{3.26}$$

Rayleigh numbers less than 10^8 indicate a buoyancy-induced laminar flow, with a transition to turbulence occurring over the range of $10^8 < Ra < 10^{10}$. In our case, the Rayleigh number is about (2×10^8) which means the flow in the SD system is turbulent and one of turbulence models needs to be used in the analysis.

3.6.6 Turbulence Equations

The turbulence kinetic energy, k, and its rate of dissipation, ε, are obtained from the following transport equations (Fluent, 2017);

$$\frac{\partial}{\partial t}(\rho k) + \frac{\partial}{\partial x_j}(\rho k u_j) = \frac{\partial}{\partial x_j}\left[\left(\mu + \frac{\mu_t}{\sigma_k}\right)\frac{\partial k}{\partial x_j}\right] + \mathrm{G_k} + G_b + \rho\varepsilon - Y_M + S_k \qquad (3.27)$$

and;

$$\frac{\partial}{\partial t}(\rho \varepsilon) + \frac{\partial}{\partial x_j}(\rho \varepsilon u_j) = \frac{\partial}{\partial x_j}\left[\left(\mu + \frac{\mu_t}{\sigma_\varepsilon}\right)\frac{\partial \varepsilon}{\partial x_j}\right] + C_{1\varepsilon}\frac{\varepsilon}{k}(G_k + C_{3\varepsilon}G_b) - \mathrm{C_{2\varepsilon}}\rho\frac{\varepsilon^2}{k} + S_\varepsilon \qquad (3.28)$$

Two-equation turbulence models allow the determination of both, a turbulent length and time scale by solving two separate transport equations. The $(k-\varepsilon)$ model has become the workhorse of practical engineering flow calculations in the time since proposed by Launder and Spalding (1972). Robustness, economy, and accuracy for a wide range of turbulent flows explain its popularity in flow and heat transfer simulations. This model has been extensively validated for a wide range of flows (Kim et al, 1999).

In these equations, G_k represents the generation of turbulence kinetic energy due to the mean velocity gradients, G_b is the generation of turbulence kinetic energy due to buoyancy, Y_M represents the contribution of the fluctuating dilatation in compressible turbulence to the overall dissipation rate, $\sigma_k \; and \; \sigma_\varepsilon$ are the turbulent Prandtl numbers for k and ε, respectively, and $S_k \;\; and \;\; S_\varepsilon$ are user-defined source terms.

The turbulent or eddy viscosity μ_t is computed by combining k and ε as follows:

$$\mu_t = \rho C_\mu \frac{k^2}{\varepsilon} \qquad (3.29)$$

While the model constants in equations (3.18, 19, 20) have the following default values;

$$C_{1\varepsilon} = 1.44, \;\; C_{2\varepsilon} = 1.92, \;\; C_\mu = 0.09, \;\; \sigma_k = 1.0, \sigma_\varepsilon = 1.3$$

These default values have been determined from experiments for fundamental turbulent flows. They have been found to work fairly well for a wide range of wall-bounded and free shear flows and they are most widely accepted (Fluent, 2017).

3.6.7 Mass Transfer Equations

In ANSYS-Fluent, evaporation-condensation problems can be modelled using the model of Lee (1979). The Lee model is a mechanistic model with a physical basis. It can be used in conjunction with the VOF multiphase model. The phase-change model proposed by Lee (1979) has been extensively used for evaporation- condensation problem (Sun & Chen, 2014).

In the Lee model, the liquid-vapour mass transfer (evaporation-condensation) is governed by the vapour transport equation (Fluent, 2017);

$$\frac{\partial}{\partial t}(\alpha_v \rho_v) + \nabla \cdot \left(\alpha_v \rho_v \vec{V}_v\right) = \dot{m}_{lv} - \dot{m}_{vl} \tag{3.30}$$

Where

- $v =$ vapour phase
- $\alpha_v =$ vapour volume fraction
- $\rho_v =$ vapour density
- $\vec{V}_v =$ vapour phase velocity
- $\dot{m}_{lv},\ \dot{m}_{vl} =$ the rates of mass transfer due to evaporation and condensation, respectively. These rates have the units of kg/s/m^3

Based on the following temperature regimes, mass transfer can be described as follows:

- If $T_l > T_{sat}$ (Evaporation)

$$\dot{m}_{lv} = coeff * \alpha_l \rho_l \frac{(T_l - T_{sat})}{T_{sat}} \tag{3.31}$$

- If $T_v < T_{sat}$ (Condensation)

$$\dot{m}_{vl} = coeff * \alpha_v \rho_v \frac{(T_{sat} - T_v)}{T_{sat}} \tag{3.32}$$

Where; $T_l,\ T_v,\ T_{sat}$ are the liquid, vapour, and saturation temperature, respectively, $coeff$ is a coefficient that must be fine-tuned and can be derived from the experimental results, α and ρ are the phase volume fraction and density, respectively.

3.7 Initial and Boundary Conditions

After providing all the governing equations, the Initial and Boundary Condition have been applied to the domain as follows;

The Initial Condition of the SD system:

The initial temperature of the system is 298 K under atmospheric pressure 101325 Pa. The SD system has been treated as one domain and the water-liquid zone has been adapted and patched. The water depth has been patched to the adapted region of 40 mm with a Volume Fraction 1 for the liquid phase. The solar radiation intensity and direction have been set using solar calculator embedded in Solar Ray Tracing model in the Fluent solver according to the geometry orientation, the location Longitude and Altitude, and according to the day of the year, and time of the day. In this location, the Longitude is 151.9ºE and Altitude is 27.6ºS.

Regarding the Boundary Conditions:

The basin base has been considered fully insulated with 0-heat flux and it participates in the solar radiation as an opaque material with absorptivity $(\alpha) = 0.8$. The base material is 3 mm thick aluminium. The cover and walls material is 3 mm thick plexiglass. The cover and walls participate in the solar radiation as a semi-transparent medium with transmissivity $(\tau) = 0.8$. The cover and the walls have been set as mixed thermal boundary condition including the effect of radiation and convection heat transfer. The free stream temperature was taken as 300-310 K and the free convection heat transfer coefficient (h_∞), which depends on the free stream velocity (wind speed U_∞), was taken according to the following correlation (Badran et al, 2007).

$$h_\infty = 5.7 + 3.8U_\infty \qquad (3.33)$$

Where; $\left\{0.1\frac{m}{s} \leq U_\infty \leq 5\frac{m}{s}\right\}$ within a temperature range $(10 - 40\ ℃)$

The inlet and outlet have been set as pressure-inlet and pressure-outlet, respectively. The inlet Volume Fraction of the liquid phase is 1 and for the outlet, this value is calculated from neighbouring cells. For the Modified SD system, the three revolving tubes have been set as moving walls with a rotational speed of 4.2 rad/s (40 rpm). The revolving tubes material is PVC and they participate in the solar radiation as an opaque material with absorptivity $(\alpha) = 0.8$.

3.8 Solution Method

Using the Pressure-Based Solver (Fluent, 2017), ANSYS Fluent solves the governing integral equations for the conservation of mass, momentum, energy, and other scalars such as turbulence and mass transfer. A control-volume-based technique is used that consists of:

- Division of the domain into discrete control volumes using a computational grid.
- Integration of the governing equations on the individual control volumes to construct algebraic equations for the discrete dependent variables ("unknowns") such as velocities, pressure, temperature, volume fraction and conserved scalars such as energy and turbulence.
- Linearization of the discretized equations and solution of the resultant linear equations system to yield updated values of the dependent variables.

The pressure-based solver employs an algorithm which belongs to a general class of methods called the projection method (Chorin, 1968). In the projection method the constraint of mass conservation (the continuity equation) i.e. the velocity field, is achieved by solving a pressure (or pressure correction) equation. The pressure equation is derived from the continuity and momentum equations in such a way that the velocity field, corrected by the pressure, satisfies the continuity equation.

The pressure-based solver uses a solution algorithm where the governing equations are solved sequentially (that is, segregated from one another). Since the governing equations are nonlinear and coupled to one another, the solution process involves iterations wherein the entire set of governing equations is solved repeatedly until the solution converges. The solution converges when the results have varied from the previous iteration with only very small value defined by the user (with subsequent iterations and all mass, momentum, energy, and scalar balances have been achieved).

The segregated algorithm is memory-efficient since the discretized equations need only to be stored in the memory one at a time. The individual governing equations for the variables (for example $u, v, w, p, T, k, \varepsilon$, and so on) are solved one after another.

Each governing equation, while being solved, is "decoupled" or "segregated" from other equations.

With the segregated algorithm, each iteration consists of the steps illustrated in Figure 3.6 and outlined below:

1. Update fluid properties (for example, density, viscosity, specific heat) including turbulent viscosity (diffusivity) based on the temperature obtained in the current solution.
2. Solve the momentum equations, one after another, using the recently updated values of pressure and face mass fluxes.
3. Solve the pressure correction equation using the recently obtained velocity field and the mass-flux.
4. Correct face mass fluxes, pressure, and the velocity field using the pressure correction obtained from Step 3.
5. Solve the equations for the additional scalars, such as turbulent quantities, energy, species, and radiation intensity using the current values of the solution variables.
6. Update the source terms arising from the interactions among different phases.
7. Check for the convergence of the equations.

In transient modelling, these steps are continued until the convergence criteria are achieved to the current Time Step before advancing to the next Time Step.

The Timestep size, Δt, must be small enough to resolve time-dependent features; we need to make sure that the convergence is reached within the number of Max Iterations per Time Step. An appropriate time step size can be estimated by:

$$\Delta t = \frac{Typical\ cell\ size}{Characteristic\ flow\ velocity} \tag{3.34}$$

The Time Step value is set as 0.01 second, and the Maximum number of Iterations per Time Step is set as 1000 iterations.

In reality on the available computers, the results residuals cannot go to zero; however, the residuals decline to some small value (round-off) and then stop changing. The lower the residual value is, the more numerically accurate the solution. In ANSYS-Fluent the default convergence criterion is (10^{-3}) for all equations and (10^{-6}) for energy equations which are sufficient for most problems. The residual of the convergence

criteria has been set to the following values; (10^{-4}) for continuity, momentum, turbulent, and volume fraction equations and (10^{-8}) for energy and radiation equations.

The convergence has been achieved after 80 iterations for the first time step. Then it converged after fewer iterations when advancing in time for the next time steps until it reached 2-3 iterations after few Time Steps.

The Pressure-Implicit with Splitting Operators (PISO) Pressure-Velocity coupling scheme has been used to improve the efficiency of the calculation and accelerate the convergence. The PISO algorithm performs neighbour and skewness correction to satisfy the momentum balance after solving the pressure-correction equation.

The Pressure-Based solver includes the Under-Relaxation Factor (URF) to stabilize the iterative process and to control the update of the computed variables at each iteration as shown in the following equation (Fluent, 2017);

$$\emptyset_{new} = \emptyset_{old} + URF * \Delta\emptyset \quad (3.35)$$

Where $\emptyset$ represent the value of any variable

The default values of the URF, which are between 0.1 to 1, are suitable for a wide range of problems; however, these values can be reduced to help in achieving faster convergence when it is necessary, especially with complex nonlinear problems. In our case, the URF values were; for continuity equation = 0.1, for momentum equation = 0.2, for turbulent equations = 0.5, for volume fraction and mass transfer equations = 0.1, and for energy equation = 0.8.

The Double Precision solution option has been used to ensure highly accurate results for the 3D Transient Multiphase problem under the Implicit Formulation scheme.

Figure 3.8 shows the flowchart of the solution method using the Pressure-Based solver

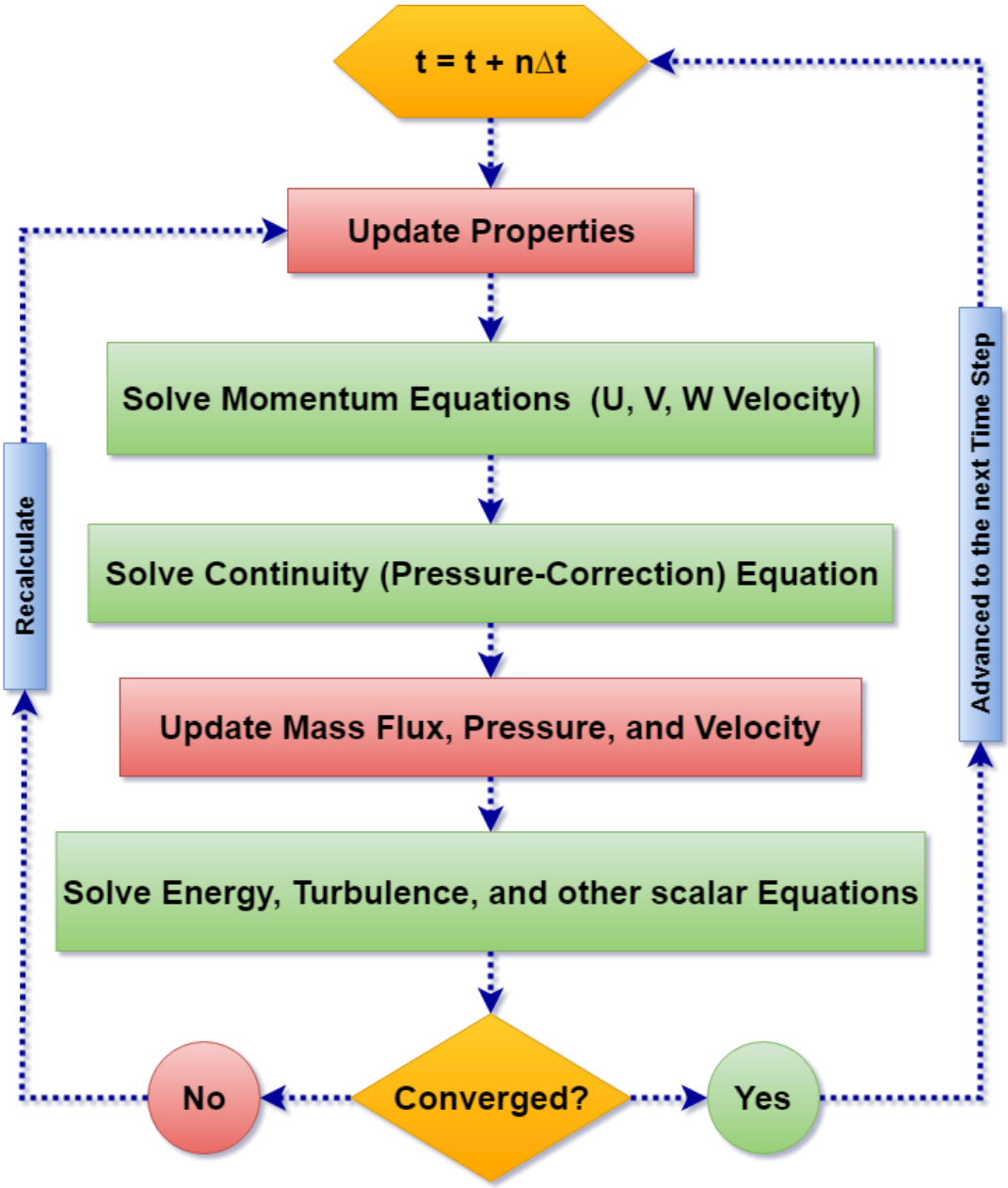

Figure 3. 8 Overview of the Pressure-Based Segregated Algorithm Solution Methods

The Iterative Time Advancement (ITA) scheme

4 Chapter Four: Experimental Investigation

After performing the CFD simulation, the experimental tests were conducted to verify the CFD model and to validate the results of the CFD simulation. The experimental tests were carried out at the University of Southern Queensland campus, in Toowoomba city (Australia) during the spring and summer seasons (from the 4th of October 2017 to the 23rd of April 2018) and further investigations (from the 1st to the 17th of April 2019). The experimental setup, instrumentation, observation, and data collection are described in this chapter.

4.1 Experimental Setup

Two apparatuses, the NSD system and the MSD system, were built to conduct the experimental examinations. As described in the previous chapters, the NSD system is a Normal Solar Still Desalination system, which has a single basin and double slope cover. The MSD system is the Modified Solar Still Desalination system, which has the proposed modification of three revolving tubes into its water basin. Both the NSD and the MSD systems have the same overall dimensions, the same operation conditions, and the same construction materials (except for the three revolving tubes). Both SD systems were run at the same time, at the same location, and under the same weather conditions. The designs, operating conditions, and the construction materials of both the NSD and the MSD systems are presented in the following sections.

4.1.1 NSD system

The NSD system, as shown in figure 4.1, has the following design parameters;

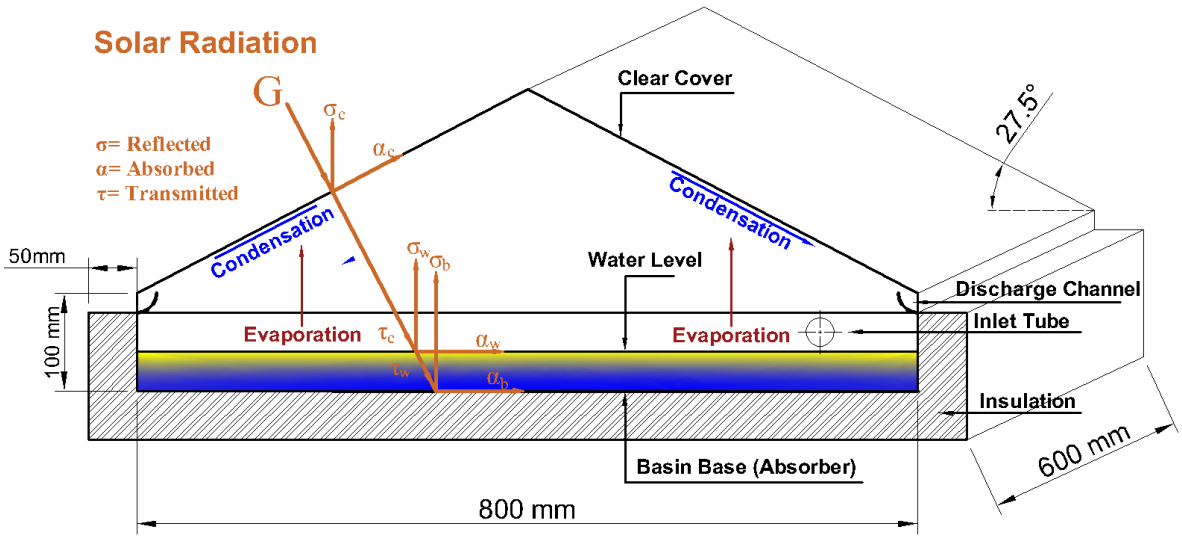

Figure 4. 1 The schematic diagram of the NSD system design

The water basin was a rectangular shape and its dimensions were; the length = 800 mm, the width = 600 mm, and the height = 100 mm. To minimize the heat loss from the water, the water basin was completely insulated from the outside by a 60 mm insulation foam layer. To enhance the solar radiation absorbance and to minimize the solar radiation reflectance, the basin liner was coated with matt black paint.

The cover was a double slope with a tilt angle of 27.6° from two opposite sides, which is the same latitude angle of the experiment's location. The two sides of the cover were facing the east and the west direction.

The NSD system has a water inlet to compensate for the amount of water that evaporates from the basin and to keep the water in the basin at a constant level. The water level in the basin was 40 ±1 mm and was controlled by a small water-float.

To measure the productivity of the NSD system through the distillate yield, the condensed water on the inner surface of the cover of the NSD system was collected and discharged using two side-channels and two outlet tubes. The condensed water was measured using a graduated flask.

4.1.2 MSD system

The MSD system, as shown in figure 4.2, has similar design parameters to the NSD system except for the addition of three identical revolving tubes to the water basin of the MSD system.

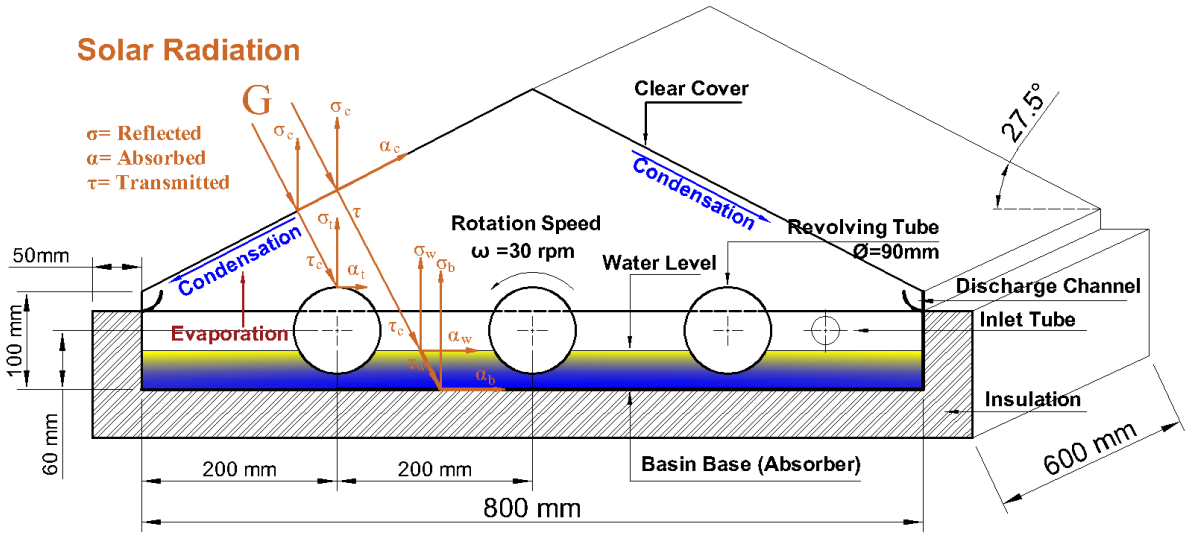

Figure 4. 2 The schematic diagram of the MSD system design

The diameter of the revolving tubes was 90 mm, the centre-to-centre distance between the tubes was 200 mm, and the tubes centre above the base of the basin was 60 mm. The water level in the basin was 40±1 mm, which means the tubes were semi-immersed in the water.

Figure 4.3 shows the revolving tubes used in the MSD system. The revolving tubes were PVC pipes plugged from both ends by push-on PVC caps with central steel shafts. The revolving tubes were wrapped with a black absorbent mat to maximize the solar radiation absorbance and to ensure that the outer circumference of the tubes was always wet.

Figure 4. 3 The three revolving tubes used in the MSD system

Figure 4.4 shows three worm gear DC motors connected to three revolving tubes of the MSD system and run by a variable DC power supply. The DC motors' specifications were; maximum voltage = 16 V, maximum power = 50 W, maximum torque = 5 N·m, and maximum rotation speed = 65 rpm. To control the rotational speed of the revolving tubes, these motors were powered by a variable (switch-mode Lab) DC power supply (0-16V/ 25A).

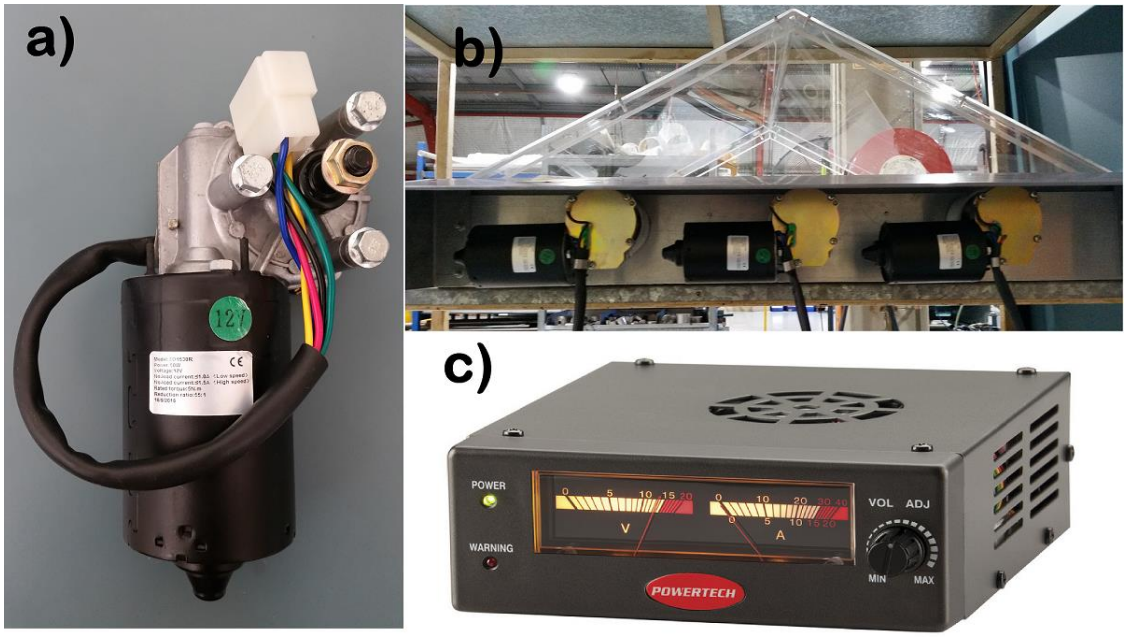

Figure 4. 4 a) The DC motor b) The coupling arrangement to the MSD system, c) The variable DC power supply that used in the experiment

4.2 Construction Materials

In both the NSD and the MSD systems, the basin was made of a 3 mm thick aluminium sheet, the cover was made of a 3 mm thick clear plexiglass sheet, and the insulation was made of a 60 mm thick XPS foam board. In the MSD system, the tubes were made of a 90 mm diameter PVC pipe. The construction materials were chosen according to their good thermal and optical properties. According to the literature review, the aluminium basins were preferable due to their good physical and thermal properties (Malaiyappan & Elumalai, 2016). Aluminium is lightweight, anti-corrosion, and the coated aluminium has a good absorbance to solar radiation. The plexiglass has many advantages over the glass, it has a lighter weight, is unbreakable, easy to fabricate, safer, has a higher transmittance to solar radiation, and is much cheaper than glass. The PVC tube is widely abundant at trivial cost and it is very lightweight, which means it requires less energy for rotating by a small DC motor. The XPS foam has good insulation properties and it is weather and rain resistant. All materials used are available in local markets at moderate prices. Table 4.1 lists the Thermal and Optical properties of the selected construction materials. Figure 4.5 shows the constructed NSD and MSD systems used in this work.

Table 4. 1 The thermal and optical properties of the construction materials used in this project

Properties	***Aluminium***	***Plexiglass***	***PVC***	***XPS foam***
Density ρ (kg/m^3)	*2790*	*1190*	*1470*	*20*
Specific Heat c_p $(J/kg \cdot K)$	*880*	*1450*	*850*	
Thermal Conductivity k $(W/m \cdot K)$	*168*	*0.7*	*0.2*	*0.02*
Absorbance	*0.88 (coated)*	*0.05*	*0.88 (coated)*	
Transmittance	*0*	*0.90*	*0*	
Reflectance	*0.12*	*0.05*	*0.12*	

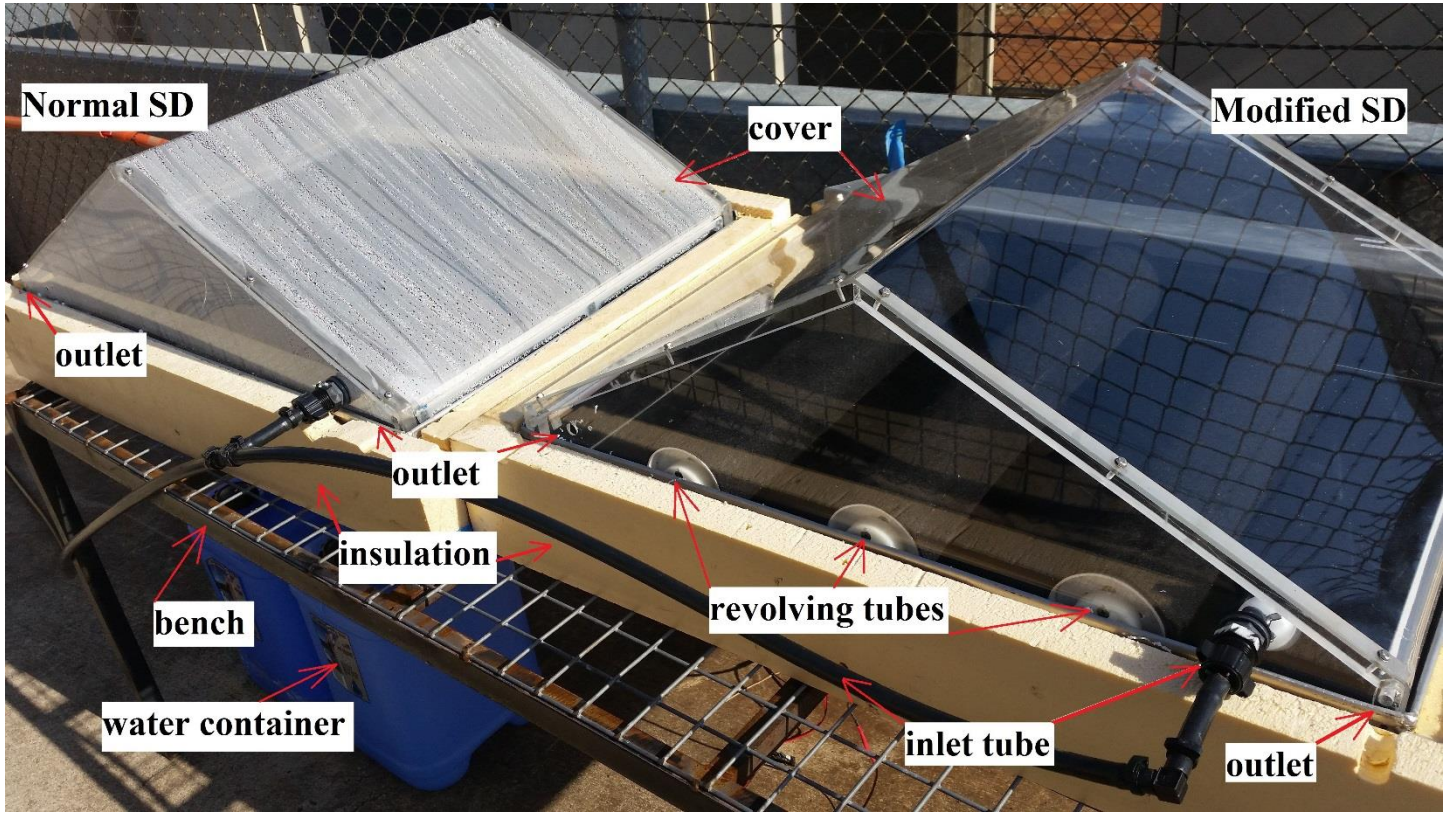

Figure 4. 5 The experimental apparatus, the NSD system (left) and the MSD system (right) the MSD was without water to show the inside

4.3 Instrumentation

Some instrumentation were used in the experiment part of this study to measure the temperatures, the output distillate water, and the weather conditions.

A calibrated thermometer Data-logger with twelve K-type thermocouples were used to measure the temperature of the water, the temperature of the vapour, the temperature of the cover, and the temperature of the basin in both the NSD and the MSD systems. The type of Datalogger was (Lutron BTM-4208SD) 12 Channels Thermometer recorder with a capability to store the data of many days as spreadsheets on an external memory card.

Two graduated measuring cylinders (500 ±5 ml) and (50 ± 0.5 ml) were used to measure the volume of the distillate yield or the productivity of each SD system. An electronic scale (0 to 5000 ±0.5 g) also was used to measure the mass of the output water.

The meteorological parameters (i.e. the weather conditions) such as the solar intensity, the wind speed, and the relative humidity were obtained from the official weather station of the University of Southern Queensland (2019). The weather station is reliable and very close to the experiment location. The data from the weather stations of the Toowoomba city that run by the Australian Government- Bureau of Meteorology (2019) also were considered reliable and were used for confirming the readings. Figure 4.6 shows the instruments used in this study and Table 4.2 lists their technical specifications as provided by the manufacturers.

Figure 4. 6 a) the thermocouples and the data logger b) the measuring cylinders and electronic scale

Table 4. 2 The technical specifications of the instruments used in the experimental tests

Instrument	***Resolution***	***Range***	***Accuracy***	***Error %***
Temperature Logger	*0.1°C*	*-50 to 999.9°C*	*±0.5°C*	*±0.4%*
K-type thermocouples		*-40 to 260°C*	*±0.5°C*	*±0.4%*
Measuring cylinder1	*5 ml*	*50 to 500 ml*	*±5 ml*	*±1%*
Measuring cylinder2	*1 ml*	*5 to 50 ml*	*±0.5 ml*	*±1%*
Electronic scale	*1 g*	*0 to 5000 g*	*±0.5 g*	*±0.1%*
Electronic stopwatch	*0.01 s*	*0 to 5999 s*	*±0.1 s*	*±0.001%*

4.4 Observation

The experimental tests were carried out at the University of Southern Queensland campus, in Toowoomba, Australia during the spring and summer seasons due to the higher levels of solar exposure in these two seasons when compared to other seasons. According to the Australian Government Bureau of Meteorology (2019), in Toowoomba city, the average daily solar exposure for the period of six months from October to April is about (21 to 24 MJ/m^2) while it is about (12 to 15 MJ/m^2) from May to September. Therefore, the experimental tests were run from the 4th of October 2017 to the 23rd of April 2018 and further investigations were undertaken from the 1st to the 17th of April 2019.

Figure 4.7 shows the average daily solar exposure in Australia during the spring and summer seasons from October to April, and Figure 4.8 during the autumn and winter seasons from May to September (Bureau of Meteorology, 2019).

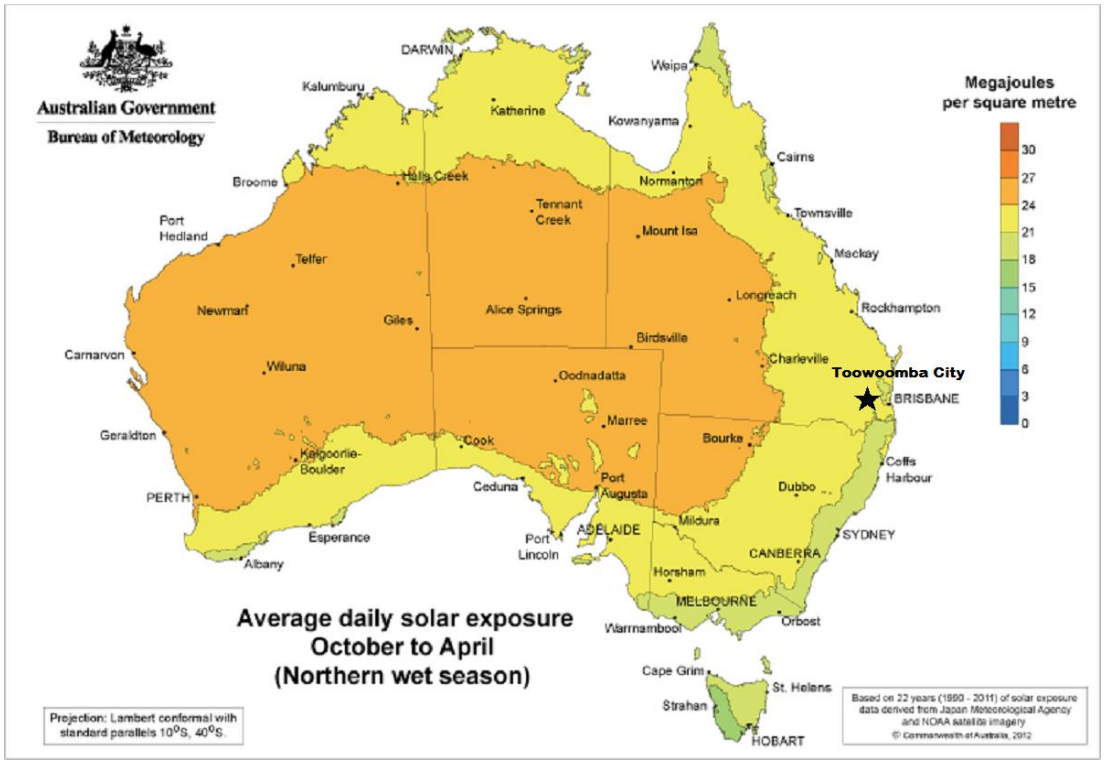

Figure 4. 7 The average daily solar exposure in Australia during the spring and summer seasons (Bureau of Meteorology, 2019). (CC licenced Product Code: IDCJCM0019). The star symbol is added to the original picture to indicate the location of Toowoomba city where the experiment was performed

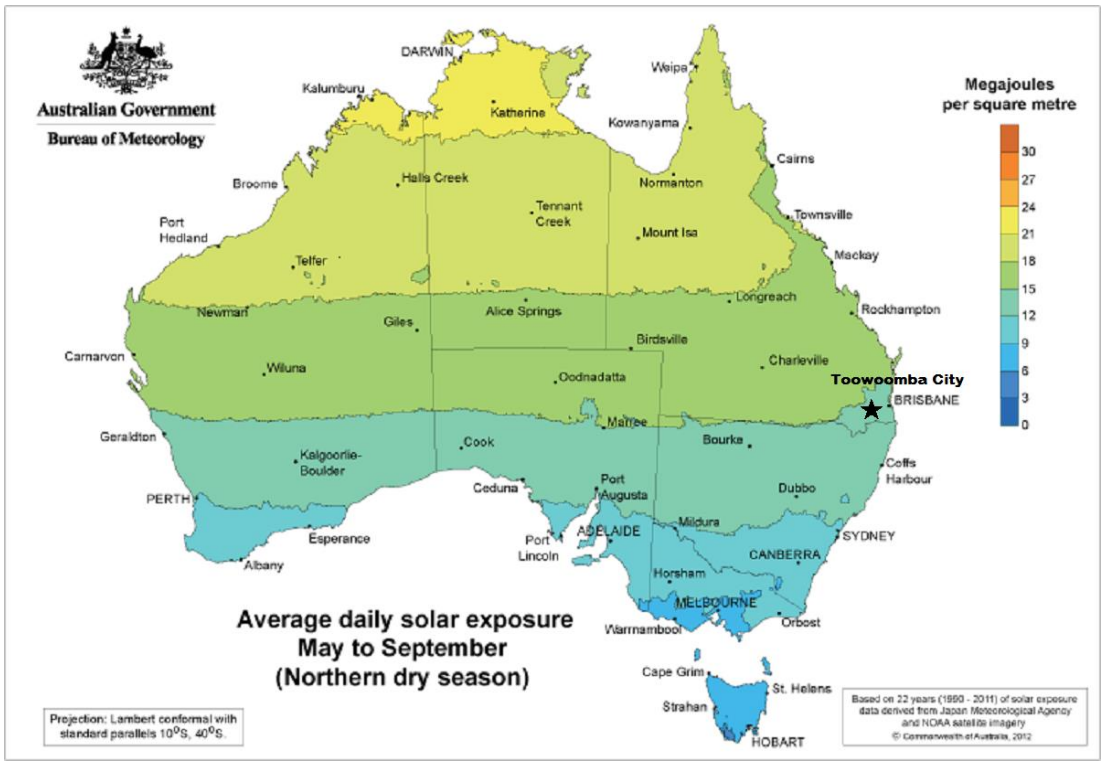

Figure 4. 8 The average daily solar exposure in Australia during the autumn and winter seasons (Bureau of Meteorology, 2019). (CC licenced Product Code: IDCJCM0019). The star symbol is added to the original picture to indicate the location of Toowoomba city where the experiment was performed

The geographical location of the experimental investigations was, Longitude = 151.931º East, Latitude = 27.601º South, and Elevation = 691 m. The orientation of the apparatuses (Both SD systems) was due north because the site was in the southern hemisphere. The two sides of the SD system cover were facing the east and the west. Figure 4.9 shows the satellite image of the experiment geographical location taken by Google Maps (2019) and figure 4.10 shows the SD systems orientation during the experimental tests.

Figure 4. 9 The satellite image of the experiment geographical location (the red circle) (Google Maps, 2019)

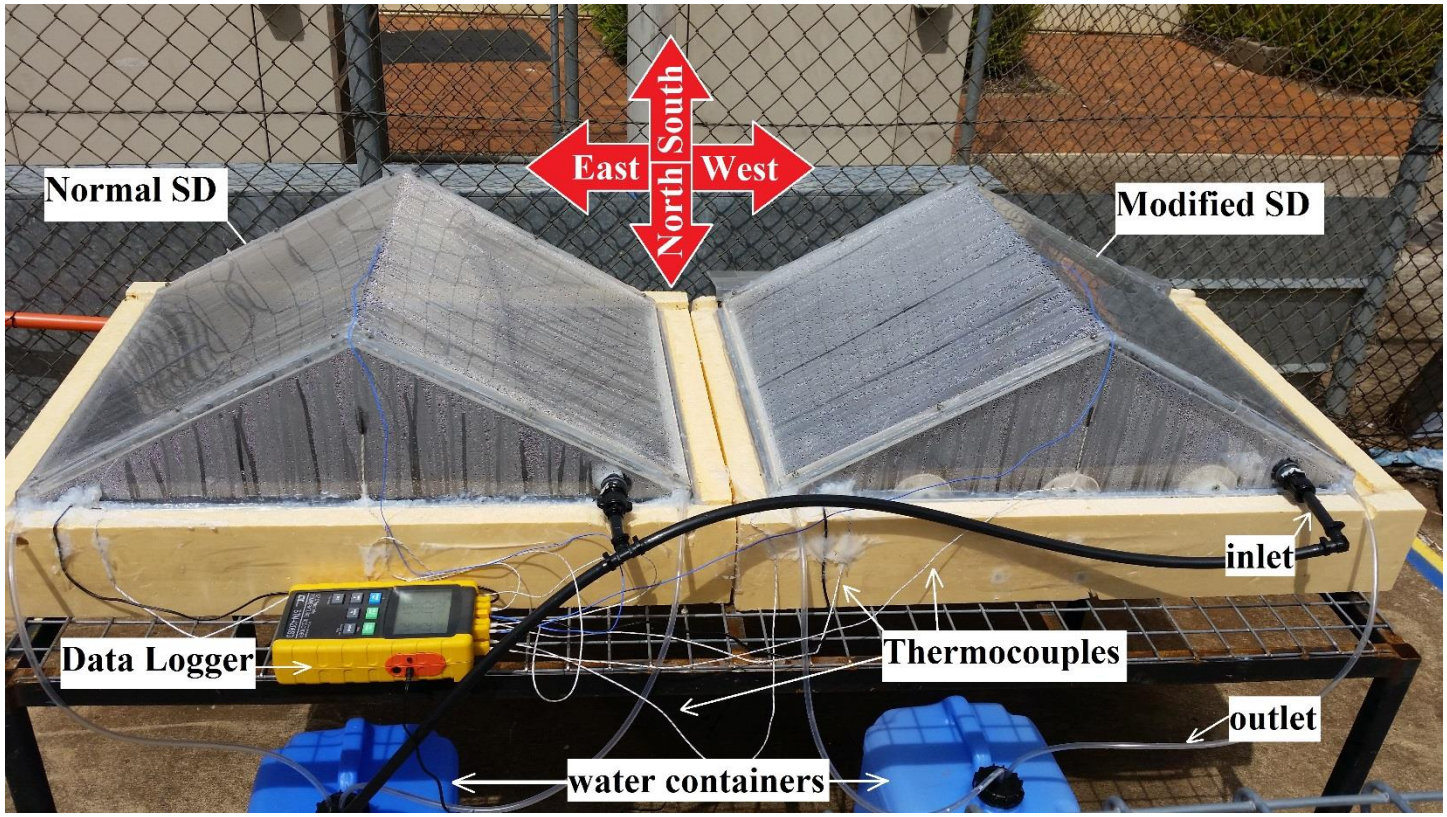

Figure 4. 10 The two SD system during the experiment and the orientation

To evaluate and compare the performance of the MSD system and the NSD system, both SD systems were run at the same time, at the same location, and under the same weather conditions. Several parameters were measured during the experimental investigations and the observation methodology was as follows;

1. The thermometer data-logger with twelve channels was set to record the temperature of the water, the temperature of the vapour, the temperature of the basin, and the temperature of the cover for both the SD systems every five minutes and stored the data into spreadsheets on an external memory card. The data was continually transferred to the computer.
2. Twelve K-type thermocouples were connected to the data-logger and distributed between the two SD systems as follows; four thermocouples placed into the water, four thermocouples placed into space above the water, two thermocouples attached to the basins, and two thermocouples attached to the covers.
3. The weather conditions such as the ambient temperature, the solar intensity, the wind speed, and the relative humidity were collected from the nearby weather station of the University of Southern Queensland and the weather stations of Toowoomba city.
4. The distillate water or the productivity of the NSD system and the MSD system were collected into two separate water containers. The collected water was measured daily in the early morning to find out the daily productivity of each SD system. A digital scale and measuring cylinders were used for measuring the daily productivity of both the SD systems.
5. The hourly yield of both the SD systems was measured on selected clear days about the middle of every month during the experimental period.

Figure 4.11 shows a schematic diagram of the experiment layout and indicates the locations of the thermocouples.

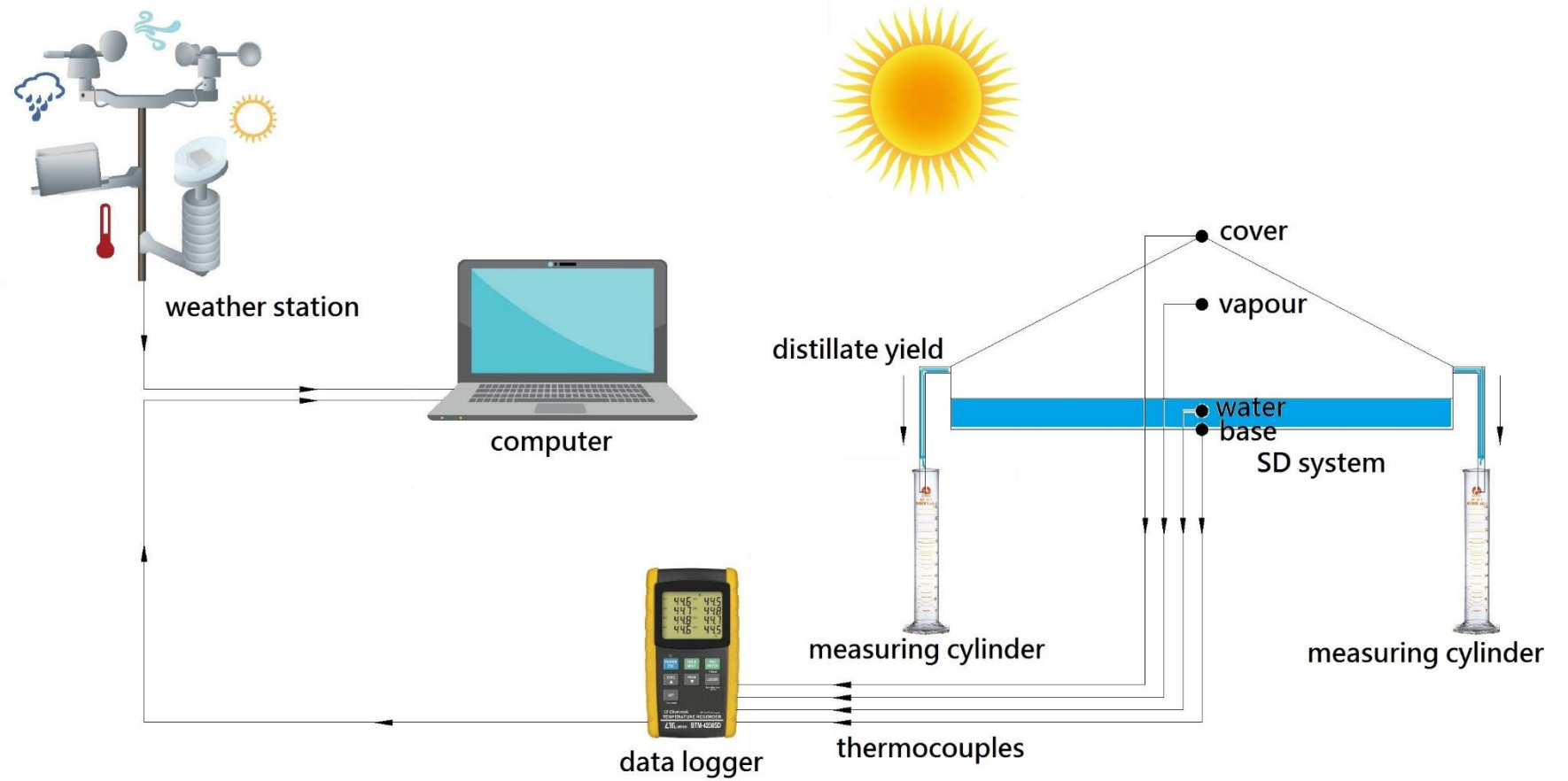

Figure 4. 11 The experiment layout and the locations of the thermocouples

4.5 Data Collection

The experimental data were recorded in three of datasheets as follows;

1. The first data sheet was used to record the following parameters every 5 minutes 24 hours a day, 7 days a week during the whole period of the experimental investigations. The data captured included the temperature of the water, the temperature of the vapour, the temperature of the basin, and the temperature of the cover of both the MSD system and the NSD system. The data also included the weather conditions, the ambient temperature, the solar intensity, the wind speed, and the relative humidity. Table 4.3 shows the first data sheet used in in the experimental part of this study.
2. The second data sheet was used to record the daily productivity (or the daily distillate yield) of both the SD systems. The data collection also included; the daily insolation (or the daily solar exposure), the maximum ambient temperature, the average wind speed, the average relative humidity, and the average cloud cover amount. The daily maximum temperature of the water, the vapour, the cover, and the basin of both the SD systems were recorded as well. The daily efficiency of both the SD systems and the enhancement in the daily efficiency and the daily productivity due to the modification were calculated and recorded daily in the same datasheet. Table 4.4 shows the second data sheet used in the experimental part of this study.
3. The third data sheet was used to record the hourly productivity and the hourly insolation of the selected days during the experimental tests. It also used to record the hourly efficiency and the enhancement in the hourly productivity and hourly efficiency. Table 4.5 shows the third data sheet used in the experimental part of this study.

Table 4. 3 The first datasheet of the experimental data collection

Time	**Water Temperature (°C)**		**Vapour Temperature (°C)**		**Basin Temperature (°C)**		**Cover Temperature (°C)**		**Ambient Temperature (°C)**	**Wind speed (km/hr)**	**Relative Humidity (%)**	**Solar intensity (W/m^2)**
	MSD	**NSD**	**MSD**	**NSD**	**MSD**	**NSD**	**MSD**	**NSD**				
06:00												
06:05												

Table 4. 4 The second datasheet of the experimental data collection

Day	Daily Solar Exposure = Daily Insolation (MJ/m2)	Daily Max. Ambient Temperature (°C)	Daily Ave. Wind Speed (km/hr)	Daily Ave. Relative Humidity (%)	Daily Ave. Cloud Amount (Oktas)	Daily Max. Water Temperature (°C)		Daily Max. Vapour Temperature (°C)		Daily Max. Basin Temperature (°C)		Daily Max. Cover Temperature (°C)		Daily Productivity ($kg/m^2.day$)		Daily Thermal Efficiency (%)		Daily Productivity Enhancement (%)	Daily Efficiency Enhancement (%)
						MSD	**NSD**	**MSD**	**NSD**	**MSD**	**NSD**	**MSD**	**NSD**	**MSD**	**NSD**	**MSD**	**NSD**		

Table 4. 5 the third datasheet of the experimental data collection

Day/Time	Hourly insolation (MJ/m^2)	Hourly Productivity (ml/hr)		Hourly efficiency (%)		Enhancement in hourly productivity (%)	Enhancement in hourly efficiency (%)
		MSD	NSD	MSD	NSD		

5 Chapter Five: Results and Discussions

This chapter presents and discusses the results of the CFD simulation and the results of the experimental investigation that were described in Chapters Three and Four, respectively. This chapter is divided into the following sections; the results of the CFD simulation, the results of the experimental investigation, and the CFD model validation.

5.1 Results of the CFD Simulation

Using the CFD Fluent solver which is part of ANSYS 19.1 software, the CFD simulation was carried out to simulate both the MSD and the NSD systems. As described in Chapter Three, the simulation was conducted as three-dimensional, transient, and multiphase (with phase change) analysis. The solution method was an iterative implicit scheme in double precision, using pressure-based solver. For the phase change (evaporation-condensation), the Lee model included in the VOF multiphase model was applied. For the turbulence flow, the $k-\epsilon$ turbulence model was used. For the solar radiation load, the solar ray-tracing model was applied.

As mentioned also in Chapter Three, mixed convection and radiation boundary conditions were applied to the walls; including the cover in both the SD systems and the revolving tubes in the MSD system. The basin wall was considered fully insulated with no heat losses. All walls participated in the solar radiation; the cover was transparent, and the basin and the revolving tubes were opaque objects. There were two pressure outlets and one velocity inlet in every SD system. The numerical model dimensions were as the experimental model dimensions; the basin was $800\ mm \times 600\ mm \times 100\ mm$, the cover slope angle was $27.5°$, the water depth was $40\ mm$, the revolving tubes' diameter was $90\ mm$, the tubes centre-to-centre was $200\ mm$ and the tube centre to the basin was $60\ mm$. The results obtained from the CFD simulation are presented in the following sections.

5.1.1 Solar Radiation

Figure 5.1 shows the rate of the absorbed solar radiation (solar heat flux) into the absorber of the MSD and NSD systems. The results show that in addition to the solar radiation absorbed by the base in both the SD systems, the MSD system has the advantage of absorbing solar radiation by the revolving tubes. According to the results, the MSD system absorbs more solar energy than the NSD system. As solar radiation is the only input heat source, solar radiation is the most important factor that affects the performance of the SD systems. Increasing the amount of absorbed solar radiation by the SD system means an SD system with higher productivity and higher thermal efficiency.

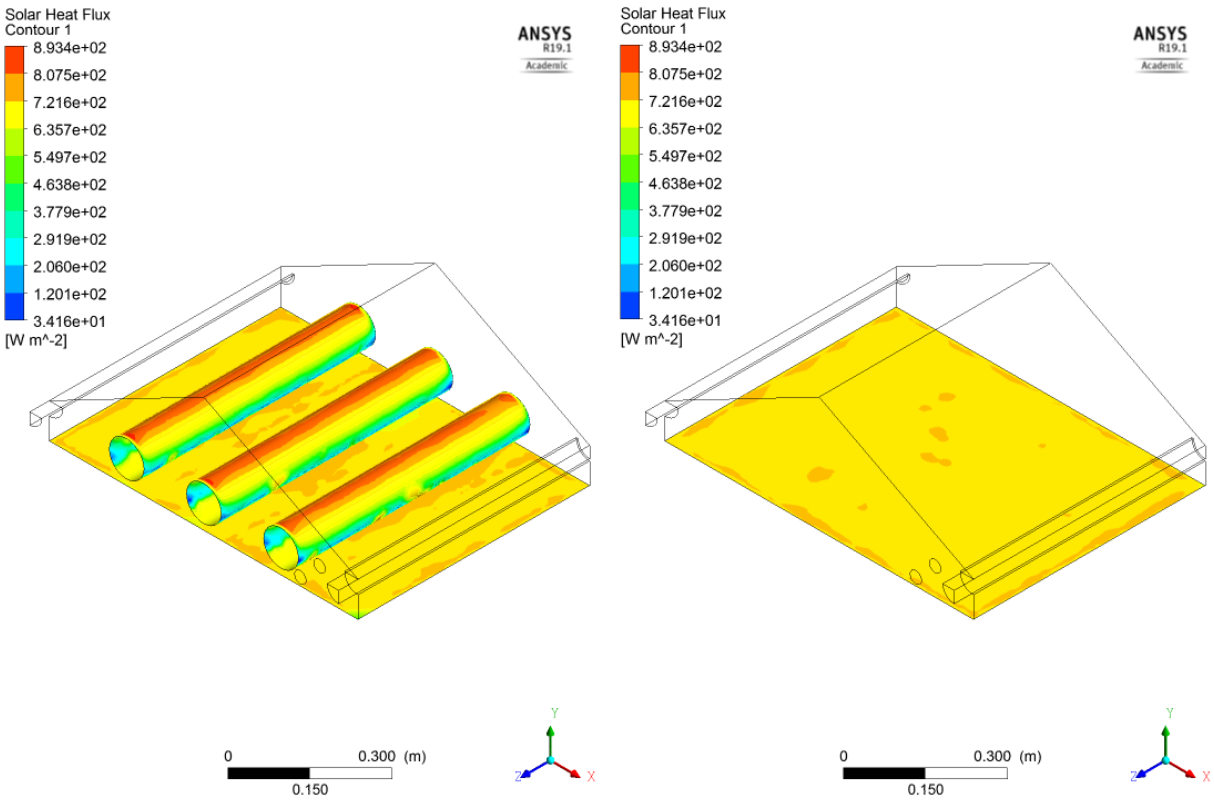

Figure 5. 1 The solar radiation distribution of the MSD system (left) and the NSD system (right)

Orthogonal solar radiation = 1000 W/m^2, ambient temperature = 300 K, wind Speed = 5 m/s, atmospheric pressure = 1 bar, tube's rotation speed = 40 rpm, water depth = 40 mm, tube's diameter = 90 mm

5.1.2 Temperature

Figures 5.2 and 5.3 show the temperature distribution in the mid plane of the MSD system and the NSD system at two different time steps. The results showed that the temperature of the MSD system was a little higher than the NSD system. The explanation to this case is the revolving tubes of the MSD system was heated by the solar radiation. The rotational movement of these tubes raise the temperature of the water in the basin and heats up the surrounding vapour. According to the results, there was about 5ºC difference between the temperature of the MSD system and the temperature of the NSD system. Increasing the absorbance of solar radiation in the MSD system was the reason for increasing the difference in the temperature between the two SD systems. Temperature is a very important factor for the SD systems' performance. Higher water temperature means more evaporation and hotter air carries more moisture, which leads to an increase in the productivity of the SD system.

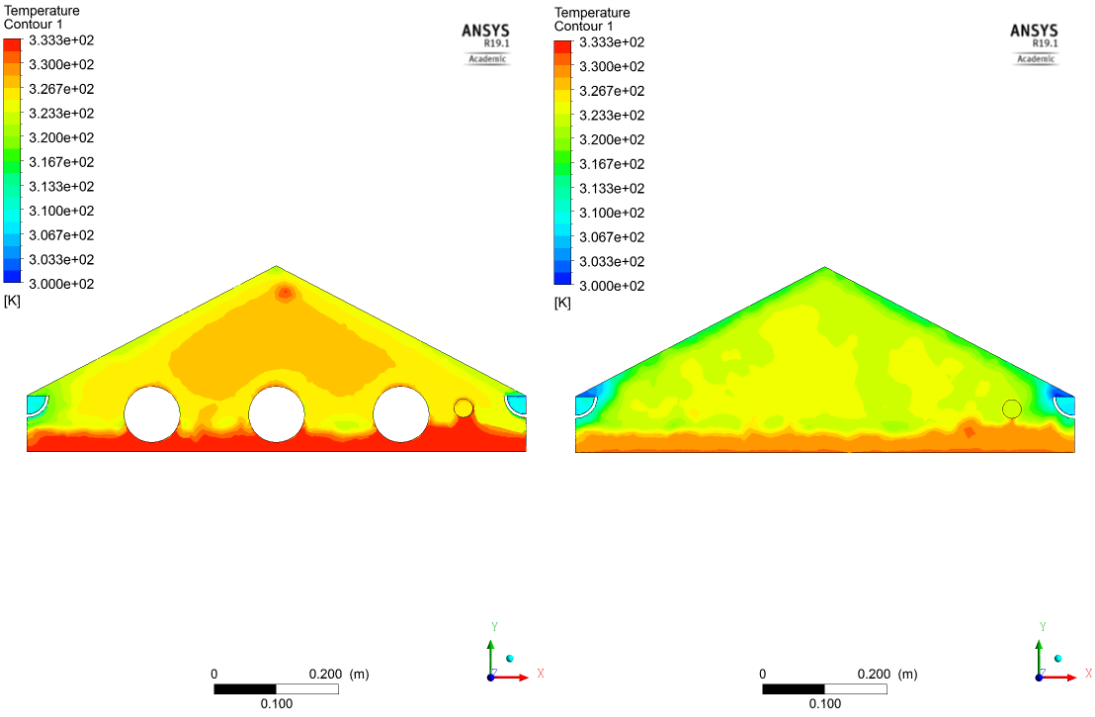

Figure 5. 2 The temperature distribution in the midplane of the MSD system (left) and the NSD system (right) after one hour. Orthogonal solar radiation = 1000 W/m^2, ambient temperature = 300 K, wind Speed = 5 m/s, atmospheric pressure = 1 bar, tube's rotation speed = 40 rpm, water depth = 40 mm, tube's diameter = 90 mm

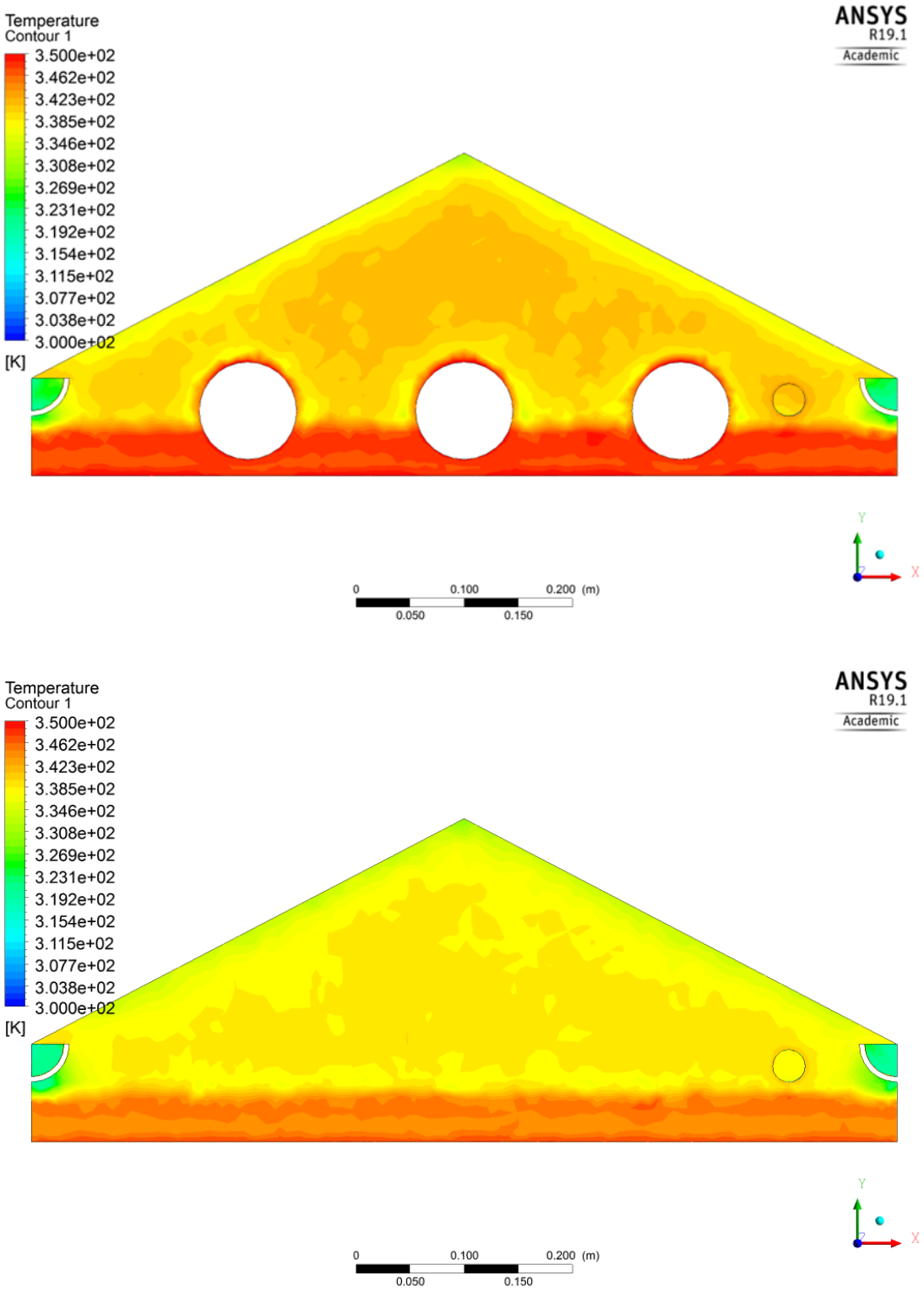

Figure 5. 3 The temperature distribution in the midplane of the MSD system (upper) and the NSD system (lower) after two hours. Orthogonal solar radiation = 1000 W/m^2, ambient temperature = 300 K, wind Speed = 5 m/s, atmospheric pressure = 1 bar, tube's rotation speed = 40 rpm, water depth = 40 mm, tube's diameter = 90 mm

5.1.3 Pressure

Figure 5.4 shows the contours of the static gauge pressure of a central cross-section of both the MSD and the NSD systems after one hour. The results showed that the modification of the revolving tubes that was introduced to the MSD system did not affect the pressure distribution of the SD system. The explanation to this case is, the temperature was rising slowly, and there were two pressure outlets. The outlet pressure keeps the pressure in balance with the surrounding atmosphere.

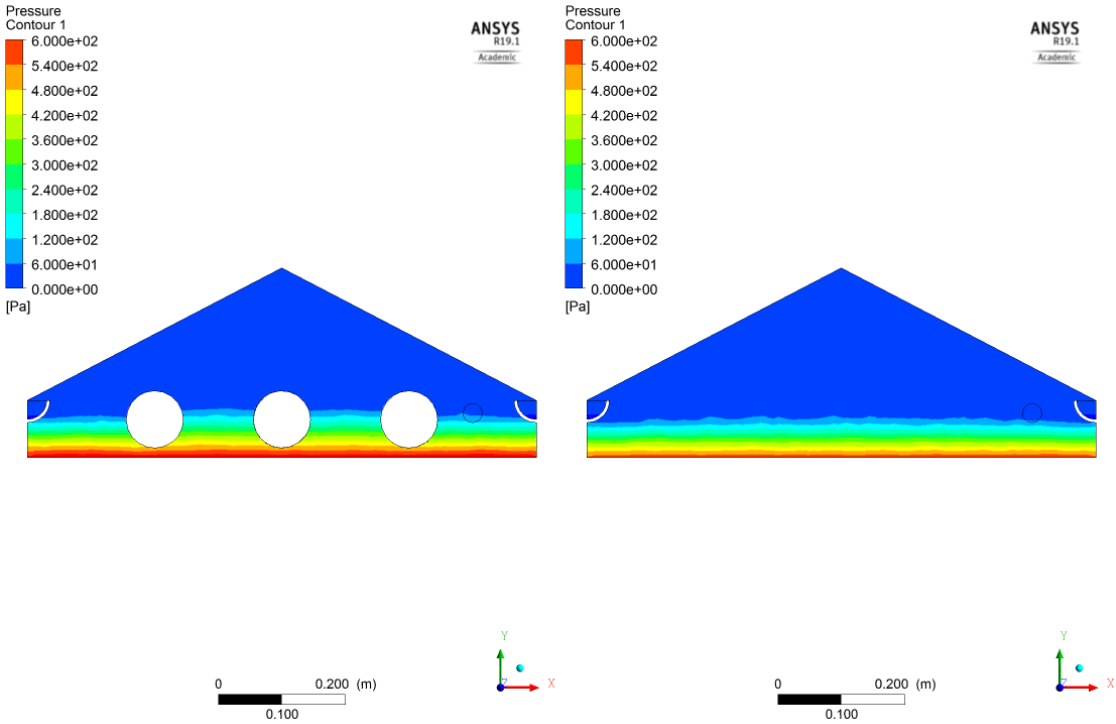

Figure 5. 4 The pressure contours of the central cross-section of the MSD system (left) and the NSD system (right). Orthogonal solar radiation = 1000 W/m^2, ambient temperature = 300 K, wind Speed = 5 m/s, atmospheric pressure = 1 bar, tube's rotation speed = 40 rpm, water depth = 40 mm, tube's diameter = 90 mm

5.1.4 Density

Figure 5.5 shows the density contours of a central cross-section of both the MSD and the NSD systems. The results showed that the density distribution within the MSD system is closely similar to that of the NSD system except for a thin layer of water density around the circumferences of the revolving tubes in the MSD system. There were three main distinctive zones; the upper zone which is occupied by the vapour with density of about (0.7 kg/m^3), the lower zone which is occupied by water with density of about (998 kg/m^3), and the in-between zone (layer), which is a mixture between the vapour and the water. According to the results, the MSD system has the advantage of increasing the surface area of the evaporation, which leads to an increase in the evaporation rate.

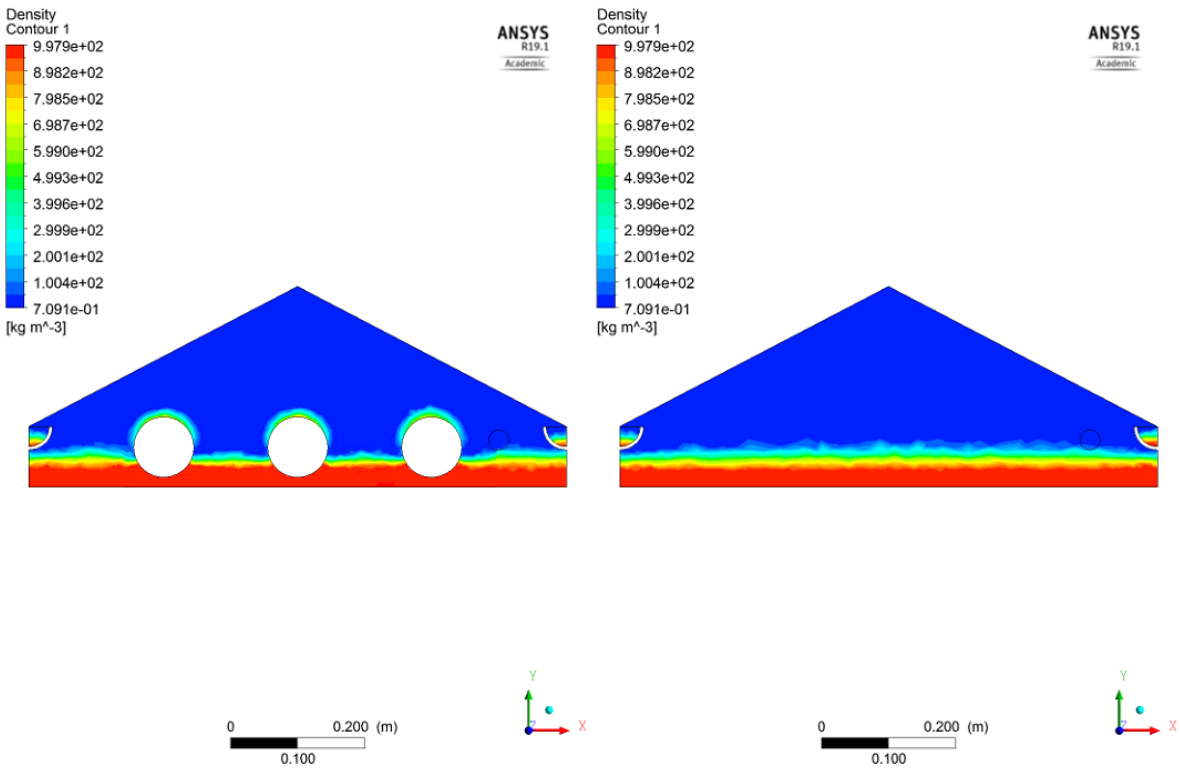

Figure 5. 5 The density contours of the central cross-section of the MSD system (left) and the NSD system (right)

Orthogonal solar radiation = 1000 W/m^2, ambient temperature = 300 K, wind Speed = 5 m/s, atmospheric pressure = 1 bar, tube's rotation speed = 40 rpm, water depth = 40 mm, tube's diameter = 90 mm

5.1.5 Velocity

Figure 5.6 shows the velocity contours of a central cross-section of both the MSD and the NSD systems. The results showed that the MSD system has a higher vapour velocity than the NSD system. The explanation to this case is that the flow inside the cavity of the MSD system was more turbulence than the NSD system due to the modification of the revolving tubes. According to the results, the vapour velocity ranged from (0 m/s) to about (0.3 m/s).

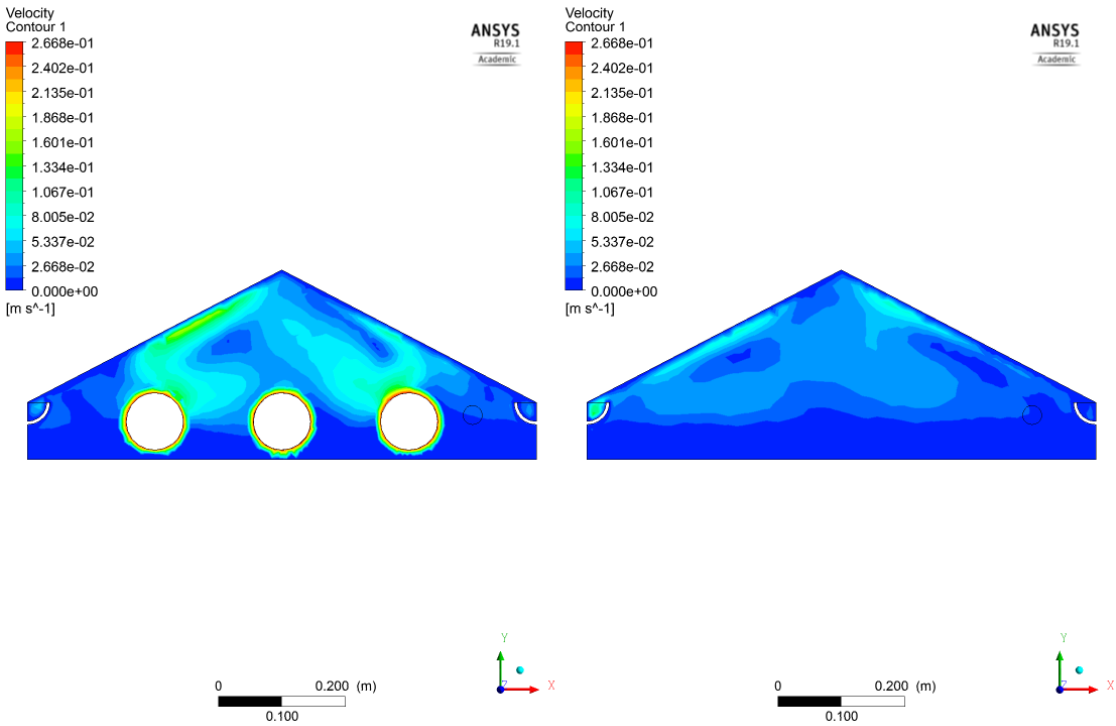

Figure 5. 6 The velocity contours of the central cross-section of the MSD system (left) and the NSD system (right)

Orthogonal solar radiation = 1000 W/m^2, ambient temperature = 300 K, wind Speed = 5 m/s, atmospheric pressure = 1 bar, tube's rotation speed = 40 rpm, water depth = 40 mm, tube's diameter = 90 mm

5.1.6 Evaporation and Condensation

Figure 5.7 shows the evaporation rate of the MSD and the NSD systems after one hour. Figure 5.8 (a) and (b) show the progressive condensation film mass of the MSD system and the NSD system at two different times. The results show that the MSD system has higher evaporation and higher condensation rates than the NSD system. According to the results, the evaporation and condensation rates of the MSD system were about double that of the NSD system. The explanation to this results is, the water temperature of the MSD system was higher than the water temperature of the NSD system (as presented in section 5.1.2, figures 5.2 & 5.3), which means faster evaporation. Since temperature is a big factor on the amount of the water particles that evaporate, causes them to move upward far from the water surface towards the cover of the SD system. Another reason is, the surface area of the evaporation in the MSD system was greater than that in the NSD system, which also leads to an increase in the evaporation rate. The increase in the evaporation enhances the possibility of an increase in the condensation hence increase the productivity of the SD system.

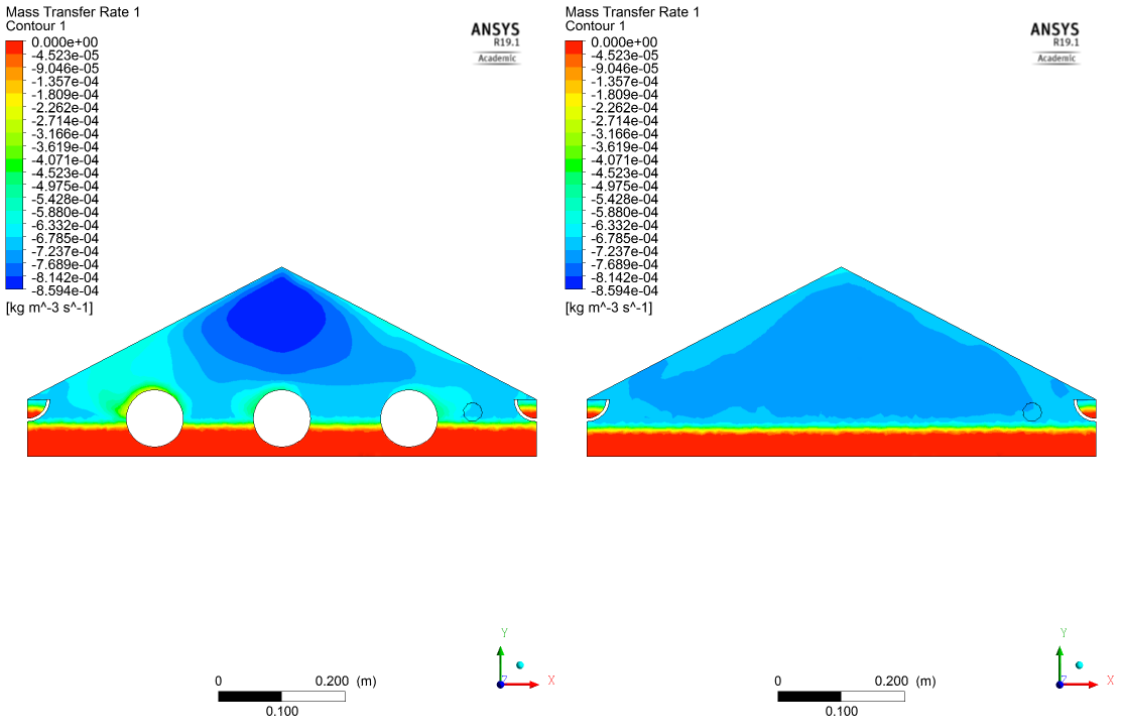

Figure 5. 7 The evaporation rate in the middle plane of the MSD system (left) and the NSD system (right) after 1 hour. Orthogonal solar radiation = 1000 W/m^2, ambient temperature = 300 K, wind Speed = 5 m/s, atmospheric pressure = 1 bar, tube's rotation speed = 40 rpm, water depth = 40 mm, tube's diameter = 90 mm

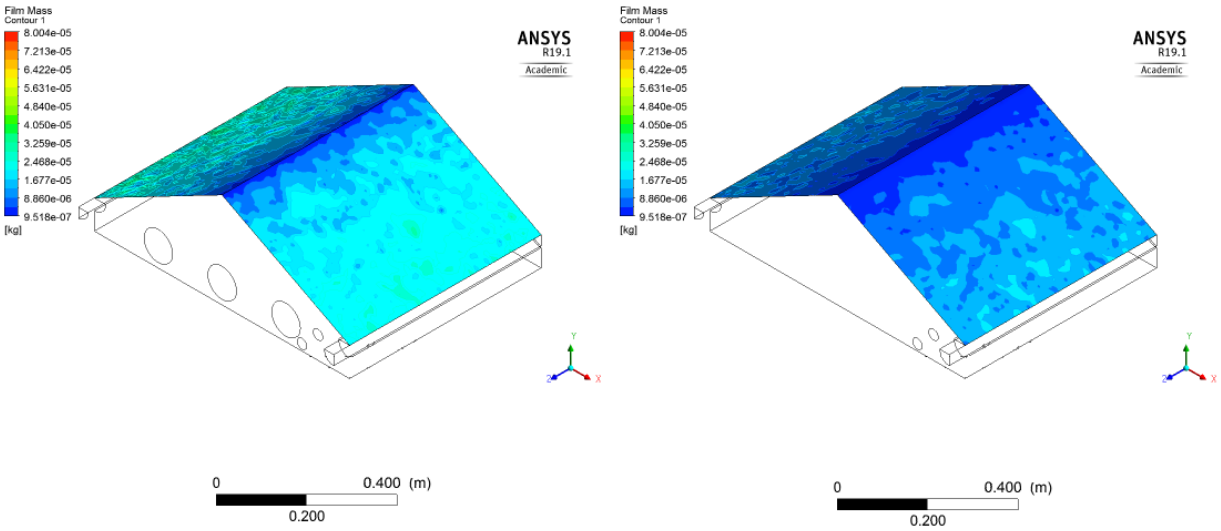

Figure 5.8 (a) The condensation film mass of the MSD system (left) and the NSD system (right) after 30 minutes

Orthogonal solar radiation = 1000 W/m^2, ambient temperature = 300 K, wind Speed = 5 m/s, atmospheric pressure = 1 bar, tube's rotation speed = 40 rpm, water depth = 40 mm, tube's diameter = 90 mm

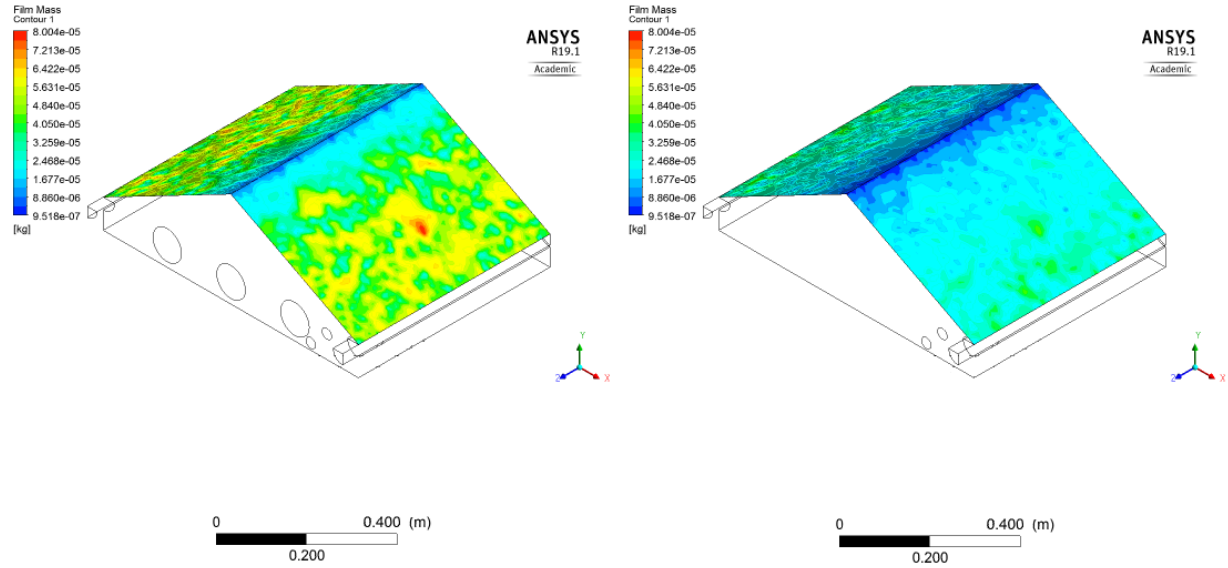

Figure 5. 8 (b) The condensation film mass of the MSD system (left) and the NSD system (right) after 1 hour

Orthogonal solar radiation = 1000 W/m^2, ambient temperature = 300 K, wind Speed = 5 m/s, atmospheric pressure = 1 bar, tube's rotation speed = 40 rpm, water depth = 40 mm, tube's diameter = 90 mm

5.2 Results of the Experimental Investigation

After conducting the experimental investigations (from the 4th of October 2017 to the 23rd of April 2018) and further investigations (from the 1st to the 17th of April 2019) to both the MSD and the NSD systems in the University of Southern Queensland-Toowoomba city- Australia, the following results were obtained.

5.2.1 Temperature Profile

The experimental data showed the following results;

1- In both the SD systems, the temperature starts rising at about 7:00 am, peaks at about 2:00 pm, and then starts declining slowly up to the next day morning.
2- In both the SD systems, the water temperature has the highest value during the peak time from about 2:00 pm to approximately 3:00 pm.
3- In both the SD systems, the vapour temperature could be a little higher than the water temperature before noon, then becomes nearly equal to the water temperature at noon, and then lower than the water temperature afternoon.
4- In both the SD systems, the basin temperature was nearly equal to the water temperature except for the noon period when the water temperature was a little higher than the basin temperature.
5- In both the SD systems, during the peak time, the highest temperature was the temperature of the water and vapour followed by the temperature of the basin and then the temperature of the cover.
6- In both the SD systems, the cover temperature had the lowest temperature values, and it could be lower than the ambient temperature during the night and up to the early morning of the next day.
7- The temperature of the MSD system was always higher than the temperature of the NSD system, especially during the noon period or the peak time.
8- During the peak time, the temperature of the MSD system was higher than the temperature of the NSD system by an average of 5℃ for the temperature of the water, vapour, and the basin, and by an average of 3℃ for the temperature of the cover.

9- During the peak time, the average temperature difference between the water and the cover was about 15℃ in the MSD system and about 12℃ in the NSD system.

Table 5.1 lists the average temperature values during the noon and the maximum-recorded temperature in both SD systems.

Table 5. 1 The temperature of the MSD system and the NSD system (the average value is from the maximum temperature of all days, and the maximum value is the maximum recorded during the whole period of the experiment)

	Average Temperature (℃)		***Maximum Temperature (℃)***	
	MSD	***NSD***	***MSD***	***NSD***
Water temperature	*55.7*	*50.5*	*73.9*	*68.6*
Vapour temperature	*54.6*	*49.5*	*74.2*	*69.3*
Basin temperature	*53.4*	*48.1*	*70.1*	*65.4*
Cover temperature	*41.9*	*38.9*	*57.7*	*55.1*

Figure 5.10 shows the temperature profile of the water, the vapour, the cover, the basin, and the ambient temperature of both the MSD and the NSD systems over a period from 6:00 am of the 4th of April 2019 to 7:00 am of the next day the 5th of April 2019.

The temperature profile of selected days, during the experiment period, is presented in Appendix A.

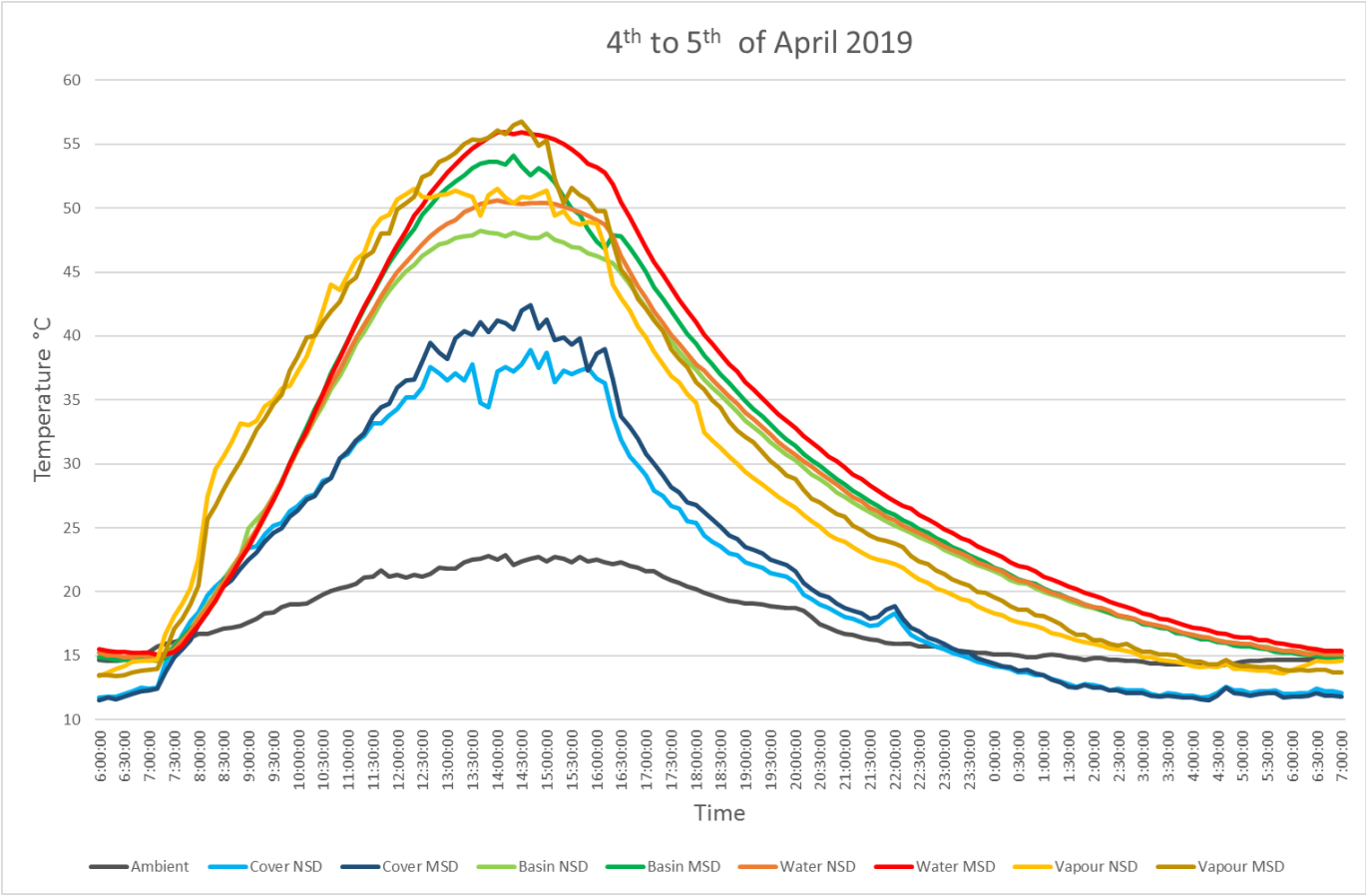

Figure 5. 9 The temperature profile of the components of the MSD system and the NSD system

5.2.2 Productivity

The productivity or the distillate yield of both the NSD and the MSD systems were recorded in two patterns, the daily productivity and hourly productivity. The daily productivity was recorded during the whole experiment period while the hourly productivity was conducted for selected clear days about the middle of every month.

5.2.2.1 Daily Productivity

The results show that the daily productivity of the MSD system was always higher than the daily productivity of the NSD system. According to the results, the average daily productivity of the MSD system and the NSD system for the whole experiment period were about ($965.5\ ml/day = 2.011\ l/m^2\ day$) and ($562.5\ ml/day = 1.172\ l/m^2\ day$), respectively. The maximum daily productivity of the MSD system and the NSD system were ($1396\ ml/day = 2.908\ l/m^2\ day$) and ($809\ ml/day = 1.685\ l/m^2\ day$), respectively. The maximum daily productivity was recorded on the 15th of December 2017 due to the high solar insolation, which was $31.4\ MJ/m^2$.

Figure 5.11 shows the daily productivity of the first experiment period from the 4th to the 15th of October 2017 and Figure 5.12 shows the daily productivity from the 1st of November 2017 to the 23rd of April 2018 for both the MSD and the NSD systems.

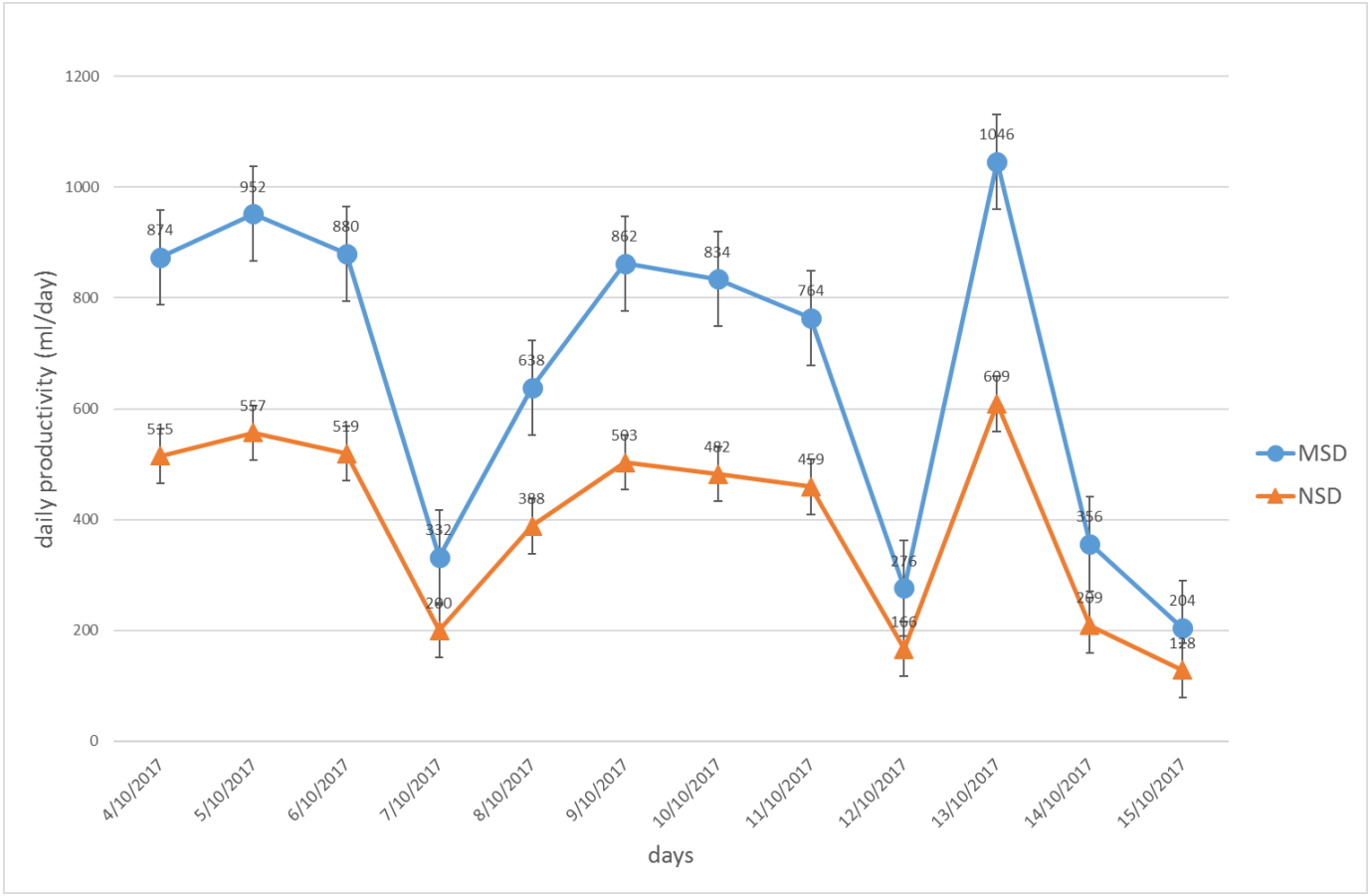

Figure 5. 10 The daily productivity of the MSD system and the NSD system during October 2017

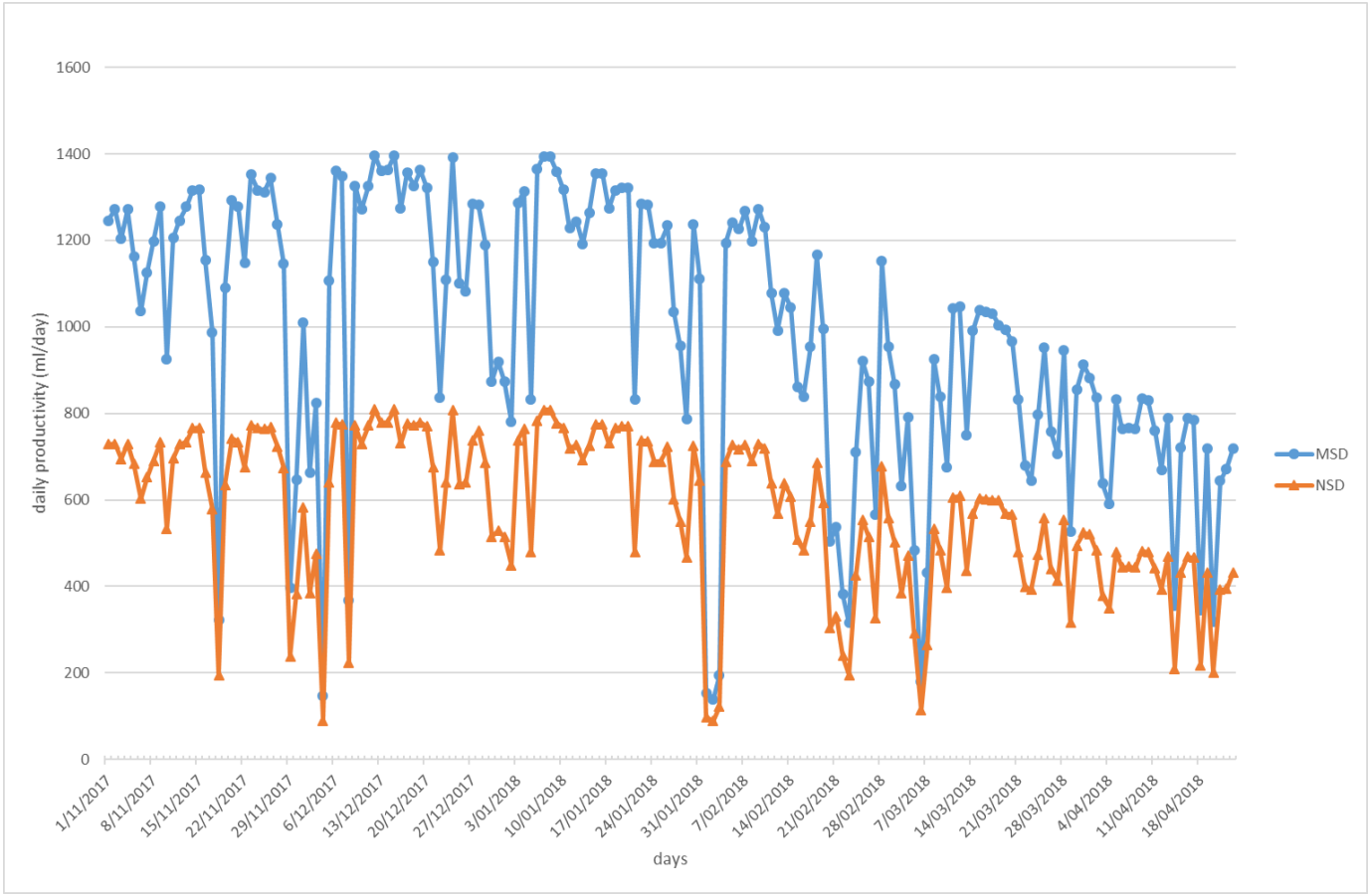

Figure 5. 11 The daily productivity of the MSD system and the NSD system from the 1st of November 2017 to the 23rd of April 2018

5.2.2.2 Hourly Productivity

The results show that the hourly productivity of the MSD system was always higher than the productivity of the NSD system. The hourly data collection was conducted for selected clear days around the middle of every month during the experimental period. The hourly productivity was measured every hour from 9:00 am to 5:00 pm. According to the results, the maximum hourly productivity was during noon or the peak time about 2:00 pm. The selected days are; the 13th of October 2017, the 15th of November 2017, the 14th of December 2017, the16th of January 2018, the 14th of February 2018, the16th of March 2018, and the 16th of April 2018.

Figures 5.13 and 5.14 show the hourly productivity and the cumulative hourly productivity on the 13th of October 2017 of both the MSD and the NSD systems.

The hourly productivity and the cumulative hourly productivity of selected days are presented in Appendix A.

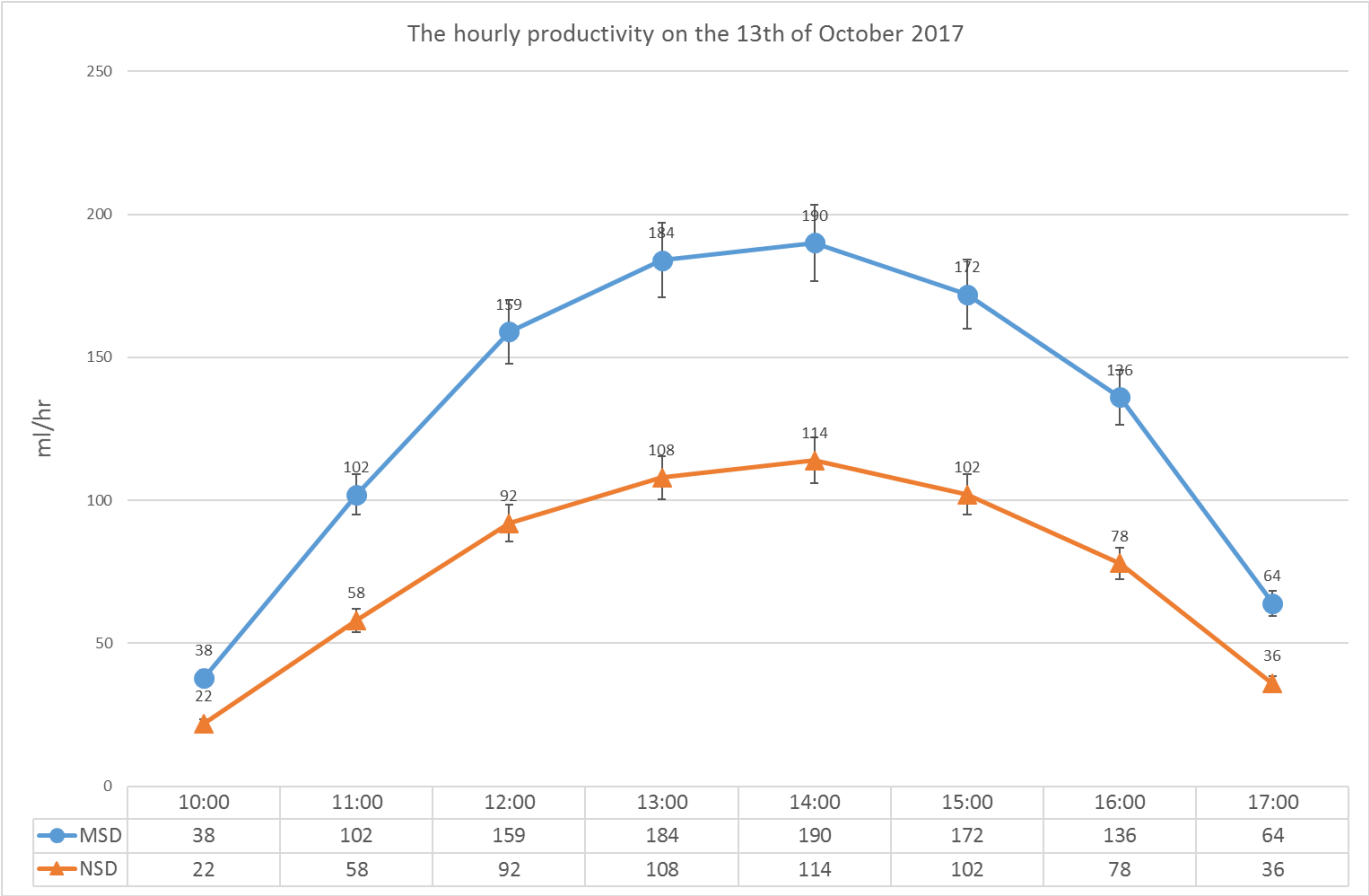

	10:00	11:00	12:00	13:00	14:00	15:00	16:00	17:00
MSD	38	102	159	184	190	172	136	64
NSD	22	58	92	108	114	102	78	36

Figure 5. 12 The hourly productivity the MSD and the NSD systems on the 13th of October 2017

The daily insolation 24.7 MJ/m^2, Max. Ambient temperature 27.5 ºC, Mean wind speed 16 km/hr, average relative humidity 56%

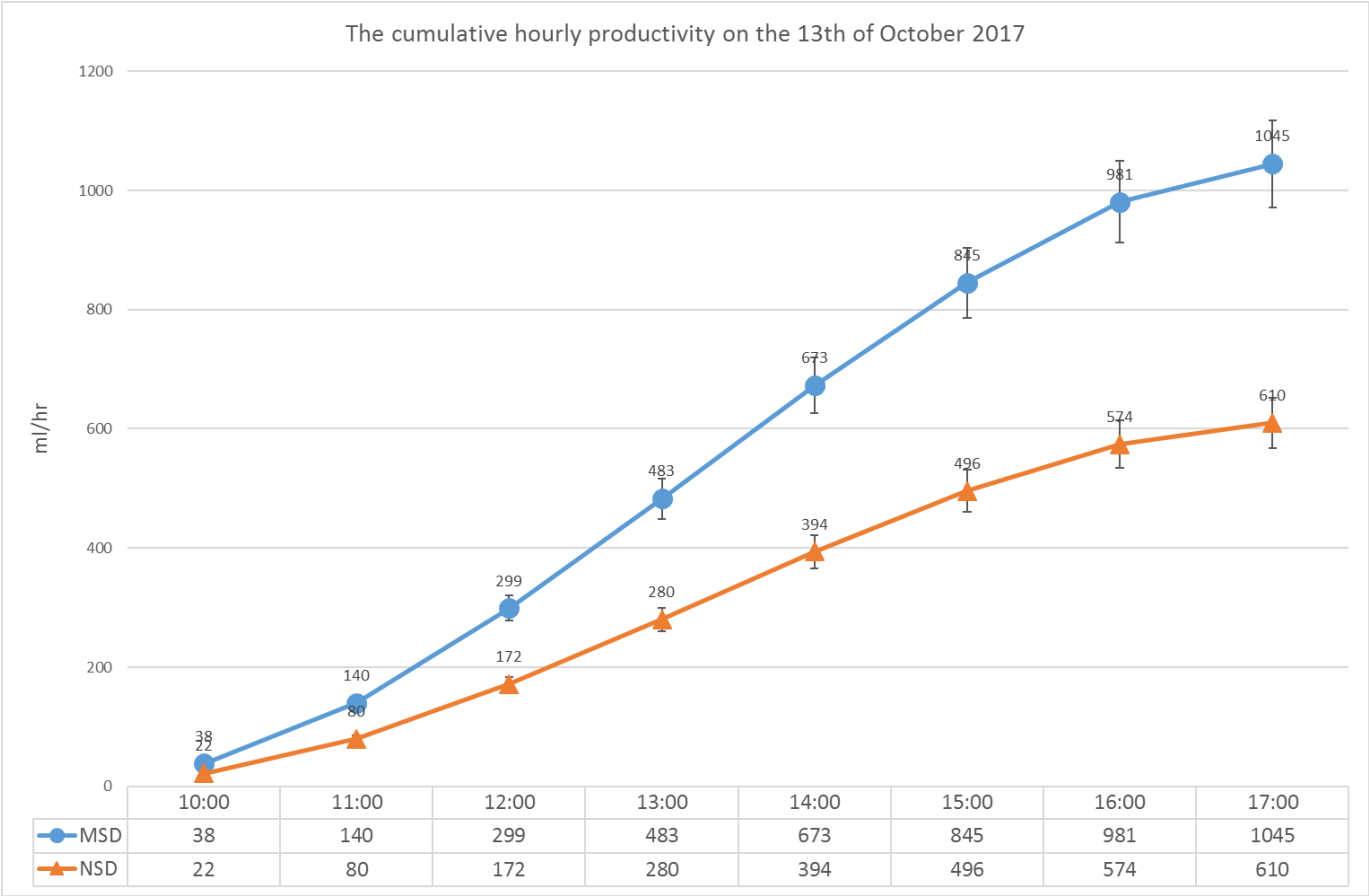

Figure 5. 13 The cumulative hourly productivity the MSD and the NSD systems on the 13th of October 2017

The daily insolation 24.7 MJ/m^2, Max. Ambient temperature 27.5 ºC, Mean wind speed 16 km/hr, average relative humidity 56%

5.2.3 Efficiency

The daily and the hourly efficiency for both the SD systems were estimated as follows;

5.2.3.1 Daily efficiency

The daily efficiency η can be found from equations 3.2 and 3.3 in Chapter Three, or as follows;

$$\eta\% = \frac{The\ heat\ used\ in\ the\ evaporation\ (output)}{The\ total\ supplied\ heat\ (input)} \times 100\% \quad (5.1)$$

From the above equation, the efficiency of the NSD system η_{NSD} will be;

$$\eta_{NSD}\% = \frac{\dot{m}_e \times L_v}{G_s \times A_s} \times 100\% \quad (5.2)$$

While the efficiency of the MSD system η_{MSD} will be;

$$\eta_{MSD}\% = \frac{\dot{m}_e \times L_v}{(G_s \times A_s) + E_m} \times 100\% \quad (5.3)$$

Where; $\dot{m}_e$ is the daily distillate yield or daily productivity, L_v is the latent heat of vaporisation, G_s is the daily solar exposure or the daily insolation, A_s is the surface area of the SD system, and E_m is the electric energy used to run the revolving tubes in the MSD system.

$$E_m = V \times A \times number\ of\ hours \times 3600 \quad (5.4)$$

Where; $V\ and\ A$ are the voltage and the current that required to run three motors and were recorded from the power supply. ($V = 10\ V\ , and\ A = 5\ A$).

The results showed that the daily efficiency of the MSD system was always higher than the daily efficiency of the NSD system. According to the results, the average daily efficiency was 18.77% and 12.11% for the MSD system and the NSD system, respectively. The maximum daily efficiency was 21.01% and 13.12% for the MSD system and the NSD system, respectively.

Figure 5.15 shows the daily efficiency for the period from the 4th to the 15th of October 2017 and Figure 5.16 shows the daily efficiency from the 1st of November 2017 to the 23rd of April 2018 for both systems.

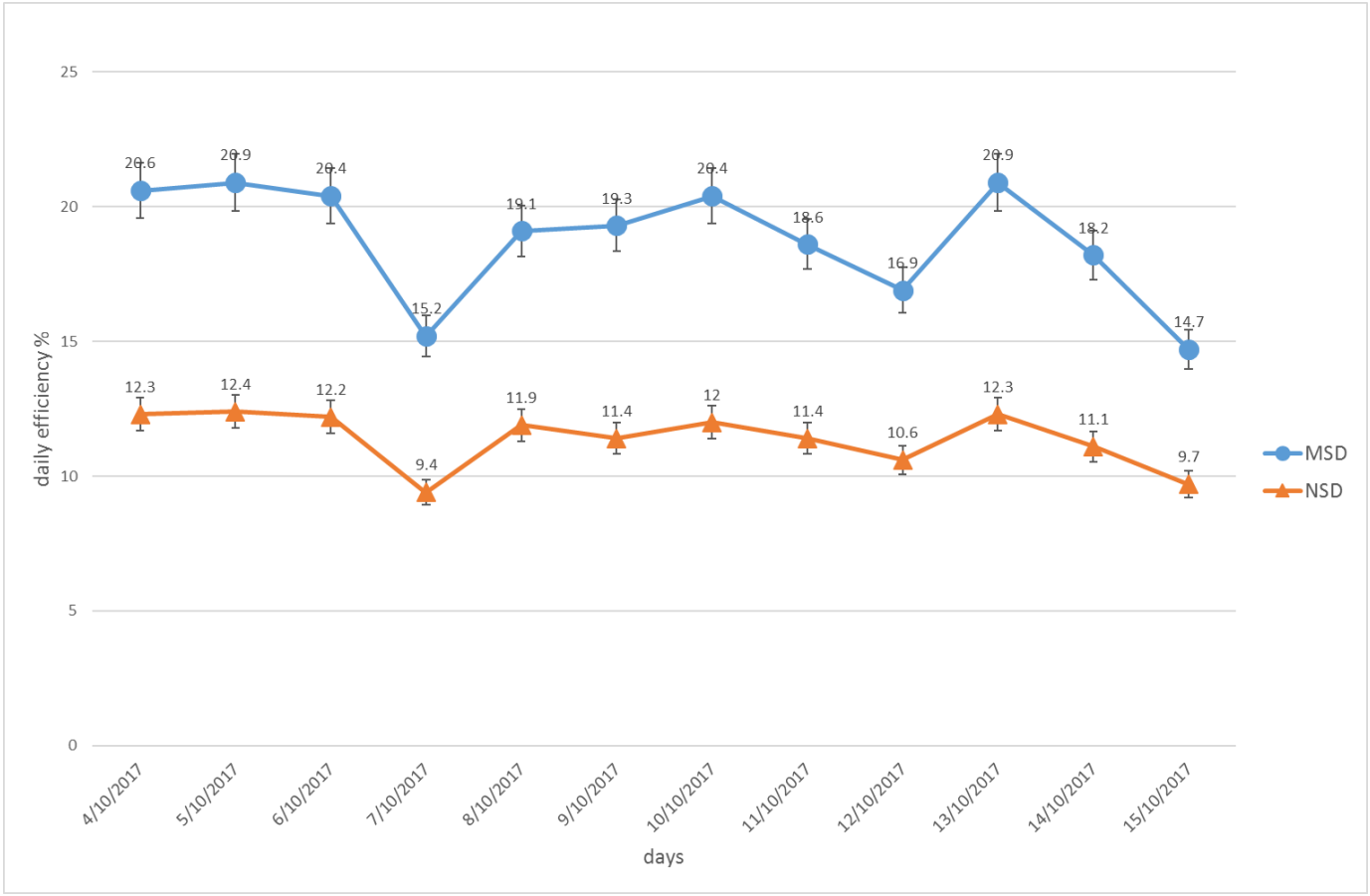

Figure 5. 14 The daily efficiency of the MSD system and the NSD system during October 2017

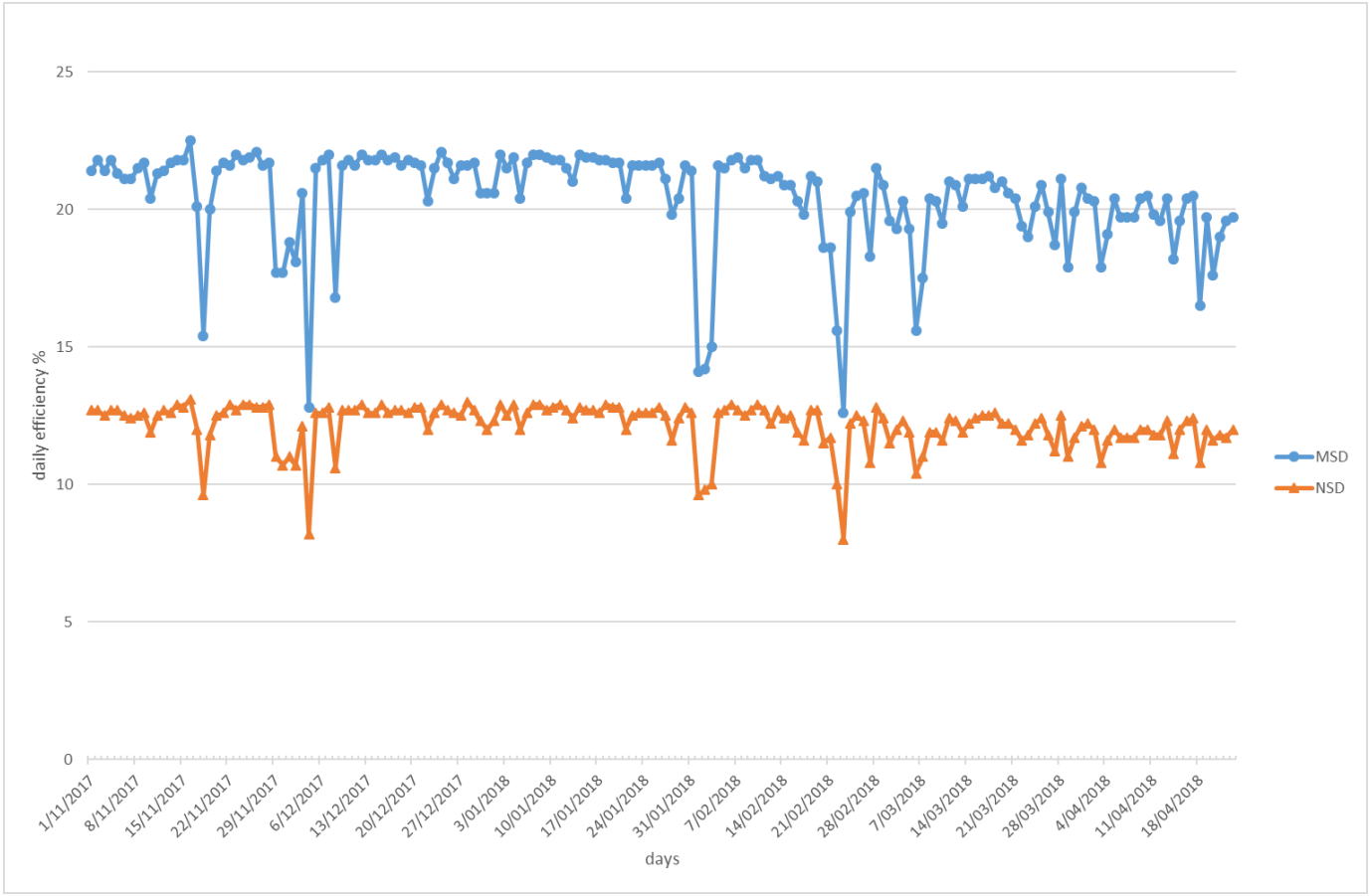

Figure 5. 15 The daily efficiency of the MSD system and the NSD system from the 1st of November 2017 to the 23rd of April 2018

5.2.3.2 Hourly efficiency

The same equations used in calculating the daily efficiency were used to calculate the hourly efficiency using the values of the hourly productivity and the hourly insolation. Similar to the hourly productivity the hourly efficiency was estimated to every hour from 10:00 am to 5:00 pm for the same selected days to conduct the hourly productivity as presented in section 5.2.2.2.

The results showed that the hourly efficiency of the MSD system was always higher than the hourly efficiency of the NSD system. According to the results, the average hourly efficiency for the conducted hours was 24.8% and 15.5% for the MSD system and the NSD system, respectively. The maximum hourly efficiency was recorded during the peak time about 2:00 pm on the 15th of November 2017 and it was 37.4% and 23.9% for the MSD system and the NSD system, respectively.

Figure 5.17 shows the hourly efficiency on the 13th of October 2017.

The hourly efficiency of selected days are presented in Appendix A. Table of the hourly insolation, hourly productivity, hourly efficiency, and the enhancement in the hourly productivity and hourly efficiency is presented in Appendix B.

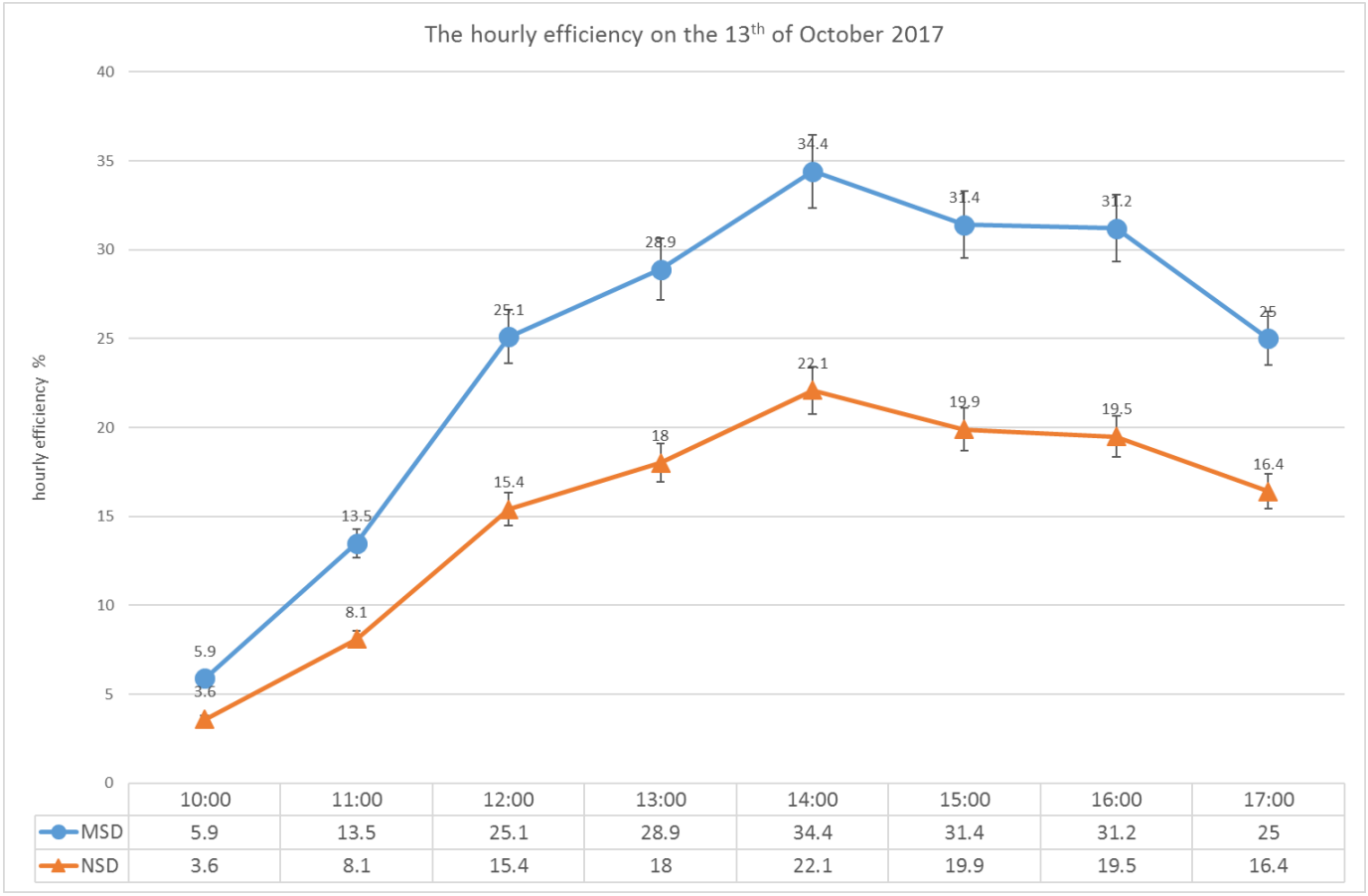

Figure 5. 16 The hourly efficiency of the MSD system and the NSD system on the 13th of October 2017

5.2.4 Enhancement in Productivity and Efficiency

The enhancement in daily productivity and the daily efficiency was found from the following relations;

$$Productivity\ Enhancement\% = \frac{MSD\ productivity - NSD\ productivity}{NSD\ productivity} \times 100\% \quad (5.5)$$

$$Efficiency\ Enhancement\% = \frac{MSD\ efficiency - NSD\ efficiency}{NSD\ efficiency} \times 100\% \quad (5.6)$$

According to the results, the average enhancement in daily productivity and daily efficiency was approximately 70.7% and 54.3%, respectively. The maximum enhancement in the daily productivity and the daily efficiency were about 74.8% and 63.4%, respectively.

Figure 5.18 shows the enhancement in the daily productivity and the daily efficiency of the MSD system with respect to NSD system for the period from the 4th to the 15th of October 2017. Figure 5.19 shows the enhancement in the daily productivity and the daily efficiency of the MSD system with respect to NSD system for the period from the 1st of November 2017 to the 23rd of April 2018.

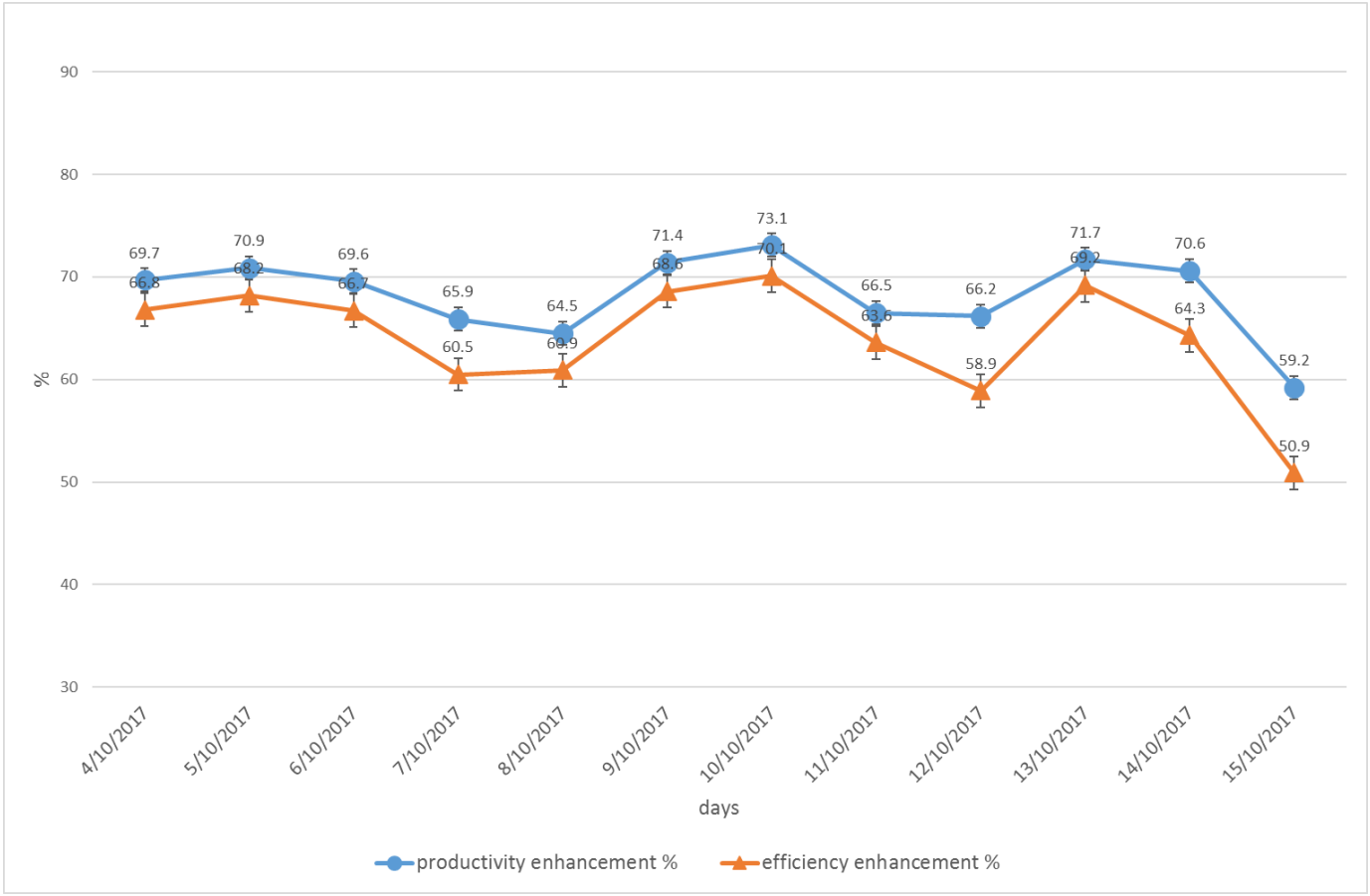

Figure 5. 17 The enhancement in the daily productivity and the daily efficiency of the MSD system respect to NSD system during October 2017

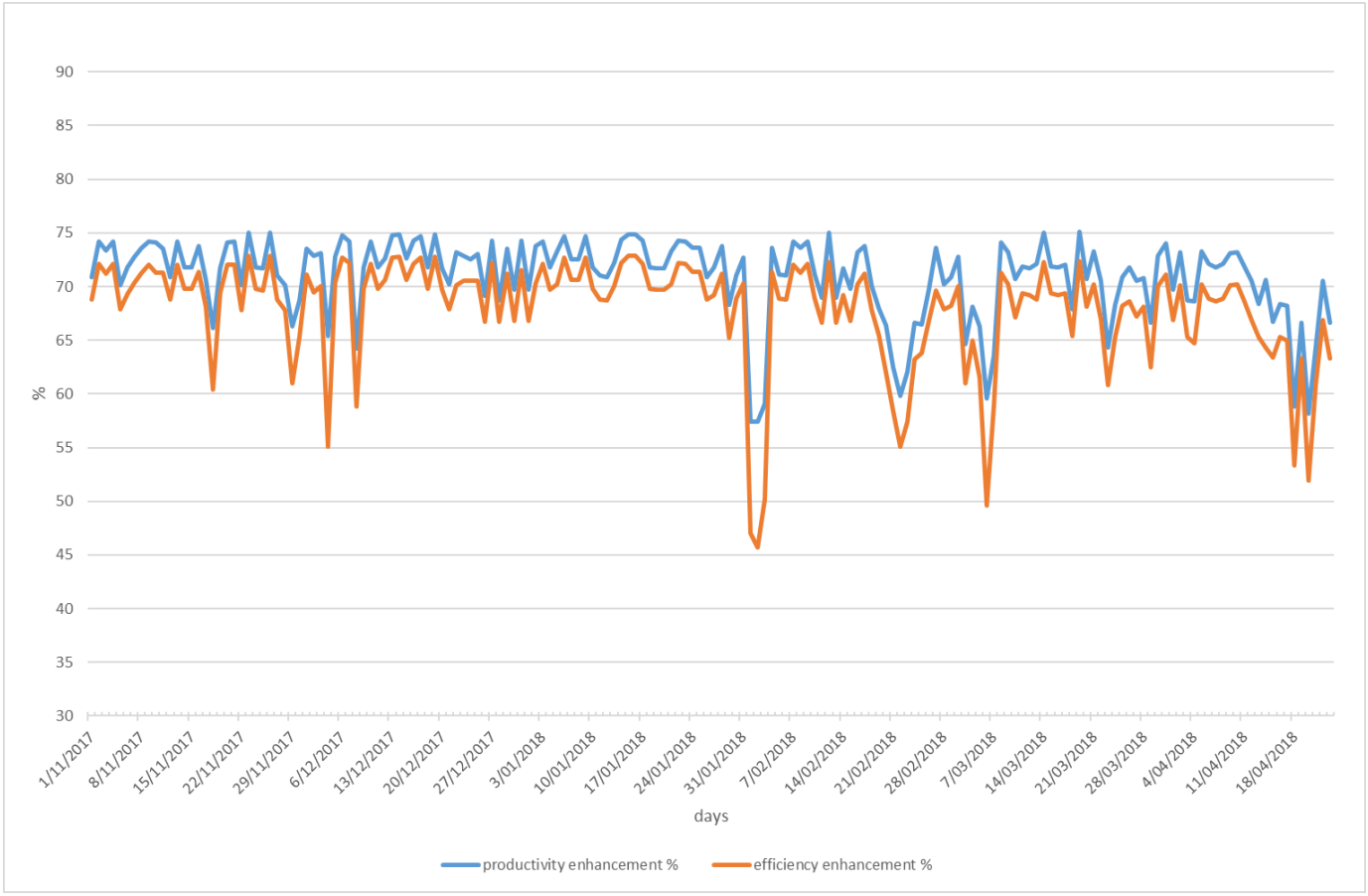

Figure 5. 18 The enhancement in the daily productivity and the daily efficiency of the MSD system respect to NSD system from the 1st of November 2017 to the 23rd of April 2018

5.2.5 Datasheets

As presented in Chapter Four, the data collection was recorded into three types of datasheets. The data from these data sheets were used in the previous sections to present the temperature profile, the hourly and daily productivity, the hourly and daily efficiency, and the enhancement in the daily productivity and efficiency.

Table 5.1 and Table 5.2 show a sample of the first and the second datasheets, respectively. The first datasheets of some selected days, the second datasheets of all days, and the third data sheet of all selected days are presented in Appendix B.

Table 5. 2 The first pattern of datasheets- the data of the 4th of April 2019 (the temperature used in figure 5.10)

Time	Water Temperature (ºC)		Vapour Temperature (ºC)		Basin Temperature (ºC)		Cover Temperature (ºC)		Ambient Temperature (ºC)	Wind speed (km/hr)	Relative Humidity (%)	Solar intensity (W/m^2)
	MSD	NSD	MSD	NSD	MSD	NSD	MSD	NSD				
10:00:00	31.3	30.2	38.4	37.2	31.4	31.1	26.4	26.7	19	2	67	703
10:10:00	32.6	31.4	39.9	38.1	32.9	32.3	27.2	27.4	19.1	21	65	722
10:20:00	34.1	32.6	40	38.5	34.3	33.5	27.5	27.6	19.4	23	64	742
10:30:00	35.5	33.9	41.1	39.7	35.5	34.6	28.5	28.7	19.8	2	64	759
10:40:00	36.9	35	41.9	40.3	37.1	35.8	28.9	28.9	20.1	27	58	775
10:50:00	38.3	36.2	42.7	41.5	38.4	36.9	30.4	30.4	20.3	23	56	789
11:00:00	39.6	37.4	44.1	42.8	39.7	38.1	31	30.8	20.4	31	57	798
11:10:00	41	38.5	44.6	44.1	40.9	39.4	31.8	31.7	20.6	18	58	809
11:20:00	42.3	39.6	46.1	44.5	42.1	40.3	32.4	32.2	21.1	11	56	819
11:30:00	43.5	40.8	46.6	46.2	43.4	41.5	33.7	33.2	21.2	6	57	826
11:40:00	44.7	41.8	48	46.6	44.6	42.6	34.4	33.2	21.7	27	54	831
11:50:00	46	42.7	48	47	45.7	43.5	34.7	33.8	21.2	24	57	828
12:00:00	47.1	43.6	49.9	48	46.6	44.3	36	34.3	21.3	19	55	833
12:10:00	48.2	44.4	50.4	48.8	47.6	45.1	36.5	35.2	21.1	26	57	830
12:20:00	49.4	45.1	50.9	47.9	48.4	45.6	36.6	35.2	21.3	13	56	830
12:30:00	50.2	45.7	52.4	48.8	49.5	46.3	38	36	21.2	5	56	823
12:40:00	51.2	46.4	52.7	49.7	50.2	46.7	39.5	37.6	21.4	23	55	817
12:50:00	52	47	53.6	50.1	51	47.2	38.7	37.1	21.9	21	53	812
13:00:00	52.8	47.5	53.9	49.8	51.6	47.3	38.2	36.5	21.8	5	54	802

Table 5. 3 the second pattern of datasheets- the daily data of October 2017 (the data used in figure 5.11, 5.15, and 5.17)

Day	Daily Solar Exposure = Daily Insolation (MJ/m^2)	Daily Max. Ambient Temperature (°C)	Daily Ave. Wind Speed (km/hr)	Daily Ave. Relative Humidity (%)	Daily Ave. Cloud Amount (Oktas)	Daily Max. Water Temperature (°C)		Daily Max. Vapour Temperature (°C)		Daily Max. Basin Temperature (°C)		Daily Max. Cover Temperature (°C)		Daily Productivity (ml/day)		Daily Thermal Efficiency (%)		Daily Productivity Enhancement (%)	Daily Efficiency Enhancement (%)
						MSD	NSD	MSD	NSD	MSD	NSD	MSD	NSD	MSD	NSD	MSD	NSD		
4	20.9	26	6.5	62	3	53.3	50.4	54.3	48.7	50.3	45.1	42.2	37.7	874	515	19	12.3	69.7	53.8
5	22.4	28	9	60	5	57	54.5	55	52	56	50	45	42	952	557	19.4	12.4	70.9	55.9
6	21.2	29.3	22.5	45	1	52	49.3	51	48	50	48	43	40	880	519	18.8	12.2	69.6	53.9
7	10.6	18.8	25	88	1	35	33	34	32	34	32	30	29	332	200	13	9.4	65.9	37.9
8	16.3	22.6	14	73	1	50	48	49	47	48	45	40	38	638	388	17.3	11.9	64.5	45.2
9	22	28.9	22	63	1	54.9	53.3	56.4	55.3	54.4	52.1	44.6	43.6	862	503	17.8	11.4	71.4	56.1
10	20.1	30	6.5	44	2	59.4	56.5	55.2	54.6	57.4	55	42.5	41.2	834	482	18.7	12	73.1	56.2
11	20.2	26	17.5	74	2	57.1	56.8	59.7	57.1	55	54.7	39.9	38.6	764	459	17.1	11.4	66.5	50.4
12	7.8	22.9	23	91	8	32.4	31.4	31.6	29.7	31.7	30.7	25	23.7	276	166	13.9	10.6	66.2	30.2
13	24.7	27.5	16	56	2	59.5	56.8	57.1	55.8	56	54.4	41	40.2	1045	610	19.5	12.3	71.7	57.5
14	9.4	22	14	87	7	28.7	26.6	26.1	26.1	27.4	26.3	20.9	19.9	356	209	15.4	11.1	70.6	38.5
15	6.6	17.2	23	89	8	20.3	18.9	20.5	19.1	19.5	18.8	15.9	15.5	204	128	11.6	9.7	59.2	20.1

5.3 Mesh Independence Study

Mesh independence test has been conducted to show the sensitivity of the CFD results to the space discretization and to find the optimal mesh size that best represents the heat/mass flow within the SD systems in the shortest time possible without sacrificing the accuracy.

In this study, different mesh cell sizes (five grid-resolutions) have been considered from the coarser to the finer as presented in Table 5.4. to compare the results.

Table 5. 4 Mesh statistics and numerical results at different design points (grid size)

Design point	***Mesh cell Size*** (mm)	***Mesh Nodes***		***Mesh Elements***		***Mean Velocity*** (m/s)	
		MSD	***NSD***	***MSD***	***NSD***	***MSD***	***NSD***
1	*25*	*7995*	*7207*	*36996*	*34756*	*0.0734*	*0.0205*
2	*20*	*14260*	*12703*	*67690*	*62421*	*0.0704*	*0.0149*
3	*15*	*28217*	*24794*	*138762*	*125521*	*0.0681*	*0.0123*
4	*10*	*73122*	*62644*	*370205*	*323771*	*0.0675*	*0.0126*
5	*5*	*385288*	*341068*	*2038793*	*1839800*	*0.0678*	*0.0131*

According to the numerical results, the optimum mesh cell-size, which is considered in this CFD simulation, is 15 mm. The new finer meshing results differ by approximately $\pm 2\%$ of the previous mesh size. The current CFD simulation is considered to be as a mesh independent solution as long as the numerical results approximately stop varying with successive mesh refinements.

Figure 5.19 shows the mean velocity magnitude at different design points (grid size).

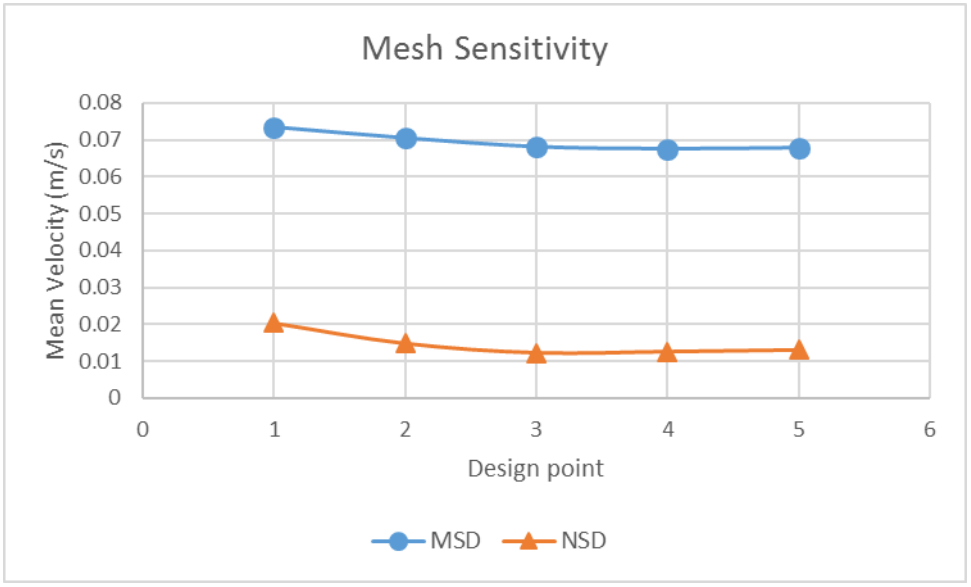

Figure 5. 19 Mean velocity at different design point (grid size) in the MSD and NSD systems. Operating conditions: Orthogonal solar radiation = 1000 W/m2, ambient temperature = 300 K, wind Speed = 5 m/s, atmospheric pressure = 100 kPa, water depth = 40 mm, tube's diameter = 90 mm, and tube's rotation speed = 40 rpm.

5.4 CFD Model Validation

In order to validate the CFD results of this work, the experimental data were used to compare with the results of the CFD simulation. The data included the hourly temperature of the water and the hourly productivity of both the MSD system and the NSD system.

The percentage differences between the CFD results and the experimental data were calculated using the following relation;

$$Difference\% = \frac{The\ CFD\ Value - The\ Experimental\ Value}{The\ Experimental\ Value} \times 100\% \qquad (5.7)$$

According to the results, the maximum percentage difference between the results of the CFD simulation and the data of the experimental investigation was approximately (±10%).

The difference between the results of the CFD simulation and the data of the experimental investigation were due to the assumptions made in the CFD model such as a fully insulated basin and an airtight cover. In the experiment, there were some heat losses from the basin and some vapour leakage from the cover.

The CFD simulation was run to model every hour and the results were recorded at the end of the simulation of the hour period. The average experimental data of every hour was applied to the CFD model for the initial and boundary conditions such as solar radiation, the ambient temperature, and the wind speed. The CFD simulation results showed good alignment with the experimental data.

Figure 5.20 shows the experimental and the CFD results for the temperature profile and Figure 5.21 shows the experimental and the CFD results for the cumulative hourly productivity on the 15th of November 2017 for both the SD systems.

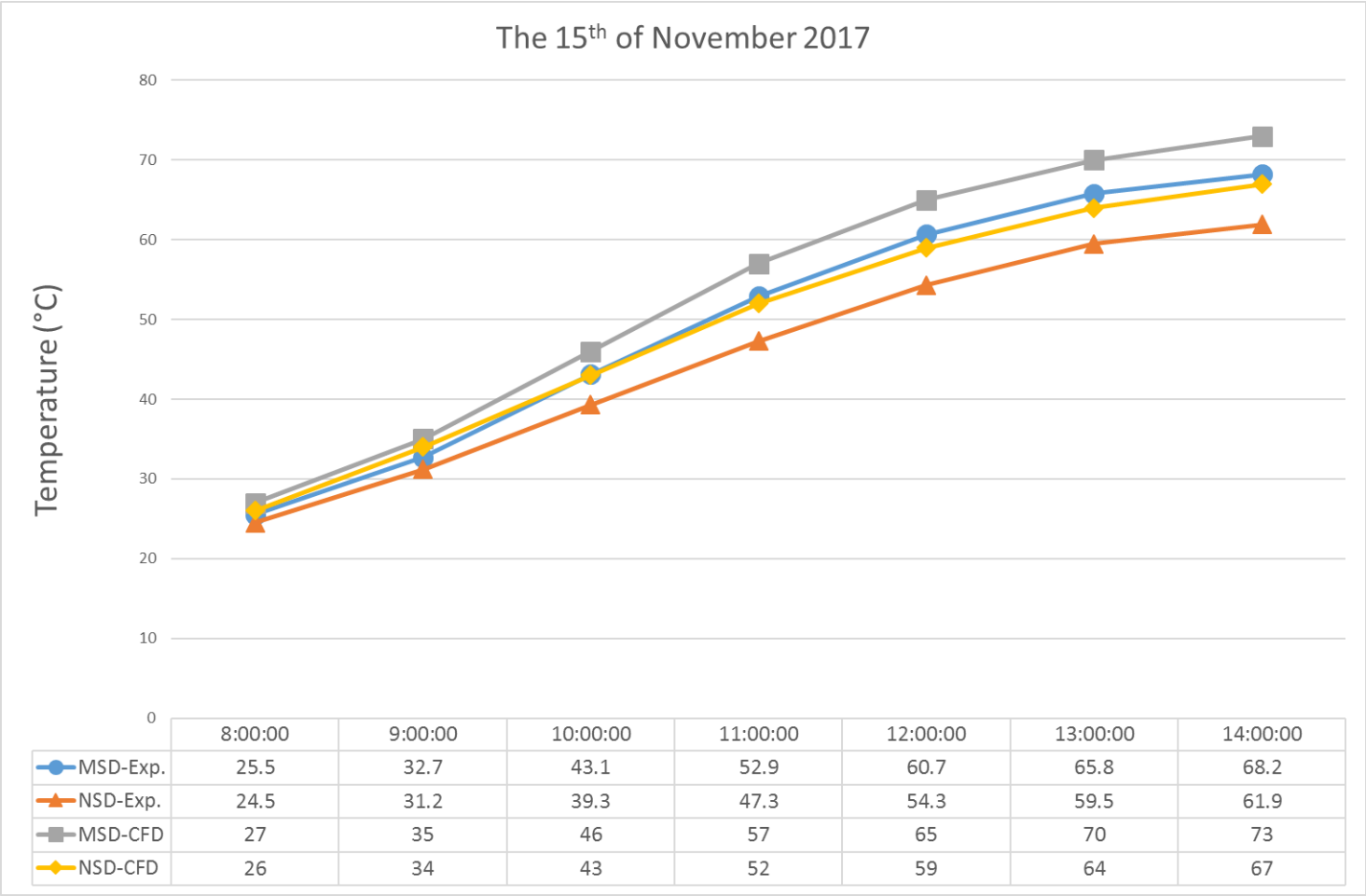

	8:00:00	9:00:00	10:00:00	11:00:00	12:00:00	13:00:00	14:00:00
MSD-Exp.	25.5	32.7	43.1	52.9	60.7	65.8	68.2
NSD-Exp.	24.5	31.2	39.3	47.3	54.3	59.5	61.9
MSD-CFD	27	35	46	57	65	70	73
NSD-CFD	26	34	43	52	59	64	67

Figure 5. 20 The water temperature profile of the MSD system and the NSD system on the 15th of November 2017 using the experimental (Exp.) and the simulation (CFD) data

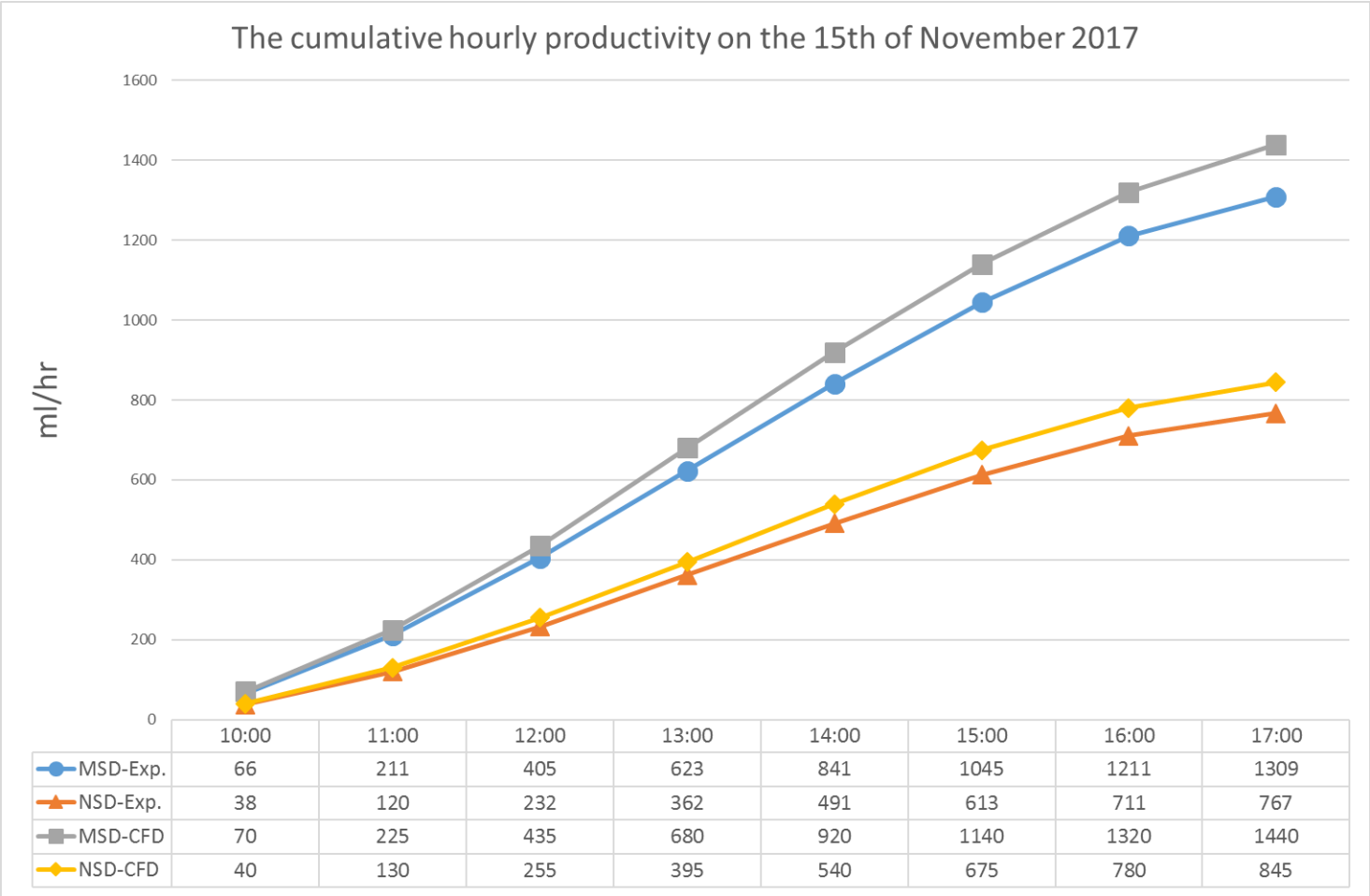

	10:00	11:00	12:00	13:00	14:00	15:00	16:00	17:00
MSD-Exp.	66	211	405	623	841	1045	1211	1309
NSD-Exp.	38	120	232	362	491	613	711	767
MSD-CFD	70	225	435	680	920	1140	1320	1440
NSD-CFD	40	130	255	395	540	675	780	845

Figure 5. 21 The hourly productivity of the MSD system and the NSD system on the 15th of November 2017 using the experimental (Exp.) and the simulation (CFD) data

6 Chapter Six: Analyses

This chapter deals with three significant analyses; which are the sensitivity analysis, the uncertainty analysis, and the cost analysis. In this work, the sensitivity analysis is used to estimate the SD system productivity depending on the input parameters such as; solar radiation, water depth, and water temperature. The uncertainty analysis is used to estimate the error in the measurements of the experimental data. The cost analysis is used to determine the cost-effectiveness of the proposed modification to the SD system. Figure 6.1 shows the flowchart of the current study and the three mentioned analysis.

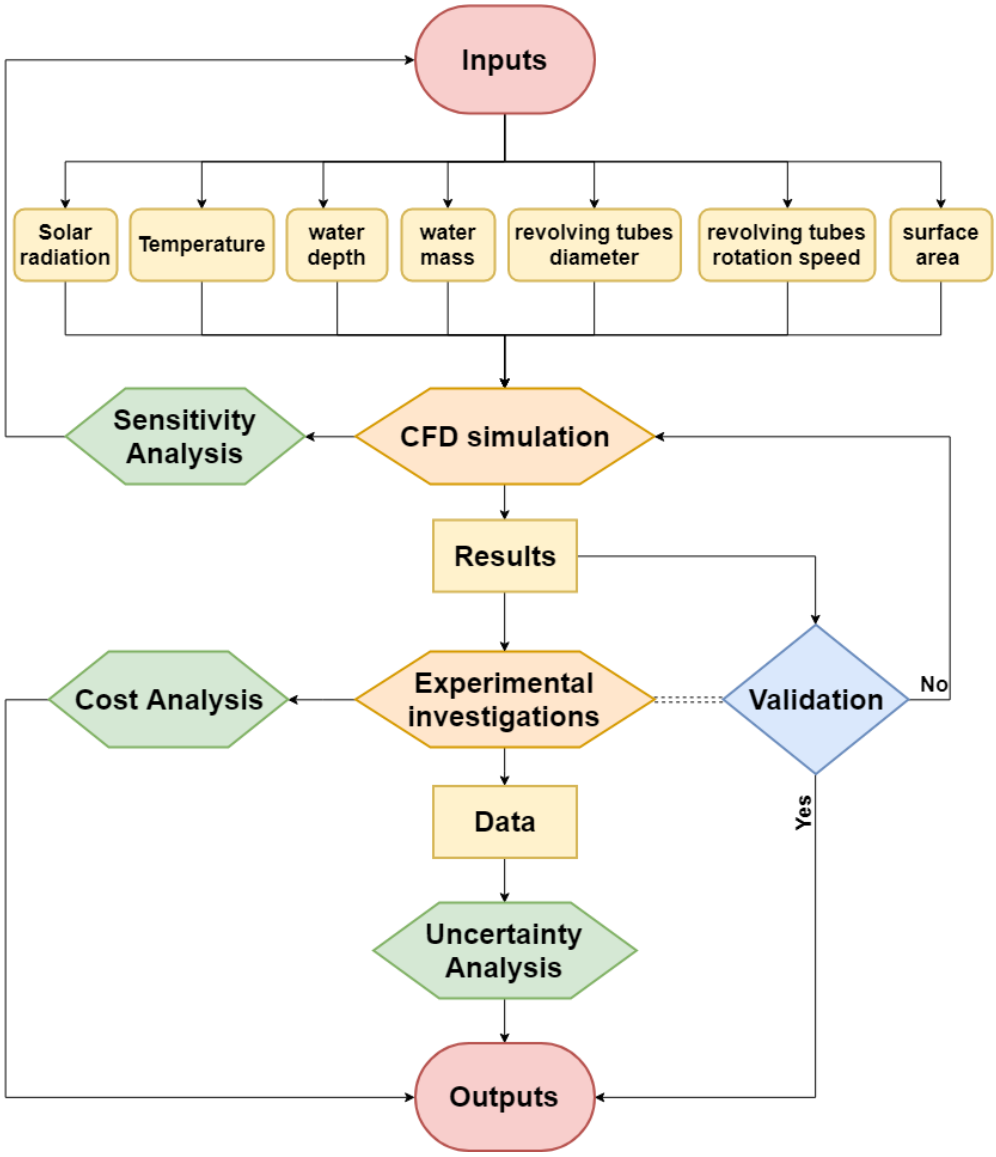

Figure 6. 1 The flowchart of the current study including the mentioned analysis

6.1 Sensitivity Analysis

As conducting several experiments under different design parameters is infeasible, the design of the SD systems was tested using the computer model before they were manufactured. Sensitivity analysis is a tool used to analyse and understand the effect of a set of independent variables on the dependent variable under certain specific conditions (Kleijnen, 2005). Sensitivity analysis is also known as (what-if) analysis to predict how changes in one variable affect the outcome.

Sensitivity analysis helps decision-makers to acquire a decent knowledge about how sensitive is the selected optimum design of the SD system to any modifications in the input values of one or more design parameters. Sensitivity analysis also helps in developing recommendations. Sensitivity analysis can be done using two different approaches, which are the regression analysis and dimensional analysis.

6.1.1 Regression Analysis

Regression analysis usually involves identifying the relationship between a dependent variable and one independent variable. Regression is a statistical measurement used to determine the strength of the relationship between one dependent variable (Y) and a series of other changing independent variables (X).

There are two kinds of regression; linear regression and nonlinear regression. Linear regression uses one independent variable (X) to predict the outcome of the dependent variable (Y) as follows Draper & Smith, 2014),

$$Y = a + bX + u \qquad (6.1)$$

In this case, the dependent variable Y is the SD system productivity; the independent variable X is the variable that affects the dependent variable Y, which in our case can be the solar radiation, the water temperatures, the cover temperature, the water depth, the rotation speed of the revolving tubes, or the diameter of the revolving tubes.

While, a and b are constant parameters (the intercept and the slope, respectively), and u is the regression residual or the unobserved random error or the uncertainty.

Nonlinear regression models are more complicated than linear regression because the function is created through a series of approximations (iterations) that may be obtained by trial-and-error (Draper & Smith, 2014).

Figure 6.2 shows the concept of the linear regression that is used in this study. Where the Y-axis is the dependent variable, which is the SD system productivity and the X-axis is the independent variable or the sensitive parameter, which is the solar radiation, the temperature of the water, the temperature of the cover, the water depth, the tubes diameter, or the tubes rotation speed.

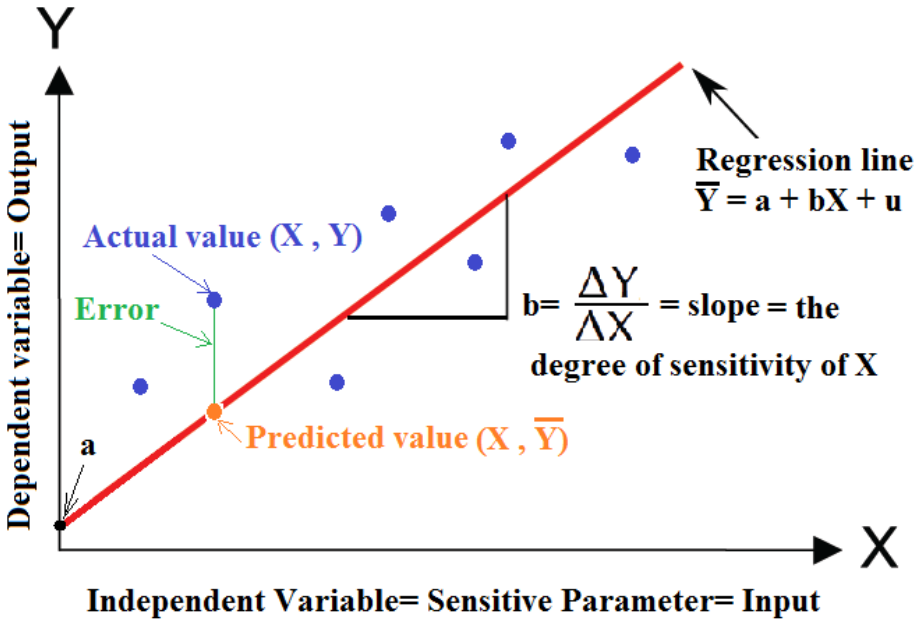

Figure 6. 2 The linear regression

The following sections present the sensitivity of each parameter (input) that affects the productivity (output) of both the SD systems using the CFD simulation data and the linear regression analysis.

6.1.1.1 Solar Radiation

Figure 6.3 shows the effects of solar radiation on the productivity of the MSD and the NSD systems. The readings of one hour modelling under the standard conditions were recorded. By changing the value of the solar radiation intensity and keeping other parameters at constant values, it can be noticed that the productivity increases as the solar radiation increases.

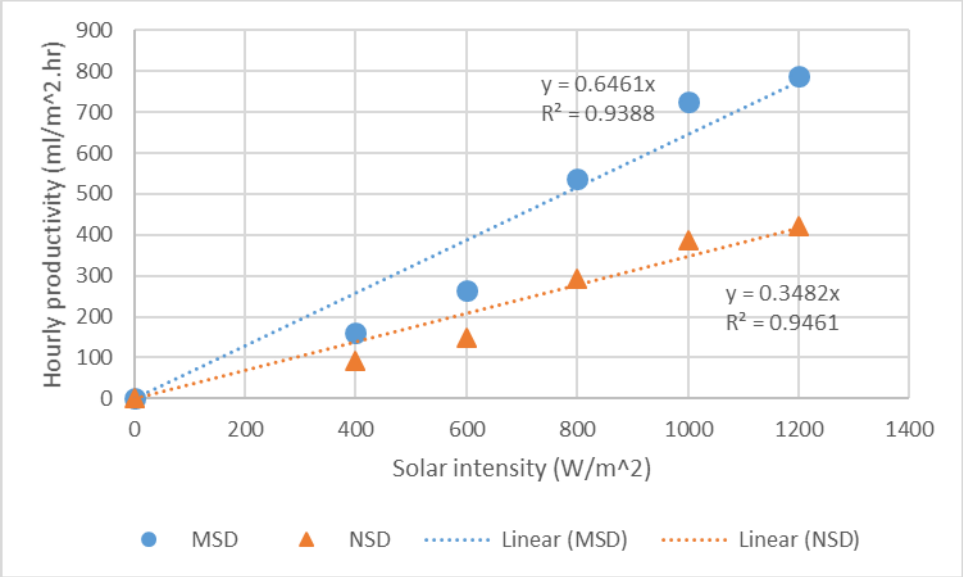

Figure 6. 3 A computational exploration of the effect of the solar radiation value on the hourly productivity of the MSD and the NSD systems. Ambient temperature = 300 K, wind Speed = 5 m/s, atmospheric pressure = 100 kPa, water depth = 40 mm, tube's rotation speed = 40 rpm, tube's diameter = 90 mm.

6.1.1.2 Temperature

Figures 6.4 and 6.5 show the effects of the water temperature and the cover temperature on the productivity of the MSD and NSD systems. By changing the initial values of the water temperature or the cover temperature and keeping other parameters at constant values, it can be noticed that the productivity of the SD systems increases with the increase of the water temperature or with the decrease of the cover temperature.

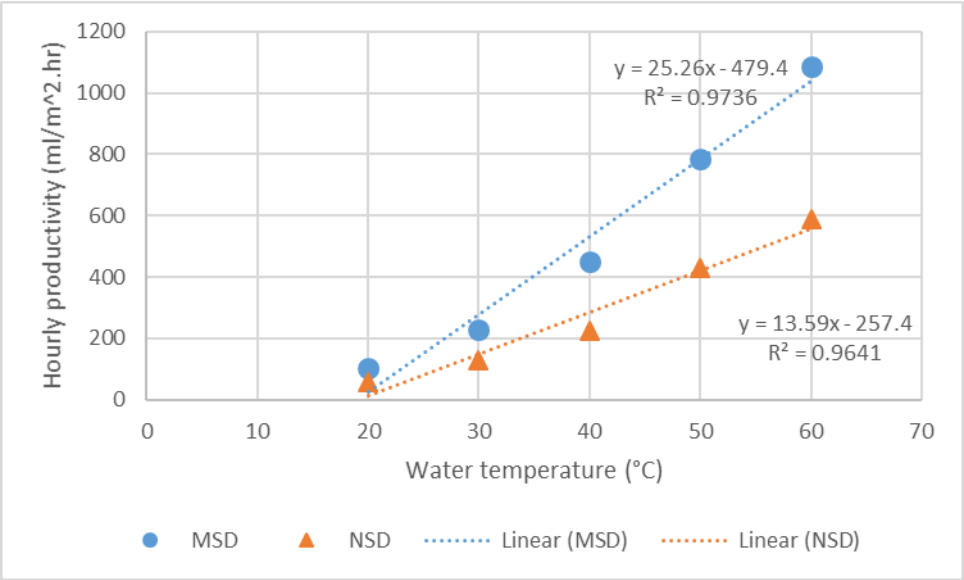

Figure 6. 4 A computational exploration of the effect of the water temperature on the hourly productivity of the MSD and the NSD systems. Orthogonal solar radiation = 1000 W/m^2, ambient temperature = 300 K, wind Speed = 5 m/s, atmospheric pressure = 100 kPa, water depth = 40 mm, tube's rotation speed = 40 rpm, tube's diameter = 90 mm.

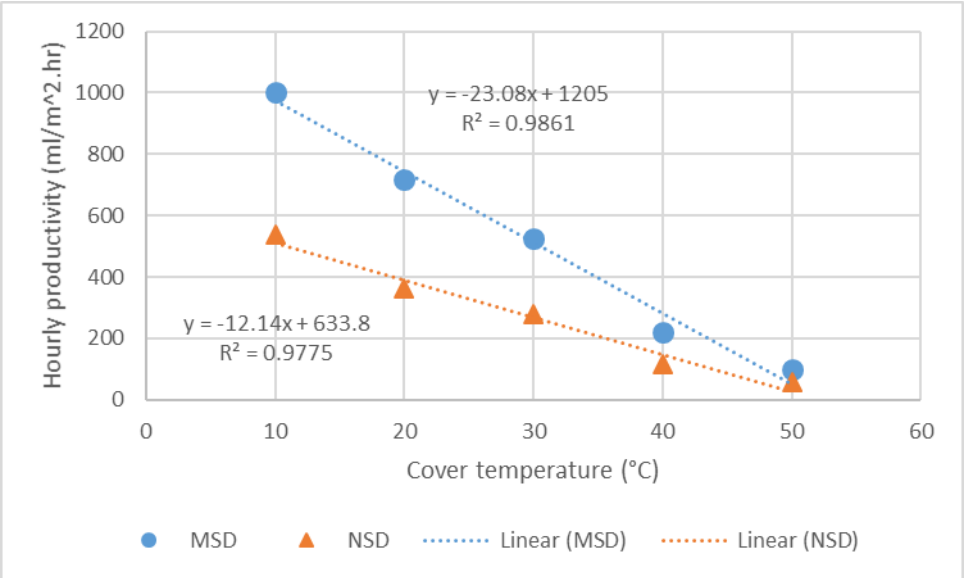

Figure 6. 5 A computational exploration of the effect of the cover temperature on the hourly productivity of the MSD and the NSD systems. Orthogonal solar radiation = 1000 W/m^2, ambient temperature = 300 K, wind Speed = 5 m/s, atmospheric pressure = 100 kPa, water depth = 40 mm, tube's rotation speed = 40 rpm, tube's diameter = 90 mm.

6.1.1.3 Water Depth

Figure 6.6 shows the effect of the water depth in the basin on the productivity of the MSD and the NSD systems. By changing the value of the water depth and keeping other parameters at constant values, it can be noticed that productivity of the SD systems increases with the decrease of the water depth. The changing in the water depth has less influence on the MSD system than the NSD system.

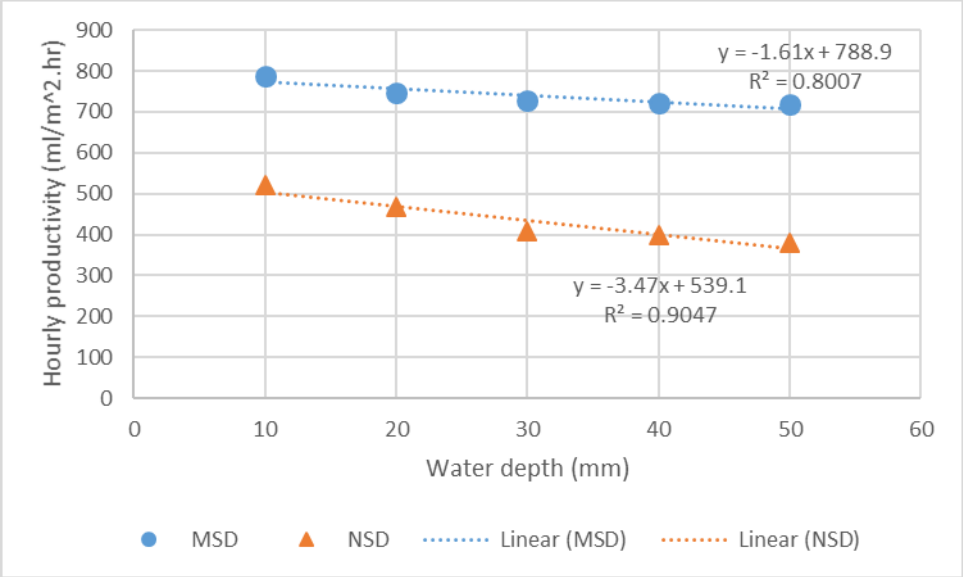

Figure 6. 6 A computational exploration of the effect of the water depth on the hourly productivity of the MSD and the NSD systems. Orthogonal solar radiation = 1000 W/m^2, ambient temperature = 300 K, wind Speed = 5 m/s, atmospheric pressure = 100 kPa, tube's rotation speed = 40 rpm, tube's diameter = 90 mm.

6.1.1.4 Revolving Tubes Diameter

Figures 6.7 shows the effect of the diameter of the revolving tubes on the productivity of the MSD system. By changing the value of the diameter of the revolving tubes and keeping other parameters at constant values, it can be noticed that productivity of the MSD system increases with the increase of the diameter of the revolving tubes. Figure 6.8 shows the percentage of enhancement in the productivity of the MSD system compared to the productivity of the NSD system at different values of the diameter of the revolving tubes for the MSD system. Note that the NSD system has no tubes and presented for comparison purpose.

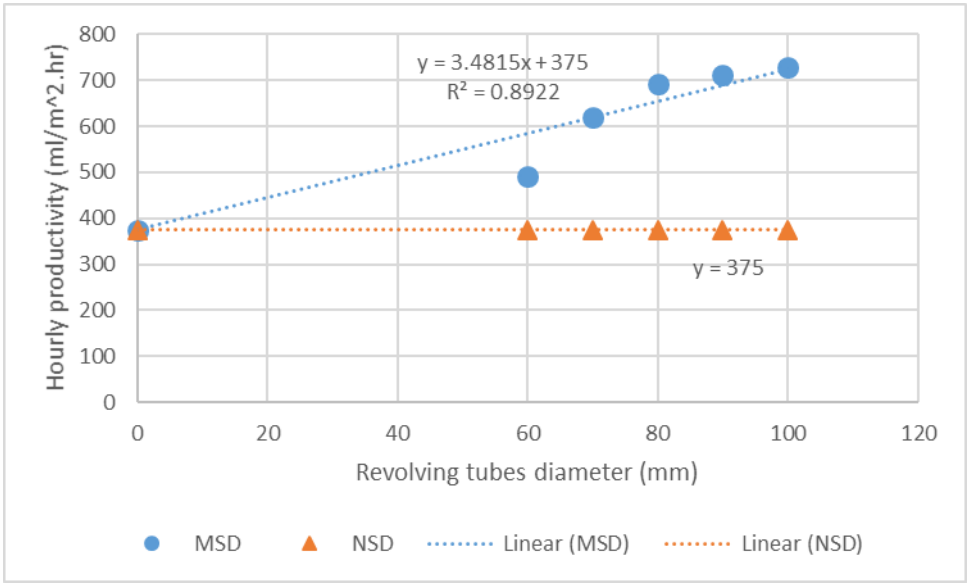

Figure 6. 7 A computational exploration of the effect of the diameter of the revolving tubes on the hourly productivity of the MSD system including the Zero value of the tube diameter whereas the MSD productivity is equal to the NSD productivity. Orthogonal solar radiation = 1000 W/m^2, ambient temperature = 300 K, wind Speed = 5 m/s, atmospheric pressure = 100 kPa, water depth = 40 mm, tube's rotation speed = 40 rpm.

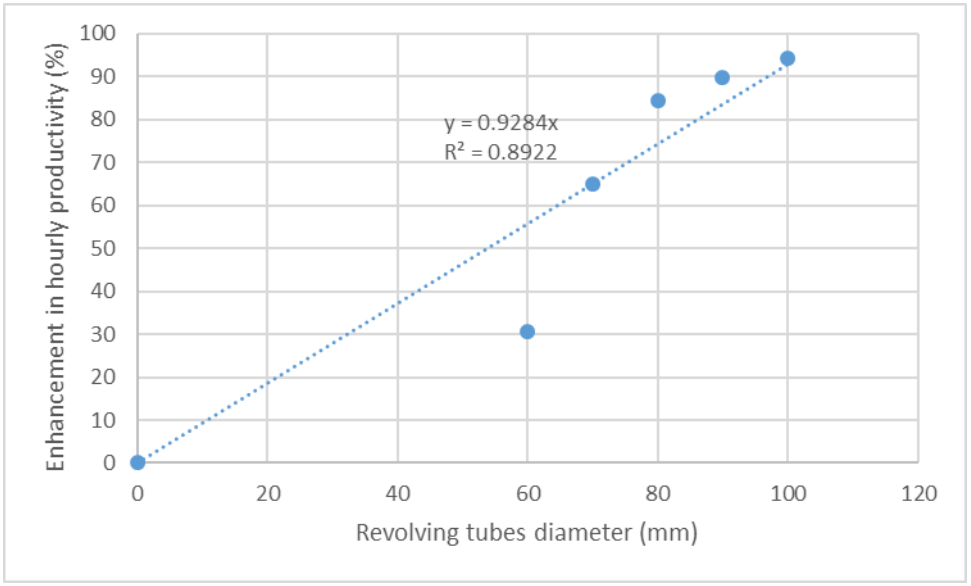

Figure 6. 8 A computational exploration of the percentage enhancement in hourly productivity of the MSD system according to the tube diameter. Orthogonal solar radiation = 1000 W/m^2, ambient temperature = 300 K, wind Speed = 5 m/s, atmospheric pressure = 100 kPa, water depth = 40 mm, tube's rotation speed = 40 rpm.

6.1.1.5 Revolving Tubes Rotation Speed

Figure 6.9 shows the effects of the rotation speed of the revolving tubes on the productivity of the MSD system. By changing the value of the rotation speed of the revolving tubes and keeping other parameters at constant values, it can be noticed that productivity of the MSD system increases with the increase of the rotation speed of the revolving tubes. Figure 6.10 shows the percentage of enhancement in the productivity of the MSD system compared to the productivity of the NSD system at different values of the rotation speed of the revolving tubes. It can be noticed that the revolving tubes have a negative effect on the productivity of the MSD system when they are stagnant or rotating at a low speed lower than 12 rpm. Note that the NSD system has no tubes and presented for comparison purpose.

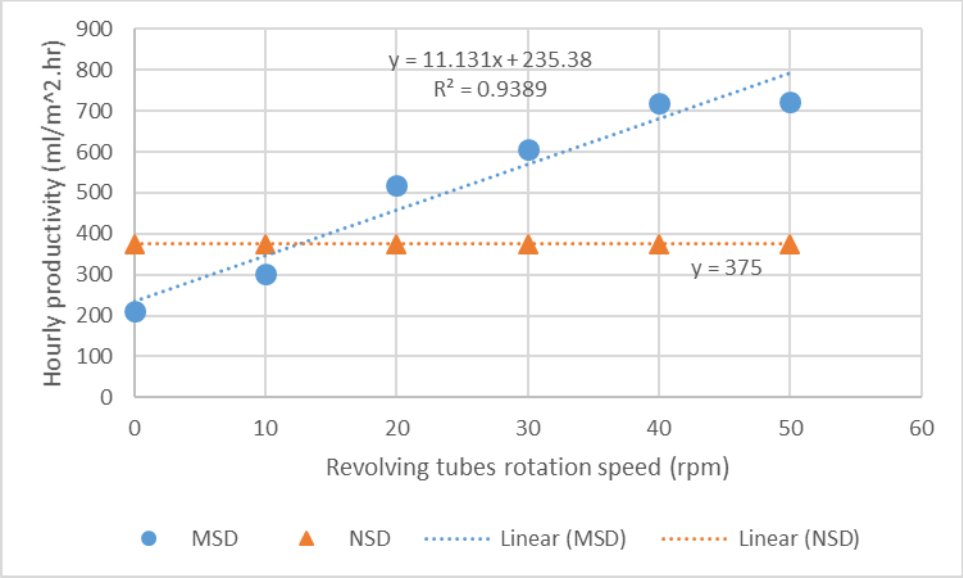

Figure 6. 9 A computational exploration of the effect of the rotation speed of the revolving tubes on hourly productivity of the MSD system. Orthogonal solar radiation = 1000 W/m^2, ambient temperature = 300 K, wind Speed = 5 m/s, atmospheric pressure = 100 kPa, water depth = 40 mm, tube's diameter = 90 mm.

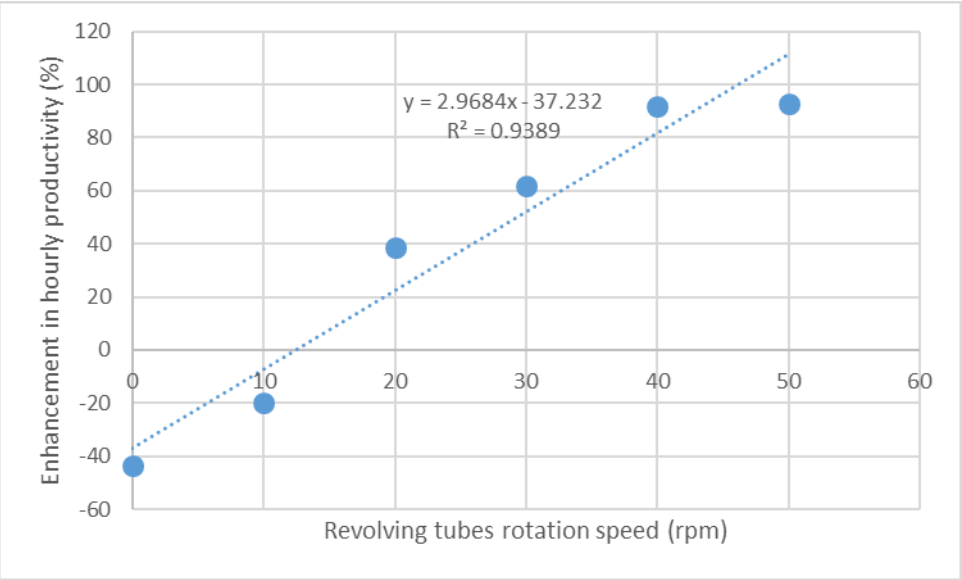

Figure 6. 10 A computational exploration of the percentage enhancement in hourly productivity of the MSD system according to the rotation speed of the revolving tubes. Orthogonal solar radiation = 1000 W/m^2, ambient temperature = 300 K, wind Speed = 5 m/s, atmospheric pressure = 100 kPa, water depth = 40 mm, tube's diameter = 90 mm.

6.1.2 Dimensional Analysis

The dimensional analysis is a mathematical technique used to predict physical parameters that influence engineering problems such as fluid flow and heat transfer problems (White, 2016). Dimensional analysis is commonly used to determine the relationships between several variables and to obtain a correlation to relate those variables or parameters. Dimensional analysis is important in experimental work to minimize the time and expenses spent on experiments and to acquire valuable information from the fewest number of experiments possible. To reduce the number of required experiments, the independent variables are grouped together to form dimensionless parameters with the help of their units of measurements using several dimensional analysis techniques. One of the most famous dimensional analysis techniques is the Pi method which is a theorem introduced by Edgar Buckingham (1914). The advantage of this theorem is that one can predict the number of dimensionless groups that could be expected from the number of variables that affect a given physical phenomenon. The number of dimensionless groups (π) can be obtained from the following relation;

$$\pi = k - r \tag{6.2}$$

Where k is the number of the effective variables and r is the number of the repeating variables

Table 6.1 lists the effective independent variables that affect the dependent variable, which is the productivity of the SD system($\dot{m}_e$);

Table 6. 1 The effective parameters

Quantity	*Symbol*	*SI units*	*Dimensional units*
SD system productivity	$\dot{m}_e$	$\frac{kg}{m^2 \cdot hr}$	$ML^{-2}T^{-1}$
Solar radiation	G_s	$W = \frac{kg.m^2}{s^3}$	ML^2T^{-3}
Water mass	m_w	kg	M
Water depth	h_w	mm	L
Water surface area	A_w	m^2	L^2
Rotation speed of the revolving tubes	ω	rad/s	T^{-1}
Radius of the revolving tubes	R	mm	L
Temperature of the cover and water	T_c, T_w	℃	θ
Time	t	hr	T

The SD system productivity $\dot{m}_e$ is a function to the above-mentioned parameters as follows,

$$\dot{m}_e = f(G_s, m_w, h_w, A_w, \omega, R, T_c, T_w, t) \quad (6.3)$$

The repeating variables should represent all basic dimensional units in the problem under study, these are the mass (M), the length (L), the time (T), and the temperature (θ). In this study, the repeating variables $M,\ L,\ T,\ and\ \theta$ are chosen to be the water mass m_w, the water depth h_w, the time t, and the cover temperature T_c, respectively.

From equation 6.2, $(\pi = 10 - 4 = 6)$, which means there are six dimensionless groups, and by applying the Buckingham Pi theorem the following relation is found;

$$\pi 1 = \emptyset\,[\,\pi 2,\ \pi 3,\ \pi 4,\ \pi 5,\ \pi 6] \quad (6.4)$$

Where;

$$\pi 1 = \frac{\dot{m}_e\, h_w^2\, t}{m_w} \quad (6.5)$$

$$\pi 2 = \frac{G_s\, t^3}{m_w\, h_w^2} \quad (6.6)$$

$$\pi 3 = \frac{A}{h_w^2} \quad (6.7)$$

$$\pi 4 = \omega\, t \quad (6.8)$$

$$\pi 5 = \frac{R}{h_w} \quad (6.9)$$

$$\pi 6 = \frac{T_w}{T_c} \quad (6.10)$$

By substituting equations 6.5 to 6.10 in equation 6.4, the following relation can be found;

$$\frac{\dot{m}_e\, h_w^2\, t}{m_w} = \emptyset\left[\frac{G_s\, t^3}{m_w\, h_w^2}\,,\ \frac{A}{h_w^2}\,,\ \omega\, t\,,\ \frac{R}{h_w},\ \frac{T_w}{T_c}\right] \quad (6.11)$$

From the first glance to the above relation 6.11, it can be noticed that the productivity of the SD system increases with the increase of the solar radiation, time, water surface-area, tube diameter, tube rotation speed, and the temperature of the water. While, the productivity of the SD system decreases with the increase of the water mass, water depth, and the temperature of the cover.

To find the relation between these dimensionless groups, the repeating variables were fixed at constant values. The water mass was assumed to be 19.2 kg, the water depth is 40 mm, the time is 1 hr, and the cover temperature is 30℃.

Then after determining the values of the repeating variable, every two dimensionless groups have two unknown variables, one input and another output. For instance, π1 and π2 have only two unknown variables; the solar radiation G_s and the productivity $\dot{m}_e$. By varying the value of the solar radiation, the productivity can be found; hence, the relation between π1 and π2 can be found too. The same procedure is followed to find the relations between other dimensionless groups.

Figures 6.8 to 6.12 represent the relation between the dimensionless groups of the equations 6.4 and 6.11.

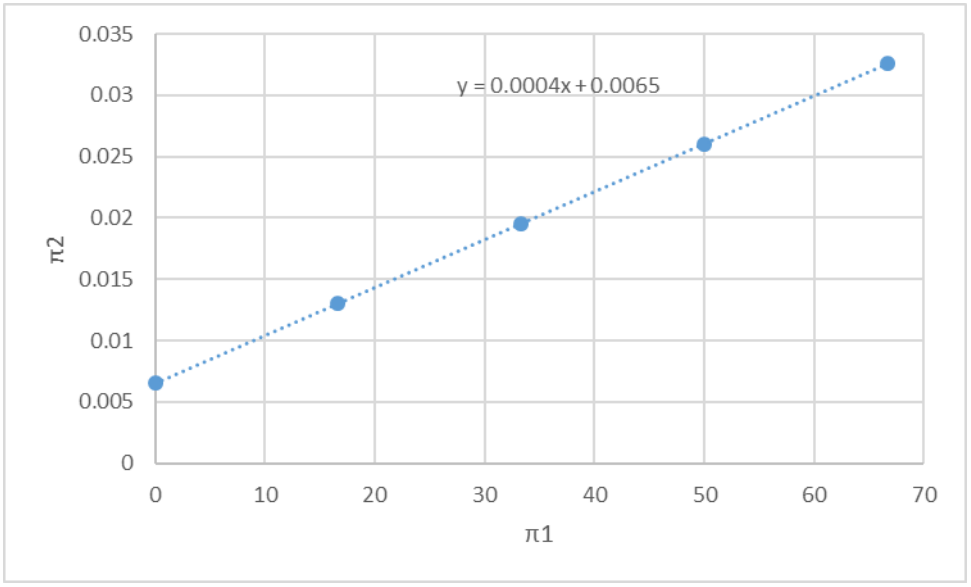

Figure 6. 11 The relation between $\pi 1 = \frac{\dot{m}_e h_w^2 t}{m_w}$ *and* $\pi 2 = \frac{G_s t^3}{m_w h_w^2}$

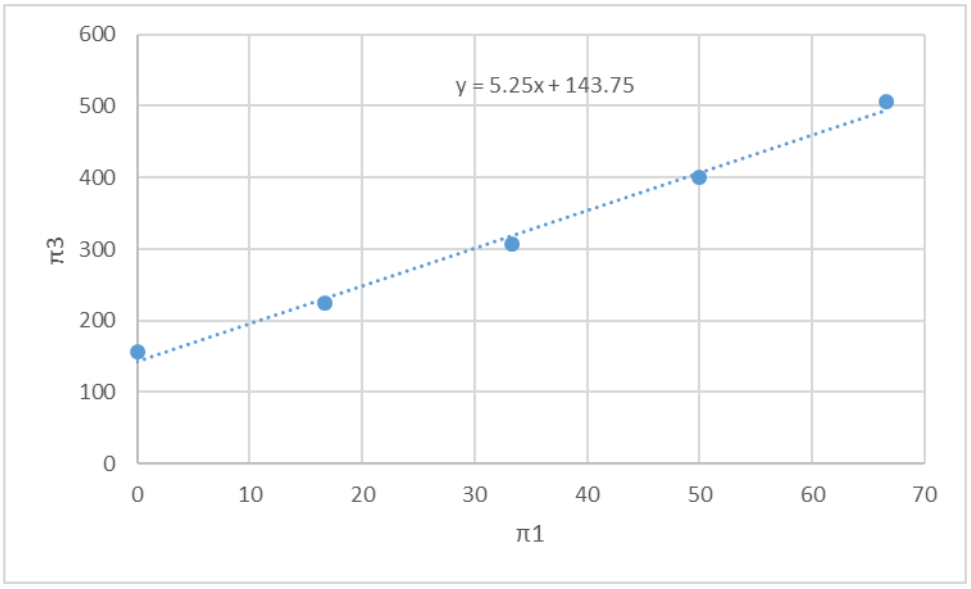

Figure 6. 12 The relation between $\pi 1 = \frac{\dot{m}_e h_w^2 t}{m_w}$ *and* $\pi 3 = \frac{A}{h_w^2}$

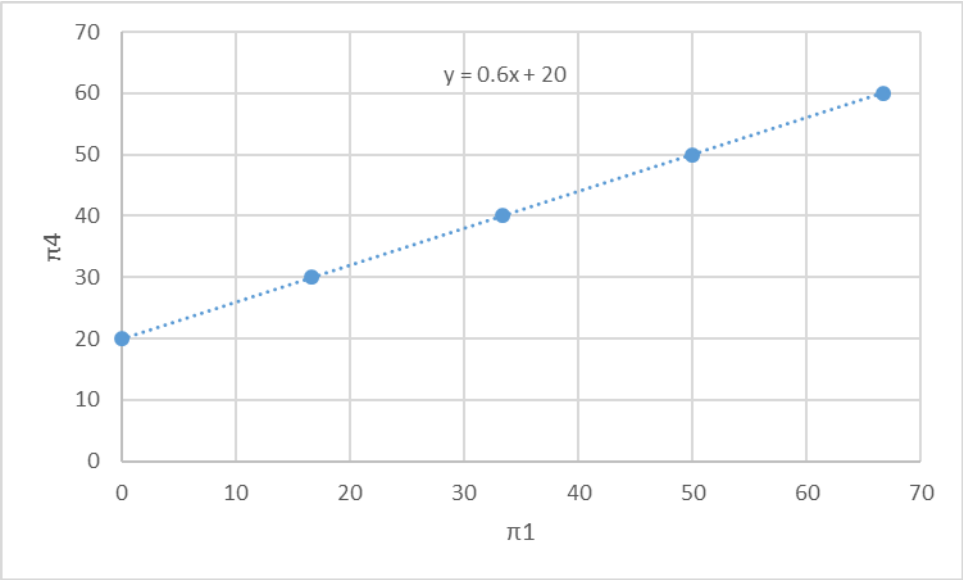

Figure 6. 13 The relation between $\pi 1 = \frac{\dot{m}_e h_w^2 t}{m_w}$ *and* $\pi 4 = \omega t$

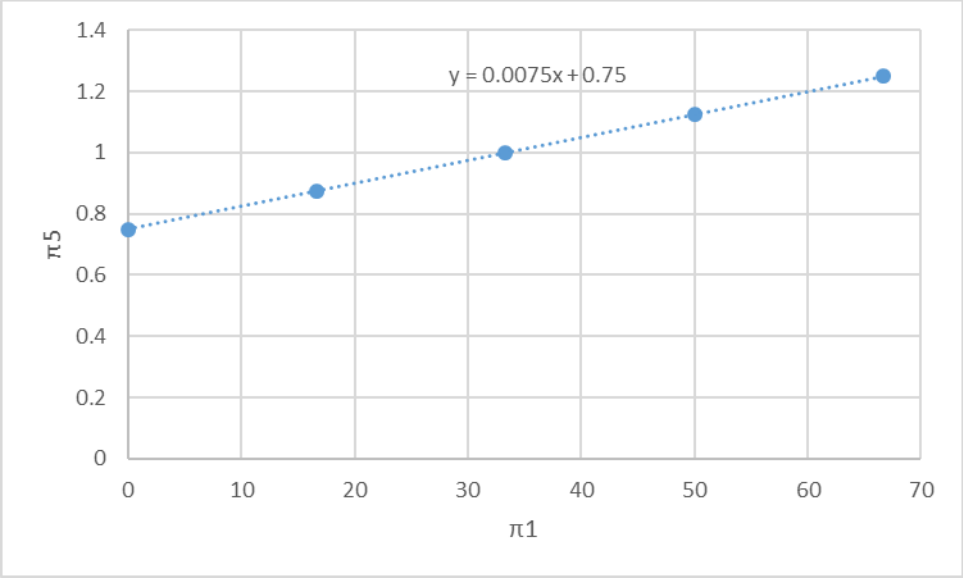

Figure 6. 14 The relation between $\pi 1 = \frac{\dot{m}_e h_w^2 t}{m_w}$ *and* $\pi 5 = \frac{R}{h_w}$

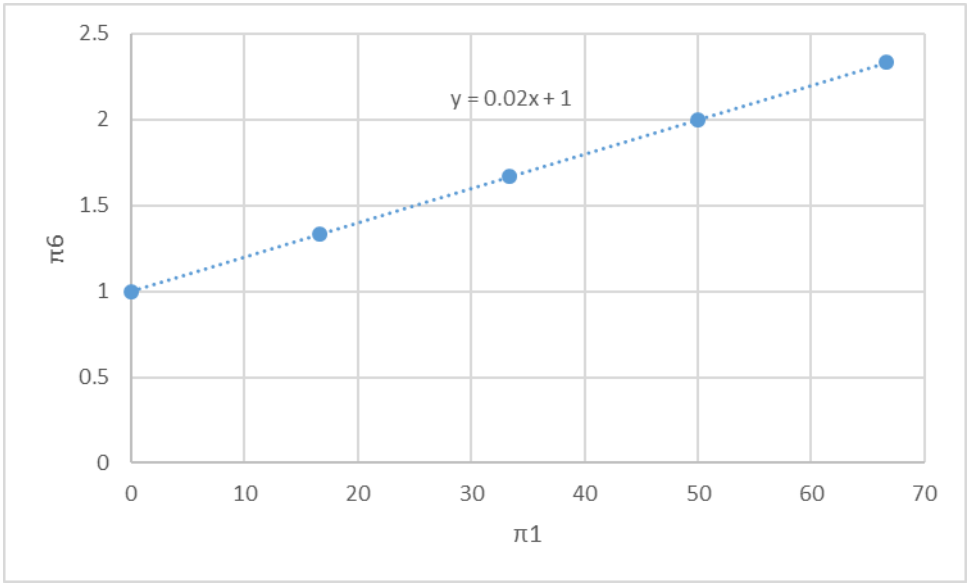

Figure 6. 15 The relation between $\pi 1 = \frac{\dot{m}_e h_w^2 t}{m_w}$ *and* $\pi 6 = \frac{T_w}{T_c}$

6.2 Uncertainty Analysis

All experimental measurements have a certain amount of uncertainty or inevitable error. There are three main types of potential errors in the measurements: the random errors, the systematic errors, and the gross errors. The random errors are caused by uncontrollable fluctuations in the variables and they are difficult to be eliminated, while systematic errors are instrumental, methodological, or personal mistakes and they can be identified and eliminated by careful inspection and instruments calibration. The gross errors are caused by carelessness or equipment failure resulting in data values that are far above or below the true value data, which are usually disregarded during the assessment (Coleman & Steele, 2018).

It is important to estimate the uncertainty value in the measured and calculated parameters of any experiment to ensure that the errors in the measurements are as small as reasonably possible.

To estimate the uncertainty in the experimental data, Holman and Gajda (2001) used the following formula;

Presume a set of 'n' of measurements $(X_1, X_2, \ldots\ldots, X_n)$ is conducted to find a required value 'R' from an experiment hence;

$$R = f\,(X_1, X_2, \ldots\ldots, X_n) \tag{6.12}$$

And the uncertainty in the R value is estimated as;

$$U_R = \sqrt{\left(\frac{\partial R}{\partial X_1} U_{X_1}\right)^2 + \left(\frac{\partial R}{\partial X_2} U_{X_2}\right)^2 + \cdots + \left(\frac{\partial R}{\partial X_n} U_{X_n}\right)^2} \tag{6.13}$$

Where $U_{X_1}, U_{X_2}, \ldots, U_{X_n}$ are the uncertainty in the measured values of $X_1, X_2, \ldots\ldots, X_n$, respectively.

Since the productivity of the SD system $\dot{m}_e$ depends on the measured values of the volume of the distillate yield V and the measured values of time t as follows;

$$\dot{m}_e = \frac{V}{t} \tag{6.14}$$

And the efficiency of the SD system η depends on the measured values of the daily productivity of the SD system $\dot{m}_e$ and the measured values of solar radiation G_s (in

addition to the latent heat of evaporation l_v and the surface area of the SD system A_s which are considered constant values) as follows;

$$\eta = \frac{\dot{m}_e \times l_v}{A_s \times G_s} \tag{6.15}$$

The uncertainty in the measured productivity $U_{\dot{m}_e}$ of the SD system can be found from the following relation (Holman & Gajda, 2001);

$$U_{\dot{m}_e} = \sqrt{\left(\frac{\partial \dot{m}_e}{\partial V} U_V\right)^2 + \left(\frac{\partial \dot{m}_e}{\partial t} U_t\right)^2} \tag{6.16}$$

In the same way, the uncertainty in the estimated efficiency U_η of the SD system can be found from the following relation;

$$U_\eta = \sqrt{\left(\frac{\partial \eta}{\partial \dot{m}_e} U_{\dot{m}_e}\right)^2 + \left(\frac{\partial \eta}{\partial G} U_{G_s}\right)^2} \tag{6.17}$$

Where U_V, U_t, $and\ U_{G_s}$ are the uncertainties in the values of the measured volume of the distillate yield, the values of the measured time, and the values of the measured solar radiation; respectively.

The results showed that the maximum estimated uncertainty was $\pm 4.6\%$ and $\pm 5.25\%$ for the productivity and efficiency, respectively. The full calculations of the uncertainty analysis is presented in Appendix C.

6.3 Cost Analysis

The cost analysis was conducted for the NSD and the MSD systems under study, to estimate the cost of the water produced by the NSD system and the MSD system, and to find out if the modification of the MSD system is justified or not?

The Cost of the water produced Per Litre (CPL) can be found from the following equations (Rajaseenivasan & Srithar, 2016);

$$CPL = TC/AY \tag{6.18}$$

Where;

$AY =$ Average Yield in litres

$TC =$ Total Cost in AUD

The total cost of the NSD system is;

$$TC_{NSD} = FC + MC - SV \tag{6.19}$$

The total cost of the MSD system is;

$$TC_{MSD} = FC + MC + PC - SV \tag{6.20}$$

Where;

$FC =$ Fixed Cost (capital cost)

$MC =$ Maintenance Cost (for two years) $\cong 20\%\ FC$

$SV =$ Salvage Value (resale value at the end of use) $\cong 20\%\ FC$

$PC =$ Power Cost for the MSD system

Table 6.2 lists the fixed or the capital cost of the NSD system and the MSD system

Table 6. 2 The capital cost or the fixed cost FC of the NSD system and the MSD system

Item	Quantity	Cost ($AUD)	
		NSD	MSD
Aluminium sheet (1200 mm ×2400 mm ×3 mm)	1	60	60
Plexiglas sheet (1220 mm ×2440 mm ×3 mm)	1	50	50
Insulation XPS foam board (1200 mm ×600 mm ×60 mm)	3	30	30
Worm-gear DC motor (12 V, 50 W, 29 Nm, 65 rpm)	3		120
Variable DC power supply (16 V, 25 A)	1		120
PVC pipe (90 mm × 3 m)	1		10
PVC push-on cap (90 mm)	6		15
Tubing, float, and other accessories	sum	30	50
Total		170	455

If we assumed that;

1. The life span of both the SD systems is two years only.
2. Both the SD systems are working 300 days per year assuming 65 days per year for the maintenance

And if we knew that;

3. The average daily productivity of the NSD system and the MSD system was about 0.562 l/day and 0.965 l/day, respectively
4. The energy consumed by the DC motors in the MSD system was about 50 $Watt$, they were working 12 hours per day, and the electricity cost is 0.1 $\$AUD/kWhr$

We can find that;

1. The AY of the NSD system and the MSD system during two years period will be about 337.2 $litre$ and 579 $litre$, respectively
2. The $PC = \frac{50\ W}{1000} \times 12\ hr \times 600\ days \times 0.1\ \$AUD/kWhr = 36\ \$AUD$
3. The $TC_{NSD} = 170\ \$AUD$ and the $TC_{MSD} = 455 + 36 = 491\ \$AUD$.
4. The CPL of the NSD system and the MSD system will be (0.5 $AUD/l= 0.34 $USD/l) and (0.85 $AUD/l= 0.57 $USD/l), respectively. The exchange rate from AUD to USD was 0.67.

According to the cost analysis, the capital or the fixed cost FC of the MSD system was higher by 167.6% than the capital cost of the NSD system. The total cost TC of the MSD system was higher by 188.8% than the total cost of the NSD system. The cost of the water produced per litre CPL of the MSD system was higher by 67.6% than that of the NSD system. The cost analysis showed that the modification to the SD system was unjustified even though the modification had increased the productivity (average yield) AY of the SD system by an average of 71.7%. The reason for the increase in the cost was the cost of the extra items required for the modification and the cost of the power that was used to run the motors to rotate the tubes. It is worth mentioning that the present SD systems used in this experiment were small-sized to fulfil the research budget and the lifespan was considered to be only two years (other researchers considered longer lifetime up to 30 years). Besides a longer lifespan, if the present MSD system manufactured in a larger-scale the cost of the extra items that are required for the modification will be diminished, thereby the price of the water produced by this system will be much cheaper.

7 Chapter Seven: Conclusions and Recommendations

This chapter provides a summary of the thesis, presents the conclusions of this work, and suggests recommendations for future work.

7.1 Thesis Summary

Water is an essential need, and there is an ethical obligation to provide all people with clean and fresh water. Some more impoverished regions have limited, or no access to potable water, especially the small communities that live in remote and arid areas. Some of these areas have no resources or suitable infrastructure with which to build desalination plants. In addition, transporting water to these remote areas is costly and connecting these areas to the electricity grid that is needed to operate the desalination plants may be a challenge. One of the simplest and most effective solutions is employing abundant solar energy to run small and inexpensive solar desalination systems. Solar Still Desalination (SD) systems consist of a basin of saline water covered with a tilted transparent cover that is exposed to solar radiation. The solar radiation heats the brackish water in the basin, producing vapour that condenses on the inner surface of the cover providing fresh water. SD systems do not require complicated maintenance or special skills to run. SD systems are very simple, low-cost, can be constructed from locally available materials, and can be operated by anyone. Despite the advantages of the SD systems, low productivity is the only drawback of these systems.

Increasing the productivity of the SD systems is the main purpose of this study. The proposed modification to achieve this goal was introducing three symmetrical and parallel revolving tubes in the water basin of the SD system. The revolving tubes were semi-immersed in the water in the basin. The Modified SD system (MSD) has advantages over the Normal SD system (NSD) of adding extra surfaces for the water evaporation, preventing water stagnation, and enhancing the solar absorption. Increasing the surface area of evaporation led to an increase in the evaporation rate,

which led to increases in productivity. Increasing the SD system productivity under the same unit area means enhancing the efficiency of the SD system.

This study was conducted in the following sequence. Firstly, a CFD model using ANSYS-FLUENT software was developed to simulate the NSD system and the MSD system and to estimate the productivities of both systems to confirm the possibility of the enhancement of performance. Then experimental tests for both the SD systems were carried out in the University of Southern Queensland campus, Toowoomba, Australia for about seven months from the 4th of October 2017 to the 23rd of April 2018. After validating the simulation results with the experimental data, the numerical model was then employed to perform the sensitivity analysis for some design and operation parameters. The uncertainty in the experimental measurements was estimated for reliability. Finally, the cost analysis of both the SD systems was implemented to justify the extra cost of the modification to the MSD system.

The conclusions of the present study and the recommendations for future work are presented in the following sections.

7.2 Conclusions

After conducting the numerical simulation, the experimental investigation, the sensitivity analysis, and the cost analysis to the MSD system and the NSD system, the following conclusions were reached:

1. The maximum and the average daily productivity of the MSD system were 2.908 l/m^2 and 2.011 l/m^2 , respectively.
2. The maximum and the average daily productivity of the NSD system were 1.685 l/m^2 and 1.172 l/m^2 , respectively.
3. The daily productivity of the MSD system was higher than the daily productivity of the NSD system by an average of 71.7%.
4. The maximum and the average daily efficiency of the MSD system were 21.01% and 18.77% , respectively.
5. The maximum and the average daily efficiency of the NSD system were 13.12% and 12.11% , respectively.

6. The daily efficiency of the MSD system was higher than the daily efficiency of the NSD system by an average of 54.3%.
7. The maximum enhancement in the daily productivity and in the daily efficiency of the MSD system were 74.8% and 63.4% higher than the NSD system, respectively.
8. The results of the CFD simulation showed a good agreement with the experimental results with a maximum error of $\pm 10\%$.
9. The numerical modelling using ANSYS- Fluent proved to be a successful tool to simulate the SD system performance and to analyse the operation and design parameters of the SD systems.
10. According to the sensitivity analysis, the increase in the solar radiation intensity, the temperature of the feed water, the surface area, the diameter of the revolving tubes, and the rotation speed of the revolving tubes have a positive effect on the productivity of the SD systems.
11. According to the sensitivity analysis, the increase in the water depth, water mass, and the temperature of the SD cover have a negative effect on the productivity of the SD systems.
12. The initial or the capital cost of the MSD system and the NSD system were \$455 AUD and \$170 AUD , respectively.
13. According to the cost analysis, the cost of the water produced by the MSD system and the NSD system were \$0.85 $AUD = 0.57\ \$USD\ per\ litre$ and \$0.5 $AUD = 0.34\ \$USD\ per\ litre$, respectively.
14. According to the cost analysis, the capital cost of the MSD system was higher by 167.6% than the capital cost of the NSD system, and the value of the produced water by the MSD system was higher by 67.6% than the value of the water produced by the NSD system.

In brief, the SD system has low productivity per unit area. The modification of the revolving tubes that were added to the basin of the SD system had enhanced the productivity of the system significantly. However, this modification was not cost-effective due to the extra cost of the additional items and the cost of power required to run the motors that rotate the tubes. Noting that, the size of the SD system was small and the lifespan considered short being only two years. The effect of the cost of the

power and the extra items on the cost of the produced water can be mitigated using a bigger sized SD system and considering a longer working life.

7.3 Recommendations

Finally, the researcher would like to suggest the following recommendations for future work:

1. Establish and conduct experimental tests to a more extensive sized SD system, at least $1.5\ m \times 1\ m$ or larger if possible. The reason is the larger system will have higher productivity and the cost of the extra items required for the modification would be close to the present system used in this work, which may lead to decrease the cost of the water produced significantly.
2. Use revolving tubes wrapped with other alternative absorbent materials such as a sponge layer or other porous materials and/or change the tube's material and/or the tube's cross-section shape. The current research used PVC tubes wrapped with a black absorbent mat. Using other materials or other tubes configurations such as polygon tube may have a good effect on the productivity of the SD system and will need to be tested experimentally to verify this expectation.
3. Study the feasibility of using a small solar panel or a small wind turbine to run the motors instead of electrical power. Using renewable sources to run the motors may reduce the cost of the power, the power supply and the wiring. It is more environmentally friendly and more practical for remote areas without power connections.
4. Use other enhancements to the SD system in conjunction with the present enhancement of the revolving tubes, such as reflective surfaces, heat exchangers to preheat the feed water, and/or film cooling to reduce the cover temperature. Using multiple enhancements or modifications in one system may have a great combined effect on the productivity and it will require further study.
5. Go further with dimensional analysis and Pi-groups to develop empirical correlations.

References

Abdallah, S., & Badran, O. O. (2008). Sun tracking system for productivity enhancement of solar still. *Desalination, 220*(1-3), 669-676.

Abdallah, S., Badran, O. O., & Abu-Khader, M. M. (2008). Performance evaluation of a modified design of a single slope solar still. *Desalination, 219*(1-3), 222-230.

Abdel-Rehim, Z. S., & Lasheen, A. (2007). Experimental and theoretical study of a solar desalination system located in Cairo, Egypt. *Desalination, 217*(1-3), 52-64.

Abu-Hijleh, B. A. K., & Rababa'h, H. M. (2003). Experimental study of a solar still with sponge cubes in basin. *Energy Conversion and Management, 44*(9), 1411-1418.

Abu-Qudais, M., & Othman, O. N. (1996). Experimental study and numerical simulation of a solar still using an external condenser. *Energy, 21*(10), 851-855.

Ahmed, M. I., Hrairi, M., & Ismail, A. F. (2009). On the characteristics of multistage evacuated solar distillation. *Renewable Energy, 34*(6), 1471-1478

Ahsan, A., Imteaz, M., Rahman, A., Yusuf, B., & Fukuhara, T. (2012). Design, fabrication and performance analysis of an improved solar still. *Desalination, 292*, 105-112.

Ahsan, A., Imteaz, M., Thomas, U. A., Azmi, M., Rahman, A., & Daud, N. N. (2014). Parameters affecting the performance of a low cost solar still. *Applied energy, 114*, 924-930.

Akther, N., Sodiq, A., Giwa, A., Daer, S., Arafat, H. A., & Hasan, S. W. (2015). Recent advancements in forward osmosis desalination: a review. *Chemical Engineering Journal, 281*, 502-522.

Al-Hinai, H., Al-Nassri, M. S., & Jubran, B. A. (2002). Effect of climatic, design and operational parameters on the yield of a simple solar still. *Energy Conversion and Management, 43*(13), 1639-1650.

Al-Kharabsheh, S., & Yogi, D. (2003). Analysis of an innovative water desalination system using low-grade solar heat. *Desalination, 156*(1-3), 323-332.

Al-Sulttani, A. O., Ahsan, A., Rahman, A., Daud, N. N., & Idrus, S. (2017). Heat transfer coefficients and yield analysis of a double-slope solar still hybrid with rubber scrapers: an experimental and theoretical study. *Desalination, 407*, 61-74.

Ansari, O., Asbik, M., Bah, A., Arbaoui, A., & Khmou, A. (2013). Desalination of the brackish water using a passive solar still with a heat energy storage system. *Desalination, 324*, 10-20.

Appadurai, M., & Velmurugan, V. (2015). Performance analysis of fin type solar still integrated with fin type mini solar pond. *Sustainable Energy Technologies and Assessments, 9*, 30-36.

Arunkumar, T., Jayaprakash, R., Denkenberger, D., Ahsan, A., Okundamiya, M. S., Tanaka, H., & Aybar, H. Ş. (2012). An experimental study on a hemispherical solar still. *Desalination, 286*, 342-348.

Australian Water Association. (2009). *Desalination Fact sheet*. National Water Week 18-24 October. Australia: AWA.

Baawain, M., Choudri, B. S., Ahmed, M., & Purnama, A. (Eds.). (2015). *Recent progress in desalination, environmental and marine outfall systems*. Cham, Switzerland: Springer.

Badran, O. O., & Abu-Khader, M. M. (2007). Evaluating thermal performance of a single slope solar still. *Heat and mass transfer, 43*(10), 985-995.

Badran, O. O., & Al-Tahaineh, H. A. (2005). The effect of coupling a flat-plate collector on the solar still productivity. *Desalination, 183*(1-3), 137-142.

Banat, F., & Jwaied, N. (2008). Economic evaluation of desalination by small-scale autonomous solar-powered membrane distillation units. *Desalination*, *220*(1-3), 566-573.

Buckingham, E. (1914). On physically similar systems; illustrations of the use of dimensional equations. *Physical review*, *4*(4), 345.

Bureau of Meteorology, Australia. (2019). *Latest Weather Observations for Queensland*. Retrieved from http://www.bom.gov.au/qld/observations/

Chorin, A. J. (1968). Numerical solution of the Navier-Stokes equations. *Mathematics of computation*, *22*(104), 745-762.

Coleman, H. W., & Steele, W. G. (2018). *Experimentation, validation, and uncertainty analysis for engineers*. John Wiley & Sons.

Dashtban, M., & Tabrizi, F. F. (2011). Thermal analysis of a weir-type cascade solar still integrated with PCM storage. *Desalination*, *279*(1-3), 415-422.

Dev, R., Abdul-Wahab, & Tiwari, G. N. (2011a). Characteristic equation of the inverted absorber solar still. *Desalination*, *269*(1-3), 67-77.

Dev, R., Abdul-Wahab, S. A., & Tiwari, G. N. (2011b). Performance study of the inverted absorber solar still with water depth and total dissolved solid. *Applied energy*, *88*(1), 252-264.

Dimri, V., Sarkar, B., Singh, U., & Tiwari, G. N. (2008). Effect of condensing cover material on yield of an active solar still: an experimental validation. *Desalination*, *227*(1-3), 178-189.

Draper, N. R., & Smith, H. (2014). *Applied regression analysis* (Vol. 326). John Wiley & Sons.

Duffie, J. A., & Beckman, W. A. (2013). *Solar engineering of thermal processes*. John Wiley & Sons.

Dunkle, R. V. (1961). Solar water distillation: the roof type still and a multiple effect diffusion still. In Proc. *International Heat Transfer Conference*, University of Colorado, USA (Vol. 5, p. 895).

Dwivedi, V. K., & Tiwari, G. N. (2009). Comparison of internal heat transfer coefficients in passive solar stills by different thermal models: an experimental validation. *Desalination, 246*(1-3), 304-318.

Eakins, B.W., & Sharman, G.F. (2010). Volumes of the World's Oceans from ETOPO1. *National Geophysical Data Centre, Boulder*. CO: NOAA.

Edalatpour, M., Aryana, K., Kianifar, A., Tiwari, G. N., Mahian, O., & Wongwises, S. (2016). Solar stills: A review of the latest developments in numerical simulations. *Solar Energy, 135*, 897-922.

El-Agouz, S. A. (2014). Experimental investigation of stepped solar still with continuous water circulation. *Energy Conversion and Management, 86*, 186-193.

El-Bahi, A., & Inan, D. (1999a). A solar still with minimum inclination, coupled to an outside condenser. *Desalination, 123*(1), 79-83.

El-Bahi, A., & Inan, D. (1999b). Analysis of a parallel double glass solar still with separate condenser. *Renewable Energy, 17*(4), 509-521

El-Mudir, W., El-Bousiffi, M., & Al-Hengari, S. (2004). Performance evaluation of a small size TVC desalination plant. *Desalination, 165*, 269-279.

El-Samadony, Y. A. F., Abdullah, A. S., & Omara, Z. M. (2015). Experimental study of stepped solar still integrated with reflectors and external condenser. *Experimental Heat Transfer, 28*(4), 392-404.

El-Sebaii, A. A., Al-Ghamdi, A. A., Al-Hazmi, F. S., & Faidah, A. S. (2009). Thermal performance of a single basin solar still with PCM as a storage medium. *Applied Energy, 86*(7-8), 1187-1195.

El-Sebaii, A. A., Ramadan, M. R. I., Aboul-Enein, S., & Salem, N. (2008). Thermal performance of a single-basin solar still integrated with a shallow solar pond. *Energy conversion and Management, 49*(10), 2839-2848.

Eltawil, M. A., & Omara, Z. M. (2014). Enhancing the solar still performance using solar photovoltaic, flat plate collector and hot air. *Desalination, 349*, 1-9.

Estahbanati, M. K., Ahsan, A., Feilizadeh, M., Jafarpur, K., Ashrafmansouri, S. S., & Feilizadeh, M. (2016). Theoretical and experimental investigation on internal reflectors in a single-slope solar still. *Applied Energy, 165*, 537-547.

Fatchurrohman, N., & Chia, S. T. (2017). Performance of hybrid nano-micro reinforced mg metal matrix composites brake calliper: simulation approach. *Fourth International Conference on Mechanical Engineering Research*, (Vol. 257, p. 012060). IOP.

Fath, H. E., El-Samanoudy, M., Fahmy, K., & Hassabou, A. (2003). Thermal-economic analysis and comparison between pyramid-shaped and single-slope solar still configurations. *Desalination, 159*(1), 69-79.

Fluent, A. (2017). *ANSYS Fluent Theory Guide*, Release 18.2. USA: ANSYS Inc.

Ghaffour, N., Bundschuh, J., Mahmoudi, H., & Goosen, M. F. (2015). Renewable energy-driven desalination technologies: A comprehensive review on challenges and potential applications of integrated systems. *Desalination, 356*, 94-114.

Gleick, P. H. (1993). *Water in crisis: a guide to the world's fresh water resources*. Oxford University Press.

Google Maps Australia. (2019). Retrieved from https://www.google.com/maps/

Goosen, M. F., Sablani, S. S., Shayya, W. H., Paton, C., & Al-Hinai, H. (2000). Thermodynamic and economic considerations in solar desalination. *Desalination, 129*(1), 63-89.

Gude, V. G., Nirmalakhandan, N., & Deng, S. (2010). Renewable and sustainable approaches for desalination. *Renewable and sustainable energy reviews, 14*(9), 2641-2654.

Gupta, B., Sharma, R., Shankar, P., & Baredar, P. (2016). Performance enhancement of modified solar still using water sprinkler: An experimental approach. *Perspectives in Science, 8*, 191-194.

Helal, A. M., & Al-Malek, S. A. (2006). Design of a solar-assisted mechanical vapor compression (MVC) desalination unit for remote areas in the UAE. *Desalination, 197*(1-3), 273-300.

Hirunpinyopas, W., Prestat, E., Worrall, S. D., Haigh, S. J., Dryfe, R. A., & Bissett, M. A. (2017). Desalination and nanofiltration through functionalized laminar MoS2 membranes. *ACS nano, 11*(11), 11082-11090.

Holman, J. P., & Gajda, W. J. (2001). *Experimental methods for engineers* (Vol. 2). NY: McGraw-Hill.

Huttner, K. R. (2013). Overview of existing water and energy policies in the MENA region and potential policy approaches to overcome the existing barriers to desalination using renewable energies. *Desalination and Water Treatment, 51*(1-3), 87-94.

Ibrahim, A. G., Allam, E. E., & Elshamarka, S. E. (2015). A modified basin type solar still: Experimental performance and economic study. *Energy, 93*, 335-342.

Ismail, B. I. (2009). Design and performance of a transportable hemispherical solar still. *Renewable Energy, 34*(1), 145-150.

Jamil, B., & Akhtar, N. (2017). Effect of specific height on the performance of a single slope solar still: An experimental study. *Desalination, 414*, 73-88

Kabeel, A. E. (2009). Performance of solar still with a concave wick evaporation surface. *Energy, 34*(10), 1504-1509.

Kabeel, A. E., & Abdelgaied, M. (2016). Improving the performance of solar still by using PCM as a thermal storage medium under Egyptian conditions. *Desalination, 383*, 22-28.

Kabeel, A. E., & Abdelgaied, M. (2017). Observational study of modified solar still coupled with oil serpentine loop from cylindrical parabolic concentrator and phase changing material under basin. *Solar Energy, 144*, 71-78.

Kabeel, A. E., Omara, Z. M., & Essa, F. A. (2014a). Enhancement of modified solar still integrated with external condenser using nanofluids: an experimental approach. *Energy conversion and management, 78*, 493-498.

Kabeel, A. E., Omara, Z. M., & Essa, F. A. (2014b). Improving the performance of solar still by using nanofluids and providing vacuum. *Energy Conversion and Management, 86*, 268-274.

Kang, K. C., Linga, P., Park, K. N., Choi, S. J., & Lee, J. D. (2014). Seawater desalination by gas hydrate process and removal characteristics of dissolved ions (Na+, K+, Mg2+, Ca2+, B3+, Cl−, SO42−). *Desalination, 353*, 84-90.

Karagiannis, I. C., & Soldatos, P. G. (2008). Water desalination cost literature: review and assessment. *Desalination, 223*(1-3), 448-456.

Khalifa, A. J. N. (2011). On the effect of cover tilt angle of the simple solar still on its productivity in different seasons and latitudes. *Energy conversion and management, 52*(1), 431-436.

Khalifa, A. J. N., & Hamood, A. M. (2009). Performance correlations for basin type solar stills. *Desalination, 249*(1), 24-28.

Khalifa, A. J. N., & Ibrahim, H. A. (2009). Effect of inclination of the external reflector on the performance of a basin type solar still at various seasons. *Energy for Sustainable Development, 13*(4), 244-249.

Kianifar, A., Heris, S. Z., & Mahian, O. (2012). Exergy and economic analysis of a pyramid-shaped solar water purification system: active and passive cases. *Energy, 38*(1), 31-36.

Kim, S. E., Choudhury, D., & Patel, B. (1999). Computations of complex turbulent flows using the commercial code FLUENT. In M. D. Salas, J. N. Hefner, & L. Sakell (Eds.), *Modeling complex turbulent flows* (pp. 259-276). Dordrecht: Springer- Science+ Business Medea.

Kleijnen, J. P. (2005). An overview of the design and analysis of simulation experiments for sensitivity analysis. *European Journal of Operational Research, 164*(2), 287-300.

Kumar, S., Dubey, A., & Tiwari, G. N. (2014). A solar still augmented with an evacuated tube collector in forced mode. *Desalination, 347,* 15-24.

Lamei, A., Van der Zaag, P., & Von Muench, E. (2008). Impact of solar energy cost on water production cost of seawater desalination plants in Egypt. *Energy Policy, 36*(5), 1748-1756.

Launder, B. E., & Spalding, D. B. (1972). *Mathematical models of turbulence*. Academic press.

Lee, W. H. (1979). *A Pressure Iteration Scheme for Two-Phase Flow Modeling* (Technical Paper No. LA-UR-79-975). USA: Los Alamos National Laboratory.

Lethea, L. (2017). Impact of water hardness on energy consumption of geyser heating elements. *Water SA, 43*(4), 614-625.

Löhner, R. (2008). *Applied computational fluid dynamics techniques: an introduction based on finite element methods*. John Wiley & Sons.

Malaiyappan, P., & Elumalai, N. (2016). Numerical investigations: basin materials of a single-basin and single-slope solar still. *Desalination and Water Treatment, 57*(45), 21211-21233.

Malik, M. A. S., Tiwari, G. N., Kumar, A., & Sodha, M. S. (1982). *Solar distillation: a practical study of a wide range of stills and their optimum design, construction, and performance*. Oxford: Pergamon press.

Mamouri, S. J., Derami, H. G., Ghiasi, M., Shafii, M. B., & Shiee, Z. (2014). Experimental investigation of the effect of using thermosyphon heat pipes and vacuum glass on the performance of solar still. *Energy, 75*, 501-507.

Maroo, S. C., & Goswami, D. Y. (2009). Theoretical analysis of a single-stage and two-stage solar driven flash desalination system based on passive vacuum generation. *Desalination, 249*(2), 635-646.

Minocha, N., Joshi, J. B., Nayak, A. K., & Vijayan, P. K. (2016). 3D CFD simulation of passive decay heat removal system under boiling conditions: Role of bubble sliding motion on inclined heated tubes. *Chemical Engineering Science, 145*, 245-265.

Monowe, P., Masale, M., Nijegorodov, N., & Vasilenko, V. (2011). A portable single-basin solar still with an external reflecting booster and an outside condenser. *Desalination, 280*(1-3), 332-338.

Moustafa, S. M. A., Jarrar, D. I., & El-Mansy, H. I. (1985). Performance of a self-regulating solar multistage flash desalination system. *Solar Energy, 35*(4), 333-340.

Murugavel, K. K., Sivakumar, S., Ahamed, J. R., Chockalingam, K. K., & Srithar, K. (2010). Single basin double slope solar still with minimum basin depth and energy storing materials. *Applied Energy, 87*(2), 514-523.

Nafey, A. S., Abdelkader, M., Abdelmotalip, A., & Mabrouk, A. A. (2002). Enhancement of solar still productivity using floating perforated black plate. *Energy Conversion and Management, 43*(7), 937-946.

Omara, Z. M., Hamed, M. H., & Kabeel, A. E. (2011). Performance of finned and corrugated absorbers solar stills under Egyptian conditions. *Desalination, 277*(1-3), 281-287.

Omara, Z. M., Kabeel, A. E., & Younes, M. M. (2014). Enhancing the stepped solar still performance using internal and external reflectors. *Energy conversion and management, 78*, 876-881.

Panchal, H. N., & Patel, S. (2017). An extensive review on different design and climatic parameters to increase distillate output of solar still. *Renewable and sustainable energy reviews, 69*, 750-758.

Panchal, H. N., & Shah, P. K. (2012). Effect of Varying Glass cover thickness on Performance of Solar still: in a Winter Climate Conditions. *International Journal of Renewable Energy Research (IJRER), 1*(4), 212-223.

Parekh, S., Farid, M. M., Selman, J. R., & Al-Hallaj, S. (2004). Solar desalination with a humidification-dehumidification technique: a comprehensive technical review. *Desalination, 160*(2), 167-186.

Peluffo, A., & Neger, Y. (2013). *Seawater desalination: technical, environmental and social aspects*. Paris: Environmental Research and Teaching Institute, CERES-ERTI. Retrieved from http://www.environnement.ens.fr/IMG/Desalination.pdf

Perlman, H. (2016). *The distribution of water on, in, and above the Earth.* Where is Earth's water? USGS, Water science school. Retrieved from https://www.usgs.gov/media/images/distribution-water-and-above-earth

Qiblawey, H. M., & Banat, F. (2008). Solar thermal desalination technologies. *Desalination, 220*(1-3), 633-644.

Rahbar, N., & Esfahani, J. A. (2012). Experimental study of a novel portable solar still by utilizing the heatpipe and thermoelectric module. *Desalination, 284*, 55-61.

Rahbar, N., & Esfahani, J. A. (2013). Productivity estimation of a single-slope solar still: Theoretical and numerical analysis. *Energy, 49*, 289-297.

Rahbar, N., Esfahani, J. A., & Fotouhi-Bafghi, E. (2015). Estimation of convective heat transfer coefficient and water-productivity in a tubular solar still–CFD simulation and theoretical analysis. *Solar Energy, 113*, 313-323.

Rajaseenivasan, T., & Murugavel, K. K. (2013). Theoretical and experimental investigation on double basin double slope solar still. *Desalination, 319*, 25-32.

Rajaseenivasan, T., & Srithar, K. (2016). Performance investigation on solar still with circular and square fins in basin with CO2 mitigation and economic analysis. *Desalination, 380*, 66-74.

Rashidi, S., Akar, S., Bovand, M., & Ellahi, R. (2018). Volume of fluid model to simulate the nanofluid flow and entropy generation in a single slope solar still. *Renewable Energy, 115*, 400-410.

Rayan, M. A., Djebedjian, B., & Khaled, I. (2001). Water supply and demand and a desalination option for Sinai, Egypt. *Desalination, 136*(1-3), 73-81.

Rijsberman, F. R. (2006). Water scarcity: fact or fiction?. *Agricultural water management, 80*(1-3), 5-22.

Sadrzadeh, M., & Mohammadi, T. (2008). Sea water desalination using electrodialysis. *Desalination, 221*(1-3), 440-447.

Sahota, L., & Tiwari, G. N. (2016). Effect of nanofluids on the performance of passive double slope solar still: a comparative study using characteristic curve. *Desalination, 388*, 9-21.

Sakthivel, M., Shanmugasundaram, S., & Alwarsamy, T. (2010). An experimental study on a regenerative solar still with energy storage medium Jute cloth. *Desalination, 264*(1-2), 24-31.

Sarray, Y., Hidouri, N., Mchirgui, A., & Brahim, A. B. (2017). Study of heat and mass transfer phenomena and entropy rate of humid air inside a passive solar still. *Desalination, 409*, 80-95.

Setoodeh, N., Rahimi, R., & Ameri, A. (2011). Modeling and determination of heat transfer coefficient in a basin solar still using CFD. *Desalination, 268*(1-3), 103-110.

Shalaby, S. M., El-Bialy, E., & El-Sebaii, A. A. (2016). An experimental investigation of a v-corrugated absorber single-basin solar still using PCM. *Desalination, 398*, 247-255.

Sharaf, M. A., Nafey, A. S., & García-Rodríguez, L. (2011). Exergy and thermo-economic analyses of a combined solar organic cycle with multi effect distillation (MED) desalination process. *Desalination, 272*(1-3), 135-147.

Sharshir, S. W., Peng, G., Wu, L., Essa, F. A., Kabeel, A. E., & Yang, N. (2017). The effects of flake graphite nanoparticles, phase change material, and film cooling on the solar still performance. *Applied energy, 191*, 358-366.

Sharshir, S. W., Yang, N., Peng, G., & Kabeel, A. E. (2016). Factors affecting solar stills productivity and improvement techniques: a detailed review. *Applied Thermal Engineering, 100*, 267-284.

Shatat, M., Worall, M., & Riffat, S. (2013). Opportunities for solar water desalination worldwide. *Sustainable cities and society, 9*, 67-80.

Singh, H. N., & Tiwari, G. N. (2004). Monthly performance of passive and active solar stills for different Indian climatic conditions. *Desalination, 168*, 145-150.

Slesarenko, V. V. (2001). Heat pumps as a source of heat energy for desalination of seawater. *Desalination, 139*(1-3), 405-410.

Somwanshi, A., & Tiwari, A. K. (2014). Performance enhancement of a single basin solar still with flow of water from an air cooler on the cover. *Desalination, 352*, 92-102.

Srivastava, P. K., & Agrawal, S. K. (2013a). Experimental and theoretical analysis of single sloped basin type solar still consisting of multiple low thermal inertia floating porous absorbers. *Desalination, 311*, 198-205.

Srivastava, P. K., & Agrawal, S. K. (2013b). Winter and summer performance of single sloped basin type solar still integrated with extended porous fins. *Desalination, 319*, 73-78.

Sun, D., Xu, J., & Chen, Q. (2014). Modeling of the evaporation and condensation phase-change problems with FLUENT. *Numerical Heat Transfer, Part B: Fundamentals, 66*(4), 326-342.

Tanaka, H., & Nakatake, Y. (2006). Theoretical analysis of a basin type solar still with internal and external reflectors. *Desalination, 197*(1-3), 205-216.

Tiwari, A. K., & Tiwari, G. N. (2006). Effect of water depths on heat and mass transfer in a passive solar still: in summer climatic condition. *Desalination, 195*(1-3), 78-94.

Tiwari, G. N. (2002). *Solar energy: fundamentals, design, modelling and applications*. Alpha Science Int'l Ltd.

Tiwari, G. N., & Sahota, L. (2017). Review on the energy and economic efficiencies of passive and active solar distillation systems. *Desalination, 401*, 151-179.

University of Southern Queensland. (2019). *Toowoomba weather station.* Retrieved from http://foesweather.usq.edu.au/

Velmurugan, V., & Srithar, K. (2007). Solar stills integrated with a mini solar pond—analytical simulation and experimental validation. *Desalination, 216*(1-3), 232-241.

Velmurugan, V., & Srithar, K. (2011). Performance analysis of solar stills based on various factors affecting the productivity: a review. *Renewable and sustainable energy reviews, 15*(2), 1294-1304.

Velmurugan, V., Deenadayalan, C. K., Vinod, H., & Srithar, K. (2008a). Desalination of effluent using fin type solar still. *Energy, 33*(11), 1719-1727.

Velmurugan, V., Gopalakrishnan, M., Raghu, R., & Srithar, K. (2008b). Single basin solar still with fin for enhancing productivity. *Energy Conversion and Management, 49*(10), 2602-2608.

Velmurugan, V., Kumar, K. N., Haq, T. N., & Srithar, K. (2009). Performance analysis in stepped solar still for effluent desalination. *Energy, 34*(9), 1179-1186.

Versteeg, H. K., & Malalasekera, W. (2007). *An introduction to computational fluid dynamics: the finite volume method*. Pearson education.

Wang, P., & Chung, T. S. (2015). Recent advances in membrane distillation processes: Membrane development, configuration design and application exploring. *Journal of membrane science, 474*, 39-56.

Welch, S. W., & Wilson, J. (2000). A volume of fluid based method for fluid flows with phase change. *Journal of computational physics, 160*(2), 662-682.

White, F. M. (2016). *Fluid mechanics* (8th Ed.). NY: McGraw-Hill Education.

World Health Organization, & UNICEF. (2017). *Progress on drinking water, sanitation and hygiene: 2017 update and SDG baselines*. Switzerland: JMP.

World Health Organization. (2011). Guidelines for drinking-water quality (4th Ed.). Malta: Gutenberg.

Yang, Y., Shen, S., Zhou, S., Mu, X., & Zhang, K. (2015). Research for the adjustable performance of the thermal vapour compressor in the MED–TVC system. *Desalination and Water Treatment, 53*(7), 1725-1734.

Appendix A: Figures

1. The temperature profile of selected days

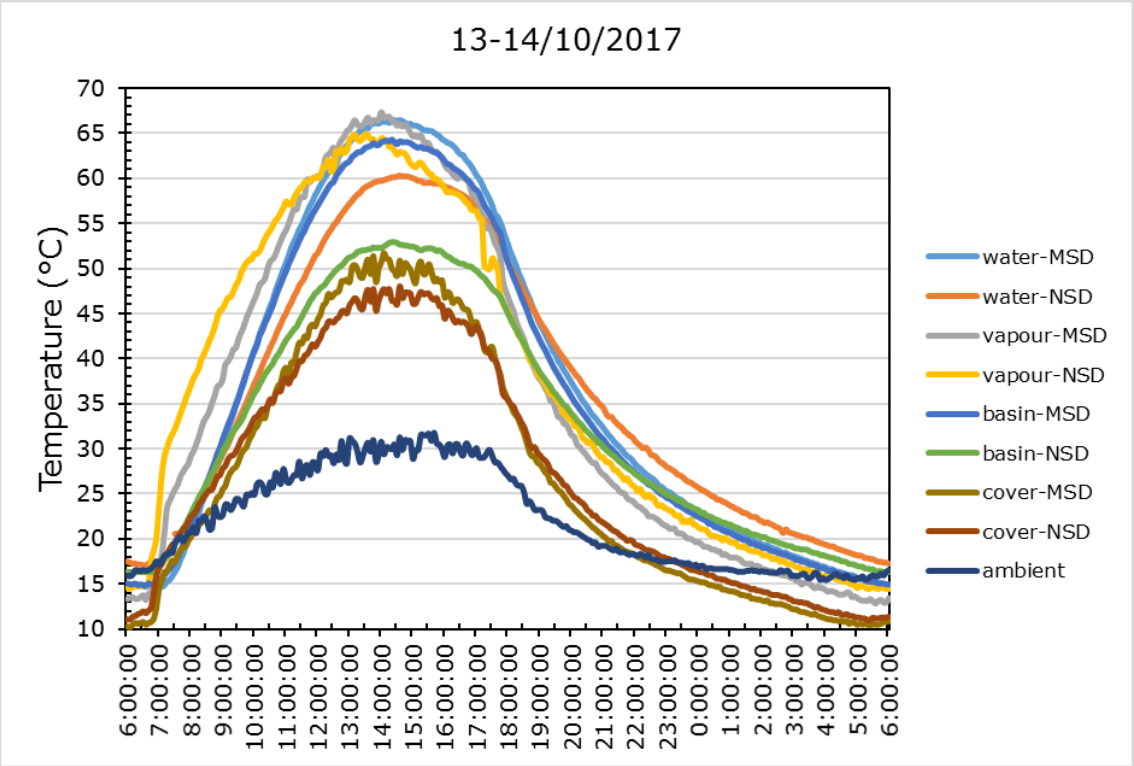

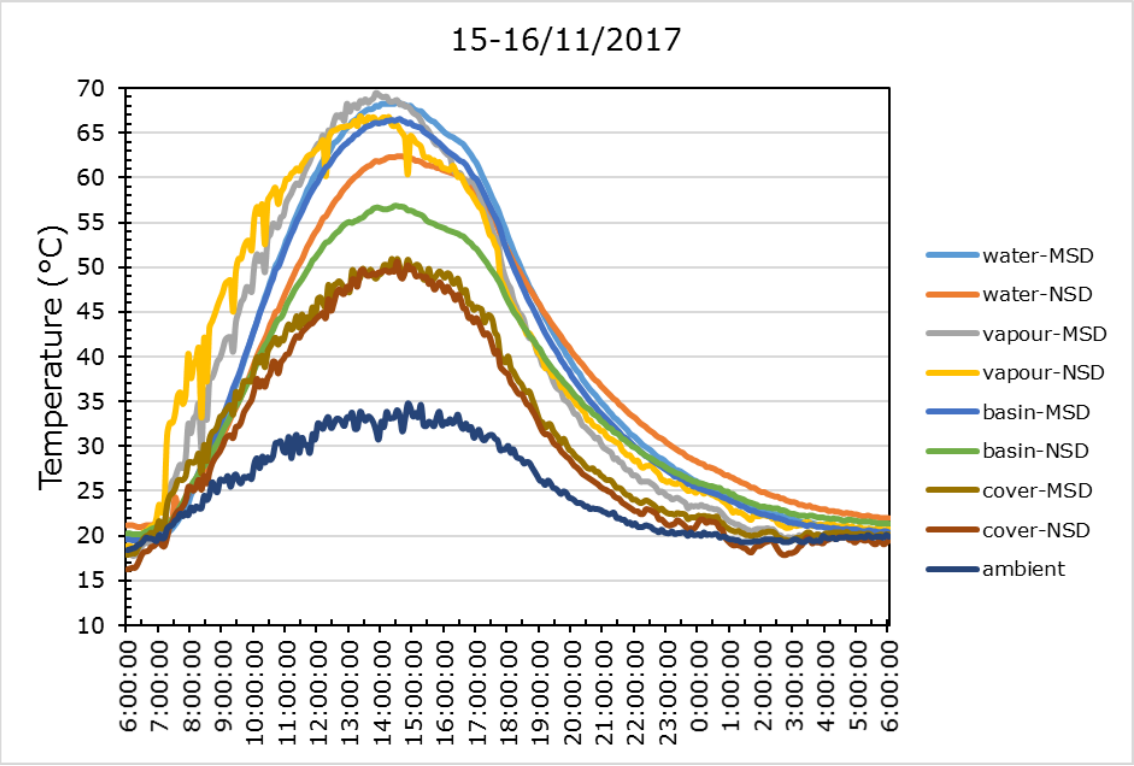

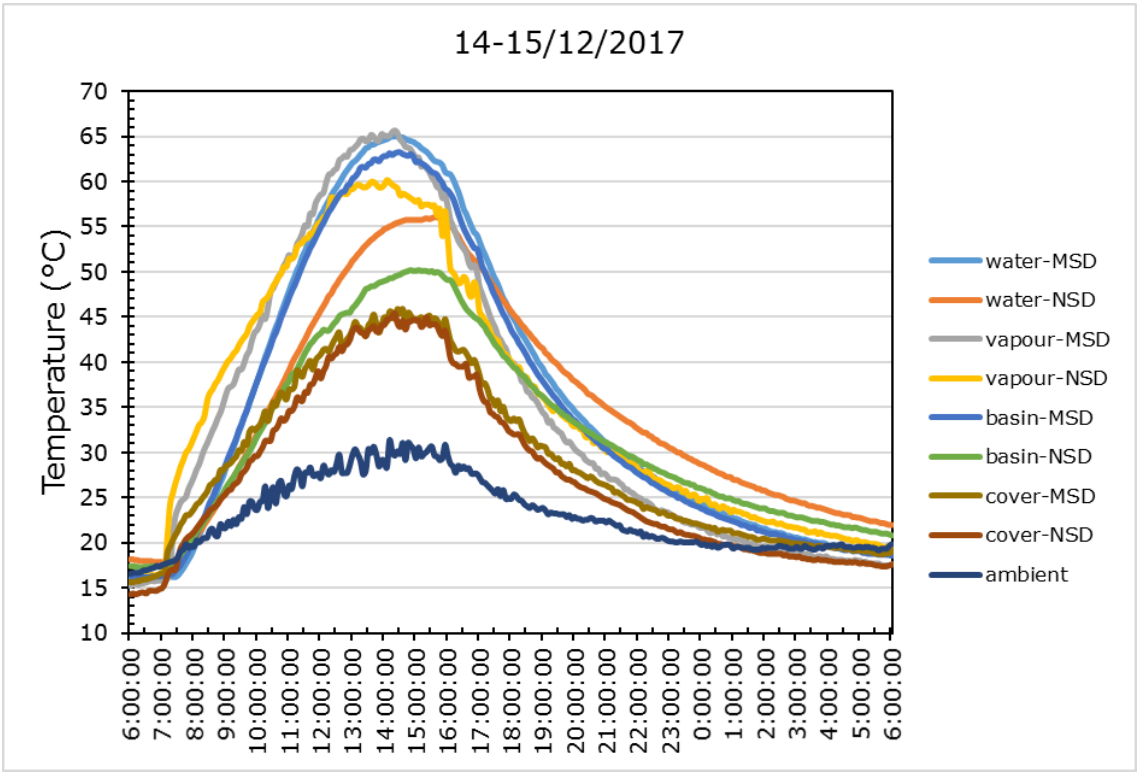
14-15/12/2017
Temperature (°C)
70
65
60
55
50
45
40
35
30
25
20
15
10
6:00:00
7:00:00
8:00:00
9:00:00
10:00:00
11:00:00
12:00:00
13:00:00
14:00:00
15:00:00
16:00:00
17:00:00
18:00:00
19:00:00
20:00:00
21:00:00
22:00:00
23:00:00
0:00:00
1:00:00
2:00:00
3:00:00
4:00:00
5:00:00
6:00:00
water-MSD
water-NSD
vapour-MSD
vapour-NSD
basin-MSD
basin-NSD
cover-MSD
cover-NSD
ambient

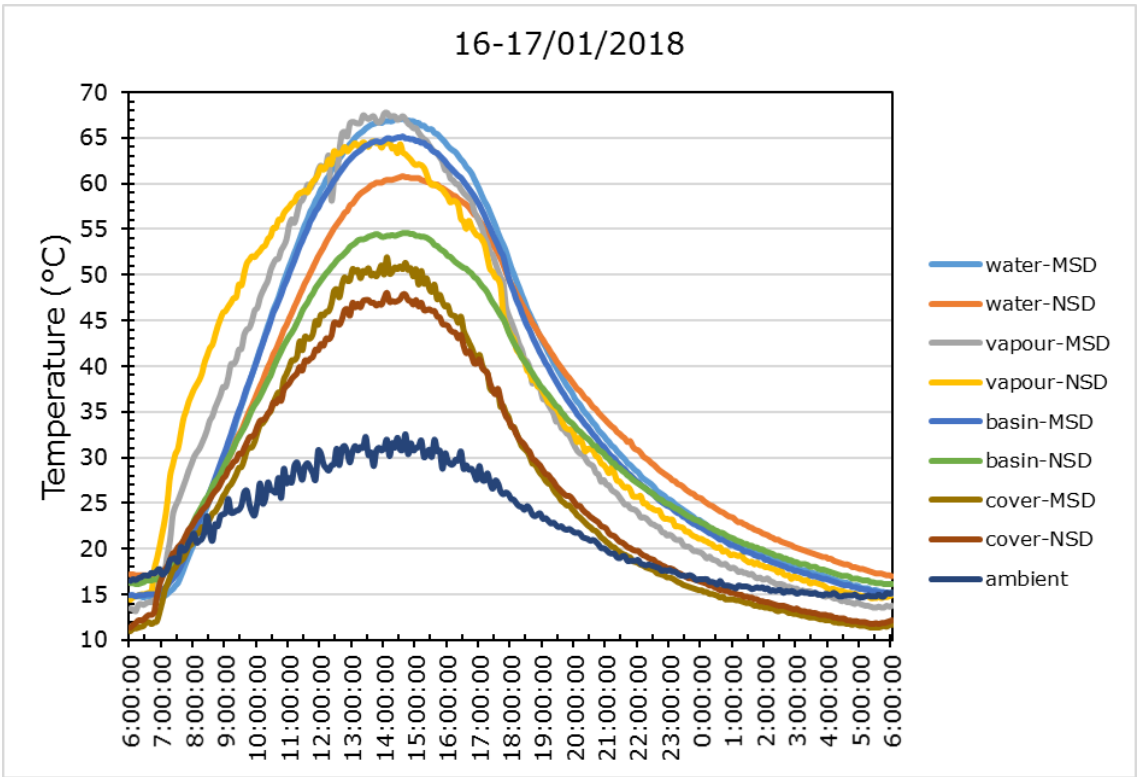
16-17/01/2018
Temperature (°C)
70
65
60
55
50
45
40
35
30
25
20
15
10
6:00:00
7:00:00
8:00:00
9:00:00
10:00:00
11:00:00
12:00:00
13:00:00
14:00:00
15:00:00
16:00:00
17:00:00
18:00:00
19:00:00
20:00:00
21:00:00
22:00:00
23:00:00
0:00:00
1:00:00
2:00:00
3:00:00
4:00:00
5:00:00
6:00:00
water-MSD
water-NSD
vapour-MSD
vapour-NSD
basin-MSD
basin-NSD
cover-MSD
cover-NSD
ambient

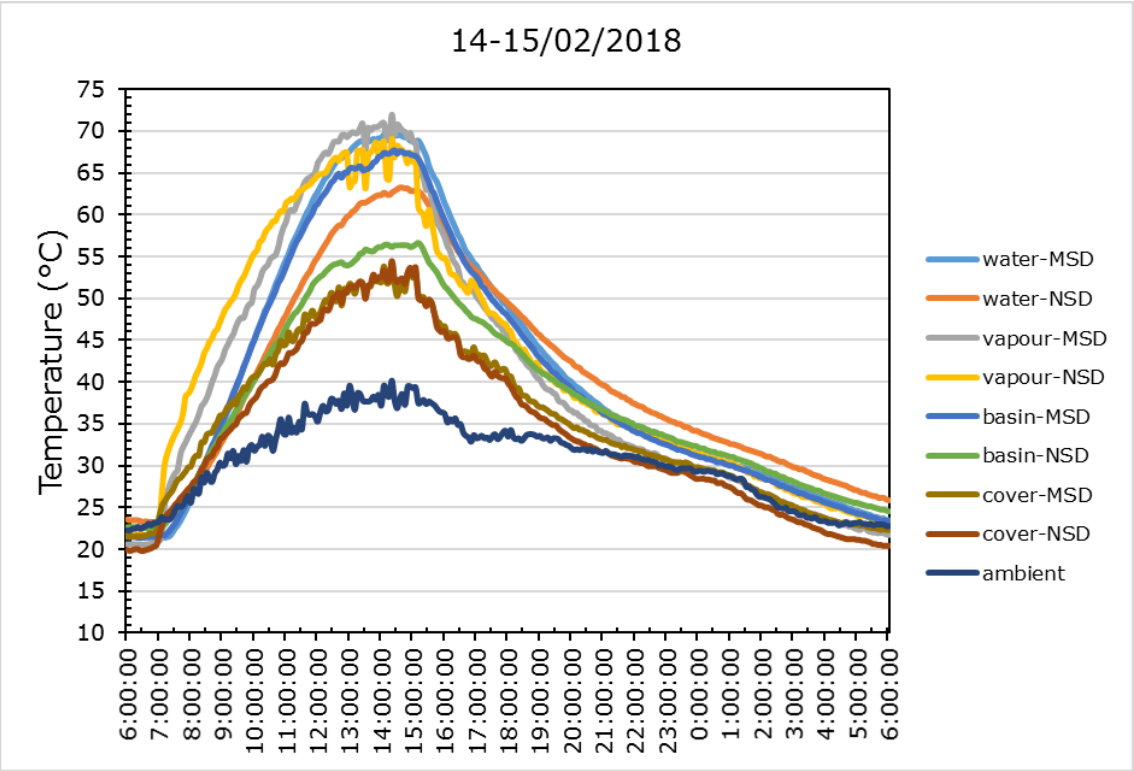
14-15/02/2018
Temperature (°C)
75
70
65
60
55
50
45
40
35
30
25
20
15
10
6:00:00
7:00:00
8:00:00
9:00:00
10:00:00
11:00:00
12:00:00
13:00:00
14:00:00
15:00:00
16:00:00
17:00:00
18:00:00
19:00:00
20:00:00
21:00:00
22:00:00
23:00:00
0:00:00
1:00:00
2:00:00
3:00:00
4:00:00
5:00:00
6:00:00
water-MSD
water-NSD
vapour-MSD
vapour-NSD
basin-MSD
basin-NSD
cover-MSD
cover-NSD
ambient

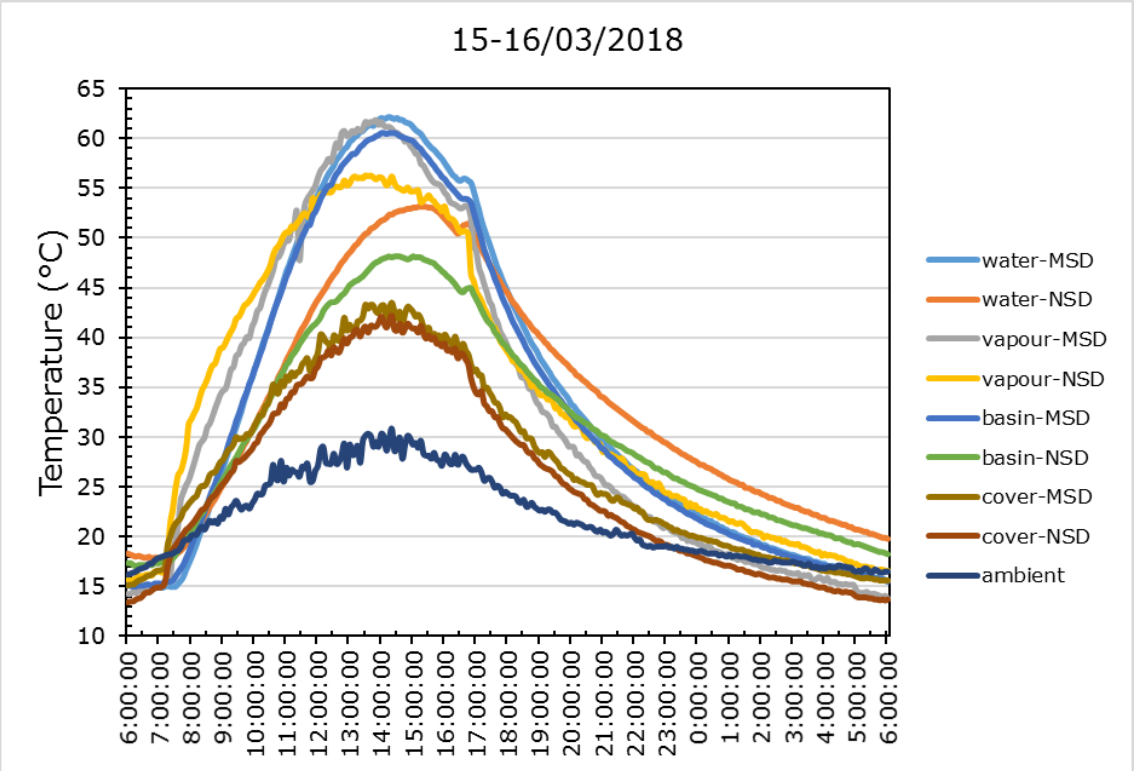
15-16/03/2018
Temperature (°C)
65
60
55
50
45
40
35
30
25
20
15
10
6:00:00
7:00:00
8:00:00
9:00:00
10:00:00
11:00:00
12:00:00
13:00:00
14:00:00
15:00:00
16:00:00
17:00:00
18:00:00
19:00:00
20:00:00
21:00:00
22:00:00
23:00:00
0:00:00
1:00:00
2:00:00
3:00:00
4:00:00
5:00:00
6:00:00
water-MSD
water-NSD
vapour-MSD
vapour-NSD
basin-MSD
basin-NSD
cover-MSD
cover-NSD
ambient

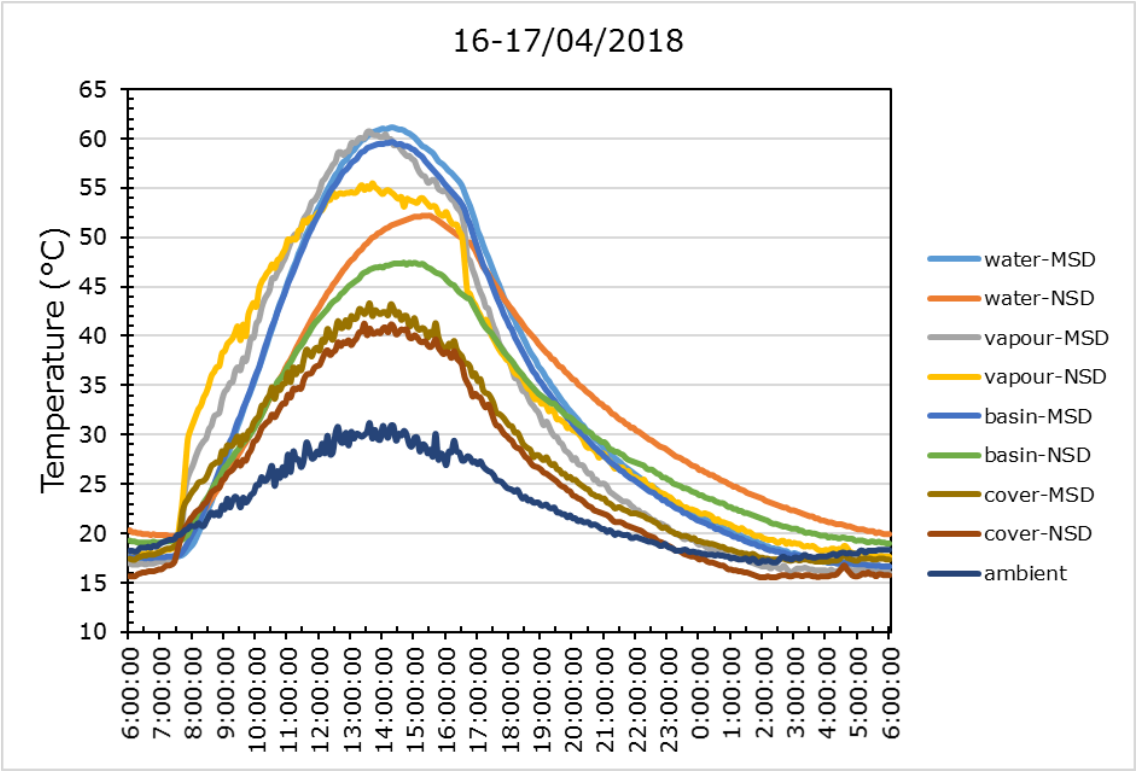
16-17/04/2018
Temperature (°C)
65
60
55
50
45
40
35
30
25
20
15
10
6:00:00
7:00:00
8:00:00
9:00:00
10:00:00
11:00:00
12:00:00
13:00:00
14:00:00
15:00:00
16:00:00
17:00:00
18:00:00
19:00:00
20:00:00
21:00:00
22:00:00
23:00:00
0:00:00
1:00:00
2:00:00
3:00:00
4:00:00
5:00:00
6:00:00
water-MSD
water-NSD
vapour-MSD
vapour-NSD
basin-MSD
basin-NSD
cover-MSD
cover-NSD
ambient

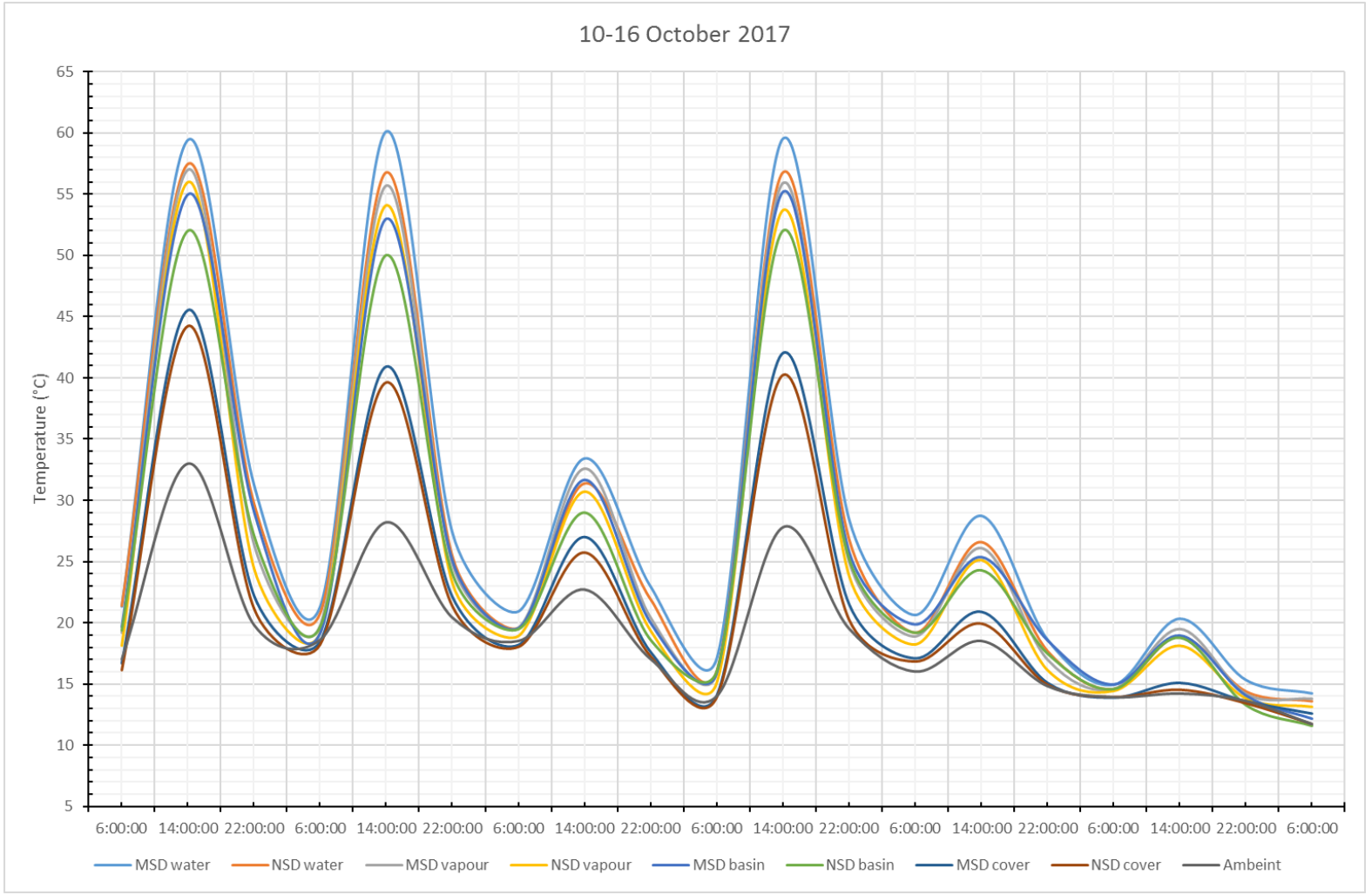
10-16 October 2017
Temperature (°C)
65
60
55
50
45
40
35
30
25
20
15
10
5
6:00:00 14:00:00 22:00:00 6:00:00 14:00:00 22:00:00 6:00:00 14:00:00 22:00:00 6:00:00 14:00:00 22:00:00 6:00:00 14:00:00 22:00:00 6:00:00 14:00:00 22:00:00 6:00:00
MSD water
NSD water
MSD vapour
NSD vapour
MSD basin
NSD basin
MSD cover
NSD cover
Ambeint

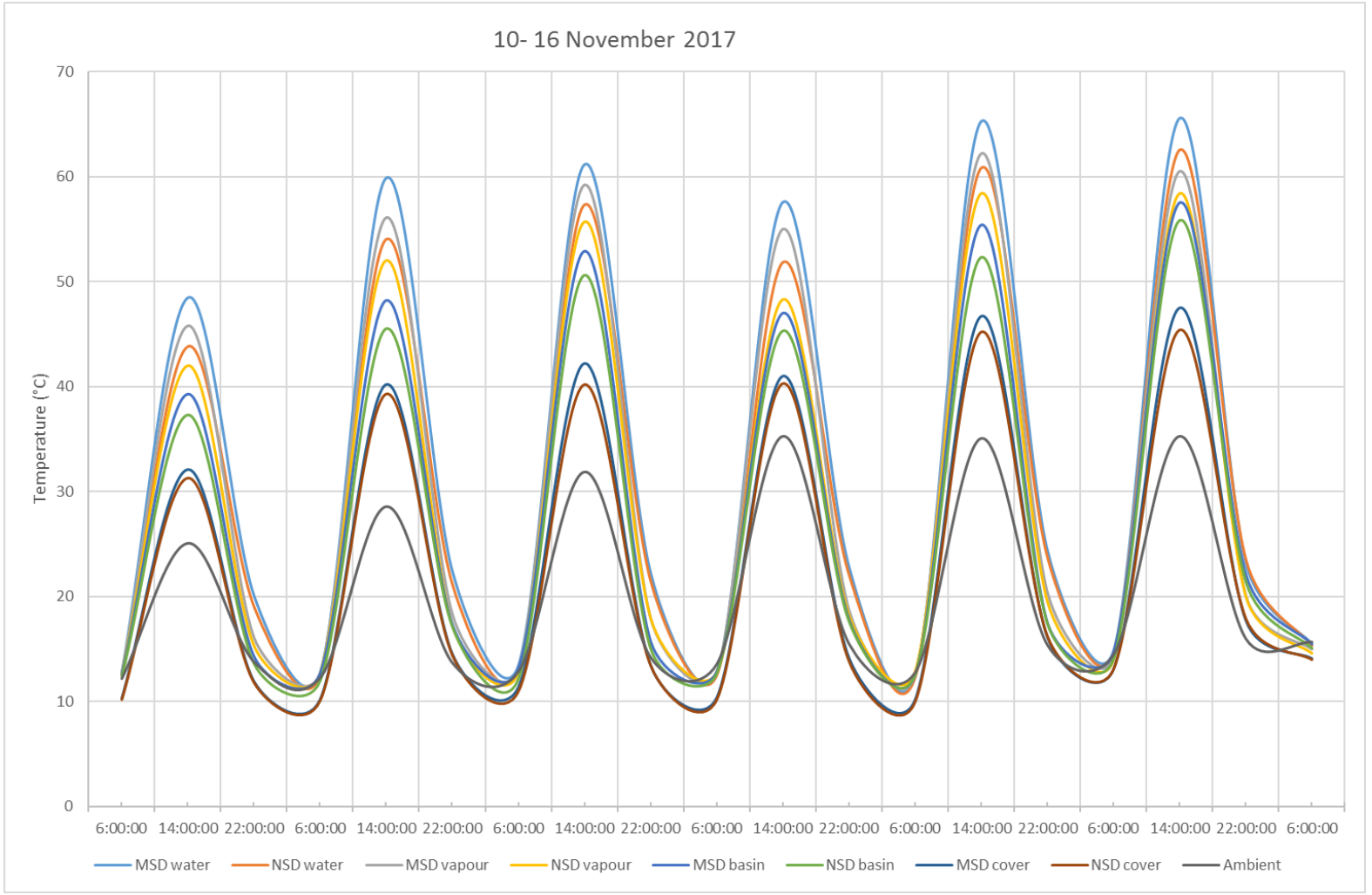
10- 16 November 2017
Temperature (°C)
70
60
50
40
30
20
10
0
6:00:00 14:00:00 22:00:00 6:00:00 14:00:00 22:00:00 6:00:00 14:00:00 22:00:00 6:00:00 14:00:00 22:00:00 6:00:00 14:00:00 22:00:00 6:00:00 14:00:00 22:00:00 6:00:00
MSD water
NSD water
MSD vapour
NSD vapour
MSD basin
NSD basin
MSD cover
NSD cover
Ambient

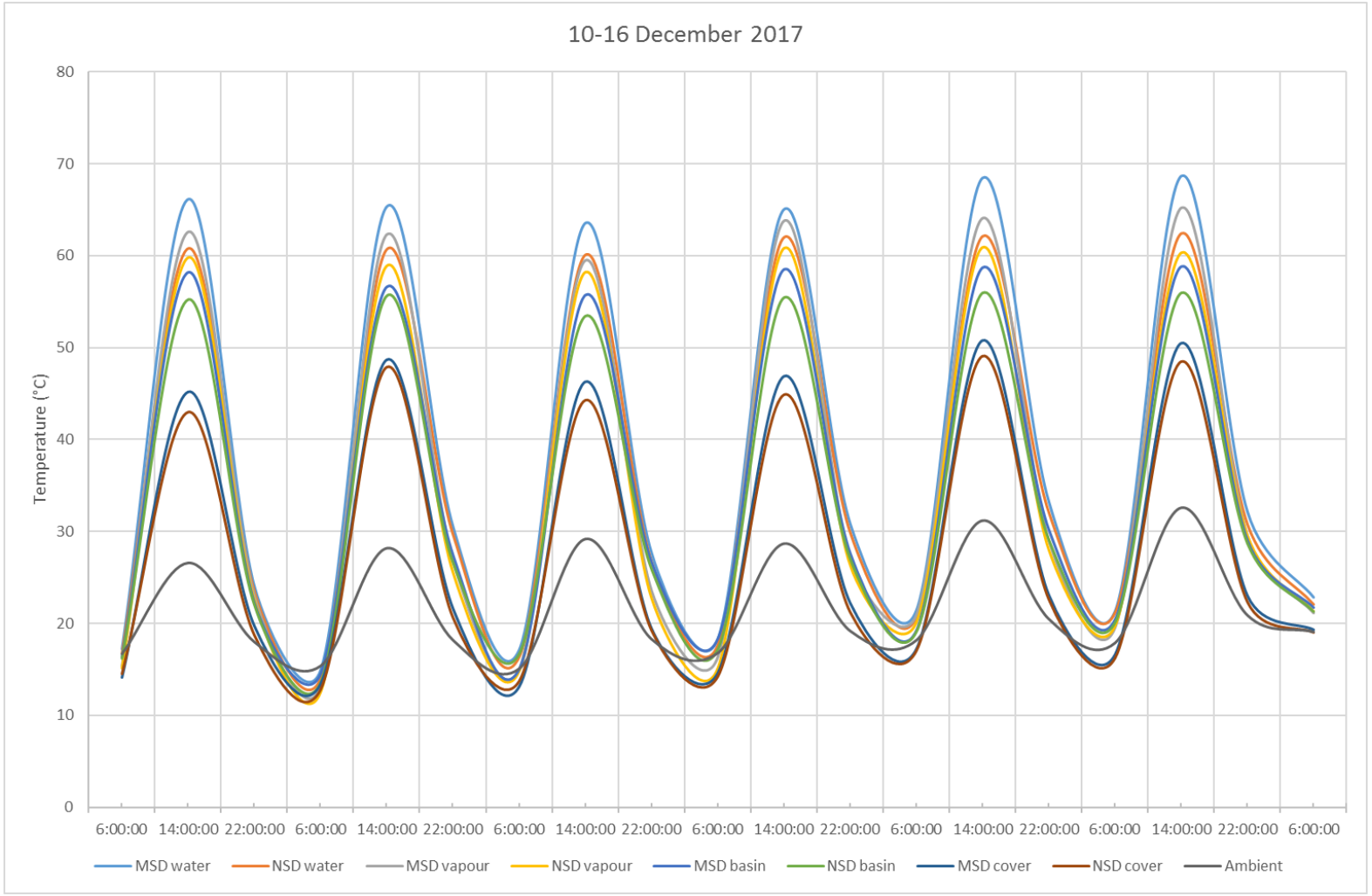
10-16 December 2017
Temperature (°C)
80
70
60
50
40
30
20
10
0
6:00:00 14:00:00 22:00:00 6:00:00 14:00:00 22:00:00 6:00:00 14:00:00 22:00:00 6:00:00 14:00:00 22:00:00 6:00:00 14:00:00 22:00:00 6:00:00 14:00:00 22:00:00 6:00:00
MSD water
NSD water
MSD vapour
NSD vapour
MSD basin
NSD basin
MSD cover
NSD cover
Ambient

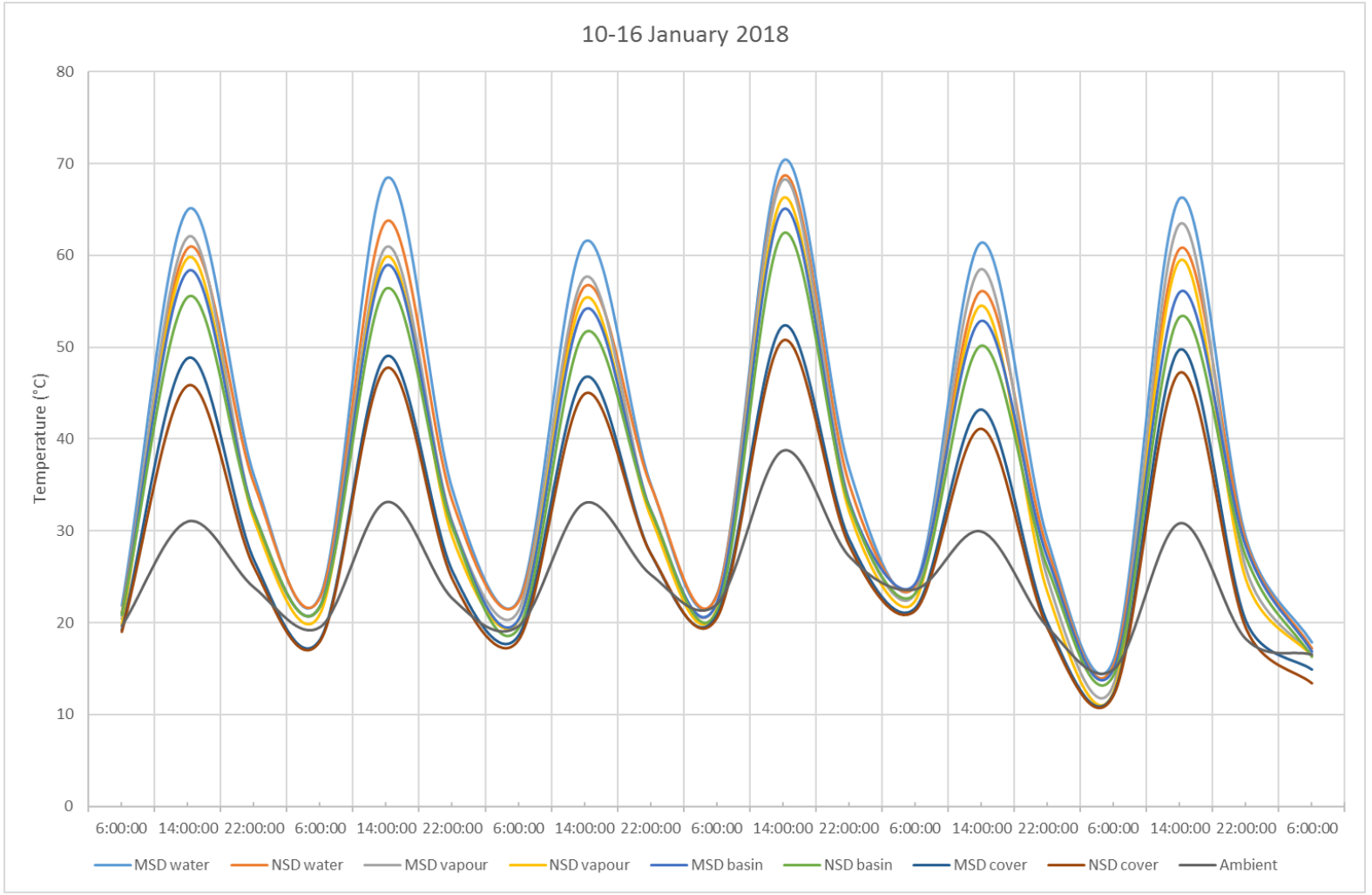
10-16 January 2018
Temperature (°C)
80
70
60
50
40
30
20
10
0
6:00:00 14:00:00 22:00:00 6:00:00 14:00:00 22:00:00 6:00:00 14:00:00 22:00:00 6:00:00 14:00:00 22:00:00 6:00:00 14:00:00 22:00:00 6:00:00 14:00:00 22:00:00 6:00:00
MSD water
NSD water
MSD vapour
NSD vapour
MSD basin
NSD basin
MSD cover
NSD cover
Ambient

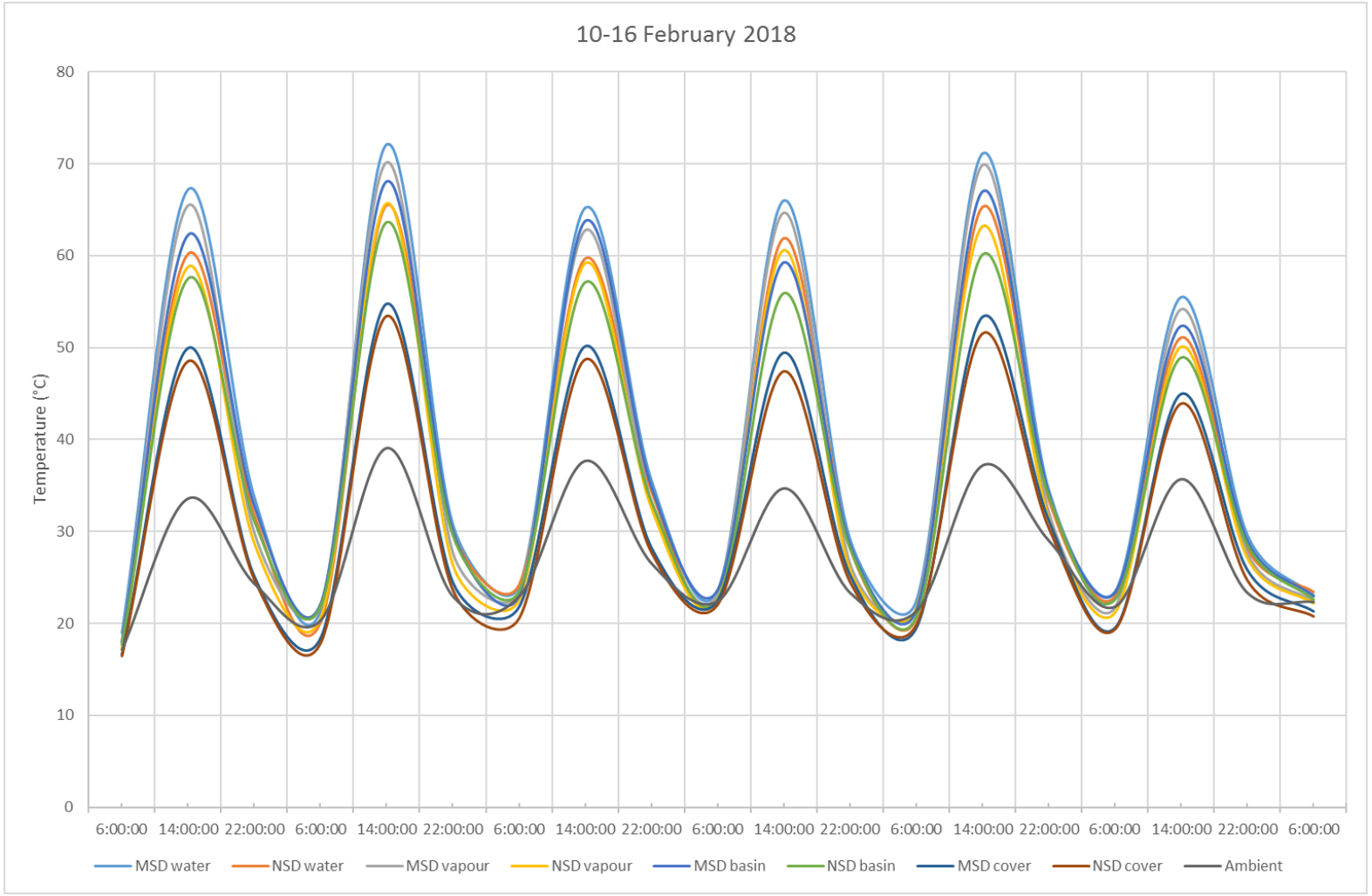
10-16 February 2018
Temperature (°C)
80
70
60
50
40
30
20
10
0
6:00:00 14:00:00 22:00:00 6:00:00 14:00:00 22:00:00 6:00:00 14:00:00 22:00:00 6:00:00 14:00:00 22:00:00 6:00:00 14:00:00 22:00:00 6:00:00 14:00:00 22:00:00 6:00:00
MSD water
NSD water
MSD vapour
NSD vapour
MSD basin
NSD basin
MSD cover
NSD cover
Ambient

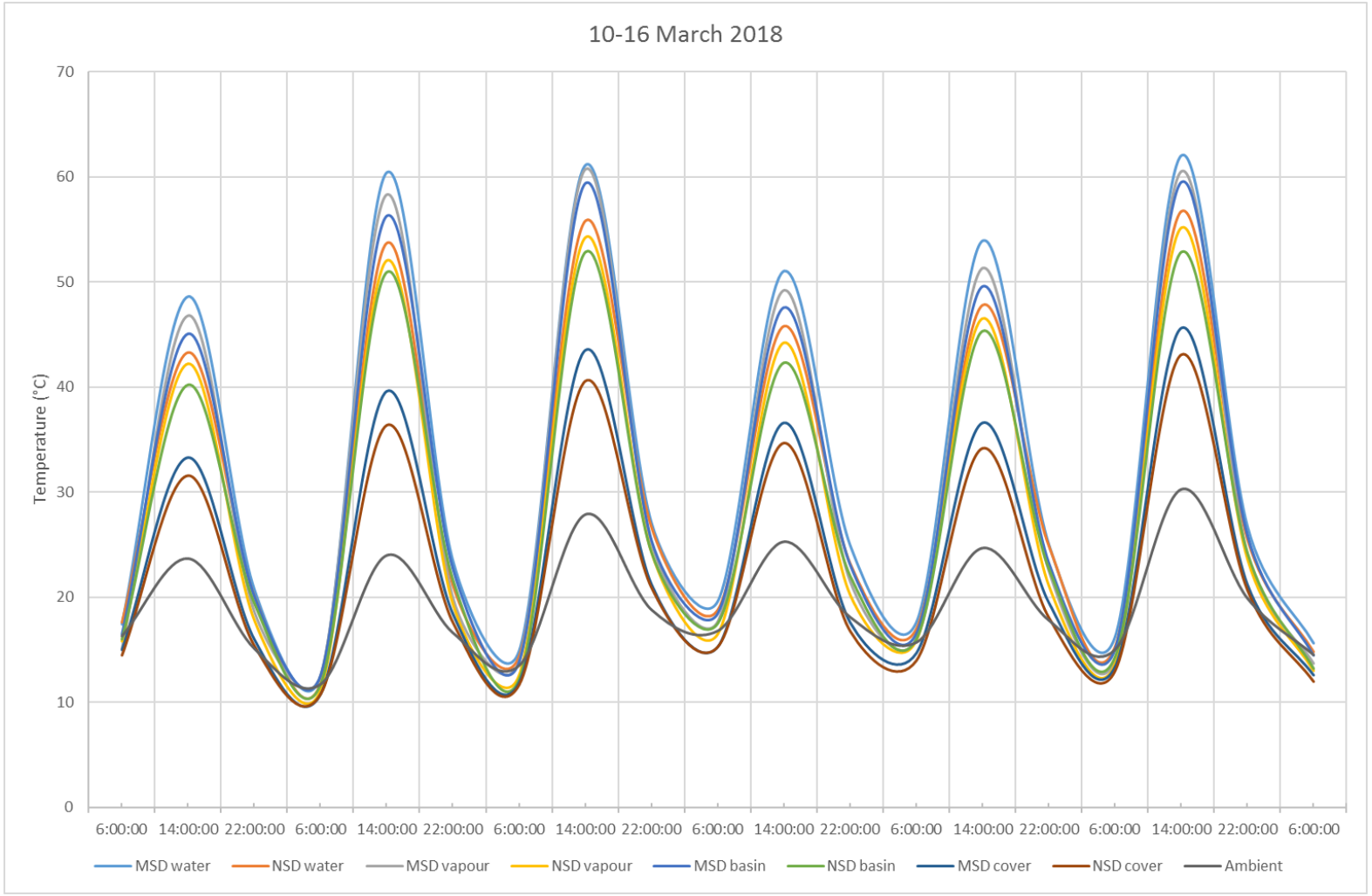
10-16 March 2018
Temperature (°C)
70
60
50
40
30
20
10
0
6:00:00 14:00:00 22:00:00 6:00:00 14:00:00 22:00:00 6:00:00 14:00:00 22:00:00 6:00:00 14:00:00 22:00:00 6:00:00 14:00:00 22:00:00 6:00:00 14:00:00 22:00:00 6:00:00
MSD water
NSD water
MSD vapour
NSD vapour
MSD basin
NSD basin
MSD cover
NSD cover
Ambient

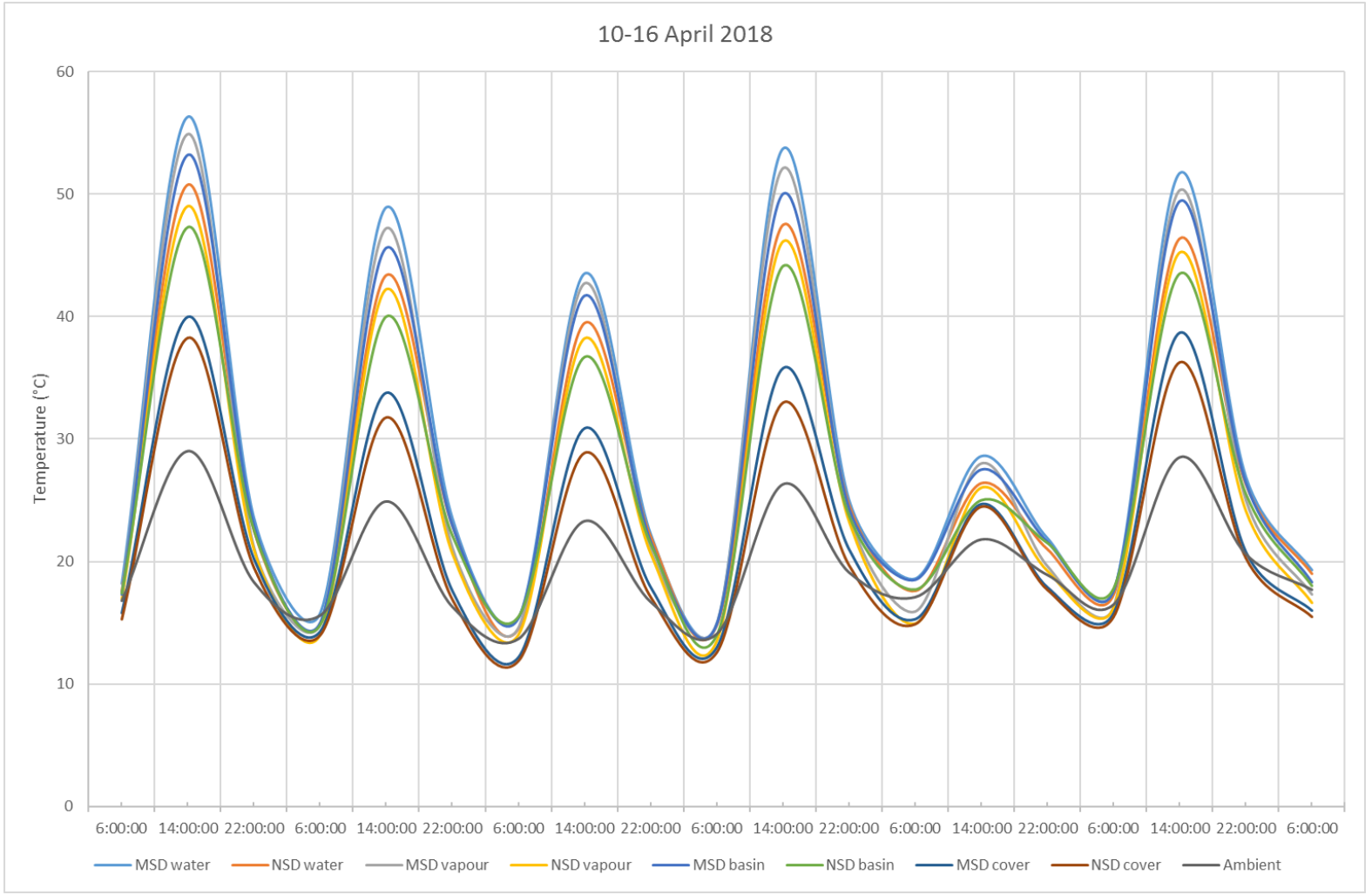
10-16 April 2018
Temperature (°C)
60
50
40
30
20
10
0
6:00:00 14:00:00 22:00:00 6:00:00 14:00:00 22:00:00 6:00:00 14:00:00 22:00:00 6:00:00 14:00:00 22:00:00 6:00:00 14:00:00 22:00:00 6:00:00 14:00:00 22:00:00 6:00:00
MSD water
NSD water
MSD vapour
NSD vapour
MSD basin
NSD basin
MSD cover
NSD cover
Ambient

2. The hourly productivity of selected days

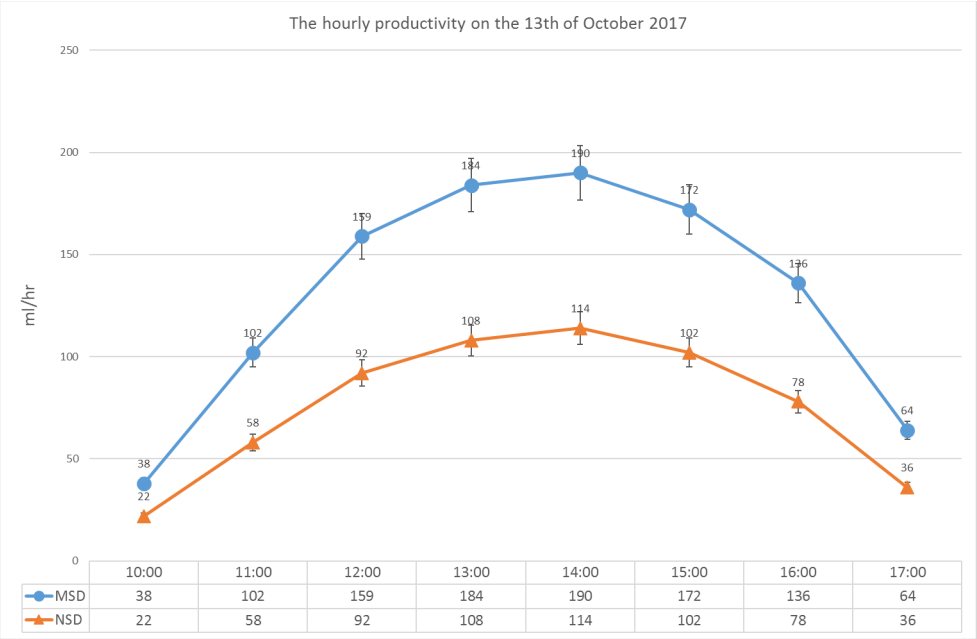

	10:00	11:00	12:00	13:00	14:00	15:00	16:00	17:00
MSD	38	102	159	184	190	172	136	64
NSD	22	58	92	108	114	102	78	36

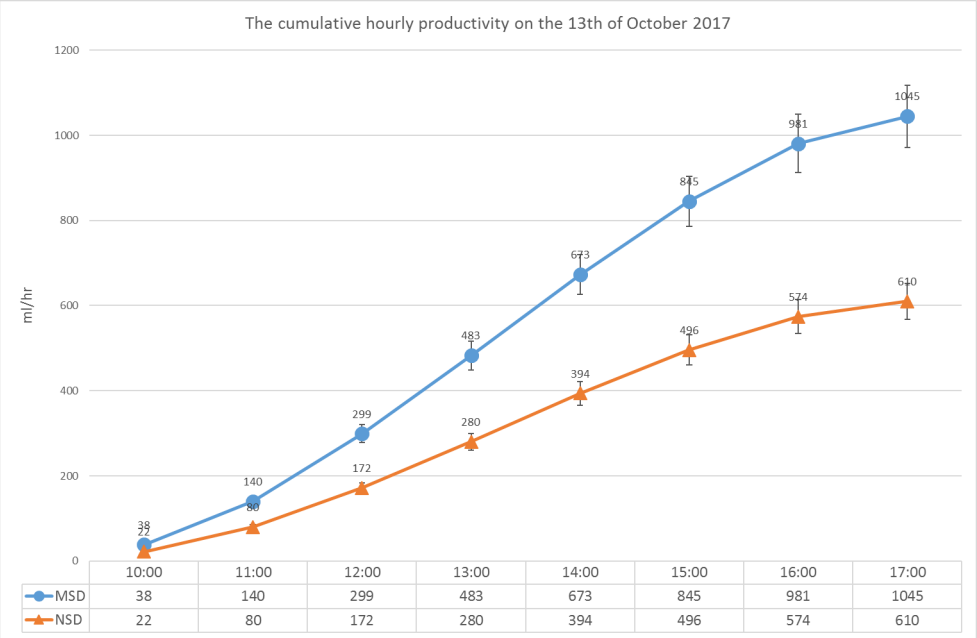

	10:00	11:00	12:00	13:00	14:00	15:00	16:00	17:00
MSD	38	140	299	483	673	845	981	1045
NSD	22	80	172	280	394	496	574	610

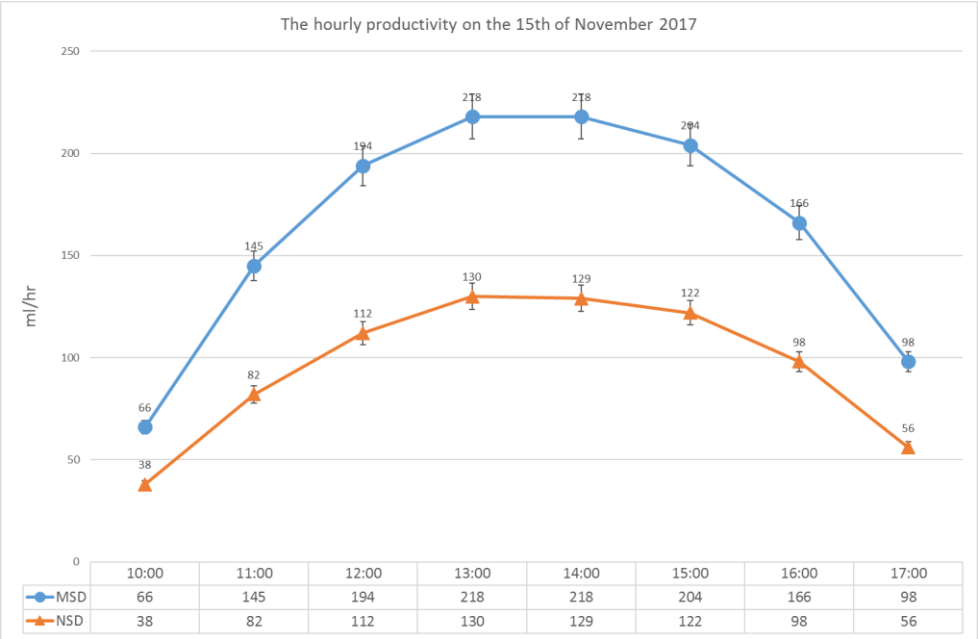

	10:00	11:00	12:00	13:00	14:00	15:00	16:00	17:00
MSD	66	145	194	218	218	204	166	98
NSD	38	82	112	130	129	122	98	56

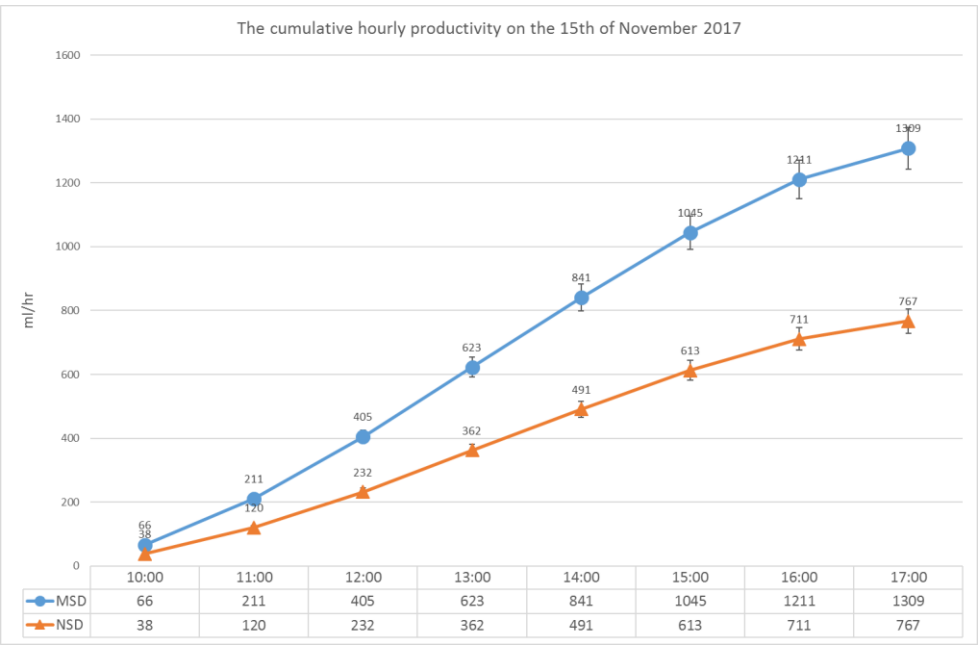

	10:00	11:00	12:00	13:00	14:00	15:00	16:00	17:00
MSD	66	211	405	623	841	1045	1211	1309
NSD	38	120	232	362	491	613	711	767

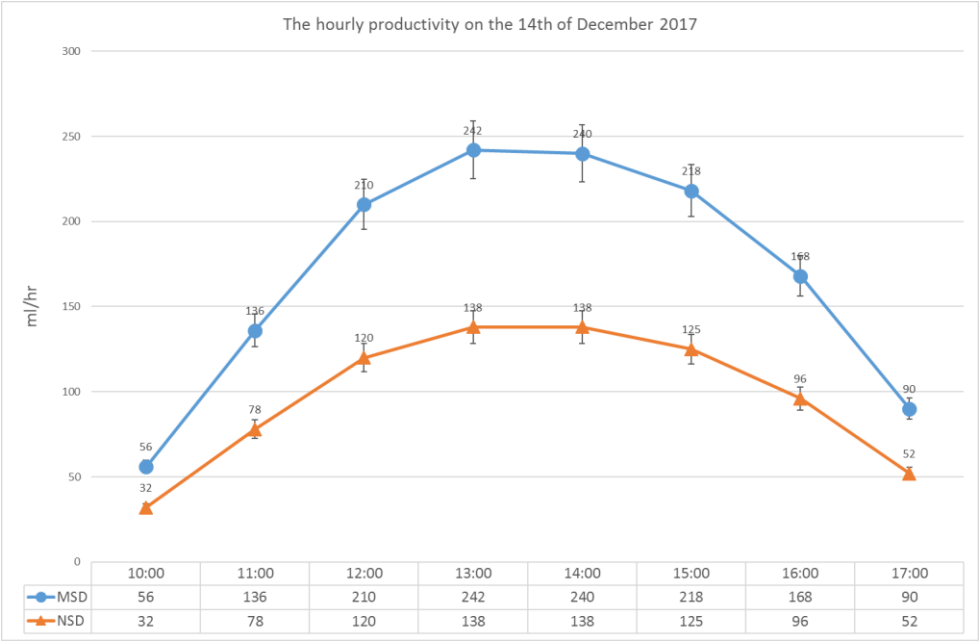

	10:00	11:00	12:00	13:00	14:00	15:00	16:00	17:00
MSD	56	136	210	242	240	218	168	90
NSD	32	78	120	138	138	125	96	52

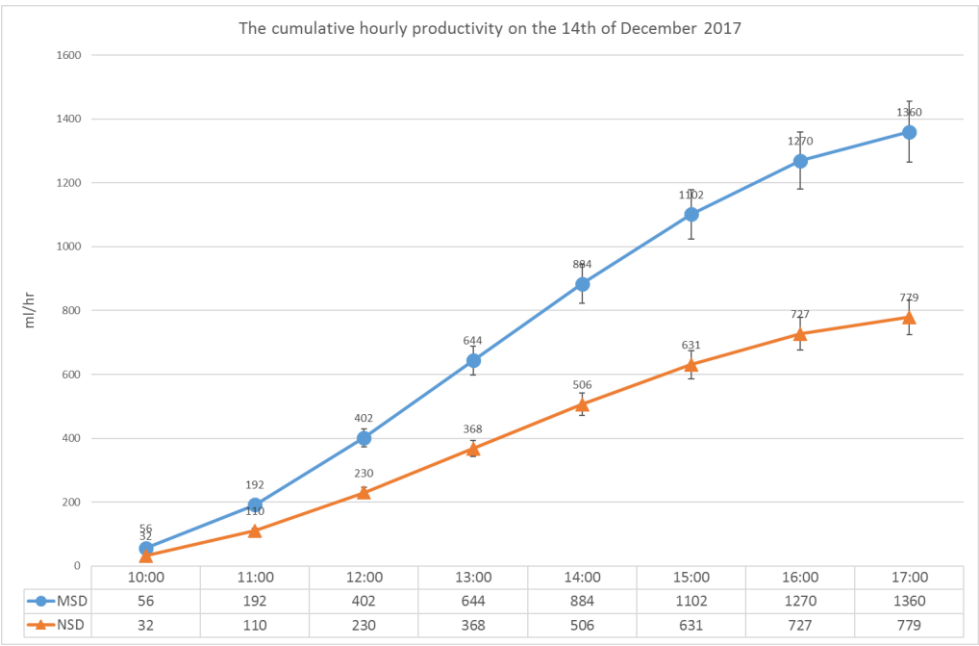

	10:00	11:00	12:00	13:00	14:00	15:00	16:00	17:00
MSD	56	192	402	644	884	1102	1270	1360
NSD	32	110	230	368	506	631	727	779

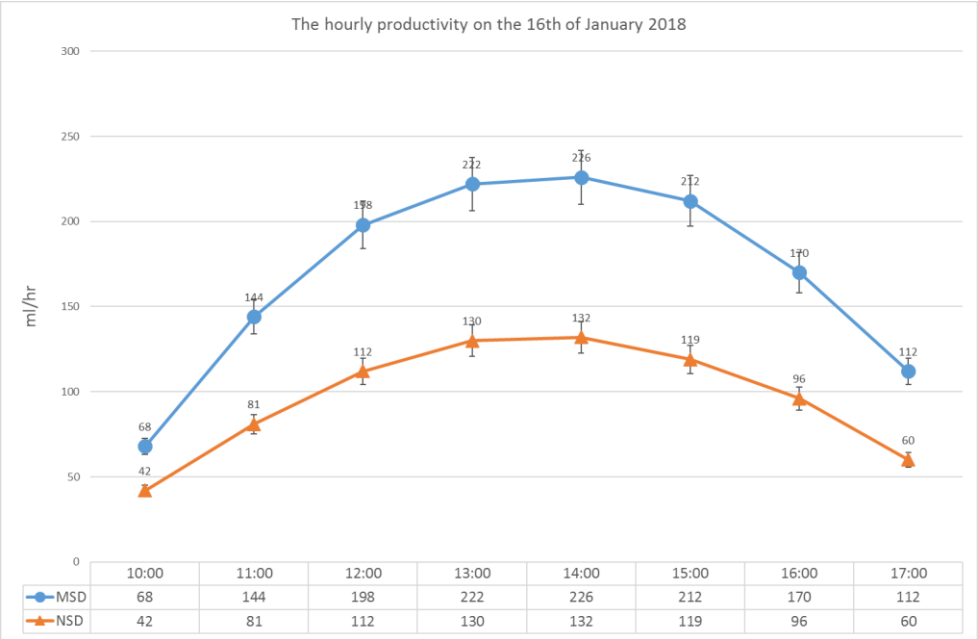

	10:00	11:00	12:00	13:00	14:00	15:00	16:00	17:00
MSD	68	144	198	222	226	212	170	112
NSD	42	81	112	130	132	119	96	60

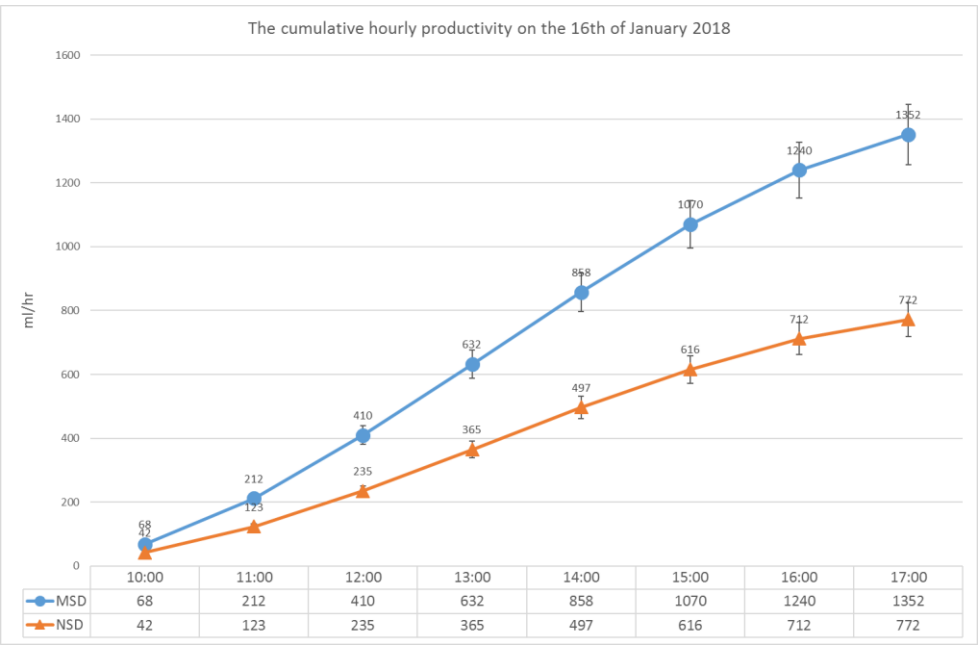

	10:00	11:00	12:00	13:00	14:00	15:00	16:00	17:00
MSD	68	212	410	632	858	1070	1240	1352
NSD	42	123	235	365	497	616	712	772

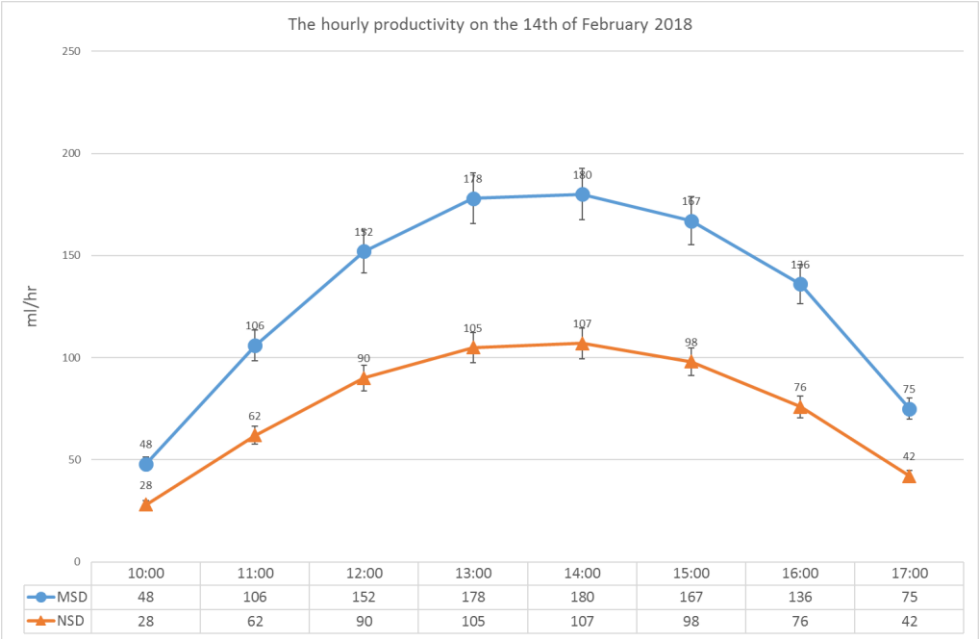

	10:00	11:00	12:00	13:00	14:00	15:00	16:00	17:00
MSD	48	106	152	178	180	167	136	75
NSD	28	62	90	105	107	98	76	42

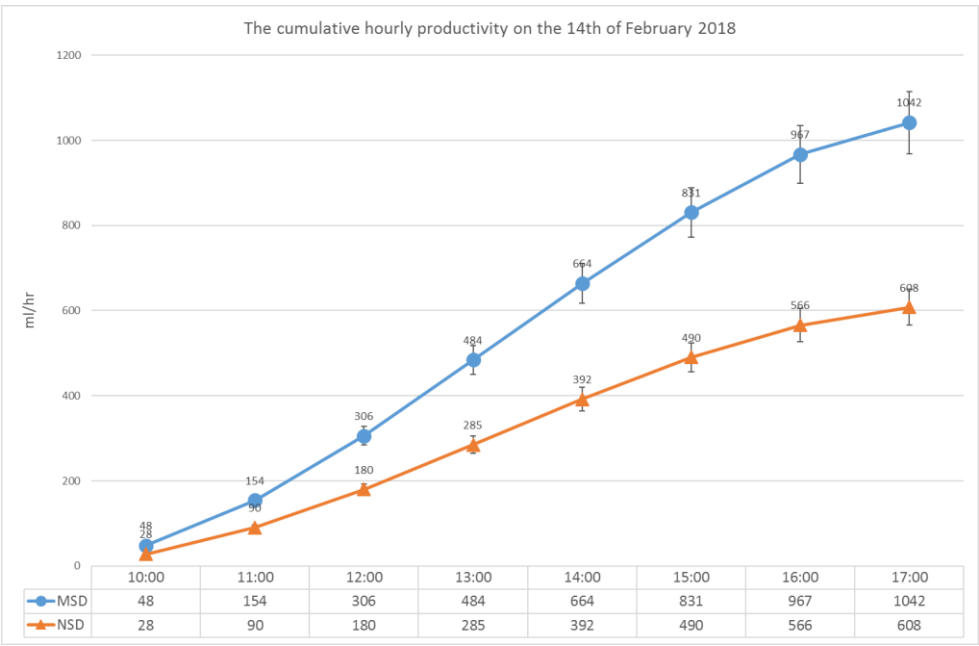

	10:00	11:00	12:00	13:00	14:00	15:00	16:00	17:00
MSD	48	154	306	484	664	831	967	1042
NSD	28	90	180	285	392	490	566	608

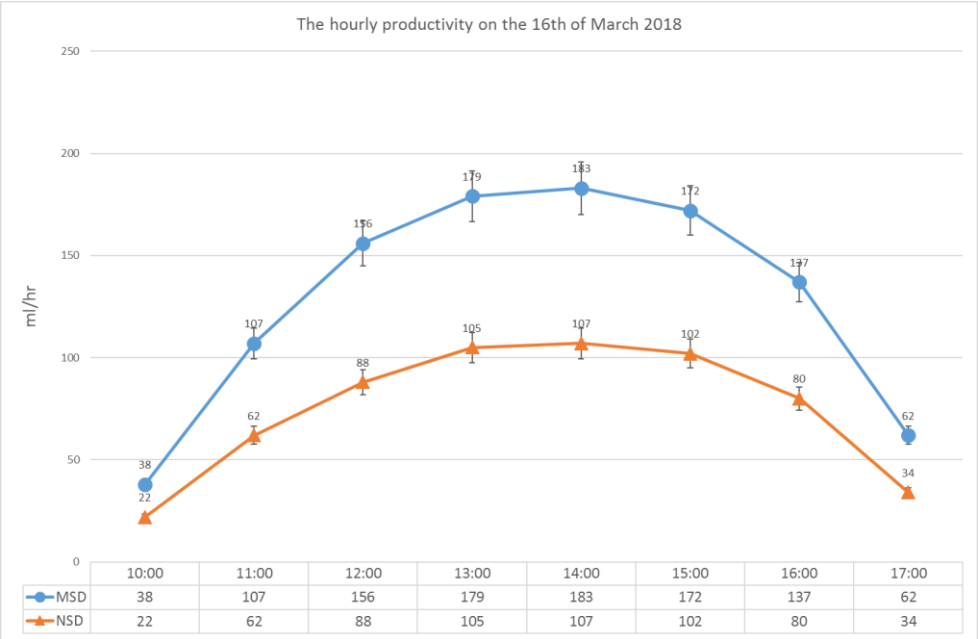

	10:00	11:00	12:00	13:00	14:00	15:00	16:00	17:00
MSD	38	107	156	179	183	172	137	62
NSD	22	62	88	105	107	102	80	34

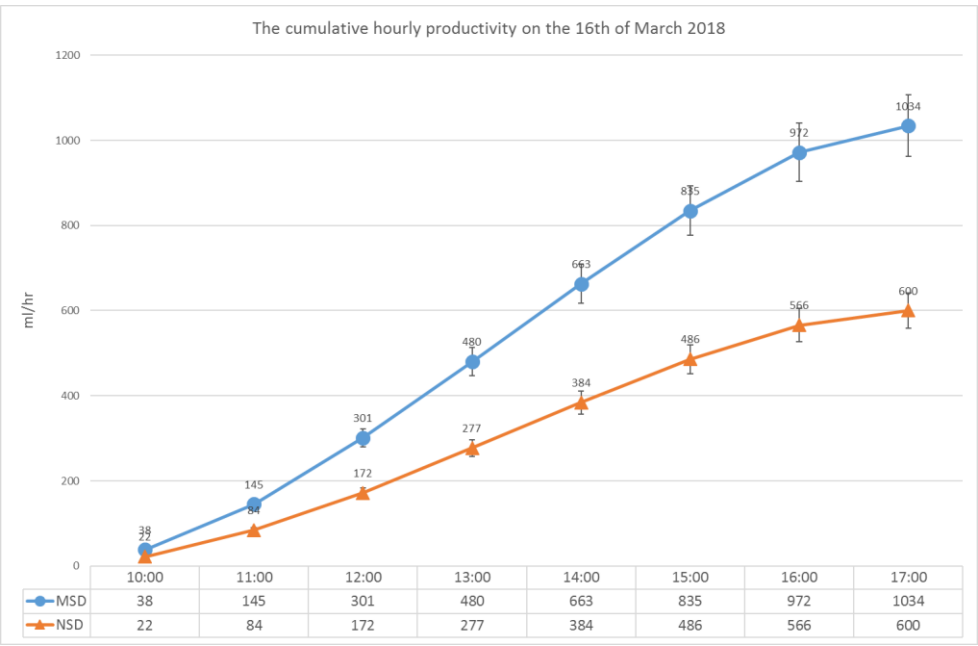

	10:00	11:00	12:00	13:00	14:00	15:00	16:00	17:00
MSD	38	145	301	480	663	835	972	1034
NSD	22	84	172	277	384	486	566	600

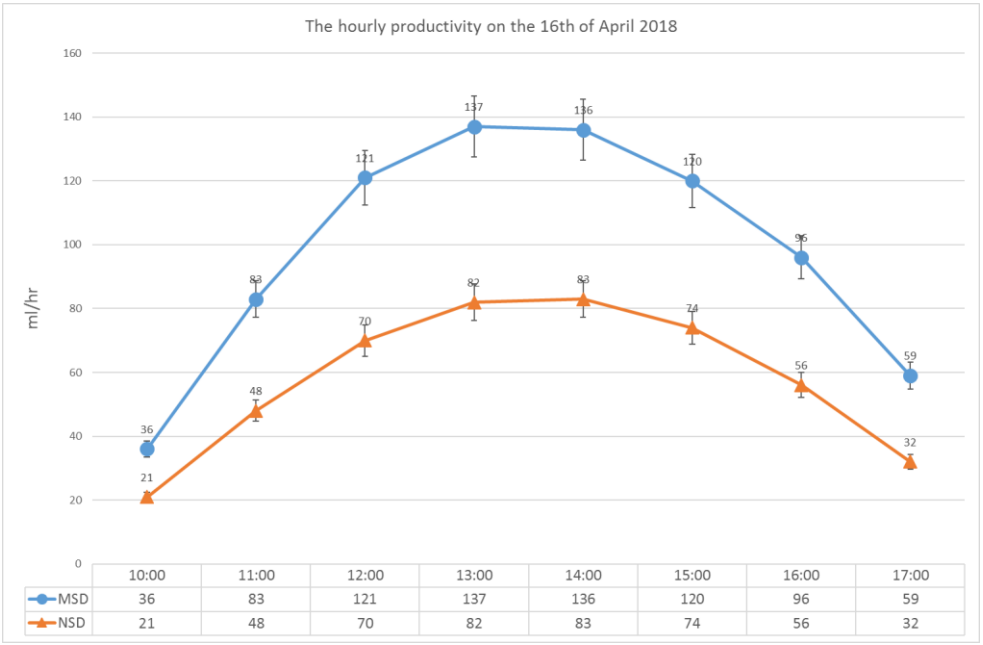

	10:00	11:00	12:00	13:00	14:00	15:00	16:00	17:00
MSD	36	83	121	137	136	120	96	59
NSD	21	48	70	82	83	74	56	32

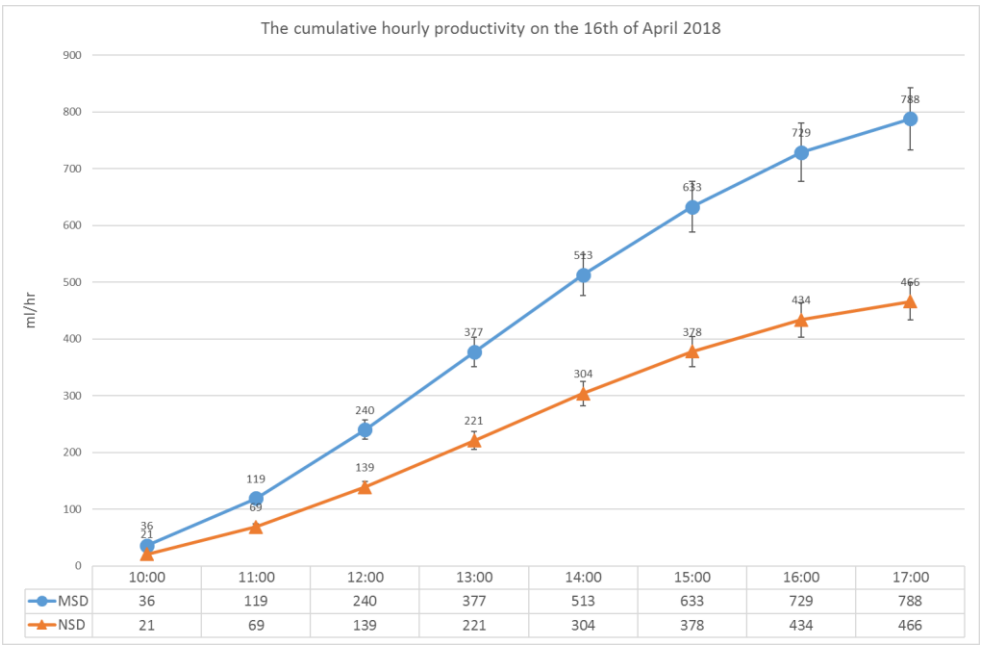

	10:00	11:00	12:00	13:00	14:00	15:00	16:00	17:00
MSD	36	119	240	377	513	633	729	788
NSD	21	69	139	221	304	378	434	466

3. The hourly efficiency of selected days

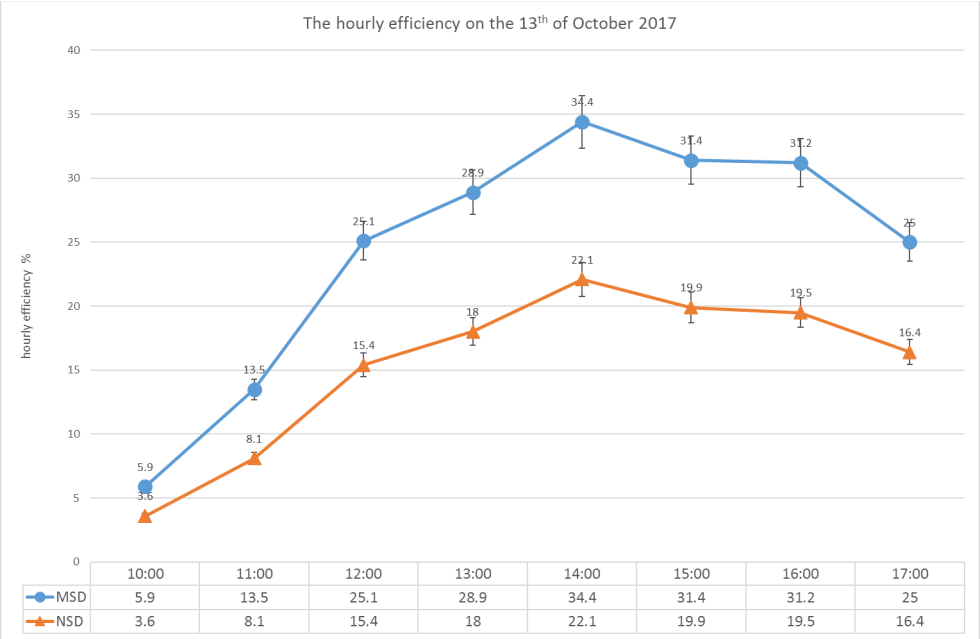

	10:00	11:00	12:00	13:00	14:00	15:00	16:00	17:00
MSD	5.9	13.5	25.1	28.9	34.4	31.4	31.2	25
NSD	3.6	8.1	15.4	18	22.1	19.9	19.5	16.4

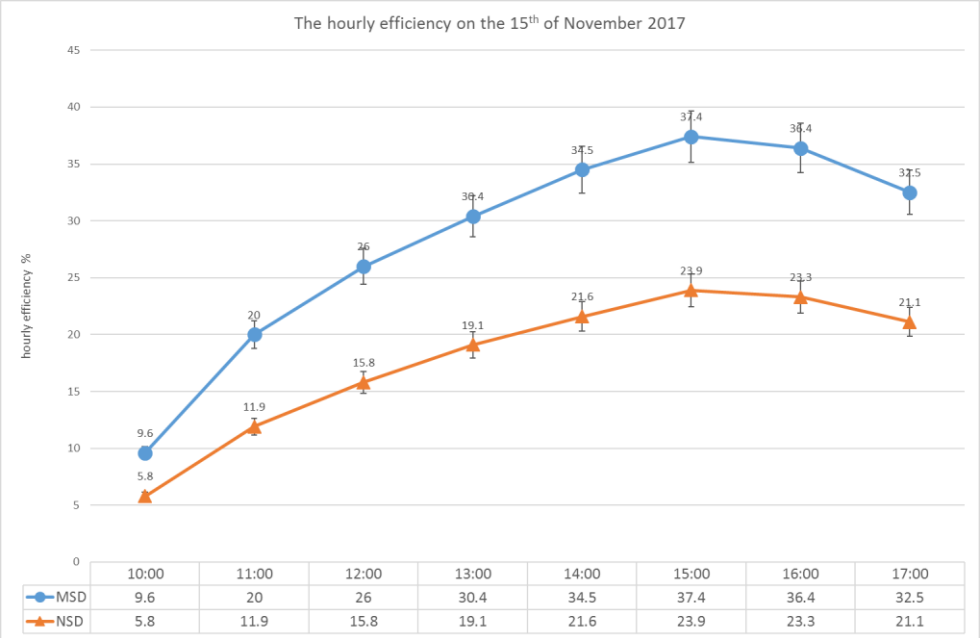

	10:00	11:00	12:00	13:00	14:00	15:00	16:00	17:00
MSD	9.6	20	26	30.4	34.5	37.4	36.4	32.5
NSD	5.8	11.9	15.8	19.1	21.6	23.9	23.3	21.1

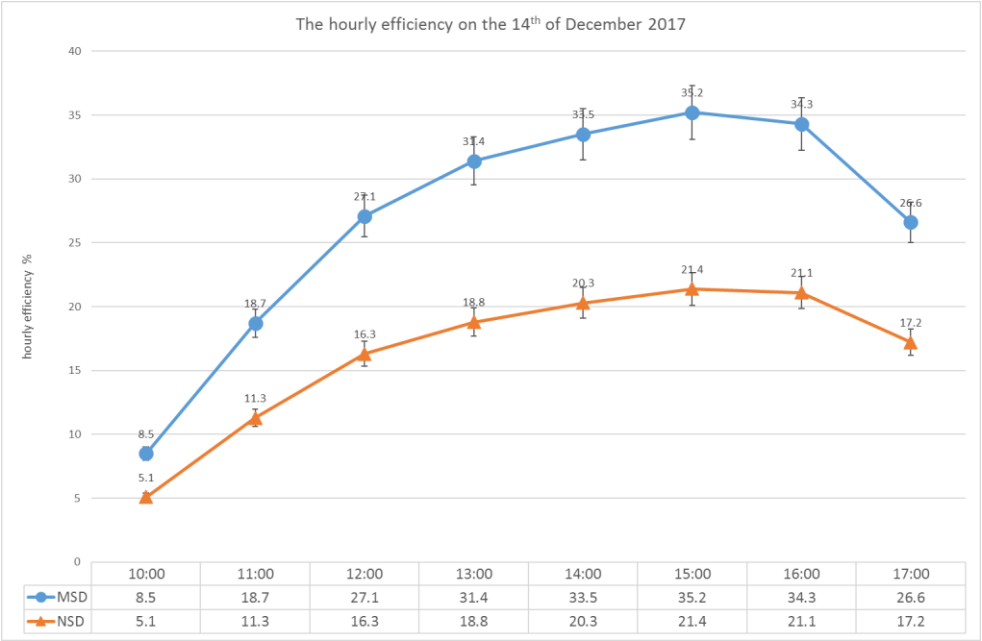

	10:00	11:00	12:00	13:00	14:00	15:00	16:00	17:00
MSD	8.5	18.7	27.1	31.4	33.5	35.2	34.3	26.6
NSD	5.1	11.3	16.3	18.8	20.3	21.4	21.1	17.2

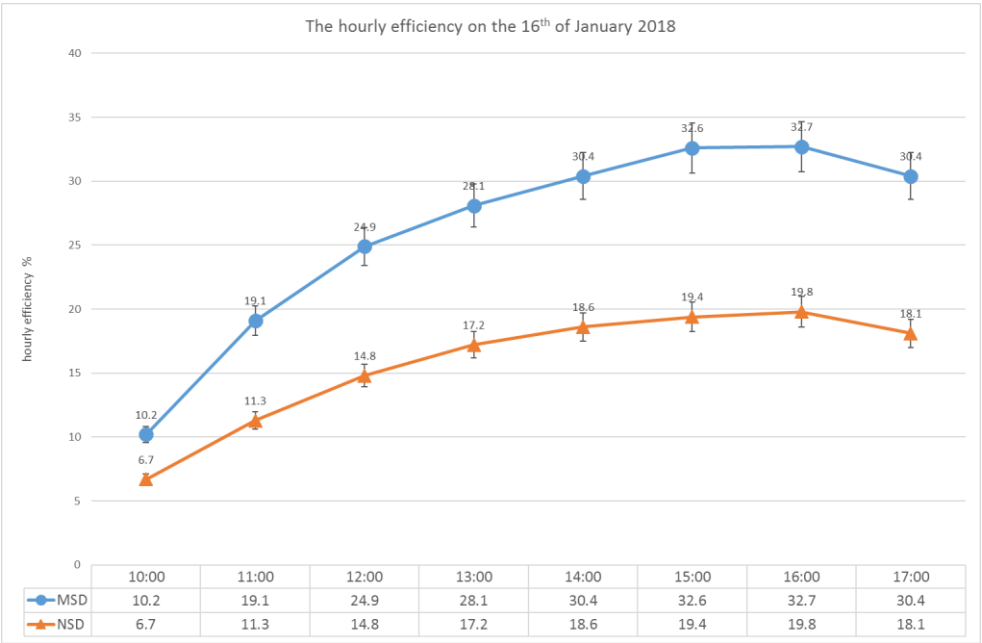

	10:00	11:00	12:00	13:00	14:00	15:00	16:00	17:00
MSD	10.2	19.1	24.9	28.1	30.4	32.6	32.7	30.4
NSD	6.7	11.3	14.8	17.2	18.6	19.4	19.8	18.1

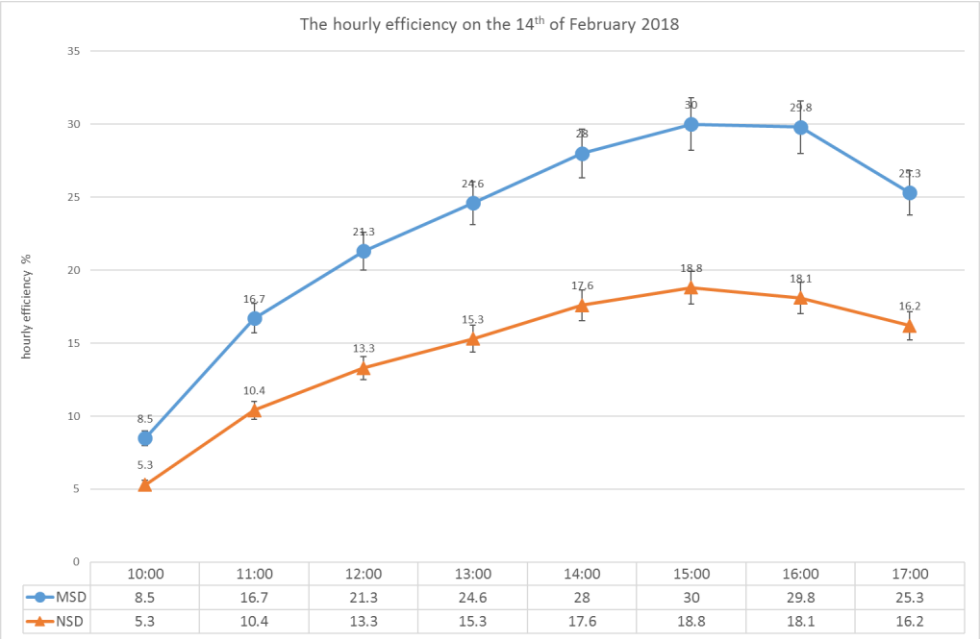

	10:00	11:00	12:00	13:00	14:00	15:00	16:00	17:00
MSD	8.5	16.7	21.3	24.6	28	30	29.8	25.3
NSD	5.3	10.4	13.3	15.3	17.6	18.8	18.1	16.2

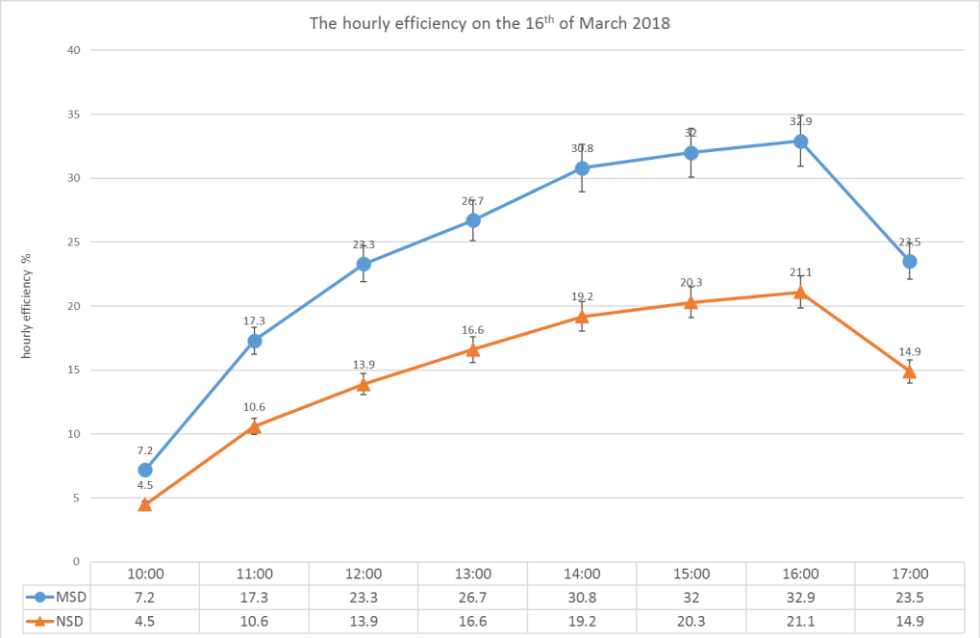

	10:00	11:00	12:00	13:00	14:00	15:00	16:00	17:00
MSD	7.2	17.3	23.3	26.7	30.8	32	32.9	23.5
NSD	4.5	10.6	13.9	16.6	19.2	20.3	21.1	14.9

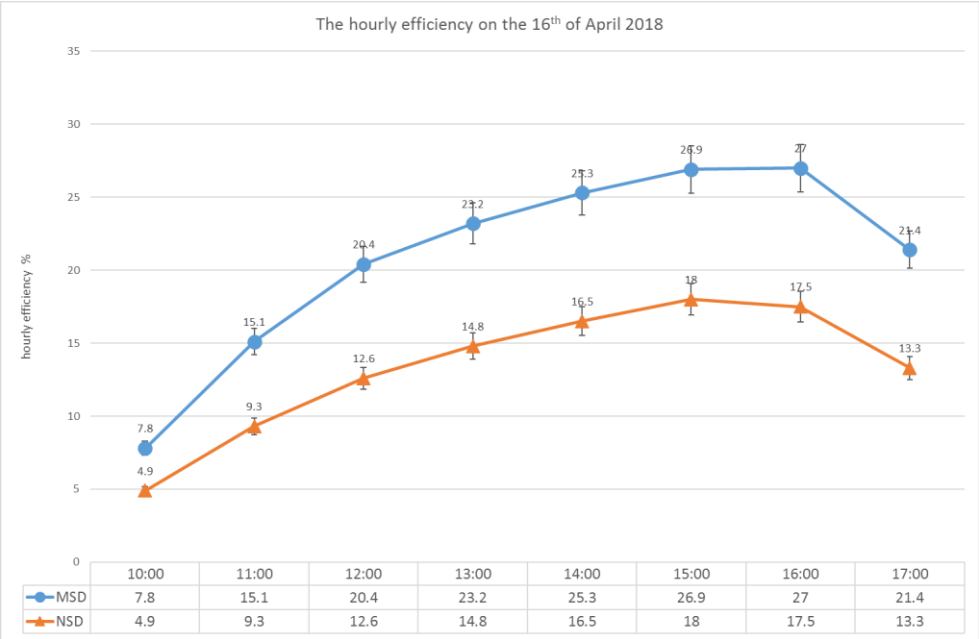

	10:00	11:00	12:00	13:00	14:00	15:00	16:00	17:00
MSD	7.8	15.1	20.4	23.2	25.3	26.9	27	21.4
NSD	4.9	9.3	12.6	14.8	16.5	18	17.5	13.3

Appendix B: Tables

1. The recorded data of selected days of every month

The recorded data on the 4th of October 2017

Time	Water Temperature (°C)		Vapour Temperature (°C)		Basin Temperature (°C)		Cover Temperature (°C)		Ambient Temperature (°C)	Wind speed (km/hr)	Relative Humidity (%)	Solar intensity (W/m²)
	MSD	NSD	MSD	NSD	MSD	NSD	MSD	NSD				
6:00:00	20.1	22.5	19.3	20.7	20	21.4	19.2	19.8	19.4	0	98	21
6:05:00	20.1	22.5	19.1	20.4	20	21.4	18.9	19.7	19.2	0	98	28
6:10:00	20.1	22.4	19.1	20.6	20	21.4	18.9	19.7	19.5	0	98	33
6:15:00	20	22.4	19.1	20.6	20	21.4	19	19.7	19.4	3	98	42
6:20:00	20	22.4	19	20.6	19.9	21.4	18.9	19.7	19.4	2	98	54
6:25:00	19.9	22.3	19	20.5	19.8	21.3	18.6	19.6	19.4	0	98	51
6:30:00	20	22.3	19.4	20.7	19.9	21.3	18.8	19.6	19.4	0	98	74
6:35:00	20	22.3	19.2	20.6	19.9	21.3	18.8	19.8	19.4	0	98	84
6:40:00	20	22.2	19.4	20.8	19.9	21.3	19.3	19.9	19.5	0	98	69
6:45:00	19.9	22.2	19.5	21.1	19.9	21.2	19.4	20	19.5	0	98	93
6:50:00	20	22.2	19.5	21.2	20	21.3	19.7	20.1	19.5	5	98	128
6:55:00	20.1	22.3	19.9	21.5	20.1	21.4	20	20.3	19.6	6	98	137
7:00:00	20.1	22.2	19.7	21.5	20.1	21.3	19.6	20.4	19.6	2	98	155
7:05:00	20.2	22.3	19.8	21.3	20.3	21.5	19.5	20.5	19.7	0	98	178
7:10:00	20.3	22.3	20	21.5	20.4	21.5	19.8	20.5	19.7	2	98	178
7:15:00	20.2	22.3	20	21.5	20.3	21.4	19.9	20.3	19.4	2	98	278
7:20:00	20.4	22.4	20.3	22.6	20.6	21.6	20.3	21.4	20.1	8	98	186
7:25:00	20.6	22.5	20.9	22.7	20.7	21.7	20.5	21.3	20.1	5	98	220
7:30:00	20.6	22.5	22.2	23.8	20.8	21.8	20.3	22.2	20	2	98	172
7:35:00	20.7	22.7	25.6	27.4	21.2	22	21.2	23.7	20.3	3	98	169
7:40:00	20.9	22.8	26.7	31.3	21.6	22.2	21.7	24.2	20.4	0	98	178
7:45:00	21.2	23	24.5	28.2	22	22.7	21.5	23.4	20.4	5	98	195
7:50:00	21.8	23.4	24.7	28.3	22.5	23.2	21.8	23.6	20.7	0	98	227
7:55:00	22.3	23.5	23.1	25.7	22.7	23.4	21.6	22.8	20.3	2	98	239
8:00:00	22.6	23.7	25.6	29	23	23.4	21.7	23.4	20.8	3	98	207
8:05:00	22.8	24	30.1	34.2	23.5	23.6	23	25.5	21.1	5	98	243
8:10:00	23.2	24.2	29.6	33.8	24	24	23.6	26.6	22.2	5	97	211
8:15:00	23.7	24.6	28.9	33.3	24.6	24.5	23.9	25.9	21.6	2	97	288
8:20:00	24.5	24.7	25.7	28.4	25.1	25	22.6	24	20.8	5	97	237
8:25:00	24.9	25	26.2	28.9	25.3	25.1	22.8	24.2	21.6	2	96	216
8:30:00	25.2	25.4	30.3	34	25.5	25.1	23.9	26.3	22.3	0	96	246
8:35:00	25.6	25.6	29.2	33.1	26.1	25.4	23.9	25.9	21.9	0	96	274
8:40:00	26	25.9	32.6	36.5	26.5	25.6	24.4	27	22.7	0	96	295
8:45:00	26.7	26.3	31.6	35.3	27.2	26.1	24.6	26.3	22.3	0	95	336
8:50:00	27.2	26.7	35	39.5	27.8	26.5	25.9	28.7	23.7	0	94	315
8:55:00	27.6	27.1	35	40.1	28.4	27	26.1	28.9	23.1	0	93	257
9:00:00	28.3	27.5	36	41.3	29.2	27.7	26.7	29.6	23.7	0	91	257
9:05:00	29.2	27.9	36.7	41	29.8	28.3	26.8	29.6	23.3	0	90	336
9:10:00	29.9	28.3	36.2	40.3	30.5	28.8	27.2	30	23.6	5	90	404
9:15:00	30.7	28.7	36.7	41.2	31.1	29.1	27	29.5	23.3	5	89	234
9:20:00	31.4	29.1	34.1	37.2	31.8	29.4	26.3	28	22.3	0	87	299
9:25:00	32	29.5	37.6	41	32.1	29.6	27.4	29.9	23.6	3	87	387
9:30:00	32.5	29.8	37.1	40.8	32.9	29.7	27.3	29.3	23.7	0	87	380
9:35:00	33.1	30.1	38.3	41.9	33.2	30	27.8	30.3	23.9	13	87	311
9:40:00	33.7	30.6	39.5	43.8	33.9	30.3	28.7	31.3	24.1	8	86	308
9:45:00	34.4	31.1	41.3	45.2	34.9	30.9	29.7	32	24.9	3	87	364
9:50:00	35.3	31.4	36.9	39.1	35.5	31.5	28.2	29.6	23.5	2	86	606
9:55:00	35.9	32	40.5	44.3	36	31.8	29.3	31.5	24.4	6	87	508
10:00:00	36.5	32.4	41.4	44.9	36.6	32.1	29.8	31.9	24.5	10	87	1088
10:05:00	37.3	32.9	42.8	46.5	37.4	32.6	30.5	32.7	24.8	5	83	1021
10:10:00	38.1	33.3	43.2	46.7	38.2	33	31.1	33.1	25.4	10	83	1037
10:15:00	38.9	33.8	42.6	44.9	38.9	33.6	30.9	32.7	24.9	2	83	582
10:20:00	39.5	34.4	44.9	48.6	39.6	34	32.2	34.6	27	2	83	759
10:25:00	40.4	35	45.4	49.1	40.6	34.7	32.8	35.2	27.5	6	80	373
10:30:00	41.3	35.6	45.4	49.3	41.5	35.4	32.8	35.4	25.7	2	81	524
10:35:00	42.1	36.1	45.9	49.2	42.3	36.1	32.4	34.9	25.6	5	79	431
10:40:00	43	36.7	46.8	49.9	43.1	36.7	33	35.9	27	6	79	490
10:45:00	43.8	37.2	47.4	49.8	43.8	37.1	33	35.5	26	6	79	411
10:50:00	44.7	37.8	48.6	50.2	44.6	37.6	33.7	36.1	27.1	8	78	1266
10:55:00	45.5	38.3	49.3	50.5	45.3	38	33.6	35.6	26.2	8	77	515
11:00:00	46.1	38.8	50.1	51.5	46	38.4	34.7	37.1	28.1	8	77	594
11:05:00	46.9	39.3	50.5	51.3	46.7	38.8	34.9	37	27.5	6	77	1253
11:10:00	47.8	39.9	50.9	51.5	47.4	39.3	35.1	37.3	27.7	3	78	367
11:15:00	48.4	40.3	51.3	51.4	48	39.7	35.9	37.9	28.8	8	76	415
11:20:00	49.2	40.9	52.2	52.8	48.8	40.2	35.5	37.8	26.9	2	75	415
11:25:00	49.9	41.4	52.5	52.5	49.5	40.8	35.7	38.1	27.3	3	75	406
11:30:00	50.6	41.9	53.3	53.1	50.1	41.3	35.7	38.5	27.8	6	74	322
11:35:00	51.1	42.4	53.7	53.2	50.7	41.6	36.3	39.3	28.9	3	74	401
11:40:00	51.8	42.9	53.8	53.4	51.2	41.9	36.3	38.5	27.6	0	74	323
11:45:00	52.4	43.4	54.7	53.1	51.8	42.4	36.8	39.7	28.8	5	74	1208
11:50:00	53.1	43.8	55.3	53.8	52.3	42.7	37.1	38.8	26.8	3	74	1118

Time	Water Temperature (°C)		Vapour Temperature (°C)		Basin Temperature (°C)		Cover Temperature (°C)		Ambient Temperature (°C)	Wind speed (km/hr)	Relative Humidity (%)	Solar intensity (W/m^2)
	MSD	NSD	MSD	NSD	MSD	NSD	MSD	NSD				
11:55:00	53.7	44.4	55.7	53.9	52.9	43.1	37.2	38.8	27.1	8	70	1060
12:00:00	54.3	44.9	56.4	54.4	53.5	43.5	38.3	40.7	29.6	6	70	1069
12:05:00	54.7	45.3	56.5	54.5	54	43.7	38.5	41.2	29.5	0	69	1069
12:10:00	55.2	45.6	57	55	54.4	44	38.5	40.7	28.9	11	69	316
12:15:00	55.8	46.2	57.3	54.5	54.9	44.4	38.7	40.8	29	8	66	1055
12:20:00	56.3	46.5	57.5	54.5	55.1	44.5	38.4	39.5	27.5	13	69	1079
12:25:00	56.7	47	58.2	54.4	55.3	44.5	38.5	39.2	27.5	2	66	1090
12:30:00	57.2	47.3	57.6	54.7	55.7	44.5	38.3	39.4	27.4	3	68	1206
12:35:00	57.5	47.7	58.6	55.3	56.1	44.5	38.7	40.5	28.2	5	65	250
12:40:00	57.8	47.9	58.7	54.9	56.5	44.6	39.1	41.6	29.3	6	65	1058
12:45:00	58.1	48.2	60.1	55.7	56.9	44.9	39.8	42.2	29.5	0	64	1139
12:50:00	58.2	48.4	58.7	55	56.8	45.2	39.4	39.9	27.9	10	64	1076
12:55:00	58.5	48.7	59.2	56.4	57.1	45.3	39.8	41.4	29.2	5	63	1034
13:00:00	58.8	49	59.7	56.3	57.3	45.4	39.5	40.2	27.9	5	61	246
13:05:00	58.9	49.3	59.8	56.3	57.5	45.7	39.8	40.6	27.6	8	57	1009
13:10:00	59.2	49.6	59.5	56	57.8	45.8	40.3	41.7	29.7	6	62	1035
13:15:00	59.4	49.8	59.6	56.2	58	45.9	40	41.6	29.8	5	61	246
13:20:00	59.6	50	59	55.1	58.1	46.1	39.8	41.1	28.3	5	61	211
13:25:00	59.8	50.3	59.6	56.2	58.3	46.4	40.1	41.3	28.9	5	60	1002
13:30:00	59.9	50.6	59.7	56.3	58.5	46.5	40	41.5	29.6	3	59	972
13:35:00	60.1	50.7	59.5	55.3	58.5	46.5	39.8	41.3	28.9	11	59	933
13:40:00	60.2	50.9	60	55.4	58.6	46.6	40.1	41.9	29.2	8	59	193
13:45:00	60.4	51.1	59.6	55.2	58.7	46.7	40.5	41.3	29.2	3	60	886
13:50:00	60.4	51.3	59.7	55.2	58.7	46.7	40.1	40.8	28.9	3	58	896
13:55:00	60.3	51.4	59.5	55	58.8	46.7	40.6	42	29.8	5	56	882
14:00:00	60.4	51.5	59.2	55	58.8	46.7	40.6	40.9	28.5	8	56	831
14:05:00	60.3	51.6	58.9	54.8	58.8	46.8	40	41.2	28.7	11	55	139
14:10:00	60.3	51.7	58.7	54.5	58.8	46.9	39.9	40.9	29.2	10	58	167
14:15:00	60.2	51.8	59.1	55	58.7	46.8	40.1	41.4	29.1	6	56	195
14:20:00	60.2	51.8	58.8	54.6	58.6	46.8	40.6	42.1	30.1	2	53	185
14:25:00	60.1	51.9	58.4	54.3	58.6	46.8	40.2	41.6	29.6	3	56	749
14:30:00	60.1	51.9	58.2	53.8	58.5	46.9	40.5	41.8	30.1	2	51	754
14:35:00	59.9	51.9	57.9	54.4	58.5	46.9	39.9	41.4	29.1	3	52	754
14:40:00	59.7	52	57.4	53.8	58.1	46.9	39.9	40.2	28.7	3	48	155
14:45:00	59.6	52	57.6	54	58.1	46.8	40.2	41	28.8	8	48	701
14:50:00	59.5	52.2	57.3	53.9	58.1	46.9	40.5	41.9	30	10	49	661
14:55:00	59.5	52.2	56.9	53.5	57.9	47	39.9	40.6	29	3	49	633
15:00:00	59.2	52.3	56.5	53.8	57.7	47	40	41	28.4	8	48	589
15:05:00	58.9	52.3	56.1	53.3	57.3	46.9	39.1	39.3	27.4	2	44	566
15:10:00	58.7	52.4	55.6	52.8	57.2	46.9	39.9	40.3	28.8	3	44	557
15:15:00	58.4	52.3	55.2	52.9	57	46.7	39.6	40.3	28.3	2	45	526
15:20:00	58.2	52.3	54.9	53.4	56.6	46.6	39.1	39.4	27.3	5	44	499
15:25:00	57.7	52.3	54.3	53.4	56.3	46.5	38.8	39.1	27.7	8	44	485
15:30:00	57.6	52.3	54.2	53.4	56	46.5	38.6	39.4	27.5	6	42	471
15:35:00	57.4	52.1	53.6	52.8	55.7	46.3	38.8	39.6	28.4	3	45	457
15:40:00	57.1	52	54.1	52.7	55.5	46.2	39.1	39.8	28.7	8	44	438
15:45:00	56.8	51.8	53.7	52.3	55.1	46.1	38.1	37.8	26.5	2	44	420
15:50:00	56.4	51.7	53.2	52	54.7	45.8	37.9	37.7	26.9	3	43	399
15:55:00	56.1	51.4	53.1	52.1	54.4	45.6	38.6	39.3	28.3	5	43	380
16:00:00	55.7	51	52.5	51.6	54.1	45.3	38.4	38.9	27.8	6	42	366
16:05:00	55.4	50.7	52.4	51.8	53.8	45.1	38	38.7	27.8	2	39	346
16:10:00	55.1	50.5	52.2	51.5	53.6	44.9	38	38.4	27.8	3	45	338
16:15:00	54.7	50.1	51.8	50.9	53.2	44.6	37.4	37.4	27.1	2	44	308
16:20:00	54.4	49.8	51.5	51	53	44.4	37.7	38.2	27.8	0	44	294
16:25:00	54.1	49.5	51.3	47.9	52.6	44.2	37.1	37.4	26.8	0	43	271
16:30:00	53.9	49.3	51.2	47.8	52.4	44.1	36.6	37.3	26.8	6	44	248
16:35:00	54	49.7	50.9	47.3	52.1	43.9	36.7	36.6	27	5	44	229
16:40:00	53.6	49.7	49.1	45	51.7	43.6	35.6	36.6	27	0	44	207
16:45:00	53.2	49.5	48.7	44	51.2	43.3	35	36.1	26.8	3	43	188
16:50:00	53.2	49.5	47.3	44	51.1	43.4	34.8	36.1	27.3	2	44	174
16:55:00	52	48.7	46.4	43.2	50	42.7	34	36.1	26.8	2	45	151
17:00:00	51	48.1	45.2	42.7	49	42.1	33.3	34.9	26.3	0	43	128
17:05:00	50.1	47.7	44.6	42.4	48.1	41.6	33.1	34.1	25.8	2	42	111
17:10:00	49.4	47.2	43.7	41.5	47.4	41.2	32.9	34.2	26	0	42	88
17:15:00	48.7	46.8	42.8	41.3	46.7	40.9	32.2	33.9	25.7	0	44	72
17:20:00	47.9	46.2	42	41.1	46	40.4	31.8	33.8	25.8	0	43	56
17:25:00	47.1	45.8	41.4	40.3	45.3	40	31.4	32.8	25	0	44	42
17:30:00	46.4	45.3	40.6	39.6	44.6	39.6	31.3	32.8	25.3	0	44	32
17:35:00	45.8	45	39.5	39	44	39.3	30.6	32	24.6	0	46	23
17:40:00	45.1	44.6	39.2	38.4	43.4	39	30.4	31.7	24.6	11	54	18
17:45:00	44.4	44.2	38.6	38.3	42.7	38.6	29.9	31.7	24.3	6	58	14
17:50:00	43.8	43.7	38.3	38.1	42.2	38.2	29.6	31.1	24.2	8	61	11
17:55:00	43.3	43.3	37.7	37.3	41.5	37.8	29.2	30.1	23.6	14	64	7
18:00:00	42.6	42.9	36.9	36.9	40.9	37.4	28.7	29.9	23.7	14	64	7
18:05:00	42	42.6	36.7	36.7	40.3	37.1	28.7	30.2	23.6	8	67	7
18:10:00	41.4	42.2	36.1	36.4	39.8	36.7	28.5	29.8	23.4	8	68	0
18:15:00	40.8	41.8	35.3	36	39.3	36.4	28	29.5	23.3	11	68	0
18:20:00	40.3	41.4	34.9	35.5	38.7	36.1	27.9	29	22.9	5	69	0
18:25:00	39.8	41	34.3	35.2	38.3	35.8	27.5	28.8	23	6	69	0

Time	Water Temperature (°C)		Vapour Temperature (°C)		Basin Temperature (°C)		Cover Temperature (°C)		Ambient Temperature (°C)	Wind speed (km/hr)	Relative Humidity (%)	Solar intensity (W/m^2)
	MSD	NSD	MSD	NSD	MSD	NSD	MSD	NSD				
18:30:00	39.2	40.6	33.9	35.1	37.7	35.5	27.4	28.7	22.8	14	70	0
18:35:00	38.7	40.3	33.3	34.4	37.2	35.1	27	28.2	22.7	18	71	0
18:40:00	38.3	39.9	32.8	33.8	36.7	34.8	26.6	27.5	22.4	16	75	0
18:45:00	37.7	39.6	32.4	33.9	36.4	34.6	26.5	27.7	22.6	11	79	0
18:50:00	37.2	39.2	32.1	33.6	35.9	34.2	26.3	27.5	22.5	19	82	0
18:55:00	36.9	39	31.7	33.6	35.4	34	26	27.1	22.2	13	84	0
19:00:00	36.3	38.5	31.5	33.4	34.9	33.7	25.8	27	22.2	24	85	0
19:05:00	36	38.4	30.8	32.9	34.6	33.5	25.5	26.8	22.2	21	86	0
19:10:00	35.5	37.9	30.5	32.1	34.2	33.2	25.3	26.3	21.7	16	87	0
19:15:00	35.1	37.7	30.3	31.5	33.8	33	25	26.5	22	13	88	0
19:20:00	34.7	37.4	29.5	31.5	33.4	32.7	24.6	25.8	21.6	24	89	0
19:25:00	34.3	37.1	29.4	31	33	32.4	24.3	25.6	21.5	13	89	0
19:30:00	33.9	36.7	28.8	30.9	32.6	32.1	24	25.5	21.2	10	90	0
19:35:00	33.5	36.4	28.3	31	32.3	31.9	24	25.4	21.1	11	90	0
19:40:00	33.1	36.2	28.4	30.5	32	31.7	23.9	25.2	21.2	23	90	0
19:45:00	32.7	35.9	28.2	30.2	31.6	31.4	23.7	24.9	20.9	14	90	0
19:50:00	32.3	35.5	27.7	30.7	31.2	31.2	23.5	24.9	20.8	13	91	0
19:55:00	32.1	35.3	27.8	30.6	31	31	23.7	24.7	20.7	14	92	0
20:00:00	31.7	35	27.3	30.2	30.6	30.7	23.9	24.8	20.9	16	92	0
20:05:00	31.4	34.8	27.2	30.1	30.4	30.5	24	24.5	20.6	21	93	0
20:10:00	31.1	34.5	27.2	29.6	30.1	30.4	24.1	24.9	20.8	14	93	0
20:15:00	30.9	34.3	27	29.5	29.9	30.2	24	24.8	20.8	23	93	0
20:20:00	30.6	34.1	26.7	29.3	29.6	30	23.9	24.4	20.5	11	94	0
20:25:00	30.4	33.9	26.8	29	29.5	30	24	24.3	20.7	16	94	0
20:30:00	30.1	33.7	26.5	29.2	29.2	29.8	23.7	24.2	20.4	11	94	0
20:35:00	29.8	33.4	26	28.7	28.9	29.6	23.4	24.2	20.5	13	94	0
20:40:00	29.7	33.3	25.7	28.4	28.7	29.5	22.7	23.6	20.3	18	94	0
20:45:00	29.3	33	25.3	28.3	28.5	29.3	22.2	23.2	20	14	95	0
20:50:00	29.1	32.8	25.1	27.4	28.2	29.1	21.7	22.9	19.8	14	95	0
20:55:00	28.8	32.6	24.6	27.1	27.9	28.8	21.4	22.7	19.9	19	95	0
21:00:00	28.6	32.3	24.6	27.2	27.7	28.6	21.3	22.6	19.7	14	95	0
21:05:00	28.2	32.1	24.3	26.8	27.4	28.3	21.1	22.5	19.8	18	95	0
21:10:00	27.9	31.8	24	27	27.1	28.2	21	22.4	19.6	24	95	0
21:15:00	27.7	31.6	23.9	26.8	26.9	27.9	20.9	22.2	19.6	19	95	0
21:20:00	27.5	31.4	23.6	26.1	26.7	27.8	20.7	21.9	19.6	21	96	0
21:25:00	27.3	31.2	23.3	26.1	26.5	27.6	20.6	21.9	19.5	16	95	0
21:30:00	26.9	30.9	23.2	26.1	26.1	27.4	20.3	21.7	19.4	23	96	0
21:35:00	26.7	30.7	22.9	26	25.9	27.2	20.3	21.6	19.4	23	96	0
21:40:00	26.6	30.6	22.9	25.6	25.8	27.1	20.3	21.6	19.4	18	96	0
21:45:00	26.3	30.4	22.8	25.6	25.6	27	20.2	21.5	19.4	14	96	0
21:50:00	26.1	30.2	22.4	25.3	25.4	26.8	20.1	21.4	19.3	18	96	0
21:55:00	25.9	29.9	22.4	25.1	25.2	26.6	20	21.1	19.1	19	96	0
22:00:00	25.7	29.7	22.1	25	25	26.4	19.8	21	19.1	19	96	0
22:05:00	25.4	29.5	22	24.9	24.8	26.2	19.7	20.9	19.1	14	96	0
22:10:00	25.3	29.3	21.9	24.6	24.6	26.1	19.6	20.9	19	16	96	0
22:15:00	25.1	29.2	21.8	24.5	24.4	26	19.5	20.7	18.9	13	96	0
22:20:00	24.8	29	21.6	24.3	24.2	25.8	19.3	20.6	18.9	18	96	0
22:25:00	24.7	28.8	21.6	24.2	24.1	25.7	19.3	20.7	19.1	16	96	0
22:30:00	24.4	28.5	21.2	23.8	23.8	25.5	19.1	20.4	18.7	18	96	0
22:35:00	24.3	28.4	21.2	23.7	23.7	25.4	19	20.3	18.7	14	96	0
22:40:00	24.1	28.2	21	23.7	23.5	25.2	18.9	20.1	18.7	21	96	0
22:45:00	24	28.1	20.9	23.6	23.4	25.2	18.9	20.3	18.7	14	96	0
22:50:00	23.8	27.9	20.9	23.3	23.2	24.9	18.8	20	18.6	16	96	0
22:55:00	23.5	27.7	20.5	23.2	23	24.8	18.7	19.9	18.7	16	96	0
23:00:00	23.4	27.5	20.4	23.1	22.9	24.6	18.5	19.8	18.5	18	96	0
23:05:00	23.3	27.4	20.4	23	22.7	24.5	18.6	19.8	18.5	18	96	0
23:10:00	23.1	27.2	20.2	23.1	22.6	24.4	18.4	19.7	18.4	14	96	0
23:15:00	23	27.1	20.2	23.1	22.5	24.3	18.4	19.7	18.5	16	96	0
23:20:00	22.8	26.9	19.9	22.8	22.3	24.2	18.2	19.6	18.4	21	96	0
23:25:00	22.7	26.7	20	22.6	22.2	24.1	18.2	19.6	18.4	18	96	0
23:30:00	22.5	26.6	19.8	22.5	22	23.9	18.6	19.5	18.3	14	96	0
23:35:00	22.4	26.5	20.2	23	21.9	23.9	19.4	19.9	18.5	19	96	0
23:40:00	22.3	26.3	20.2	22.8	21.8	23.7	19.1	19.7	18.5	14	96	0
23:45:00	22.1	26.2	20	22.7	21.7	23.7	19.3	19.9	18.6	16	96	0
23:50:00	22.1	26	19.9	22.6	21.6	23.6	19.2	19.9	18.6	16	96	0
23:55:00	21.9	25.9	19.8	22.2	21.5	23.5	18.6	19.7	18.5	19	96	0
0:00:00	21.8	25.8	19.6	22.2	21.6	23.4	18.2	19.5	18.5	19	96	0

The recorded data on the 5th of November 2017

Time	Water Temperature (°C)		Vapour Temperature (°C)		Basin Temperature (°C)		Cover Temperature (°C)		Ambient Temperature (°C)	Wind speed (km/hr)	Relative Humidity (%)	Solar intensity (W/m2)
	MSD	NSD	MSD	NSD	MSD	NSD	MSD	NSD				
6:00:00	12.5	15.8	11.6	13.2	12.6	14.7	10.8	12.5	13.7	8	70	141
6:05:00	12.5	15.8	11.7	13.3	12.6	14.6	10.8	12.5	13.7	5	71	160
6:10:00	12.5	15.7	11.7	13.3	12.6	14.6	11	12.6	13.7	6	72	183
6:15:00	12.4	15.6	11.8	13.2	12.5	14.6	11.1	12.7	13.7	10	72	206
6:20:00	12.4	15.6	11.8	13.4	12.5	14.6	11.1	12.7	13.8	8	72	227
6:25:00	12.3	15.5	11.8	13.2	12.5	14.5	11.3	12.8	13.8	3	71	246
6:30:00	12.3	15.4	11.8	13.4	12.4	14.5	11.1	12.8	14	10	70	265
6:35:00	12.3	15.5	11.9	13.4	12.5	14.5	11.2	12.9	14.1	10	69	285
6:40:00	12.2	15.3	11.8	13.3	12.5	14.5	11	12.9	14.1	10	70	304
6:45:00	12.3	15.4	11.8	13.4	12.5	14.6	11.3	13	14.4	5	70	322
6:50:00	12.2	15.4	11.9	13.5	12.5	14.6	11.4	13.2	14.6	8	70	330
6:55:00	12.2	15.3	11.9	13.3	12.5	14.5	11.4	13.3	14.8	10	70	44
7:00:00	12.3	15.3	12	13.4	12.6	14.6	11.7	13.4	15	5	70	141
7:05:00	12.3	15.3	12.1	13.7	12.6	14.6	12	13.7	15.4	5	70	399
7:10:00	12.4	15.3	12.4	14.2	12.6	14.6	13.5	15.8	15.7	3	69	418
7:15:00	12.4	15.4	12.4	17.9	12.7	14.7	14.4	17.1	15.5	5	68	434
7:20:00	12.3	15.5	15.3	19.4	12.8	14.9	14.9	18.2	15.8	5	68	454
7:25:00	12.3	15.7	16.6	21.2	13.3	15.3	15.1	18.9	16.2	5	67	471
7:30:00	12.5	15.8	18.2	24.8	13.6	15.8	15.8	19.6	16.6	11	67	490
7:35:00	12.7	16	20.9	25.5	14	16.2	16.9	19.7	16.6	10	67	510
7:40:00	13	16.2	21.6	26.2	14.4	16.5	17.8	20.5	17.5	5	66	527
7:45:00	13.5	16.6	22.2	26.8	14.8	16.9	18.3	21.1	17.9	8	65	561
7:50:00	14	16.8	23	27.6	15.4	17.3	18.4	21.4	18	11	65	577
7:55:00	14.6	17.2	23.6	28.1	16.1	17.8	18.7	21.9	18	8	64	596
8:00:00	15.3	17.6	24.2	31.1	16.8	18.2	19	21.8	17.7	8	64	613
8:05:00	16.1	18.1	25	32	17.4	18.7	19.7	22.4	18.3	6	63	471
8:10:00	16.7	18.4	26.1	32.4	18	19.1	20.1	23	19.1	14	62	121
8:15:00	17.4	18.9	27.2	33.4	18.8	19.6	20.8	23.8	19.7	6	65	645
8:20:00	18.2	19.3	28	34.2	19.5	20.1	21.3	24	19.5	11	63	677
8:25:00	18.9	19.7	28.5	34.7	20.2	20.5	21.5	24.2	19.5	13	63	693
8:30:00	19.7	20.2	29	35.4	20.9	20.9	21.7	24.1	19.2	10	65	708
8:35:00	20.6	20.6	29.8	35.7	21.6	21.4	22.1	24.5	19.7	10	64	722
8:40:00	21.3	21.1	30.4	36.1	22.4	21.7	22.4	24.6	19.6	13	63	737
8:45:00	22.4	21.6	31	36.7	23.1	22.1	22.6	25.2	20.2	8	62	752
8:50:00	23	22.1	31.5	37.6	23.9	22.5	23	25.6	20.5	14	62	768
8:55:00	23.9	22.6	32	37.9	24.7	22.9	23.3	25.6	20	16	63	779
9:00:00	24.7	23	33.1	38.6	25.3	23.3	23.6	26	20.3	19	61	796
9:05:00	25.4	23.5	33.4	39.3	26.1	23.7	24	26.8	21.3	8	60	819
9:10:00	26.2	23.9	33.8	38.9	26.8	23.9	24.2	26.5	20.7	10	61	802
9:15:00	26.9	24.4	35.6	40.8	27.7	24.4	25.2	27.8	21.6	11	60	744
9:20:00	27.9	25	35.5	40.8	28.5	25	25.5	27.6	21.1	3	60	371
9:25:00	28.7	25.4	35.9	41.1	29.3	25.5	26	28.5	21.9	8	60	872
9:30:00	29.6	25.8	36.9	41.3	30.2	26	25.9	28.2	20.7	10	57	867
9:35:00	30.5	26.5	37.7	41.9	31	26.5	26.5	29.1	22.4	5	58	872
9:40:00	31.3	27	38	42.8	31.8	26.9	26.6	28.9	21.9	14	56	884
9:45:00	32.3	27.5	38.8	43.3	32.5	27.2	26.7	28.8	21.4	11	55	893
9:50:00	33.2	28.2	38.8	43.2	33.3	27.7	27.1	29	21.9	10	55	422
9:55:00	33.9	28.6	40.2	44.5	34.1	28.2	27.7	30.1	23.3	5	55	907
10:00:00	34.9	29.1	40.3	45.2	34.9	28.6	27.7	29.7	21.7	19	52	916
10:05:00	35.6	29.7	41.3	45.4	35.7	29.2	28.1	30.3	22	3	54	918
10:10:00	36.5	30.3	41.7	45.2	36.4	29.7	28.3	30.1	22.3	5	52	933
10:15:00	37.4	30.8	42	46.1	37.2	30	28.8	30.6	22.8	10	52	939
10:20:00	38.2	31.4	42.6	46.5	38.1	30.5	29	30.8	22.5	10	51	944
10:25:00	39.1	31.9	43.6	47.1	38.8	30.9	29.3	30.9	22.4	8	49	947
10:30:00	39.8	32.5	44.3	47.5	39.6	31.4	30.1	31.8	23.1	8	49	949
10:35:00	40.7	33	44.9	47.7	40.4	31.8	29.8	31.4	22.5	3	48	954
10:40:00	41.5	33.6	45.4	47.9	41.1	32.3	30.5	32	23.3	10	46	962
10:45:00	42.3	34.1	45.7	48.3	41.8	32.7	30.9	32.6	23.8	6	47	970
10:50:00	43.1	34.5	46.4	49	42.6	33.2	31.3	32.7	23.9	3	46	981
10:55:00	43.8	35.1	47.5	48.7	43	33.5	31.2	32	23	11	45	990
11:00:00	44.5	35.6	48.1	49.9	44	34	32.2	33.5	23.9	6	43	990
11:05:00	45.4	36.1	48.5	49.1	44.9	34.5	32.5	34	24.5	11	41	990
11:10:00	46.1	36.6	49.4	48.7	45.3	35	32.6	33.6	24	10	39	1009
11:15:00	46.9	37.3	49.4	49.5	46.2	35.5	32.9	34.2	24.9	5	40	1005
11:20:00	47.6	37.7	49.5	50	46.8	35.8	32.8	33.6	23.6	2	38	1020
11:25:00	48.2	38.2	49.4	50.6	47.4	36.2	34	35.1	25.4	8	35	1016
11:30:00	48.9	38.7	51	51	48.1	36.7	34.3	35.4	25.4	11	35	1007
11:35:00	49.7	39.3	51.6	51.2	48.9	37.2	34.7	36.5	26.5	18	34	1021
11:40:00	50.2	39.8	51.8	51.4	49.5	37.8	34.4	36	25.2	13	34	1021
11:45:00	51	40.3	51.4	49.8	50	38.3	34.1	34.7	24.5	11	35	1032
11:50:00	51.5	40.8	53.1	51.8	50.6	38.6	34.4	35.7	24.7	0	35	1032
11:55:00	52.2	41.3	53.4	52.1	51.2	39.1	35	35.9	25	3	33	1037
12:00:00	52.7	41.8	53.5	52.2	51.7	39.5	35.2	36.1	25	14	34	1062
12:05:00	53.2	42.2	55.6	53.5	52.3	39.8	36.5	38.4	27.4	10	35	1053

Time	Water Temperature (°C)		Vapour Temperature (°C)		Basin Temperature (°C)		Cover Temperature (°C)		Ambient Temperature (°C)	Wind speed (km/hr)	Relative Humidity (%)	Solar intensity (W/m2)
	MSD	NSD	MSD	NSD	MSD	NSD	MSD	NSD				
12:10:00	53.8	42.6	55.5	53	52.7	40.1	36.2	37.4	26.6	10	34	1002
12:15:00	54.3	43.1	55.7	53.3	53	40.3	36	36.5	25.8	11	33	997
12:20:00	54.8	43.5	56.1	53.3	53.4	40.5	36.9	37.5	27.2	6	34	998
12:25:00	55.4	43.9	56.5	54	54.1	40.7	36.7	37.6	25.8	6	35	1025
12:30:00	55.9	44.4	56.6	53.3	54.4	41	37	37.9	26.2	2	34	410
12:35:00	56.2	44.8	58	54.2	55	41.3	37.9	39.1	26.6	10	34	213
12:40:00	56.7	45.3	58.4	54.2	55.2	41.5	37.8	37.9	26.1	14	35	183
12:45:00	57.1	45.7	57.6	53.7	55.3	41.6	37	36.8	24.8	8	36	211
12:50:00	57.4	46	57.5	54.3	55.7	41.6	37.7	37.7	25.9	2	38	346
12:55:00	57.8	46.3	58.6	54.8	56.1	41.9	37.9	38.9	27.3	11	36	1027
13:00:00	58.1	46.7	59.3	55.8	56.4	42.1	38.6	39	26.9	8	38	1035
13:05:00	58.3	46.8	57.2	46.9	56.7	42.4	37.6	37.6	25.6	14	36	230
13:10:00	58.4	47.1	59.6	49.9	56.8	42.4	38.6	38.9	26.4	11	34	204
13:15:00	58.6	47.3	59.3	51.2	57	42.6	38.5	39.3	26.5	11	34	229
13:20:00	58.8	47.6	59.4	54.8	57.2	42.8	38.4	38.4	25.8	16	31	155
13:25:00	59.1	48	59.4	55	57.5	43.2	39.1	39.8	27.4	10	31	148
13:30:00	59.3	48.4	61.1	52.2	58.1	43.5	40.5	40.4	27.7	6	32	172
13:35:00	59.8	48.8	61.4	52.5	58.5	44.1	40.6	41.3	27.3	10	32	172
13:40:00	60.2	49.2	62.1	53	58.9	44.6	40.6	41.1	27.2	2	32	186
13:45:00	60.7	49.4	57.8	50.3	58.8	45.1	37.7	38.3	25	13	31	185
13:50:00	60.6	49.7	59.4	54	59.1	45	39.2	40	27	5	31	169
13:55:00	60.8	49.9	57.5	49.9	58.9	45.1	36.6	37.4	24.6	6	31	830
14:00:00	60.4	49.7	56.3	48	58.3	44.9	36.4	36.6	24	6	30	814
14:05:00	59.5	49.5	57.9	51.5	57.3	44.1	37.8	38.2	25	3	29	807
14:10:00	59.3	49.5	59.9	55.8	57.6	43.6	39.7	40.1	26.5	3	28	791
14:15:00	59.3	49.7	59.9	56.3	57.8	43.5	39.9	40.1	26.7	11	27	779
14:20:00	59.5	49.8	58.8	54.9	57.8	43.9	39.1	38.6	25.6	16	27	754
14:25:00	59.6	49.9	55.6	48.8	57.4	44.2	36.9	36.8	24.4	16	26	735
14:30:00	59.1	49.8	57.6	52.9	57	43.8	38.7	38.9	26.1	6	28	717
14:35:00	58.8	49.7	57.7	53.2	56.9	43.4	39	39	26.6	8	27	712
14:40:00	58.7	49.7	57.2	53.2	57.1	43.4	38.1	38	24.8	21	26	700
14:45:00	58.7	49.9	57.2	52.6	57.1	43.6	38.6	37.8	25.1	2	26	682
14:50:00	58.5	49.8	55.5	50.3	56.6	43.8	38	38.7	26.1	6	26	673
14:55:00	58.1	49.8	56.2	52.3	56.6	43.7	37.8	38.2	26.3	6	27	661
15:00:00	58.3	50	54.1	47.6	56.6	44	37.1	38	25.6	23	26	645
15:05:00	57.6	49.8	55	51.1	55.9	43.7	37.7	37.7	25.6	23	26	635
15:10:00	57	49.6	55.2	52.8	55.5	43.6	38.4	39.2	26.3	16	27	608
15:15:00	56.8	49.7	55.1	52.6	55.4	43.5	38.1	38.3	26	6	28	585
15:20:00	57.1	49.8	52.4	46.3	55.3	43.9	35.7	37.3	24.9	10	28	571
15:25:00	56	49.4	52.8	50.5	54.3	43.6	37.3	36.8	25.2	3	29	568
15:30:00	55.7	49.3	52.2	49.4	54	43.2	37.2	37.6	26	10	29	529
15:35:00	55.2	49.2	51.9	50.5	53.8	43.2	36.6	36.8	24.9	14	29	503
15:40:00	55	49.1	51.3	50	53.5	43.2	36.6	36.9	24.8	16	30	487
15:45:00	54.7	49.1	51.5	49.9	53.2	43.1	36.4	36.7	24.8	11	30	469
15:50:00	54.5	49	51.5	49.6	52.8	43	36.4	36.4	25.2	11	32	457
15:55:00	54.3	48.7	51.9	50.1	52.8	42.9	36.5	36.9	25	19	32	436
16:00:00	54	48.5	51.6	50.4	52.6	42.5	36.5	36.2	24	14	33	142
16:05:00	53.9	48.3	50.8	48.5	52.3	42.3	35.7	36.2	24.6	19	33	302
16:10:00	53.6	48	50.3	48.3	52	41.9	35.5	36.2	24.2	19	34	76
16:15:00	53.4	47.7	49.7	47.9	51.7	41.7	34.7	35.9	24.5	31	34	79
16:20:00	53.2	47.4	49.7	47.9	51.4	41.3	34.9	36.1	24.5	23	35	76
16:25:00	53	47.2	49.5	47.6	51.2	40.9	35	35.6	24.2	19	36	84
16:30:00	52.9	47.4	49.4	47.9	51.2	41	34.9	35.4	24.3	26	36	70
16:35:00	53	48.1	49.7	48.6	51.3	41.6	35	35.8	24.5	19	35	56
16:40:00	53	48.3	48.7	47.1	51.2	41.5	34.1	34.8	23.6	14	35	60
16:45:00	52.3	48	46.5	43.1	50.4	41.4	33.1	34.5	23.7	14	35	62
16:50:00	52	47.9	48.8	47	50.2	41.2	33.6	34.3	23.4	21	35	104
16:55:00	51.8	47.7	48.6	44.4	49.9	41	33.3	33.7	23.3	19	35	67
17:00:00	51.2	47.1	45.8	41.7	49.2	40.6	31.6	32.5	23.1	24	35	67
17:05:00	50.3	46.6	44.2	41.2	48.3	39.9	31	32.4	22.7	21	35	70
17:10:00	49.6	46.1	43.4	40.4	47.5	39.4	30.5	32.2	22.6	19	35	54
17:15:00	48.7	45.6	42.5	39.8	46.7	39.1	30	31.8	22.4	19	35	53
17:20:00	47.7	45	41.3	39	45.8	38.9	30.1	31.5	22.5	27	35	60
17:25:00	46.9	44.6	41.1	38.5	44.9	38.3	29.7	31.3	22.5	24	35	54
17:30:00	46.2	44.1	40	38.1	44.1	37.8	29.5	30.3	21.6	19	35	39
17:35:00	45.5	43.7	39.2	37.3	43.4	37.3	28.4	29.4	21.2	19	35	53
17:40:00	44.7	43.2	38.7	37.4	42.6	36.9	28.4	29.4	21.3	19	35	26
17:45:00	44.1	42.9	38.2	36.5	42.2	36.8	28.6	29.5	21.4	16	35	21
17:50:00	43.4	42.4	37.3	36.1	41.5	36.2	28.5	29.2	20.9	24	43	16
17:55:00	42.8	42.1	37.1	36	40.9	36	28.2	29	20.8	23	50	11
18:00:00	42.2	41.7	36.3	36.2	40.3	35.8	28.3	28.8	20.8	19	57	9
18:05:00	41.5	41.3	35.1	34.5	39.8	35.5	24.3	28.2	20.5	16	60	7
18:10:00	40.8	40.9	33.9	33.7	39.1	35.2	24.9	27.5	20	34	61	0
18:15:00	40.2	40.5	32.9	32.9	38.5	34.9	23.3	26.6	19.3	29	61	0
18:20:00	39.5	40.1	31.7	32.5	37.8	34.5	23.1	26	19.1	24	64	0
18:25:00	38.8	39.6	31.7	32.2	37.1	34.1	22.5	24.8	19	19	66	0
18:30:00	38.2	39.2	31	31.1	36.3	33.5	22	24.8	18.6	19	68	0
18:35:00	37.5	38.8	30.9	31.3	35.7	33	21.9	23.9	18.5	34	69	0
18:40:00	37	38.5	30.3	30.8	35.1	32.6	21.7	23.6	18.1	24	69	0

Time	Water Temperature (°C)		Vapour Temperature (°C)		Basin Temperature (°C)		Cover Temperature (°C)		Ambient Temperature (°C)	Wind speed (km/hr)	Relative Humidity (%)	Solar intensity (W/m2)
	MSD	NSD	MSD	NSD	MSD	NSD	MSD	NSD				
18:45:00	36.3	37.8	29.8	30.4	34.4	32.2	21.7	22.9	18.3	35	69	0
18:50:00	35.7	37.4	29.4	30.8	34	31.8	21.9	24.4	18.6	21	69	0
18:55:00	35.2	37.2	29.5	30.6	33.6	31.7	22.1	25	18.6	39	70	0
19:00:00	34.6	36.9	29.2	30.3	33.1	31.5	21.9	25.6	18.7	37	70	0
19:05:00	34.3	36.6	28.8	30.5	32.8	31.5	22.1	25.3	18.6	35	70	0
19:10:00	33.8	36.3	28.6	30.2	32.4	31.4	21.7	25.2	18.8	31	70	0
19:15:00	33.4	36	28.4	30.1	32	31.2	21.7	25	18.7	32	70	0
19:20:00	32.9	35.6	28	29.9	31.6	30.9	20.9	24.3	18.5	13	70	0
19:25:00	32.6	35.4	27.9	29.8	31.4	30.7	20.9	24.1	18.3	32	70	0
19:30:00	32.2	35.2	27.4	29.4	31	30.5	20	23.7	18.2	21	70	0
19:35:00	31.8	34.8	26.7	29.2	30.5	30.2	19.9	23.2	18.1	32	70	0
19:40:00	31.5	34.6	25.9	28.7	30.2	29.9	20.2	22.8	18	32	70	0
19:45:00	31	34.3	25.7	28.2	29.8	29.7	20	22.4	17.8	19	70	0
19:50:00	30.7	34.1	25.6	28	29.5	29.4	20.1	22.3	17.8	26	70	0
19:55:00	30.4	33.7	25.4	28.1	29.1	29.1	20.6	22.2	17.7	26	68	0
20:00:00	29.9	33.5	25.2	28	28.7	28.9	20.7	21.9	17.6	35	67	0
20:05:00	29.6	33.1	24.6	27.4	28.4	28.6	20.6	21.9	17.6	23	65	0
20:10:00	29.2	32.9	24.4	27.3	28.1	28.4	20.7	21.7	17.5	32	64	0
20:15:00	28.9	32.8	24.4	26.9	27.9	28.3	20.5	21.7	17.4	19	62	0
20:20:00	28.6	32.4	23.9	26.6	27.4	28	20.2	21.2	17.2	29	62	0
20:25:00	28.3	32.2	23.6	26.6	27.2	27.7	20.1	21.2	17.4	26	61	0
20:30:00	28	32	23.4	26.4	26.9	27.5	20	21	17.4	23	60	0
20:35:00	27.6	31.6	23.3	26.2	26.5	27.2	19.7	20.8	17.2	19	58	0
20:40:00	27.3	31.4	22.7	26.1	26.3	27.1	19.7	21	17.3	39	57	0
20:45:00	27	31.2	22.9	25.6	26.1	27	19.6	20.9	17.4	32	56	0
20:50:00	26.8	31	22.5	25.3	25.8	26.9	19.5	20.9	17.2	37	56	0
20:55:00	26.5	30.8	22.4	25.4	25.6	26.8	19.4	20.8	17.3	29	55	0
21:00:00	26.2	30.5	22.1	25.3	25.3	26.6	19.2	20.7	17.3	34	55	0
21:05:00	26	30.4	22.1	25	25.1	26.5	19.1	20.3	17.1	23	55	0
21:10:00	25.7	30.2	21.6	25.3	24.9	26.3	19	20.4	17.1	40	54	0
21:15:00	25.5	29.9	21.5	24.8	24.6	26.1	18.7	20.2	17	27	54	0
21:20:00	25.3	29.8	21.4	24.7	24.5	26.1	18.7	20.2	17.1	19	53	0
21:25:00	25	29.6	21.1	24.2	24.2	25.8	18.6	20	17	26	52	0
21:30:00	24.7	29.3	20.8	24.5	24	25.6	18.3	19.7	16.9	27	52	0
21:35:00	24.5	29.1	20.5	24.1	23.7	25.4	18.2	19.4	16.8	21	51	0
21:40:00	24.3	28.9	20.3	24.1	23.5	25.3	18.1	19.5	16.9	24	51	0
21:45:00	24	28.7	20.2	23.7	23.3	25	18	19.2	16.7	32	50	0
21:50:00	23.9	28.6	20.2	23.5	23.1	25	17.8	19.1	16.7	37	50	0
21:55:00	23.6	28.4	19.7	23.3	22.9	24.7	17.7	19.1	16.6	34	50	0
22:00:00	23.4	28.1	19.9	23.3	22.7	24.6	17.6	19	16.6	29	49	0
22:05:00	23.3	28	19.5	23.1	22.5	24.6	17.5	19.1	16.6	29	49	0
22:10:00	23	27.8	19.3	22.5	22.3	24.4	17.3	18.7	16.4	39	48	0
22:15:00	22.8	27.6	19.3	22.8	22.2	24.3	17.2	18.7	16.4	31	48	0
22:20:00	22.6	27.5	19.2	22.4	21.9	24.1	17.1	18.4	16.3	40	48	0
22:25:00	22.5	27.3	19.2	22.4	21.8	23.9	17	18.4	16.4	21	48	0
22:30:00	22.3	27.1	18.8	22.2	21.6	23.8	16.9	18.3	16.3	23	47	0
22:35:00	22.1	26.9	18.7	22.1	21.5	23.6	16.9	18.2	16.3	18	47	0
22:40:00	21.9	26.8	18.5	22.2	21.3	23.5	16.7	18.1	16.3	23	47	0
22:45:00	21.8	26.6	18.2	22.1	21.2	23.5	16.6	18.1	16.3	29	47	0
22:50:00	21.5	26.4	18.2	21.5	20.9	23.2	16.5	17.9	16.3	29	47	0
22:55:00	21.4	26.4	18.2	21.6	20.9	23.2	16.5	17.9	16.3	34	47	0
23:00:00	21.2	26.1	17.9	21.4	20.6	23	16.2	17.8	16.2	29	47	0
23:05:00	21	26	17.7	21.3	20.5	22.9	16.2	17.7	16.1	35	47	0
23:10:00	21	25.8	17.8	21.2	20.4	22.9	16.1	17.7	16.3	23	46	0
23:15:00	20.7	25.7	17.5	21.1	20.2	22.7	15.9	17.7	16.1	23	46	0
23:20:00	20.6	25.5	17.6	21.1	20.1	22.6	16	17.6	16.5	26	46	0
23:25:00	20.4	25.4	17.4	21.1	20	22.5	15.8	17.7	16.3	31	45	0
23:30:00	20.3	25.2	17.2	20.9	19.8	22.4	15.6	17.5	16	29	45	0
23:35:00	20.1	25.1	17.1	20.7	19.7	22.2	15.7	17.3	16.4	40	44	0
23:40:00	20	24.9	17.1	20.3	19.5	22	15.7	17.1	16.3	31	44	0
23:45:00	19.9	24.7	17	20.4	19.4	21.9	15.6	17.1	16.5	33	45	0
23:50:00	19.7	24.6	16.9	20.1	19.2	21.7	15.5	17	16.4	33	45	0
23:55:00	19.6	24.4	16.8	20.2	19.1	21.6	15.5	17	16.4	32	45	0
0:00:00	19.4	24.3	16.8	20.2	19	21.5	15.5	17	16.4	33	46	0

The recorded data on the 7th of December 2017

Time	Water Temperature (°C)		Vapour Temperature (°C)		Basin Temperature (°C)		Cover Temperature (°C)		Ambient Temperature (°C)	Wind speed (km/hr)	Relative Humidity (%)	Solar intensity (W/m2)
	MSD	NSD	MSD	NSD	MSD	NSD	MSD	NSD				
6:00:00	22.1	24	21.2	22.5	22.2	23.3	19.8	20.5	23	8	44	90
6:05:00	22.1	24.1	21.5	22.7	22.2	23.3	20.2	20.8	23.1	6	44	244
6:10:00	22.2	24.1	21.5	23.1	22.3	23.5	20.5	21.2	23.5	6	45	220
6:15:00	22.2	24.1	21.7	23.2	22.4	23.5	20.5	21.2	23.5	10	45	218
6:20:00	22.3	24.2	21.9	23.4	22.5	23.6	20.6	21.4	23.7	8	45	322
6:25:00	22.2	24.2	21.9	23.3	22.5	23.6	20.7	21.4	23.9	6	45	158
6:30:00	22.4	24.2	22.1	23.3	22.5	23.7	20.9	21.6	23.7	8	45	336
6:35:00	22.3	24.1	22.2	23.5	22.6	23.7	20.8	21.5	23.9	5	45	174
6:40:00	22.5	24.2	22.5	23.8	22.6	23.8	21.1	21.6	24.2	11	43	410
6:45:00	22.6	24.3	22.7	24.9	22.8	23.9	21.2	21.8	24.1	10	43	396
6:50:00	22.5	24.3	25.7	29.6	22.7	23.9	21.4	23.2	24.2	5	43	274
6:55:00	22.5	24.4	27.7	32.6	23	24	21.6	24.1	24.4	5	44	439
7:00:00	22.6	24.6	27.7	33	23.2	24.4	22.8	24.4	24.1	5	43	436
7:05:00	22.8	24.4	29.3	34.8	23.4	24.6	23.6	25	24.7	8	42	468
7:10:00	23.1	24.9	30.2	35.4	23.7	24.9	24.1	25.5	24.8	8	42	485
7:15:00	23.3	25.4	31	35.9	24.1	25.2	24.5	26	25.2	6	41	496
7:20:00	23.6	25.6	31.8	36.7	24.5	25.6	25.1	26.5	25.6	5	39	487
7:25:00	24	26.3	32.5	37.6	24.9	26.1	25.4	27	25.8	8	39	524
7:30:00	24.4	26.5	33.1	38.5	25.3	26.5	25.6	27.2	25.5	8	39	547
7:35:00	25	26.9	33.7	38.8	25.8	27	26	27.6	26.3	3	39	540
7:40:00	25.6	27.4	34.3	39.7	26.4	27.4	26.3	28	26.3	6	38	566
7:45:00	26.4	27.8	34.8	39.8	27.2	28	26.7	28.4	26.7	6	37	552
7:50:00	27.1	28.2	35	40	27.8	28.5	26.7	28.5	26.4	6	37	656
7:55:00	27.7	28.6	35.7	40.9	28.4	28.9	27.1	28.9	27.4	8	36	253
8:00:00	28.5	29.2	36	40.8	29	29.4	27.3	29.1	26.8	2	34	650
8:05:00	28.9	29.5	36.4	41.5	29.6	29.7	27.6	29.3	27.3	10	37	687
8:10:00	29.6	30	37.5	42.7	30.2	30.2	28.3	30	27.9	6	36	731
8:15:00	30.3	30.6	38.5	43.9	30.9	30.7	28.7	30.5	27.5	5	36	735
8:20:00	31	31.1	38.5	44.1	31.6	31.2	29.2	31	28.6	6	35	691
8:25:00	31.7	31.5	39.4	44.8	32.3	31.7	29.6	31.5	28.7	8	35	710
8:30:00	32.4	32	40.2	45.8	32.8	32.1	30	31.7	29	6	35	768
8:35:00	33	32.5	41.1	47.2	33.6	32.5	30.8	32.5	29.4	3	32	817
8:40:00	33.8	33.1	41.9	48.1	34.3	33.1	31.2	32.9	29.1	2	32	817
8:45:00	34.6	33.6	42.5	48.9	35.1	33.6	31.5	33.4	29.2	2	32	425
8:50:00	35.4	34.2	42.7	49.4	35.9	34.1	32.2	33.8	29.2	0	31	844
8:55:00	36.1	34.6	42.2	47.4	36.5	34.6	31.8	33.3	29.1	3	31	731
9:00:00	36.9	35.1	43.6	49.1	37.1	34.9	32.2	33.7	29.8	5	29	659
9:05:00	37.6	35.7	43.8	49.2	37.8	35.4	32.7	34.2	29.7	3	30	965
9:10:00	38.2	36	44	48.1	38.4	35.7	32.9	34.2	30.5	3	31	700
9:15:00	38.8	36.6	46.1	51.3	39	36.1	34.3	35.3	31.5	6	30	916
9:20:00	39.5	37.2	47.1	52.4	39.9	36.7	35	36.2	31.5	6	32	889
9:25:00	40.3	37.8	47.3	53.7	40.6	37.3	35.3	36.5	31.7	2	30	914
9:30:00	41.1	38.5	48.3	54.2	41.4	38	36.3	37.4	32.2	3	31	919
9:35:00	41.9	39.1	49	54.7	42.1	38.6	37	37.9	31.9	2	31	925
9:40:00	42.8	39.8	49.5	54.7	43	39.3	37.2	38.1	32.4	2	30	939
9:45:00	43.7	40.5	50	55.2	43.8	40	37.5	38.4	32.4	13	30	970
9:50:00	44.7	41.2	50.5	55.6	44.5	40.6	37.6	38.6	31.5	2	32	1011
9:55:00	45.5	41.8	51.7	55.8	45.4	41	38.5	39.4	33.7	5	31	867
10:00:00	46.3	42.5	52.2	56.1	46.1	41.5	38.7	39.5	32.2	2	29	946
10:05:00	47.1	43.2	53.2	56.7	46.9	42	39.5	40	32.4	11	27	953
10:10:00	47.9	43.8	51.9	54.8	47.6	42.5	39.2	39.6	32.1	5	27	802
10:15:00	48.6	44.3	52.6	55.4	48.2	42.9	39.7	39.6	32.5	5	29	997
10:20:00	49.4	45	52.5	55	48.7	43.4	40	39.7	32.6	6	28	1113
10:25:00	49.8	45.3	55.1	57.5	49.2	43.4	40.8	40.4	34.3	2	26	385
10:30:00	50.4	45.9	55.8	59.1	50	43.8	42.1	41.5	35.2	13	27	1158
10:35:00	51.2	46.5	56.9	59.8	50.8	44.5	42.5	42.3	33.9	14	27	1044
10:40:00	52	47.1	56.9	60.2	51.5	45.2	43.1	42.6	33.1	14	27	721
10:45:00	52.8	47.7	57.4	60.6	52.2	45.8	43.5	42.9	35.2	6	26	788
10:50:00	53.5	48.4	57.7	61.1	52.9	46.4	44.2	43.3	33.8	13	26	1058
10:55:00	54.2	49	58	61.1	53.6	46.8	44.3	43.4	33.6	8	25	1071
11:00:00	55	49.6	58.8	61.7	54.3	47.3	45.4	44.1	35.8	2	26	1137
11:05:00	55.8	50.2	59.7	62.3	55.1	47.8	46	44.4	36.3	11	26	798
11:10:00	56.5	50.8	61.2	62.7	55.7	48.3	46	44.6	34.1	13	27	1116
11:15:00	57.2	51.5	61.7	63	56.4	48.9	46.9	45.1	34.4	11	27	575
11:20:00	57.9	52	61.4	63.2	57.1	49.4	47.2	45.5	36.2	6	26	1042
11:25:00	58.6	52.6	61.8	63.6	57.6	49.8	47.5	45.5	35.1	8	26	1065
11:30:00	59.3	53.2	63.3	63.6	58.3	50.3	48.1	46	35.2	2	28	1074
11:35:00	60	53.8	63.3	64.4	58.9	50.8	49.2	46.8	37.7	11	25	1063
11:40:00	60.6	54.3	64.2	64.8	59.5	51.2	49.4	47	36.6	3	26	1049
11:45:00	61.3	54.9	64.4	64.8	60	51.8	49.4	47	36.4	21	26	1042
11:50:00	61.8	55.5	64.5	65.3	60.7	52.2	50.2	47.8	37	21	25	1042
11:55:00	62.3	56	65	65.5	61.1	52.6	50.2	47.8	36.2	11	27	1039
12:00:00	63	56.6	65.1	65.2	61.6	53	49.4	47.5	36.6	11	28	1037
12:05:00	63.5	57.1	66.4	66.4	62.1	53.1	51.5	48.8	36.9	10	26	1034
12:10:00	63.9	57.4	66	65.6	62.6	53.4	51.9	49.3	37.7	18	28	1032

Time	Water Temperature (°C)		Vapour Temperature (°C)		Basin Temperature (°C)		Cover Temperature (°C)		Ambient Temperature (°C)	Wind speed (km/hr)	Relative Humidity (%)	Solar intensity (W/m2)
	MSD	NSD	MSD	NSD	MSD	NSD	MSD	NSD				
12:15:00	64.2	57.4	65.1	63.3	62.5	53.6	50.6	47	35.1	0	26	1030
12:20:00	64.3	57.9	67	66	62.9	53.6	52.4	49.1	38.4	19	27	1030
12:25:00	64.9	58.6	67.8	67.1	63.5	53.8	53	50.4	38	8	25	1021
12:30:00	65.2	59	67.9	67.2	63.9	54.2	53.4	50.3	38.7	3	25	1018
12:35:00	65.8	59.5	67.6	67.3	64.1	54.5	52.1	49.9	36	8	25	1014
12:40:00	66.2	59.9	68	67.1	64.5	54.9	52.6	49.5	37.7	16	25	1005
12:45:00	66.4	60.2	68.3	67.4	64.8	54.9	53.5	50.4	37.3	13	26	1004
12:50:00	66.8	60.6	68.9	67.3	64.8	55	52.8	49.7	35.8	11	26	997
12:55:00	67.2	60.8	68.8	66.6	65.3	55.2	54.2	50.8	37.7	18	26	990
13:00:00	67.3	61.2	69.8	67.8	65.6	55.2	53.9	51.1	38.1	13	25	981
13:05:00	67.6	61.5	69.8	67.7	66	55.4	53.6	51.3	37.6	6	25	976
13:10:00	67.8	61.7	65.5	68.2	66.1	55.7	54.8	51.6	36	5	25	963
13:15:00	68.2	62.1	66.6	68.4	66.3	56.1	55.2	51.5	36.7	13	24	958
13:20:00	68.4	62.3	68	68.6	66.6	56.2	55.3	52.1	36.9	24	25	949
13:25:00	68.7	62.6	70.9	68.9	66.9	56.4	56.5	52.5	37.9	19	26	940
13:30:00	68.9	62.8	71.3	69.3	67.2	56.6	55.7	53.3	38.5	16	23	930
13:35:00	69.2	63.1	70.7	68.8	67.4	56.8	56.1	52.4	38.2	8	24	921
13:40:00	69.4	63.3	71.3	69.5	67.7	56.9	57.1	53.2	37.9	16	24	914
13:45:00	69.6	63.6	71.7	69.9	67.8	57.1	57.2	53.8	40.1	21	24	900
13:50:00	69.8	63.7	71.7	69.7	68	57.3	57.3	53.8	39.4	13	25	888
13:55:00	70	63.4	68	62.9	68.1	57.7	54.2	51	37.3	11	23	879
14:00:00	69.8	63.6	70.2	67.2	68	57.4	56.3	52.7	38.7	11	24	867
14:05:00	69.7	62.9	66.5	60.6	67.5	57.4	53.1	50.1	36.1	0	24	856
14:10:00	69.2	63	69.9	66.7	67.2	56.9	55.6	52.5	37.6	8	24	847
14:15:00	69	63.4	71.6	69.3	67.3	56.5	56.1	53.5	39.8	14	22	837
14:20:00	68.9	63.4	70.7	68.8	67.3	56.5	55.8	53	39.1	21	21	526
14:25:00	69	63.5	70.4	68.1	67.4	56.7	55.3	52.6	38.6	13	22	541
14:30:00	69.2	63.8	70.8	68.4	67.6	57	56.4	53.2	38.5	8	22	687
14:35:00	69.2	63.8	70.4	68.5	67.5	57.2	55.5	53	37.7	13	21	780
14:40:00	68.9	63.5	69.9	67.4	67.2	57.2	55.9	52.7	38.5	10	22	768
14:45:00	69	63.2	67.6	63.4	67	57.1	54.5	51.6	38.6	10	22	751
14:50:00	68.6	63.1	68.3	65.9	66.8	56.7	55.3	52.4	39.2	8	22	733
14:55:00	68.6	63	67	63	66.5	56.7	53.4	51.1	37.1	10	22	717
15:00:00	68.1	62.6	66.4	62.2	66.1	56.6	53.4	51.2	37.7	13	23	703
15:05:00	67.9	62.7	67.6	64.5	66.2	56.3	54.5	52.2	38.6	16	22	691
15:10:00	67.6	62.8	69.1	67.6	66.1	56.2	55.9	53.5	39	18	23	671
15:15:00	67.7	62.6	65.9	62.4	66	56.5	53.4	51.3	38	14	22	657
15:20:00	67.4	62.2	64.8	60.9	65.6	56.5	52.9	50.6	38.9	18	22	638
15:25:00	66.9	61.9	65.5	62.2	65	56.1	53.1	51	38.1	14	22	622
15:30:00	66.6	61.8	64.5	61.8	64.7	55.8	52.4	50.6	38	19	22	603
15:35:00	66.1	61.4	63.3	60	64.1	55.4	50.1	48.8	37.2	8	22	589
15:40:00	65.4	60.9	62.3	59.2	63.2	54.9	49.9	48.3	36.5	6	21	573
15:45:00	64.9	60.5	61.4	58.2	62.6	54.4	49.9	48.4	36.4	6	22	555
15:50:00	64.2	59.9	60.2	57.2	61.8	53.9	48.2	47.2	35.8	2	22	540
15:55:00	63.4	59.4	59.4	56.4	61.1	53.2	49	47.6	36.4	13	22	520
16:00:00	62.6	58.9	58.4	55.8	60.5	52.7	48.2	47.1	36.5	8	22	506
16:05:00	61.8	58.3	57.8	55.4	59.7	52.1	47.7	46.7	36.1	10	21	482
16:10:00	61.1	58	57.4	55.2	59.1	51.8	47.5	46.8	36.7	8	21	462
16:15:00	60.4	57.5	56.5	55	58.4	51.3	46.7	46.1	36.1	6	22	446
16:20:00	59.8	57.1	56	54.7	58	51.1	46.5	45.8	36.7	10	22	431
16:25:00	59.2	56.7	55.5	53.6	57.3	50.8	46.6	46	36.3	2	21	424
16:30:00	58.5	56.1	54	52.3	56.5	50.3	43.8	43.6	34	8	22	86
16:35:00	57.9	55.6	53.2	51.9	55.7	49.7	43.3	43	34	8	21	378
16:40:00	57.1	55.2	52.4	51.1	54.7	49.1	42.3	42.4	33.2	10	21	359
16:45:00	56.4	54.6	51.6	50.4	54.1	48.5	41.9	42	32.8	13	21	338
16:50:00	55.7	54.1	51	50	53.3	48	41.2	41.3	32.5	13	22	316
16:55:00	55	53.6	50.2	49.4	52.9	47.4	40.8	41.2	32.4	10	21	297
17:00:00	54.4	53.2	49.5	49.3	52.2	46.9	40.1	40.4	32	11	21	274
17:05:00	53.8	52.7	48.9	48.8	51.4	46.4	39.8	40.2	32.1	6	22	257
17:10:00	53.1	52.2	48.5	48.4	51	46	39.2	39.7	31.4	14	21	239
17:15:00	52.6	51.7	47.6	47.5	50.6	45.7	38.9	39.4	31.3	10	21	220
17:20:00	52	51.2	47	46.7	49.7	45.2	38	38.6	30.8	13	21	202
17:25:00	51.3	50.7	46	46	49.3	44.7	37.3	36.9	30.3	2	22	188
17:30:00	50.7	50.2	45.5	45.4	48.6	44.3	36.6	37.3	29.7	8	22	169
17:35:00	50.1	49.7	44.9	45.1	47.9	43.8	36.5	37.3	29.7	6	22	148
17:40:00	49.4	49.2	44.2	44.1	47.4	43.3	35.6	36.4	29.6	6	21	130
17:45:00	48.7	48.5	42.9	43	46.6	42.8	34	34.6	29	3	22	107
17:50:00	48.1	48.1	43	43.2	46.1	42.3	35	35.7	29.4	5	22	88
17:55:00	47.5	47.6	42.5	42.8	45.6	41.9	35.1	36	29	11	22	74
18:00:00	47	47.2	41.8	42.5	45.1	41.6	34.4	35.3	28.9	16	30	58
18:05:00	46.4	46.8	40.9	42	44.5	41.2	28.2	34.5	28.4	11	32	44
18:10:00	45.7	46.2	39	39.7	44	40.8	27.5	29.2	27.5	8	33	32
18:15:00	45.1	45.6	38.3	39.2	43.4	40.4	28.9	30.7	27.4	6	34	23
18:20:00	44.4	45.2	37.9	38.9	42.7	39.9	27.7	31.2	27.7	11	35	16
18:25:00	43.9	44.8	38.2	39.1	42.3	39.5	31.1	31.8	27.7	13	36	12
18:30:00	43.2	44.3	38.4	39.6	41.7	39.1	32.1	33.2	27.8	11	36	11
18:35:00	42.8	43.9	38.2	40.2	41.4	38.9	32.5	33.6	28.1	14	37	7
18:40:00	42.3	43.5	38.2	39.5	40.9	38.5	32.2	33.4	27.9	14	37	5
18:45:00	42	43.2	37.7	39.1	40.6	38.3	32.3	33.3	28.2	13	38	0

Time	Water Temperature (°C)		Vapour Temperature (°C)		Basin Temperature (°C)		Cover Temperature (°C)		Ambient Temperature (°C)	Wind speed (km/hr)	Relative Humidity (%)	Solar intensity (W/m2)
	MSD	NSD	MSD	NSD	MSD	NSD	MSD	NSD				
18:50:00	41.5	42.9	37.3	38.6	40.2	38.1	31.9	33	27.9	10	38	0
18:55:00	41.1	42.5	37.3	38.1	39.8	37.9	31.9	33	27.8	13	38	0
19:00:00	40.7	42.2	36.8	38.2	39.5	37.7	31.5	32.5	28	11	39	0
19:05:00	40.4	42	36.5	38.2	39.2	37.5	31.5	32.6	28.1	13	39	0
19:10:00	40	41.6	36.2	37.5	38.8	37.4	31.2	32.3	28.1	11	39	0
19:15:00	39.8	41.4	35.7	37.5	38.7	37.3	30.9	32.1	28.2	10	40	0
19:20:00	39.4	41.1	35.5	36.9	38.3	37	30.8	32.1	28.3	10	40	0
19:25:00	39.2	40.9	35.5	37	38.1	36.9	30.8	32	28	10	40	0
19:30:00	38.8	40.6	35.3	36.7	37.8	36.7	30.5	31.8	28	10	40	0
19:35:00	38.5	40.4	35.2	36.5	37.6	36.5	30.4	31.6	28.2	6	40	0
19:40:00	38.3	40.1	34.9	36.7	37.3	36.3	30	31.3	27.6	6	40	0
19:45:00	38	39.8	34.6	36.1	37	36.2	29.9	31.2	27.6	10	40	0
19:50:00	37.8	39.7	34.3	36.2	36.8	36.1	29.9	31.1	28.1	6	40	0
19:55:00	37.5	39.4	33.9	36	36.5	35.8	29.6	30.9	27.8	8	40	0
20:00:00	37.2	39.1	33.9	35.7	36.2	35.7	29.5	30.8	27.6	10	40	0
20:05:00	37	39	33.5	35.5	36.1	35.5	29.5	30.7	27.7	13	41	0
20:10:00	36.7	38.7	33.5	35.2	35.8	35.3	29.4	30.7	27.5	13	41	0
20:15:00	36.6	38.6	33.5	34.8	35.7	35.3	29.3	30.6	27.6	10	41	0
20:20:00	36.3	38.3	33.1	34.6	35.4	35.1	29.1	30.4	27.6	19	41	0
20:25:00	36	38.1	33	34.8	35.2	34.9	29.1	30.5	27.7	13	42	0
20:30:00	35.8	37.9	33	34.7	35.1	34.8	29.2	30.5	28.1	14	44	0
20:35:00	35.7	37.8	32.9	34.8	34.9	34.7	29.1	30.5	28	14	45	0
20:40:00	35.5	37.6	32.6	34.4	34.7	34.7	29.2	30.5	27.7	11	47	0
20:45:00	35.2	37.4	32.3	34.2	34.5	34.4	29.1	30.4	27.8	10	48	0
20:50:00	35	37.2	32.4	34.2	34.3	34.4	29	30.4	28	11	49	0
20:55:00	34.9	37.1	32.4	34.1	34.2	34.3	28.9	30.2	28.1	11	50	0
21:00:00	34.7	37	32	34.1	34.1	34.2	28.8	30.2	28.1	16	51	0
21:05:00	34.5	36.7	32.1	33.8	33.8	34	28.7	30.1	27.9	18	52	0
21:10:00	34.3	36.5	31.8	34	33.7	34	28.5	29.9	28.1	16	52	0
21:15:00	34.2	36.4	31.7	33.4	33.5	33.8	28.4	29.7	27.8	13	53	0
21:20:00	34	36.3	31.5	33.4	33.4	33.7	28.3	29.7	27.8	16	53	0
21:25:00	33.9	36.2	31.3	33.4	33.3	33.6	28.3	29.6	27.8	16	54	0
21:30:00	33.7	36	31.2	33	33.1	33.6	28.1	29.5	27.7	16	54	0
21:35:00	33.6	35.9	31.1	33	33	33.5	28.1	29.4	27.6	13	54	0
21:40:00	33.4	35.7	30.9	32.7	32.8	33.3	27.7	29.1	27.7	18	54	0
21:45:00	33.3	35.5	30.9	32.6	32.7	33.2	27.6	28.9	27.8	13	54	0
21:50:00	33.1	35.4	30.6	32.5	32.6	33.2	27.5	28.7	27.6	16	54	0
21:55:00	33	35.3	30.6	32.1	32.5	33	27.4	28.7	27.6	11	55	0
22:00:00	32.8	35.1	30.3	32.1	32.2	32.9	27.1	28.4	27.2	14	55	0
22:05:00	32.6	35	30.2	31.6	32.1	32.8	26.8	28.2	27	16	55	0
22:10:00	32.5	34.8	30	31.8	31.9	32.6	26.7	28.1	27.2	13	55	0
22:15:00	32.4	34.7	29.8	31.7	31.9	32.5	27.1	28.4	27.4	8	56	0
22:20:00	32.2	34.5	30	31.5	31.7	32.4	27.3	28.6	27	13	56	0
22:25:00	32.1	34.4	30.1	31.7	31.6	32.3	27.6	28.8	27.4	21	56	0
22:30:00	31.9	34.3	29.7	31.5	31.4	32.1	27.4	28.7	27.1	14	56	0
22:35:00	31.8	34.1	29.7	31.5	31.4	32.1	27.1	28.4	27.3	11	56	0
22:40:00	31.7	34.1	29.6	31.4	31.2	32.1	26.9	28.2	27.1	14	56	0
22:45:00	31.6	33.9	29.4	31.1	31.2	31.9	26.7	28	27.1	13	56	0
22:50:00	31.4	33.8	29.2	31.2	30.9	31.8	26.6	27.9	26.7	14	57	0
22:55:00	31.4	33.6	29.3	31.4	30.9	31.7	26.8	28	26.5	14	57	0
23:00:00	31.2	33.6	29.2	31.3	30.8	31.6	26.8	28.1	26.8	16	57	0
23:05:00	31.1	33.4	29.2	31.1	30.7	31.5	26.7	27.9	26.9	11	57	0
23:10:00	31	33.3	29	30.7	30.6	31.4	26.5	27.8	26.9	14	57	0
23:15:00	30.9	33.2	29	30.7	30.5	31.4	26.4	27.6	26.7	6	57	0
23:20:00	30.7	33.1	28.6	30.5	30.3	31.2	26.1	27.4	26.6	13	58	0
23:25:00	30.6	33	28.8	30.4	30.2	31.1	25.9	27.2	26.5	19	58	0
23:30:00	30.6	32.9	28.2	30.2	30.2	31.1	25.7	27	26.4	18	58	0
23:35:00	30.4	32.7	28.1	30.4	30	30.9	25.4	26.7	26.6	13	58	0
23:40:00	30.4	32.6	28	30	29.9	30.9	25.3	26.5	26.6	14	58	0
23:45:00	30.2	32.5	27.8	29.5	29.8	30.7	25	26.2	26.5	11	58	0
23:50:00	30.1	32.4	27.9	29.6	29.7	30.7	25	26.2	26.6	11	59	0
23:55:00	30	32.3	27.7	29.4	29.5	30.5	24.8	26	26.5	11	58	0
0:00:00	29.8	32.1	27.6	29.4	29.4	30.3	24.8	25.9	26.2	12	58	0

The recorded data on the 16th of January 2018

Time	Water Temperature (°C)		Vapour Temperature (°C)		Basin Temperature (°C)		Cover Temperature (°C)		Ambient Temperature (°C)	Wind speed (km/hr)	Relative Humidity (%)	Solar intensity (W/m2)
	MSD	NSD	MSD	NSD	MSD	NSD	MSD	NSD				
6:00:00	14.9	17.2	13.4	14.4	14.9	16.3	10.9	11.4	16.5	13	56	14
6:05:00	14.9	17.2	13.3	14.7	14.9	16.3	11.2	11.7	16.7	13	56	14
6:10:00	14.8	17.1	13.1	14.8	14.8	16.2	11.2	11.9	16.6	13	56	14
6:15:00	14.8	17.1	13.8	14.9	14.9	16.2	11.3	12.2	16.8	13	56	14
6:20:00	14.8	17.1	13.9	15	14.9	16.3	11.4	12.2	16.9	13	56	14
6:25:00	14.7	17.1	13.8	15	14.9	16.4	11.5	12.3	17.1	13	56	14
6:30:00	14.8	17.1	14	15.1	15	16.6	11.9	12.6	17.1	13	56	14
6:35:00	14.8	17	14.1	15.2	15	16.6	11.9	12.8	17.1	13	56	14
6:40:00	14.7	17	14.1	15.3	15	16.6	11.7	12.8	17.4	13	56	14
6:45:00	14.8	17.1	14.4	17.7	15	16.7	11.9	13.1	17.3	13	56	14
6:50:00	14.7	17.1	14.7	18.9	15	16.7	12	14.8	17.6	13	56	14
6:55:00	14.7	17.1	17	20.2	15.1	16.9	13	16.1	17.8	13	56	14
7:00:00	14.6	17	17.2	21.7	15.4	17.2	14.1	16.9	17.2	13	56	14
7:05:00	14.9	17.6	17.5	23.2	15.7	17.6	15.4	17.7	17.4	13	56	14
7:10:00	15.1	17.8	19.4	25.2	16	17.9	16.1	18.1	17.8	13	56	14
7:15:00	15.4	18.1	20.9	28	16.4	18.3	16.9	18.8	18.8	13	56	14
7:20:00	15.6	18.5	23.6	29.2	16.7	18.7	17.6	19.5	18.9	13	56	14
7:25:00	16	18.9	24.6	30.4	17.1	19.2	17.9	19.7	19	13	56	14
7:30:00	16.3	19.3	25.2	31	17.5	19.7	18.4	20.2	18.6	13	56	14
7:35:00	17	20.1	26	32.6	18.1	20.3	18.6	20.5	20.2	13	56	14
7:40:00	17.7	20.3	26.8	34.2	18.7	20.9	18.9	20.9	19.8	13	56	14
7:45:00	18.5	20.8	27.6	35.1	19.4	21.4	19.5	21.5	20	13	56	14
7:50:00	19.2	21.2	28.5	36.1	20.1	21.9	20.2	22.1	20.7	13	56	14
7:55:00	19.9	21.8	29.2	36.8	20.8	22.5	20.4	22.4	21.2	13	56	14
8:00:00	20.6	22.3	30	37.5	21.6	23.1	20.9	22.9	21.7	13	56	14
8:05:00	21.5	23	30.5	38	22.3	23.7	21.6	23.4	20.7	13	56	14
8:10:00	22.2	23.6	30.9	38.5	23.1	24.2	21.7	23.7	20.9	13	56	14
8:15:00	23	24.1	31.5	39.2	23.8	24.7	22.3	24.2	21.1	13	56	14
8:20:00	23.9	24.7	32.2	40.4	24.7	25.3	22.3	24.5	21.9	13	56	14
8:25:00	24.7	25.1	33	41.2	25.4	25.7	22.7	24.8	23.6	13	56	14
8:30:00	25.4	25.8	34	42	26.2	26.2	23.2	25.4	21.8	8	55	703
8:35:00	26.3	26.3	34.5	42.4	26.9	26.9	23.8	25.9	20.9	6	53	722
8:40:00	27.1	27	35.4	43.4	27.7	27.4	24	26.3	22.7	2	54	735
8:45:00	27.9	27.5	36.1	44.4	28.5	27.7	24.5	26.6	22.5	3	54	747
8:50:00	28.7	28.1	36.8	45.2	29.3	28.2	25	27.1	23.6	6	51	766
8:55:00	29.5	28.7	37.7	45.9	30.1	28.8	25.7	27.7	23.8	8	49	784
9:00:00	30.4	29.2	37.7	46.1	30.8	29.4	26.1	28	24	8	49	800
9:05:00	31.3	29.9	38.8	46.6	31.7	30	26.7	28.7	25.5	5	49	812
9:10:00	32	30.4	40.2	47	32.5	30.5	27	29	24	6	49	826
9:15:00	32.9	31.1	40.2	47.5	33.4	31.1	27.5	29.5	24	0	48	844
9:20:00	34	31.9	40.7	47.6	34.3	31.8	28.1	29.7	24.2	5	48	854
9:25:00	34.8	32.5	41.8	49	35.1	32.3	28.8	30.4	24.3	3	46	865
9:30:00	35.7	33	41.9	48.9	35.8	32.8	28.9	30.4	24.8	10	47	879
9:35:00	36.5	33.7	43.4	50.2	36.7	33.3	29.7	31	26.2	6	44	895
9:40:00	37.4	34.4	44	51.3	37.6	33.9	30.7	31.6	26.4	0	44	907
9:45:00	38.2	35.1	44.2	51.7	38.3	34.6	31	32.2	24.9	5	45	916
9:50:00	39.1	35.7	45	52.1	39.1	35.3	31.1	32.3	24	3	43	930
9:55:00	40	36.4	46.1	52	39.9	35.8	31.7	32.6	23.7	2	43	942
10:00:00	40.9	37.1	46.4	52.4	40.7	36.2	32.7	33.4	25.2	11	41	949
10:05:00	41.8	37.8	47.5	52.7	41.6	36.7	33.5	34	27.2	6	41	956
10:10:00	42.6	38.4	48.2	53.1	42.4	37.3	33.7	34.1	25	3	43	969
10:15:00	43.5	39.2	48.8	53.3	43.3	37.9	34.1	34.3	25.5	2	45	972
10:20:00	44.4	39.9	49.4	54	44	38.5	34.7	34.8	27.3	10	39	981
10:25:00	45.2	40.5	50.5	54.3	44.9	39	35	35.2	26.5	8	40	988
10:30:00	46.1	41.3	51.2	55.2	45.8	39.8	35.9	36	26.4	10	40	1000
10:35:00	46.8	41.8	51.7	55.2	46.4	40.5	36.6	35.9	26.2	5	39	1009
10:40:00	47.5	42.5	51.8	56.1	47.1	41.1	37.1	36.4	27.8	5	40	1011
10:45:00	48.4	43.2	52.7	56.1	47.8	41.7	37	36.2	25.6	10	41	1025
10:50:00	49.3	44	53.2	56.8	48.7	42.3	38.5	37.4	28.8	8	40	1027
10:55:00	50.1	44.5	53.9	57.2	49.3	42.8	39.1	37.8	27.2	5	40	1032
11:00:00	50.9	45.2	55.4	57.5	50.1	43.3	39.8	38.1	27.8	11	41	1035
11:05:00	51.6	45.8	56.1	57.9	50.8	43.7	40.6	38.6	27.3	8	42	1041
11:10:00	52.4	46.5	55.7	58.1	51.5	44.2	40.6	38.9	29.1	5	42	1049
11:15:00	53.1	47.1	56.7	58.7	52.3	44.8	41	39.2	29.5	6	41	1048
11:20:00	53.9	47.8	57.9	59	53.1	45.4	42.7	39.9	28.5	3	41	1055
11:25:00	54.7	48.4	58.2	59.1	53.7	46.1	41.7	39.5	27.6	11	42	1053
11:30:00	55.5	49.1	58.9	59.3	54.4	46.6	43.2	40.6	29.1	3	39	1058
11:35:00	56.1	49.6	59.9	59.1	55	47	43	40.5	29.4	14	40	1060
11:40:00	56.9	50.2	59.5	59.8	55.8	47.6	43	40.8	28.9	6	41	1058
11:45:00	57.4	50.8	60	60.3	56.3	48	43.5	41	28.3	11	40	1060
11:50:00	58.1	51.4	60.5	60.6	56.9	48.6	44.9	41.8	27.6	5	39	1053
11:55:00	58.6	52	61.5	61.1	57.3	49	44.5	41.7	30.8	8	40	1051
12:00:00	59.3	52.5	62	61.9	57.9	49.4	45.6	42.4	30.5	11	40	1055
12:05:00	59.7	53	61.6	61.6	58.4	49.8	45.5	42.2	29.3	11	39	1062
12:10:00	60.4	53.6	62	61.9	58.9	50.2	45.9	43	28.9	3	39	1056

Time	Water Temperature (°C)		Vapour Temperature (°C)		Basin Temperature (°C)		Cover Temperature (°C)		Ambient Temperature (°C)	Wind speed (km/hr)	Relative Humidity (%)	Solar intensity (W/m2)
	MSD	NSD	MSD	NSD	MSD	NSD	MSD	NSD				
12:15:00	60.8	54.1	63	62.7	59.3	50.5	46	42.9	28.6	5	39	1055
12:20:00	61.4	54.6	58.2	62.2	59.8	50.9	46.8	43.3	29.2	3	38	1067
12:25:00	61.9	55.1	60.2	63.6	60.3	51.2	48.2	44.7	29.3	8	38	1049
12:30:00	62.2	55.5	60.7	63.3	60.7	51.6	48.4	44.7	31	16	38	1046
12:35:00	62.7	55.9	63.6	63.4	61.1	51.9	47.5	44.5	29.2	8	39	1049
12:40:00	63.1	56.3	65.5	63.5	61.5	52.1	48.9	45.1	31	2	39	1037
12:45:00	63.6	56.8	65.7	64.1	61.9	52.4	49.7	46.1	31.3	13	39	1039
12:50:00	63.9	57	65.2	63.6	62.3	52.7	49.3	46.2	30.6	6	38	1030
12:55:00	64.3	57.6	66.6	63.9	62.6	53.1	49.4	45.5	29.5	8	37	1034
13:00:00	64.6	57.8	66.8	64.2	62.9	53.3	50.6	46.9	30.7	6	37	1023
13:05:00	65	58.2	66.7	64.5	63.2	53.5	50.3	46.4	31.3	6	37	1021
13:10:00	65.3	58.6	66.6	64.2	63.4	53.8	50.5	46.8	30.8	5	37	1014
13:15:00	65.5	58.9	66.7	64.3	63.6	53.9	49.6	46.4	31.2	8	37	1007
13:20:00	65.7	59.1	67.5	64.6	63.9	53.9	50.4	47.1	31.1	2	36	1004
13:25:00	66	59.3	67.3	64.4	64.1	54	50.2	47.2	32.3	13	37	993
13:30:00	66.2	59.5	67.1	64.1	64.2	54.2	50.7	47.2	30.3	6	37	977
13:35:00	66.4	59.8	67.3	64.6	64.4	54.3	49.9	46.9	30.6	3	36	970
13:40:00	66.5	59.9	67.4	64.7	64.5	54.4	50.1	46.9	29.1	5	36	958
13:45:00	66.6	60.1	66.9	64.5	64.6	54.5	49.8	46.6	30.8	5	36	949
13:50:00	66.7	60.1	66.7	64.5	64.5	54.4	50.4	46.8	31.1	10	36	942
13:55:00	66.6	60.1	67	64	64.5	54.2	51	46.7	30.8	5	35	933
14:00:00	66.8	60.3	67.7	64.5	64.7	54.2	50	47.4	31.1	10	35	921
14:05:00	66.8	60.4	67.8	64.5	64.9	54.3	51.9	48	32	6	35	914
14:10:00	66.8	60.4	67.4	64.6	64.9	54.3	50.1	47	30.2	6	35	896
14:15:00	66.8	60.4	67.4	63.9	64.8	54.4	50.3	47.1	31.6	3	34	888
14:20:00	67	60.5	67.4	64.1	64.9	54.3	50.8	47	31.1	8	35	872
14:25:00	67	60.6	67	63.4	65	54.4	50.6	47.1	32.2	11	35	861
14:30:00	67	60.7	67.2	64.4	65	54.5	50.9	47.3	30.9	10	34	851
14:35:00	67.1	60.8	67.4	63.5	65.1	54.6	50.6	47.8	30.9	5	35	831
14:40:00	66.9	60.7	67.1	63.3	64.9	54.6	51.3	47.8	32.6	13	34	819
14:45:00	66.9	60.7	66.6	63	64.9	54.6	50.5	47.2	30.4	13	34	809
14:50:00	66.8	60.6	66.4	62.7	64.8	54.5	50.7	47.1	31.6	11	35	793
14:55:00	66.8	60.6	66.1	62.3	64.8	54.5	49.8	46.7	30.8	8	35	777
15:00:00	66.6	60.6	66.1	62.1	64.6	54.3	50.6	47.2	31.1	8	36	763
15:05:00	66.6	60.6	65.6	62.2	64.6	54.3	48.9	46.5	31.2	11	35	747
15:10:00	66.3	60.4	65.2	62.1	64.4	54.2	50.4	46.9	31.9	11	34	729
15:15:00	66.3	60.3	64.9	61.8	64.4	54.2	49	46.1	30.1	11	35	719
15:20:00	66	60.2	64.7	61.1	64.1	54.1	49.6	46.1	30.4	18	36	698
15:25:00	65.9	60.1	64.2	60.3	64	53.9	48.5	46.2	30.9	6	35	677
15:30:00	65.9	60	63.8	59.9	63.6	53.7	48.1	46	30.1	10	35	664
15:35:00	65.5	59.8	63.5	60	63.4	53.3	48.9	46	32	13	37	650
15:40:00	65.4	59.9	63.3	59.8	63.3	53.2	47.3	45.4	30.7	14	38	631
15:45:00	65.1	59.6	62.9	59.6	63	52.9	47.8	45.3	30.8	8	38	612
15:50:00	64.8	59.5	62.4	59.4	62.7	52.7	47	44.6	28.8	18	38	594
15:55:00	64.5	59.3	61.5	59	62.4	52.5	46.5	44.5	30.5	18	39	578
16:00:00	64.1	59.1	61.5	58.6	62	52.1	46.6	44.4	29.7	13	39	561
16:05:00	63.8	58.9	60.6	58	61.7	52	45.7	43.9	29.3	10	39	543
16:10:00	63.6	58.7	60.4	58.2	61.4	51.7	45.5	43.7	29.3	13	38	527
16:15:00	63.4	58.6	60	58.1	61.1	51.4	45.4	43.6	29.8	11	38	508
16:20:00	63	58.3	59.9	57.7	60.8	51.2	44.7	43	29.7	13	38	492
16:25:00	62.6	58.1	59.4	56.2	60.6	51	45.4	43.4	30.7	16	39	471
16:30:00	62.3	57.9	59	55.9	60.2	50.8	43.9	42.2	28.8	16	41	452
16:35:00	61.8	57.7	58.7	55.1	59.8	50.7	43.2	41.4	29.2	19	41	434
16:40:00	61.5	57.4	58.4	56	59.4	50.4	42.6	41.6	28.7	14	42	415
16:45:00	61.1	57	58.1	55.3	59	50.2	42	41.1	28.8	19	42	399
16:50:00	60.5	56.6	57	54.8	58.6	49.8	41.2	40.3	28.2	19	43	378
16:55:00	59.9	56.4	56.4	54.4	58.1	49.6	40.3	40.3	27.6	13	43	357
17:00:00	59.3	55.9	55.8	54.3	57.6	49.2	41.2	40.7	29.1	19	44	339
17:05:00	58.6	55.5	55.1	53.9	57	48.8	40.1	39.8	27.6	19	44	322
17:10:00	58	55	54.1	53.3	56.4	48.5	39.5	39.5	27.5	26	44	302
17:15:00	57.5	54.5	53.5	52	55.7	48.1	39.2	39.2	28.3	23	45	287
17:20:00	56.8	53.9	52.5	50.7	55.1	47.5	37.5	38.1	27.3	13	45	267
17:25:00	56.1	53.3	52.2	50.4	54.4	47	37.2	37.4	26.6	19	46	248
17:30:00	55.4	52.9	51.3	49.8	53.8	46.6	37.3	36.9	27.5	18	46	232
17:35:00	54.6	52.3	50.5	49.6	53.2	46.1	37.2	37.5	27.2	18	45	211
17:40:00	53.9	51.8	49.7	48.8	52.5	45.6	35.5	36.3	26.3	16	46	192
17:45:00	53.3	51.1	49.2	45.8	52	45.2	35.6	35.3	26	13	46	172
17:50:00	52.6	50.3	46.6	44.7	50.8	44.6	34.8	34.5	26.2	18	46	156
17:55:00	51.7	49.6	45.6	44	49.7	43.8	34.4	34.1	26	16	46	137
18:00:00	50.8	49	44.9	43.4	48.8	43.2	33.3	33.5	25.5	14	47	116
18:05:00	50.1	48.5	44.1	43	48.1	42.6	33.3	33.2	25.4	16	47	97
18:10:00	49.3	47.9	43.3	41.9	47.2	42.1	32.6	32.5	25	18	47	79
18:15:00	48.6	47.4	42.4	41.5	46.6	41.6	31.9	32	24.7	18	47	62
18:20:00	47.8	46.8	41.8	41	45.8	41	31.2	31.7	24.6	13	48	49
18:25:00	47.1	46.3	40.8	40.6	45.1	40.6	30.9	31.4	24.3	11	48	39
18:30:00	46.3	45.8	40.5	39.6	44.4	40.2	30.6	30.9	24.7	19	48	28
18:35:00	45.7	45.3	39.8	39.3	43.9	39.7	30.1	30.6	24.4	13	49	21
18:40:00	45.1	44.7	38.1	38.5	43.2	39.3	29.3	29.9	23.8	13	49	16
18:45:00	44.5	44.3	38.6	38.6	42.6	38.8	29.2	29.7	23.6	13	49	0

Time	Water Temperature (°C)		Vapour Temperature (°C)		Basin Temperature (°C)		Cover Temperature (°C)		Ambient Temperature (°C)	Wind speed (km/hr)	Relative Humidity (%)	Solar intensity (W/m2)
	MSD	NSD	MSD	NSD	MSD	NSD	MSD	NSD				
18:50:00	43.8	43.8	37.8	37.8	42	38.4	28.7	29.4	23.8	13	49	0
18:55:00	43.2	43.3	37.5	37.8	41.4	37.9	28.2	29.1	23.9	13	49	0
19:00:00	42.6	42.9	36.4	37.2	40.9	37.6	27.9	28.6	23.3	13	49	0
19:05:00	42.1	42.4	36.3	36.7	40.3	37.2	27.4	28.2	23.4	13	49	0
19:10:00	41.5	42	35.8	36.1	39.9	36.9	27.1	28.1	23.1	13	49	0
19:15:00	41	41.5	35.3	35.9	39.3	36.5	27	27.7	22.8	13	49	0
19:20:00	40.4	41.1	34.8	35.6	38.8	36.1	26.4	27.4	22.9	13	49	0
19:25:00	39.9	40.6	33.9	35.4	38.3	35.7	26	26.9	22.6	13	49	0
19:30:00	39.4	40.2	34	34.9	37.8	35.5	25.7	26.6	22.4	13	49	0
19:35:00	38.9	39.8	33.2	34.2	37.3	35	25.2	26.3	22.5	13	49	0
19:40:00	38.4	39.4	33	33.5	36.9	34.7	25	26	22.2	13	49	0
19:45:00	37.9	39	32.6	33.2	36.4	34.3	24.7	25.8	22.1	13	49	0
19:50:00	37.5	38.7	32.4	33.1	36	34	24.7	25.8	22.2	13	49	0
19:55:00	37.1	38.3	31.8	33	35.6	33.8	24.3	25.5	22	13	49	0
20:00:00	36.5	37.9	31.2	32.4	35.2	33.5	24	25.1	21.8	13	49	0
20:05:00	36.1	37.5	30.7	31.7	34.7	33.1	23.6	24.7	21.8	13	49	0
20:10:00	35.8	37.3	30.4	32.2	34.4	32.9	23.4	24.7	21.7	13	49	0
20:15:00	35.3	36.9	30.3	31.5	34	32.6	23.1	24.3	21.3	13	49	0
20:20:00	34.9	36.5	29.9	30.7	33.6	32.3	22.8	24	21.2	13	49	0
20:25:00	34.6	36.3	29.4	31	33.3	32.1	22.5	23.8	21.1	13	49	0
20:30:00	34.2	35.9	29.2	30.9	32.9	31.8	22.3	23.5	20.9	13	49	0
20:35:00	33.8	35.5	29	30.8	32.5	31.4	22	23.3	21	13	49	0
20:40:00	33.5	35.3	28.3	30.2	32.2	31.3	21.9	23.1	20.8	13	49	0
20:45:00	33	34.9	28.1	30	31.8	30.9	21.6	22.9	20.5	13	49	0
20:50:00	32.7	34.6	27.3	29.4	31.4	30.7	21.2	22.5	20.1	13	49	0
20:55:00	32.4	34.3	27.5	29.2	31.2	30.5	21	22.4	20.1	13	49	0
21:00:00	32	34	27	28.8	30.8	30.1	20.7	22.2	19.9	13	49	0
21:05:00	31.7	33.7	26.9	28.3	30.4	29.9	20.5	21.7	19.6	13	49	0
21:10:00	31.3	33.4	26.4	28.9	30.1	29.5	20.2	21.5	19.5	13	49	0
21:15:00	31.1	33.2	26.2	28.3	29.9	29.4	20.1	21.4	19.5	13	49	0
21:20:00	30.7	32.8	26	27.5	29.5	29	19.8	21.1	19.1	13	49	0
21:25:00	30.4	32.6	25.6	27.4	29.2	28.9	19.6	20.8	19	13	49	0
21:30:00	30.1	32.3	25.2	27	28.9	28.6	19.4	20.7	19.2	13	49	0
21:35:00	29.8	32.1	24.8	26.7	28.7	28.4	19.3	20.5	19.2	13	49	0
21:40:00	29.4	31.7	24.8	26.8	28.3	28.1	19.1	20.2	18.7	13	49	0
21:45:00	29.2	31.8	24.4	26.5	28.1	27.9	19	20.1	18.7	13	49	0
21:50:00	28.9	31.2	24.3	25.8	27.8	27.6	18.6	19.9	18.7	13	49	0
21:55:00	28.6	30.9	24.2	25.7	27.5	27.4	18.5	19.8	18.7	13	49	0
22:00:00	28.4	30.8	23.9	25.7	27.3	27.2	18.4	19.8	18.8	13	49	0
22:05:00	28	30.5	23.4	25.8	27	27	18.2	19.5	18.4	13	49	0
22:10:00	27.7	30.1	23.4	25	26.8	26.8	18.1	19.3	18.3	13	49	0
22:15:00	27.5	29.9	23.3	25	26.6	26.6	17.9	19.2	18.2	13	49	0
22:20:00	27.3	29.7	23	24.6	26.3	26.4	17.8	19	18.3	13	49	0
22:25:00	27.1	29.4	22.7	24.5	26.1	26.2	17.7	18.9	18.2	13	49	0
22:30:00	26.8	29.2	22.6	24.3	25.9	26	17.6	18.8	18.1	13	49	0
22:35:00	26.4	28.9	22.4	24.2	25.6	25.7	17.3	18.5	18	13	49	0
22:40:00	26.2	28.6	22.3	24.2	25.3	25.5	17.2	18.4	17.9	13	49	0
22:45:00	26	28.4	21.8	23.6	25.1	25.4	17.1	18.2	17.6	13	49	0
22:50:00	25.8	28.2	21.7	23.3	24.9	25.1	17	18.1	17.7	13	49	0
22:55:00	25.5	28	21.4	23.3	24.7	25	16.8	17.9	17.6	13	49	0
23:00:00	25.4	27.8	21.5	23.2	24.6	24.9	16.8	17.9	17.7	13	49	0
23:05:00	25.2	27.5	21.3	23.2	24.4	24.7	16.7	17.8	17.5	13	49	0
23:10:00	24.9	27.4	21	22.5	24.1	24.5	16.5	17.6	17.5	13	49	0
23:15:00	24.7	27.1	20.9	22.5	23.9	24.4	16.3	17.4	17.3	13	49	0
23:20:00	24.5	27	20.9	22.4	23.8	24.2	16.2	17.3	17.1	13	49	0
23:25:00	24.3	26.8	20.4	22.3	23.5	24	16	17.1	17.1	13	49	0
23:30:00	24.1	26.5	20.2	21.9	23.4	23.8	15.9	17	17	13	49	0
23:35:00	23.9	26.3	20.2	21.9	23.1	23.6	15.8	16.8	17.1	13	49	0
23:40:00	23.7	26.1	20	21.6	22.9	23.5	15.7	16.8	17.1	13	49	0
23:45:00	23.5	26	19.7	21.4	22.7	23.3	15.6	16.7	16.9	13	49	0
23:50:00	23.2	25.7	19.7	21.3	22.6	23.2	15.5	16.6	16.6	13	49	0
23:55:00	23.2	25.6	19.6	21.1	22.4	23.1	15.4	16.5	16.7	13	49	0
0:00:00	23	25.5	19.5	21.1	22.3	22.9	15.4	16.4	16.7	13	49	0

The recorded data of the 9th of February 2018

Time	Water Temperature (℃)		Vapour Temperature (℃)		Basin Temperature (℃)		Cover Temperature (℃)		Ambient Temperature (℃)	Wind speed (km/hr)	Relative Humidity (%)	Solar intensity (W/m2)
	MSD	NSD	MSD	NSD	MSD	NSD	MSD	NSD				
6:00:00	14.9	17.3	13.7	14.6	14.8	16.2	12.2	14.1	15.5	8	35	42
6:05:00	14.8	17.2	13.7	14.7	14.8	16.2	12.3	14.2	15.6	6	36	56
6:10:00	14.8	17.2	13.8	14.7	14.9	16.2	12.5	14.3	15.8	8	37	69
6:15:00	14.8	17.1	13.8	14.6	14.7	16.2	12.4	14.3	15.9	6	39	84
6:20:00	14.8	17.1	14.1	14.8	14.8	16.2	12.8	14.6	16.1	5	39	98
6:25:00	14.9	17	14.3	15.1	14.9	16.2	12.9	14.7	16.2	8	39	125
6:30:00	14.7	17	14.2	15.1	14.8	16.2	13.1	14.9	16.3	8	40	146
6:35:00	14.8	17.1	14.4	15.3	15	16.4	13.3	15	16.4	6	42	169
6:40:00	14.8	17	14.4	15.1	14.9	16.4	13.4	15.1	16.6	8	43	192
6:45:00	14.8	17	14.5	15.4	15	16.4	13.5	15.3	16.8	8	44	211
6:50:00	14.8	17	14.4	15.7	15	16.4	13.5	15.3	16.9	8	46	234
6:55:00	14.7	16.9	14.5	15.5	15	16.4	15	16.9	17	6	48	255
7:00:00	14.8	17	14.6	19.6	15	16.4	16.2	18.2	17.1	3	50	276
7:05:00	14.7	17.1	17.1	21.5	15.1	16.6	16.8	19.1	17.2	10	52	276
7:10:00	14.7	17.2	18.7	25.4	15.4	16.9	17.2	19.9	17.3	3	54	316
7:15:00	14.8	17.4	21.9	27.7	15.7	17.3	17.4	20.3	17.5	11	58	338
7:20:00	15	17.5	23	29.2	15.9	17.6	17.9	21.2	18.5	8	58	104
7:25:00	15.4	17.8	23.9	29.9	16.4	18.1	18.1	21.5	18.3	14	60	51
7:30:00	15.8	18.1	24.5	30.7	16.9	18.5	18.1	22	19.1	5	61	35
7:35:00	16.4	18.5	25.3	31.3	17.4	18.9	18.2	22.3	18.7	6	64	418
7:40:00	16.9	18.9	26	32.2	18.1	19.4	18.3	22.9	19.6	3	64	434
7:45:00	17.6	19.3	26.1	32.9	18.7	19.9	18.4	23	19	3	66	452
7:50:00	18.2	19.7	26.7	33.7	19.4	20.4	18.6	23.9	20.4	6	67	466
7:55:00	18.9	20.2	27.5	34.2	20	21	19.4	23.7	19.4	6	67	483
8:00:00	19.6	20.7	28.5	35.1	20.7	21.5	20.2	24.7	21.3	10	69	503
8:05:00	20.3	21.1	27.8	35.6	21.4	21.9	21.3	25.1	21.2	10	71	522
8:10:00	21.1	21.7	29.1	36.4	22.2	22.6	22.1	26.3	22.2	14	71	541
8:15:00	21.7	22.2	29.9	37.3	22.9	23.1	22.8	26.5	22.2	6	71	559
8:20:00	22.4	22.6	30.2	37.7	23.4	23.6	23.2	26.6	21.6	6	70	577
8:25:00	23.2	23.2	30.9	38.6	24.2	24.2	23.7	27.6	23.7	10	69	594
8:30:00	24	23.7	32	39.5	25.1	24.8	24.5	28.7	24.3	2	69	608
8:35:00	24.7	24.3	32.6	40.1	25.8	25.4	24.7	28.8	23.4	8	68	541
8:40:00	25.6	25	33.7	41.1	26.6	26.1	25.3	28.9	23.4	3	65	35
8:45:00	26.4	25.6	34	41.1	27.2	26.5	25.4	29.1	23.3	13	65	49
8:50:00	27.3	26.2	35.5	42	28.1	27.1	26	30.2	24.1	8	64	673
8:55:00	28	26.7	36.2	42.5	28.8	27.7	26.4	30.5	24.1	11	64	691
9:00:00	28.8	27.5	36.8	43.2	29.7	28.3	26.9	30.7	23.4	11	63	703
9:05:00	29.7	28.1	37.5	43.6	30.5	28.9	27.1	31.3	23.9	11	63	717
9:10:00	30.6	28.8	38.6	44	31.3	29.5	28	32	25.7	2	62	737
9:15:00	31.5	29.4	39.4	44.7	32.2	30.1	28.1	31.8	24	10	60	749
9:20:00	32.4	30.1	40.5	44.9	33	30.7	28.5	32	23.2	3	59	763
9:25:00	33.3	30.7	40.7	45.9	33.8	31.2	29.4	33.2	25.8	0	59	775
9:30:00	34.3	31.4	42.1	46.9	34.6	31.7	29.7	32.4	23.5	10	59	793
9:35:00	35.2	32.1	42.4	47.6	35.5	32.3	30.2	33.5	24.5	6	58	802
9:40:00	36.1	32.8	43.7	48.8	36.4	32.9	30.7	33.3	24.3	8	60	814
9:45:00	37	33.5	43.8	49.3	37.3	33.4	31	34.4	25.4	0	60	826
9:50:00	38	34.2	45	49.8	38.2	34	31.4	33.8	24.4	3	60	838
9:55:00	38.9	35	44.6	50.1	38.9	34.6	31.4	33.8	24.5	6	58	853
10:00:00	39.7	35.6	45.5	50.2	39.8	35	32.2	35.8	27.3	8	57	865
10:05:00	40.8	36.2	46.3	50.8	40.6	35.4	32.7	35.1	25	5	56	870
10:10:00	41.5	37	47.2	51.2	41.6	36.1	33.3	36.5	25.9	5	55	882
10:15:00	42.4	37.6	48.3	51.3	42.2	36.6	33.4	35.5	25.3	10	54	891
10:20:00	43.2	38.3	48.1	52.3	43.1	37.1	34	36.2	26.4	2	52	900
10:25:00	44.2	39.1	49.4	53.2	43.9	37.6	34.2	37.5	26.6	10	54	911
10:30:00	45	39.7	50.7	53.9	44.7	38.1	35	37.6	27.1	2	53	916
10:35:00	45.8	40.4	51.6	54.6	45.6	38.7	35.7	39.1	28	11	52	923
10:40:00	46.7	41.1	52	54.7	46.4	39.3	35.9	38.6	27.6	2	54	933
10:45:00	47.5	41.7	52.7	54.8	47.1	39.8	36.1	38.7	26.9	8	54	940
10:50:00	48.6	42.5	53.5	55.1	48	40.6	36.6	39	26.7	5	53	947
10:55:00	49.3	43.1	53.3	55.5	48.7	41	37.2	39.2	28.2	2	51	951
11:00:00	50.2	43.8	54.4	56	49.6	41.6	37.4	39.9	28.2	8	50	962
11:05:00	51	44.4	54.9	56.7	50.2	42.2	38.1	39.9	28.9	3	47	969
11:10:00	51.8	45.1	55.6	57.1	51	42.7	38.7	40.1	28.4	3	43	967
11:15:00	52.6	45.7	56.5	57.5	51.7	43.1	38.6	39.6	27.6	8	44	970
11:20:00	53.5	46.5	57.2	57.7	52.5	43.7	38.8	40.9	29.8	8	42	977
11:25:00	54.3	47.1	57	57.9	53.1	44	38.6	39.9	27.6	6	43	983
11:30:00	54.9	47.7	57.8	58.7	53.8	44.4	39.2	40.8	29.2	14	42	986
11:35:00	55.5	48.4	58.3	58.9	54.4	44.8	39.6	40.2	28.4	13	43	990
11:40:00	56.3	49	58.7	59.4	55.1	45.3	40.3	41.7	29.5	8	42	990
11:45:00	56.9	49.4	59.4	59.8	55.6	45.6	40.9	41.7	29	6	42	995
11:50:00	57.4	49.9	59.6	60.1	56.2	46	41.2	43.2	31.2	16	40	995
11:55:00	58	50.4	60.4	60.2	56.7	46.5	41.7	42.5	30.6	18	40	995
12:00:00	58.6	51	60.4	60.3	57.3	46.9	41.9	42.3	29.6	6	40	997
12:05:00	59.3	51.6	61.4	60.5	57.9	47.4	41.4	42.2	29.2	8	39	997
12:10:00	59.8	52.1	61.8	60.6	58.3	47.6	42.1	42.2	29.5	5	40	995

Time	Water Temperature (°C)		Vapour Temperature (°C)		Basin Temperature (°C)		Cover Temperature (°C)		Ambient Temperature (°C)	Wind speed (km/hr)	Relative Humidity (%)	Solar intensity (W/m2)
	MSD	NSD	MSD	NSD	MSD	NSD	MSD	NSD				
12:15:00	60.3	52.6	56.5	60.8	58.5	47.8	42.7	42.7	30.2	13	40	1000
12:20:00	60.7	53	59.3	61.7	59.2	48	44	44.3	31.3	16	40	993
12:25:00	61.1	53.5	60.8	61.7	59.6	48.4	43.2	43.4	30	8	40	988
12:30:00	61.6	53.9	63.1	61.5	60.1	48.6	43.8	44.2	30.3	13	39	988
12:35:00	62	54.4	63.5	61.9	60.5	48.9	43.8	44.7	29.5	11	40	983
12:40:00	62.5	54.9	64.5	63.3	61	49.2	44.6	45.5	31.6	11	40	983
12:45:00	62.9	55.3	64.3	62.7	61.4	49.6	44	45.1	29.9	6	39	981
12:50:00	63.2	55.6	65.1	62.6	61.4	49.8	44.7	45.7	30.7	14	39	976
12:55:00	63.6	56	65.5	62.8	61.9	50.1	45.3	45.1	31.5	6	39	974
13:00:00	63.7	56.3	65.9	62.7	62	50.3	45.2	46.4	32	11	38	969
13:05:00	64.2	56.6	65.9	63.1	62.1	50.5	45.5	45.6	31.1	10	38	963
13:10:00	64.5	56.9	65.7	64.3	62.6	50.8	45.3	45.1	30.4	6	36	541
13:15:00	64.5	57.2	66	63.6	62.7	51	46.2	46.6	32.4	13	35	954
13:20:00	64.9	57.5	66.5	64.4	63.1	51.1	46.6	47.7	32.2	5	36	944
13:25:00	65.3	57.9	66.4	63.8	63.5	51.5	46.1	45.5	29.9	13	36	937
13:30:00	65.5	58.3	66.3	63.9	63.5	51.7	46.1	45.8	30.4	5	35	928
13:35:00	65.6	58.4	66.8	63.4	63.5	51.8	46.4	46.3	31.2	14	36	923
13:40:00	65.7	58.5	67.4	55.1	63.8	51.7	46.4	46.6	30.7	16	35	914
13:45:00	65.9	58.7	62.5	58.9	63.8	51.8	46.6	45.6	30.7	3	35	900
13:50:00	65.9	58.9	66.5	59.2	64	52	47.4	47.7	32.6	8	36	895
13:55:00	66	59	66.4	60.3	64	52.1	47.1	46.5	31	11	33	886
14:00:00	66.2	59.2	66.6	63.2	64.1	52.1	47	46.4	31.5	18	34	879
14:05:00	66.3	59.3	66.6	63.4	64.2	52.2	47.7	46.8	31.9	8	34	863
14:10:00	66.3	59.4	66.9	63.5	64.4	52.3	47.6	46.6	32.1	19	33	856
14:15:00	66.4	59.4	66.6	63.9	64.3	52.4	47.1	46	30.1	10	33	844
14:20:00	66.5	59.5	67.7	63.7	64.4	52.3	47.9	46.6	31.7	10	32	831
14:25:00	66.5	59.6	66.7	63.3	64.2	51.9	47.1	46.3	31	18	31	821
14:30:00	66.4	59.7	66	62.6	64.4	51.8	46.8	45.8	31.4	23	30	809
14:35:00	66.4	59.7	66.5	62.3	64.3	51.9	47.3	47.2	32.9	16	30	793
14:40:00	66.2	59.6	65.8	62.3	64.2	51.8	47.5	47.7	32	14	30	779
14:45:00	65.8	59.5	65.5	61.7	64	52	47.4	47.6	33.5	11	32	766
14:50:00	66.1	59.5	65.9	62.1	64	52.1	47.6	46.8	32.4	8	31	754
14:55:00	65.8	59.4	65.2	61.5	63.9	52.2	47.3	47.4	32.5	16	34	738
15:00:00	65.8	59.3	64.6	60.8	63.6	52.2	46.1	46.3	31.8	23	34	722
15:05:00	65.5	59.2	64.4	61.1	63.6	52.1	47.1	49.2	33.1	18	34	708
15:10:00	65.4	59.2	64.8	61.2	63.6	52.2	48.3	48.4	33.1	5	34	694
15:15:00	65.2	59.1	64.3	61.6	63.4	52.2	48.6	48.2	32.6	5	34	686
15:20:00	65.2	59.2	64	61	63.5	52.5	47.4	49.4	33.9	13	33	682
15:25:00	65	59.2	64	60.8	63.3	52.5	48.5	48.9	33.7	10	35	657
15:30:00	64.7	59.1	63.7	60.6	63.2	52.5	48.3	48.4	32.6	10	34	650
15:35:00	64.7	59.2	63.6	60.9	63	52.6	48	48.8	33.2	2	33	628
15:40:00	64.5	59.3	62.9	60.4	63	52.7	47.1	48.5	32.9	6	34	606
15:45:00	64.2	59.3	62.4	59.9	62.6	52.6	46.6	48.7	33.5	16	36	587
15:50:00	64.1	59.2	61.8	59.6	62.4	52.5	46.1	47.8	32.5	10	36	568
15:55:00	63.7	59.2	61.4	58.9	62.1	52.5	46.6	48	33.6	3	36	547
16:00:00	63.4	59	60.8	58.8	61.7	52.3	46	47.1	32.1	13	37	529
16:05:00	63.1	58.9	60.9	59	61.3	51.9	46.7	46.7	31.9	8	36	512
16:10:00	62.9	58.6	60.3	59.2	61	51.5	45.9	47.8	32.5	11	36	494
16:15:00	62.8	58.6	60.2	59.2	60.9	51.3	45.8	47.7	32.5	16	37	483
16:20:00	62.7	58.5	60.5	58.5	60.8	51.3	44.6	46.9	32.2	11	36	457
16:25:00	62.7	58.5	60.3	58	60.7	51.3	44.4	46	31.5	10	37	443
16:30:00	62.4	58.3	59.9	57.6	60.4	51	44.5	45.8	31.8	10	37	424
16:35:00	62.2	58.1	59.6	57.8	60.2	50.8	43.7	46.1	31.7	14	38	404
16:40:00	62.1	58	59.8	56.3	60	50.6	43.7	46.1	31.5	18	38	387
16:45:00	61.7	57.8	59.3	56	59.8	50.5	43.1	46.1	31.8	19	39	369
16:50:00	61.3	57.7	58.9	56	59.5	50.3	43.2	45.4	31	14	40	350
16:55:00	60.9	57.6	58.7	55.8	59.2	50.4	42.8	44.5	30.6	8	40	330
17:00:00	60.6	57.5	58.2	55.4	59	50.3	42	44.3	30.7	19	40	315
17:05:00	59.9	57	57.9	56.1	58.5	50.1	42.3	44.6	31.1	18	41	295
17:10:00	59.3	56.7	57	55.9	57.9	49.8	42.2	44.2	30.3	13	42	276
17:15:00	58.6	56.3	55.7	55.4	57.2	49.4	42.4	44.3	30.7	16	41	257
17:20:00	58	55.9	54.5	54.6	56.7	49.1	41.4	43.5	30	6	41	239
17:25:00	57.3	55.1	53	50.2	55.8	48.6	40	41.6	29.7	18	41	220
17:30:00	56.4	54.3	51.2	48.8	54.5	47.9	38.9	40.8	29.5	14	42	206
17:35:00	55.5	53.7	50.4	48.6	53.5	47.3	38.6	41.1	29.4	19	42	186
17:40:00	54.8	53.1	49.7	48.1	52.7	46.7	38.4	40.9	29.1	13	43	169
17:45:00	53.9	52.5	48.5	47.2	51.8	46.1	37.4	39.1	28.5	6	43	148
17:50:00	53	51.9	47.7	46.5	51.1	45.5	37.2	39	28.4	18	43	128
17:55:00	52.3	51.3	47.1	45.8	50.3	44.9	36.9	38.6	28.4	18	44	107
18:00:00	51.6	50.8	46.2	45.3	49.6	44.5	36.4	38.2	28.1	23	44	88
18:05:00	50.9	50.3	45.5	44.8	49	44	35.9	37.8	28.3	16	44	72
18:10:00	50.1	49.8	45	44.3	48.3	43.5	35.6	37.7	27.8	14	45	56
18:15:00	49.5	49.3	44.2	43.8	47.6	43.2	35.1	37.2	27.6	10	45	42
18:20:00	48.8	48.8	43.6	43.3	47	42.7	34.6	35.8	27	5	45	32
18:25:00	48.2	48.3	42.9	42.7	46.4	42.3	34.3	36.1	27.2	13	46	23
18:30:00	47.5	47.8	42	42.4	45.7	41.8	33.8	35.7	27	13	47	16
18:35:00	46.9	47.4	41.5	42.1	45.1	41.5	33.8	35	26.7	11	47	12
18:40:00	46.3	46.9	41.1	41.7	44.6	41.1	33.5	34.4	26.2	13	48	11
18:45:00	45.7	46.5	40.7	41.1	44	40.7	33.2	34.6	26.6	16	48	7

Time	Water Temperature (°C)		Vapour Temperature (°C)		Basin Temperature (°C)		Cover Temperature (°C)		Ambient Temperature (°C)	Wind speed (km/hr)	Relative Humidity (%)	Solar intensity (W/m2)
	MSD	NSD	MSD	NSD	MSD	NSD	MSD	NSD				
18:50:00	45	46.1	40	40.8	43.4	40.3	32.9	34.6	26.5	13	49	0
18:55:00	44.6	45.7	39.7	40.6	43	40	32.7	34.1	26.4	11	49	0
19:00:00	44	45.2	38.9	40	42.4	39.7	32.5	34.1	26.2	10	49	0
19:05:00	43.5	44.8	38.5	39.2	42	39.4	31.9	34	26.1	11	50	0
19:10:00	42.9	44.5	38.1	39.2	41.5	39.1	31.5	33.7	26.1	13	50	0
19:15:00	42.5	44	37.6	38.9	41	38.7	31.4	33.4	25.9	13	51	0
19:20:00	42	43.7	37.5	38.4	40.6	38.5	31.2	32.9	25.9	10	51	0
19:25:00	41.5	43.4	36.7	38.1	40.1	38.1	31	32.9	25.6	10	51	0
19:30:00	41.1	43	36.6	37.7	39.7	37.9	30.8	32.4	25.4	11	51	0
19:35:00	40.7	42.7	36.1	37.6	39.3	37.7	30.5	32.4	25.3	10	52	0
19:40:00	40.2	42.3	35.4	37.6	38.8	37.3	30.1	32	25.3	10	52	0
19:45:00	39.7	42	35.2	36.9	38.5	37	29.8	31.7	25.1	13	52	0
19:50:00	39.3	41.6	34.6	36.5	38.1	36.8	29.6	31.1	24.9	14	52	0
19:55:00	39.1	41.4	34.6	36.2	37.8	36.6	29.4	30.9	25.1	14	53	0
20:00:00	38.6	41	33.8	36.1	37.3	36.3	28.9	30	24.8	11	53	0
20:05:00	38.2	40.7	33.3	35.6	36.9	36	28.5	30.1	24.4	19	53	0
20:10:00	37.8	40.3	33.1	35.3	36.5	35.6	28.2	30	24.3	27	56	0
20:15:00	37.4	40	32.8	34.2	36.1	35.3	27.7	29.2	23.7	13	60	0
20:20:00	37	39.8	32.1	34.2	35.8	35	27.3	28.7	23.4	23	64	0
20:25:00	36.6	39.4	31.9	33.5	35.4	34.7	27.1	28.9	23.4	19	66	0
20:30:00	36.2	39.1	31.5	33.6	35	34.4	26.9	28.7	23.2	19	68	0
20:35:00	35.9	38.8	31.1	33.5	34.6	34.1	26.7	28.6	23.1	16	68	0
20:40:00	35.5	38.5	31	33.9	34.3	33.8	26.5	28	22.8	11	69	0
20:45:00	35.1	38.2	30.7	32.9	34	33.6	26.5	28	22.9	11	69	0
20:50:00	34.8	37.9	30.3	33	33.6	33.4	26.3	27.7	22.6	13	69	0
20:55:00	34.4	37.5	29.6	32.1	33.3	33.1	25.9	27.5	22.2	10	69	0
21:00:00	34.1	37.3	29.6	32	33	32.9	25.5	27	22.1	13	69	0
21:05:00	33.8	37	29.2	31.5	32.7	32.6	25.3	26.8	22	18	69	0
21:10:00	33.4	36.7	28.8	31.6	32.3	32.3	25	26.2	21.7	11	69	0
21:15:00	33.2	36.5	28.7	31.1	32.1	32.1	24.8	26.2	21.6	18	69	0
21:20:00	32.9	36.2	28.5	31	31.8	31.9	24.5	25.8	21.4	13	68	0
21:25:00	32.5	35.8	28	30.6	31.4	31.6	24.4	25.9	21.5	10	68	0
21:30:00	32.2	35.6	27.9	30.4	31.1	31.3	24.2	25.8	21.6	18	67	0
21:35:00	32	35.4	27.7	30.5	30.9	31.1	24.1	25.7	21.4	13	67	0
21:40:00	31.6	35.1	27.4	30.4	30.6	30.9	23.8	25.4	21.3	13	67	0
21:45:00	31.3	34.8	27	30.1	30.3	30.7	23.5	25.4	21.2	14	67	0
21:50:00	31.1	34.6	27.1	29.9	30.1	30.5	23.4	25.3	21.1	16	67	0
21:55:00	30.7	34.3	26.3	29.5	29.8	30.2	23.3	24.9	20.9	8	66	0
22:00:00	30.5	34.1	26.4	29.3	29.6	30.1	23.2	24.8	20.9	6	66	0
22:05:00	30.3	33.9	26.4	29.1	29.4	30	23.2	24.9	21	10	66	0
22:10:00	30	33.6	26.2	28.7	29.1	29.8	22.9	24.7	20.9	8	66	0
22:15:00	29.7	33.3	25.8	28.6	28.8	29.6	22.7	24.4	20.8	13	65	0
22:20:00	29.5	33.1	25.5	28.4	28.7	29.4	22.4	24	20.5	11	65	0
22:25:00	29.1	32.8	25.2	28.1	28.3	29.1	22.1	23.9	20.4	16	65	0
22:30:00	28.9	32.6	25	27.8	28.1	28.9	22	23.7	20.2	11	64	0
22:35:00	28.7	32.4	24.7	27.7	27.9	28.7	21.9	23.2	19.9	14	64	0
22:40:00	28.5	32.2	24.5	27.3	27.6	28.5	21.7	23.3	20.2	13	63	0
22:45:00	28.2	32	24.4	27.4	27.4	28.3	21.5	23.1	20	13	62	0
22:50:00	28	31.8	24.2	27.2	27.2	28.2	21.4	23.1	20	13	62	0
22:55:00	27.8	31.6	24	26.8	27	28	21.2	23	19.9	11	62	0
23:00:00	27.6	31.3	23.7	26.6	26.8	27.8	21	22.9	19.9	13	61	0
23:05:00	27.3	31.2	23.9	26.5	26.6	27.7	21	22.8	19.9	11	61	0
23:10:00	27.2	30.9	23.4	26.4	26.4	27.5	20.9	22.5	19.8	6	60	0
23:15:00	26.9	30.7	23.4	26.3	26.2	27.3	20.6	22.5	19.6	14	60	0
23:20:00	26.7	30.5	23	25.9	26	27.1	20.5	22.2	19.6	16	60	0
23:25:00	26.5	30.3	22.8	25.6	25.8	27	20.4	22.2	19.4	14	60	0
23:30:00	26.3	30.1	22.9	25.5	25.6	26.8	20.2	21.9	19.3	14	59	0
23:35:00	26.1	29.9	22.6	25.3	25.4	26.6	20.1	21.9	19.4	14	59	0
23:40:00	25.9	29.7	22.4	25.3	25.2	26.4	20	21.6	19.3	18	59	0
23:45:00	25.7	29.5	22.1	24.9	25	26.2	19.8	21.5	19.1	16	58	0
23:50:00	25.5	29.2	22	24.5	24.8	26.1	19.7	21.4	18.9	14	57	0
23:55:00	25.4	29.2	22.1	24.8	24.7	26	19.7	21.4	19.1	14	57	0
0:00:00	25.2	29	21.7	24.7	24.5	25.8	19.6	21.2	18.9	14	57	0

The recorded data of the 15th of March

Time	Water Temperature (°C)		Vapour Temperature (°C)		Basin Temperature (°C)		Cover Temperature (°C)		Ambient Temperature (°C)	Wind speed (km/hr)	Relative Humidity (%)	Solar intensity (W/m2)
	MSD	NSD	MSD	NSD	MSD	NSD	MSD	NSD				
6:00:00	15.2	18.3	14.2	15.7	15.1	17.3	13.4	15.1	16.2	13	70	5
6:05:00	15.1	18.2	14.2	15.6	15.1	17.3	13.5	15.2	16.3	6	70	7
6:10:00	15	18.1	14.4	15.7	15	17.1	13.5	15.2	16.4	18	70	11
6:15:00	15	18	14.3	15.8	15	17	13.7	15.4	16.5	13	71	18
6:20:00	15	18.1	14.5	16.1	15.1	17.1	13.8	15.6	16.7	16	71	28
6:25:00	15	18	14.5	16	15.1	17.1	13.9	15.7	16.8	16	71	42
6:30:00	14.9	17.9	14.6	16.1	15.1	17.1	14.2	15.8	16.9	10	72	56
6:35:00	14.9	17.9	14.6	16.2	15.2	17.1	14.4	16	17	14	72	72
6:40:00	15	18	14.7	16.2	15.2	17.2	14.4	16.1	17.3	16	72	91
6:45:00	14.9	17.8	14.7	16.1	15.1	17.1	14.6	16.2	17.3	11	72	113
6:50:00	14.9	17.9	14.8	16.5	15.3	17.3	14.8	16.4	17.6	18	72	91
6:55:00	14.9	17.9	14.9	16.5	15.3	17.3	14.9	16.6	17.8	13	72	26
7:00:00	14.9	17.8	14.9	16.5	15.3	17.3	14.9	16.6	17.9	16	72	181
7:05:00	14.9	17.8	15	16.4	15.3	17.4	15	16.7	18	14	72	206
7:10:00	15	17.8	15.2	16.6	15.5	17.4	15.4	16.9	18.1	8	72	158
7:15:00	15.1	17.8	15.4	18.3	15.5	17.5	16.9	19.1	18.2	14	72	197
7:20:00	15	17.9	15.8	21.3	15.5	17.5	18	20	18.2	19	71	265
7:25:00	15	18.1	18.6	22.8	15.6	17.8	18.7	20.8	18.3	16	71	285
7:30:00	15	18.2	19.5	24.8	16	18.1	19.1	21.3	18.5	11	71	304
7:35:00	15.3	18.4	21.1	26.2	16.4	18.6	19.5	21.6	18.6	18	71	323
7:40:00	15.6	18.6	23.6	26.6	16.8	19	19.9	21.9	18.9	16	71	343
7:45:00	16	18.9	24.4	27.5	17.2	19.4	20.3	22.6	19.5	13	71	360
7:50:00	16.7	19.2	25.1	28.8	17.8	19.8	20.7	22.9	19.7	16	71	373
7:55:00	17.3	19.6	25.6	31.3	18.4	20.1	20.9	23.3	19.7	14	71	385
8:00:00	17.9	19.9	26.4	31.8	19.1	20.6	21.2	23.6	20.1	24	71	32
8:05:00	18.6	20.3	27.3	32.4	19.8	21	21.5	23.9	20.2	14	71	33
8:10:00	19.3	20.8	28.2	32.9	20.4	21.5	21.9	24.1	20.2	16	70	53
8:15:00	20.1	21.2	29.1	33.8	21.1	22	22.3	24.8	20.7	18	68	469
8:20:00	20.8	21.6	29.5	34.7	21.8	22.3	22.7	25.1	21	23	67	483
8:25:00	21.5	22.1	29.9	35.2	22.5	22.7	22.8	25.1	20.7	23	67	504
8:30:00	22.2	22.5	30.9	35.8	23.2	23.2	23.2	25.5	21.2	21	66	522
8:35:00	23.1	23	31.3	36.6	24	23.6	23.7	26.2	21.6	14	67	540
8:40:00	23.8	23.4	32	37.2	24.7	24	24	26.4	21.4	13	67	555
8:45:00	24.6	23.8	32.8	37.4	25.3	24.4	24.2	26.5	21.6	23	66	571
8:50:00	25.3	24.3	33.5	38.2	26.1	24.8	24.6	27	21.3	10	67	584
8:55:00	26.1	24.8	34.2	38.9	26.8	25.3	25	27.5	22	8	66	601
9:00:00	26.9	25.2	34.6	39	27.6	25.7	25.3	27.7	21.8	23	67	615
9:05:00	27.7	25.7	34.8	39.5	28.3	26.1	25.6	28.2	22.8	19	66	631
9:10:00	28.5	26.2	35.7	40.1	29.2	26.6	26	28.7	22.2	14	66	647
9:15:00	29.4	26.7	36.7	40.6	30	27.1	26.4	28.9	22.9	13	66	663
9:20:00	30.2	27.2	37	41.1	30.7	27.5	26.7	29.3	23.2	21	66	673
9:25:00	31	27.6	38.1	41.9	31.6	27.9	27.6	30	23.6	16	66	691
9:30:00	31.8	28.1	38.3	42.1	32.3	28.4	27.5	29.8	23.1	18	67	700
9:35:00	32.6	28.6	39.1	42.6	33.1	28.9	27.7	29.9	22.7	21	67	714
9:40:00	33.6	29.2	39.4	43.2	33.9	29.4	27.9	29.9	23	24	67	728
9:45:00	34.4	29.6	40	43.4	34.5	29.7	28.2	30.3	23.1	16	67	740
9:50:00	35.3	30.3	39.9	43.7	35.3	30.2	28.5	30.2	22.8	21	66	752
9:55:00	35.9	30.7	41	44.1	36	30.5	28.8	30.6	23.3	11	66	763
10:00:00	36.8	31.2	41.6	44.6	36.8	30.9	29.3	31.2	23.7	23	66	770
10:05:00	37.6	31.7	42.6	45	37.5	31.4	29.5	31.7	24.3	27	66	782
10:10:00	38.4	32.3	42.9	45.5	38.3	31.9	30.2	32.2	24.2	14	66	791
10:15:00	39.3	32.8	43.8	45.8	39	32.3	30.5	32.2	24.3	14	66	803
10:20:00	40	33.3	44.6	46.2	39.9	32.8	30.9	33.1	25.1	14	65	812
10:25:00	40.8	33.9	45.2	46.7	40.6	33.4	31.2	33.3	25.2	13	65	823
10:30:00	41.6	34.3	45.9	47.3	41.5	33.9	31.6	34.1	25.4	14	65	831
10:35:00	42.4	34.8	46.7	48.3	42.3	34.4	32.3	35.3	27.2	18	64	837
10:40:00	43.2	35.3	47.8	48.9	43.1	35.1	32.4	34.6	25.8	29	64	846
10:45:00	44	36	48	49.2	43.8	35.7	32.5	34.4	25.7	18	64	851
10:50:00	44.9	36.5	48.5	49.7	44.5	36.2	33.3	35.6	27.6	8	65	858
10:55:00	45.7	37	49.3	50.3	45.3	36.6	33	35.1	25.5	5	65	863
11:00:00	46.6	37.7	49.7	50.6	46.1	37.2	33.8	36.1	26.9	14	65	870
11:05:00	47.2	38.2	49.7	50.6	46.7	37.5	33.9	35.7	26.1	24	65	410
11:10:00	48	38.7	51	51.2	47.5	38.1	34.5	36.5	26.7	18	67	877
11:15:00	48.7	39.2	51.2	51	48	38.4	34.5	36.1	26.5	11	66	879
11:20:00	49.4	39.8	52.6	51.5	48.8	38.8	35.2	36.5	26.4	19	66	886
11:25:00	50.2	40.4	47.7	51.8	49.4	39.3	35.3	36.6	26	18	67	889
11:30:00	50.8	40.9	51.2	52.3	50.1	39.7	35.4	37.3	27	18	67	904
11:35:00	51.4	41.3	53.2	52.5	50.6	40.1	35.8	37.6	26.8	14	66	896
11:40:00	52.1	41.8	53.9	52.2	51.2	40.5	36.1	37.9	27.3	13	66	904
11:45:00	52.7	42.4	54.3	52.1	51.3	40.8	35.9	36.6	25.5	8	66	902
11:50:00	53.4	42.9	54.7	54	52.2	41.1	36	37.2	25.6	6	65	904
11:55:00	53.8	43.4	55.2	53.5	52.6	41.3	36.8	37.9	26.6	14	65	902
12:00:00	54.3	43.8	56	53.8	53.2	41.6	37.1	38.5	27.1	14	65	900
12:05:00	54.9	44.2	56.7	54.4	53.9	42	37.9	40.3	28.7	11	64	905
12:10:00	55.3	44.6	57	54.5	54.4	42.6	38	40.1	29	14	61	900

Time	Water Temperature (°C)		Vapour Temperature (°C)		Basin Temperature (°C)		Cover Temperature (°C)		Ambient Temperature (°C)	Wind speed (km/hr)	Relative Humidity (%)	Solar intensity (W/m2)
	MSD	NSD	MSD	NSD	MSD	NSD	MSD	NSD				
12:15:00	55.9	45	57.4	54.6	54.9	43	38.2	39.6	27.4	18	62	902
12:20:00	56.4	45.5	57.9	54.6	55.2	43.3	38.7	39.4	27.3	11	61	900
12:25:00	56.8	45.9	57.6	54.6	55.3	43.5	38.2	38.7	27.3	19	60	896
12:30:00	57.2	46.3	58.5	55	55.9	43.5	39	40.2	28.3	11	59	896
12:35:00	57.8	46.6	59.5	55.2	56.4	43.6	38.7	39.9	27.3	16	61	893
12:40:00	58.1	47.1	59	55.1	56.7	43.9	38.5	39.7	27.5	18	61	889
12:45:00	58.5	47.5	60.5	55.2	57.2	44.2	39.2	40.5	28.2	14	61	886
12:50:00	58.9	47.8	60.7	55.8	57.5	44.4	39.9	42	29.3	2	60	884
12:55:00	59.1	48.2	60.2	55.3	57.8	44.8	39.4	40.7	26.9	21	58	882
13:00:00	59.6	48.5	60.3	55.5	58.1	45.2	40	41.3	29.2	19	59	870
13:05:00	59.8	48.8	60.7	56	58.4	45.4	40.1	40.8	28.2	11	57	867
13:10:00	60.1	49.2	60.5	56.2	58.4	45.6	40.7	40.5	28.3	13	57	861
13:15:00	60.3	49.4	60.9	56	58.7	45.7	40.7	41.6	29.1	10	56	853
13:20:00	60.6	49.8	60.7	56.1	59.1	45.9	40.1	41.7	27.4	16	56	846
13:25:00	60.7	50.1	60.9	56	59.3	46.1	40.8	42.1	29.6	18	57	837
13:30:00	61	50.4	61.6	56.3	59.6	46.4	41.1	43.3	30.1	23	57	831
13:35:00	61.2	50.5	61.4	56.2	59.8	46.7	40.5	42.9	30.3	6	56	821
13:40:00	61.4	50.9	61.6	56.3	59.9	47	41.2	43.3	30.1	10	54	817
13:45:00	61.2	51	61.6	56.1	60	47.3	41.1	43.2	29	13	54	805
13:50:00	61.6	51.2	61.8	55.9	60.2	47.5	41.1	42.6	29.5	14	54	798
13:55:00	61.8	51.5	61.3	56.1	60.3	47.6	41.5	42.5	29	11	53	786
14:00:00	62	51.7	61.6	56.1	60.5	47.8	42.1	43.2	30.3	16	52	779
14:05:00	61.9	51.8	61.2	55.8	60.5	47.9	41.5	43.2	30	3	53	766
14:10:00	62	52	61.1	55.3	60.4	48	41	42	28.6	14	52	758
14:15:00	62.1	52.3	61.1	55.6	60.5	48.1	41.6	42.9	29.7	3	53	745
14:20:00	62	52.3	60.9	56.2	60.5	48	42.2	43.5	30.8	18	53	733
14:25:00	61.9	52.5	60.6	55.5	60.5	48.1	40.8	42.6	28.6	16	53	721
14:30:00	62	52.6	60.5	55.1	60.4	48.1	40.7	41.9	29.1	16	52	707
14:35:00	61.8	52.7	60.3	55	60.2	48.1	41.4	42.6	29.9	18	52	694
14:40:00	61.8	52.7	60.1	54.8	60.1	48	40.5	41.3	27.8	21	53	682
14:45:00	61.6	52.8	59.6	54.8	60	47.9	40.9	42.4	29.2	5	53	664
14:50:00	61.5	52.9	59.8	55.1	59.9	47.8	41.4	43.1	30.1	16	53	650
14:55:00	61.4	52.9	59.2	54.7	59.8	47.9	41.1	42.9	29.8	8	53	635
15:00:00	61.1	53	58.9	54.7	59.7	48.1	40.9	42.6	29.2	13	52	621
15:05:00	60.8	53	58.4	54.7	59.4	48	40.9	42.1	29.4	26	52	606
15:10:00	60.6	53.1	58.3	54.8	59.1	48	40.5	42.3	28.9	19	51	596
15:15:00	60.4	53.1	57.4	53.6	58.9	48	41.2	41.9	29.6	10	51	580
15:20:00	60	53.1	57.2	53.8	58.5	47.8	40.4	41.1	28.3	18	52	561
15:25:00	59.6	53.1	56.7	54	58.2	47.7	39.9	40.7	28.1	21	53	540
15:30:00	59.3	53	56.2	54.3	57.9	47.6	40.2	41	28.1	21	53	524
15:35:00	59	53	55.8	53.9	57.5	47.5	39.8	40.1	27.8	21	52	508
15:40:00	58.8	52.9	55.5	53.7	57.2	47.4	40	40.4	28.4	18	53	492
15:45:00	58.5	52.7	55.4	53.3	56.8	47.1	39.4	40.1	27.7	23	54	475
15:50:00	58.2	52.5	55.3	53.1	56.5	46.9	39.4	40.2	27.6	21	55	459
15:55:00	57.9	52.2	55	52.7	56.1	46.6	39.1	39.4	27.1	13	55	438
16:00:00	57.5	51.9	54.5	53.2	55.9	46.4	39.4	40.3	28.2	13	56	420
16:05:00	57.1	51.6	54.2	52.3	55.5	46.1	38.7	39.9	27.9	11	57	401
16:10:00	56.7	51.3	53.6	52	55.2	45.9	38.8	39.6	27.3	23	56	385
16:15:00	56.3	51	53.4	51.9	54.9	45.6	38.5	39.3	27.3	18	56	366
16:20:00	56.1	50.7	53.3	51.6	54.6	45.3	38.9	40.1	28.2	24	56	350
16:25:00	55.8	50.4	53.1	51	54.3	44.9	37.9	39.2	27.2	13	56	330
16:30:00	55.7	50.7	52.9	50.6	54	44.6	38.4	38.8	27.8	16	56	313
16:35:00	55.9	51.2	53	50.7	53.9	44.5	38.3	39.4	28	13	57	292
16:40:00	55.9	51.3	53.2	50.7	53.9	44.8	37.8	38.7	27.4	16	56	272
16:45:00	55.7	51.4	53	50.3	53.8	44.9	37.3	38.3	27	21	56	251
16:50:00	55.5	51.1	51.9	46.4	53.5	44.9	35.9	37.3	26.7	19	56	237
16:55:00	54.7	50.4	49.2	45.7	52.6	44.3	35	36.6	26.7	14	56	221
17:00:00	53.7	49.9	48.6	44.7	51.6	43.8	34.4	36.8	26.7	19	56	202
17:05:00	52.8	49.4	47	44.2	50.7	43.3	34.3	36.2	26.9	21	56	186
17:10:00	51.7	48.8	46.2	43.7	49.8	42.7	34.6	36.2	26.4	18	55	165
17:15:00	50.9	48.3	45.3	43	48.8	42.2	33.4	34.9	25.6	5	55	144
17:20:00	50.1	47.8	44.5	42.5	48.1	41.7	33.1	35	25.8	18	55	123
17:25:00	49.4	47.4	43.6	41.8	47.3	41.4	32.6	34.5	25.9	14	55	102
17:30:00	48.6	46.9	43.1	41.2	46.7	41.1	32.6	34.1	25.5	19	55	86
17:35:00	47.8	46.4	42	41	45.9	40.5	32	33.5	24.9	24	56	69
17:40:00	47	46	41.5	40.4	45.3	40.2	32	33.4	25.1	18	56	53
17:45:00	46.4	45.6	40.6	39.7	44.6	39.8	31.4	32.9	24.9	14	56	39
17:50:00	45.7	45.1	40.1	39.3	43.9	39.4	30.9	32	24.3	16	56	28
17:55:00	45.1	44.7	39.6	38.9	43.3	39.2	30.8	32.3	24.5	14	57	19
18:00:00	44.5	44.4	39	38.5	42.8	38.8	30.5	32	24.3	18	58	16
18:05:00	43.9	43.9	38.3	38.1	42.1	38.5	30.2	32	24.1	11	58	12
18:10:00	43.2	43.5	37.8	37.6	41.5	38.1	29.9	31.7	24.1	14	58	9
18:15:00	42.7	43.2	37.3	37.8	41	37.9	29.6	31.5	24	8	58	5
18:20:00	42.1	42.8	36.9	37	40.5	37.5	29.4	31	23.5	13	59	0
18:25:00	41.6	42.4	36	36.7	40	37.2	29.2	30.5	23.4	11	60	0
18:30:00	41	42.1	35.9	36.7	39.5	37	29.2	30.6	23.7	10	60	0
18:35:00	40.5	41.7	35.6	36.1	38.9	36.6	28.7	29.9	23	13	60	0
18:40:00	39.9	41.4	34.8	35.8	38.5	36.3	28.4	29.9	23.1	11	61	0
18:45:00	39.4	41	34.8	35.1	38	36	28.4	29.8	23.4	10	61	0

Time	Water Temperature (°C)		Vapour Temperature (°C)		Basin Temperature (°C)		Cover Temperature (°C)		Ambient Temperature (°C)	Wind speed (km/hr)	Relative Humidity (%)	Solar intensity (W/m2)
	MSD	NSD	MSD	NSD	MSD	NSD	MSD	NSD				
18:50:00	39	40.7	34	35.4	37.5	35.7	27.9	29.1	23	14	61	0
18:55:00	38.6	40.5	33.4	34.9	37.1	35.5	27.7	28.7	22.8	6	62	0
19:00:00	38	40.1	33.1	34.3	36.7	35.1	27.3	28.4	22.6	11	62	0
19:05:00	37.6	39.9	32.5	34.2	36.3	34.9	27.1	28.5	22.7	10	62	0
19:10:00	37.2	39.5	32.4	34.2	35.9	34.7	26.9	28	22.5	11	63	0
19:15:00	36.8	39.3	32.2	33.8	35.5	34.4	26.8	28.5	22.7	11	63	0
19:20:00	36.4	38.9	31.8	33.8	35.1	34.3	26.7	28.4	22.7	10	63	0
19:25:00	35.9	38.7	31	33.6	34.8	34.1	26.5	28	22.4	11	64	0
19:30:00	35.6	38.4	31	32.9	34.4	33.9	26.1	27.7	22.4	10	64	0
19:35:00	35.2	38.1	30.5	33	34	33.7	26	27.4	22.1	14	64	0
19:40:00	34.9	37.9	30.2	32.4	33.7	33.4	25.6	26.9	21.7	13	65	0
19:45:00	34.5	37.6	29.9	32.3	33.3	33.1	25.3	26.8	21.6	13	65	0
19:50:00	34.2	37.4	29.5	32	33	32.9	25.2	26.5	21.5	11	66	0
19:55:00	33.8	37.1	29	32	32.6	32.6	24.9	26.3	21.3	16	66	0
20:00:00	33.3	36.8	29	31.5	32.3	32.4	24.7	26.2	21.4	10	66	0
20:05:00	33.1	36.6	28.9	31.1	32	32.1	24.5	25.7	21.2	13	66	0
20:10:00	32.7	36.2	28.1	31.1	31.6	31.9	24.4	25.8	21.4	13	66	0
20:15:00	32.4	36.1	28.2	31.2	31.4	31.8	24.3	25.6	21.3	8	67	0
20:20:00	32.1	35.8	27.8	30.9	31.1	31.6	24.2	25.5	21.2	13	67	0
20:25:00	31.8	35.6	27.5	30.2	30.7	31.4	23.8	25.4	21	13	67	0
20:30:00	31.5	35.4	27.4	29.9	30.5	31.3	23.7	25.2	20.9	11	67	0
20:35:00	31.1	35.1	26.9	30	30.2	31.1	23.3	25.2	21	11	67	0
20:40:00	30.8	34.9	26.6	29.9	29.9	30.8	23.2	25.1	20.9	11	67	0
20:45:00	30.6	34.7	26.1	29.5	29.6	30.7	23	24.5	20.6	13	68	0
20:50:00	30.3	34.5	26	29.4	29.4	30.5	22.8	24.2	20.5	10	68	0
20:55:00	29.9	34.1	25.9	29.3	29	30.2	22.6	24.4	20.7	13	68	0
21:00:00	29.7	34	25.5	28.5	28.8	30.1	22.6	24.3	20.4	14	68	0
21:05:00	29.4	33.8	25.1	28.7	28.6	30	22.5	24.3	20.5	11	68	0
21:10:00	29.1	33.5	25.1	28.2	28.2	29.7	22.1	24.1	20.3	8	68	0
21:15:00	28.9	33.3	24.9	28.3	28	29.5	22.2	23.7	20.1	11	68	0
21:20:00	28.6	33.1	24.5	28.1	27.8	29.4	22	23.6	20.3	11	68	0
21:25:00	28.4	32.9	24.4	28	27.5	29.2	21.9	23.9	20.7	10	68	0
21:30:00	28.1	32.7	24.1	27.7	27.3	29.1	21.7	23.9	20.4	10	68	0
21:35:00	27.9	32.5	24	27.9	27.1	29	21.5	23.5	20.1	10	68	0
21:40:00	27.7	32.3	23.9	27.6	26.9	28.8	21.4	23.4	20.2	10	69	0
21:45:00	27.4	32.1	23.6	27	26.6	28.6	21.1	23.3	20.1	11	69	0
21:50:00	27.1	31.9	23.4	26.8	26.4	28.5	21	23.2	20.2	10	70	0
21:55:00	26.9	31.7	23	26.9	26.2	28.4	20.8	23.1	20.3	8	71	0
22:00:00	26.7	31.5	23	26.6	25.9	28.2	20.7	22.8	19.9	6	71	0
22:05:00	26.5	31.3	22.8	26.3	25.8	28	20.5	22.9	19.6	11	72	0
22:10:00	26.2	31.1	22.6	26.3	25.6	27.9	20.4	22.5	19.7	10	72	0
22:15:00	26	30.9	22.3	26.3	25.3	27.7	20.3	22.5	19.2	10	72	0
22:20:00	25.8	30.8	22.1	26.2	25.1	27.5	20.2	22	19.1	8	72	0
22:25:00	25.5	30.5	21.9	25.4	24.9	27.4	20.1	21.7	19	10	71	0
22:30:00	25.5	30.5	21.9	25.4	24.8	27.3	20	21.7	19.1	10	71	0
22:35:00	25.2	30.2	21.5	25.5	24.5	27	19.8	21.6	18.9	11	70	0
22:40:00	24.9	30	21.4	25	24.3	26.8	19.6	21.7	19	8	69	0
22:45:00	24.8	29.9	21.3	25.4	24.2	26.8	19.6	21.6	19	14	68	0
22:50:00	24.6	29.7	21	25	24	26.6	19.5	21.5	19	13	67	0
22:55:00	24.3	29.5	20.8	24.5	23.8	26.4	19.2	21.3	19	13	65	0
23:00:00	24.2	29.4	21	24.4	23.7	26.4	19.2	21.2	19.1	14	64	0
23:05:00	24	29.2	20.8	24.4	23.4	26.2	19.1	21	18.9	13	62	0
23:10:00	23.8	29	20.5	24.1	23.3	26	18.9	20.9	19	16	60	0
23:15:00	23.6	28.8	20.4	24.1	23.2	25.8	18.9	20.6	18.8	13	59	0
23:20:00	23.5	28.7	20.3	24.1	23	25.8	18.8	20.7	19	18	57	0
23:25:00	23.3	28.5	20.2	23.9	22.8	25.6	18.6	20.5	18.8	13	55	0
23:30:00	23.1	28.3	19.8	23.8	22.7	25.5	18.6	20.4	18.8	18	54	0
23:35:00	23	28.2	20	23.7	22.5	25.4	18.5	20.4	18.7	11	53	0
23:40:00	22.8	28	19.5	23	22.3	25.2	18.3	20.2	18.7	13	52	0
23:45:00	22.7	27.9	19.6	23.4	22.2	25.1	18.3	20.1	18.6	14	51	0
23:50:00	22.5	27.7	19.4	23	22.1	25	18.2	20.1	18.6	8	50	0
23:55:00	22.4	27.6	19.4	23.2	21.9	24.9	18.1	20	18.5	9	51	0
0:00:00	22.2	27.4	19.2	22.8	21.8	24.7	18	19.9	18.5	10	52	0

The recorded data of the 11th of April 2018

Time	Water Temperature (°C)		Vapour Temperature (°C)		Basin Temperature (°C)		Cover Temperature (°C)		Ambient Temperature (°C)	Wind speed (km/hr)	Relative Humidity (%)	Solar intensity (W/m2)
	MSD	NSD	MSD	NSD	MSD	NSD	MSD	NSD				
6:00:00	15.8	18.9	14.9	16.2	15.8	17.8	14	15.3	15.6	14	8	0
6:05:00	15.8	18.8	14.9	16.1	15.7	17.7	13.8	15.2	15.5	19	7	0
6:10:00	15.8	18.8	14.8	16.1	15.7	17.7	13.9	15.2	15.6	13	7	0
6:15:00	15.7	18.7	14.8	16	15.6	17.6	13.7	15.1	15.5	18	7	5
6:20:00	15.7	18.7	14.9	16.1	15.6	17.5	13.9	15.1	15.6	27	8	9
6:25:00	15.6	18.6	14.6	16	15.5	17.4	13.8	15.1	15.6	19	11	14
6:30:00	15.5	18.5	14.8	16	15.5	17.4	13.7	15.2	15.8	24	14	19
6:35:00	15.5	18.5	14.8	16	15.5	17.4	13.7	15.2	15.8	19	19	21
6:40:00	15.5	18.4	14.7	16	15.5	17.4	13.8	15.3	15.8	26	23	32
6:45:00	15.5	18.4	14.8	16.2	15.5	17.4	13.8	15.3	15.9	24	30	53
6:50:00	15.5	18.3	14.8	16	15.5	17.3	13.7	15.4	16	23	40	58
6:55:00	15.5	18.3	14.8	16.2	15.5	17.3	13.7	15.5	16.1	37	49	69
7:00:00	15.4	18.3	14.8	16.2	15.5	17.3	13.7	15.6	16.2	21	56	104
7:05:00	15.4	18.1	14.7	16.2	15.4	17.2	13.6	15.6	16.2	11	60	121
7:10:00	15.4	18.2	14.9	16.2	15.5	17.3	13.7	15.7	16.2	23	61	144
7:15:00	15.4	18.1	14.8	16.2	15.5	17.3	13.9	15.7	16.2	19	63	165
7:20:00	15.5	18.1	14.8	16.3	15.6	17.3	14.1	15.9	16.4	23	64	188
7:25:00	15.4	18.1	14.8	16.3	15.6	17.3	14.2	15.9	16.5	21	67	211
7:30:00	15.5	18.1	14.7	16.3	15.6	17.4	14.4	16	16.6	18	68	230
7:35:00	15.6	18.1	15	16.5	15.7	17.4	14.5	16.2	16.7	18	69	251
7:40:00	15.5	18	14.9	16.6	15.7	17.3	14.6	16.2	16.7	26	69	267
7:45:00	15.6	18	15.1	16.6	15.7	17.4	14.7	16.4	16.8	23	70	287
7:50:00	15.5	18	15.1	16.6	15.7	17.4	14.9	16.4	17	18	70	306
7:55:00	15.6	17.9	15.2	16.9	15.8	17.4	15	16.6	17.2	16	71	322
8:00:00	15.7	18	15.3	17	15.9	17.4	15.2	16.8	17.5	21	72	339
8:05:00	15.7	18	15.6	17.3	16	17.5	15.9	17	17.5	11	72	359
8:10:00	15.7	18.1	16	18.1	16.1	17.5	17.2	17.4	17.8	31	72	376
8:15:00	15.8	18.1	18.4	20.2	16.2	17.5	17.9	18.3	17.9	21	71	388
8:20:00	16.1	18.4	20.4	22.6	16.5	17.7	18.6	20.6	18.1	27	72	406
8:25:00	16.6	18.6	23.7	27.3	17.1	17.9	19.1	21.3	18	19	72	424
8:30:00	17	18.9	24.4	28.8	17.8	18.2	19.3	21.5	18	24	72	441
8:35:00	17.5	19.2	25	29.7	18.6	18.8	19.9	22.4	18.5	26	72	464
8:40:00	17.9	19.5	25.5	29.7	19	19.5	20.3	22.7	18.8	31	72	490
8:45:00	18.4	19.8	26.3	30.3	19.6	20.2	20.3	22.5	18.2	37	72	517
8:50:00	19	20.2	25.9	30.1	20.2	20.8	20.2	22	18.4	29	72	114
8:55:00	19.7	20.3	22.6	25.3	20.4	21.3	19.5	20.7	18.1	23	72	114
9:00:00	20.2	20.8	26.4	29.8	21	21.4	20.4	22.2	18.7	34	72	151
9:05:00	20.9	21	24	26.5	21.4	21.6	19.8	20.9	18.5	29	72	214
9:10:00	21.3	21.3	25.8	28.8	21.9	21.7	21	22.3	19	21	72	232
9:15:00	21.8	21.4	23.1	25.1	22.1	21.8	20.4	20.8	18.5	37	72	214
9:20:00	22.2	21.7	26.8	29.5	22.3	21.7	21	22.4	18.8	27	72	214
9:25:00	22.4	22	26.6	28.9	22.8	21.8	21	22.3	18.7	32	72	700
9:30:00	22.9	22.3	26	28.3	23.4	22.2	20.6	21.7	19	23	72	169
9:35:00	23.2	22.6	29.9	32.9	23.5	22.4	21.7	23	19.1	32	72	677
9:40:00	23.7	23	32.8	35.8	24.5	22.9	23.1	24.6	19.8	27	72	339
9:45:00	24.6	23.1	27.8	29.9	25.3	23.5	22	23.1	19.4	26	71	737
9:50:00	25.3	23.8	33.8	35.7	26	24	23.1	25.3	20.5	23	70	262
9:55:00	26.1	23.8	25.9	26.5	26.2	24.4	21	22.3	19.3	42	70	816
10:00:00	26.5	24	29.7	29.6	26.4	24.2	22.3	23.2	19.6	31	69	199
10:05:00	26.9	24.5	33.2	34.4	27.1	24.1	22.7	25	21	27	69	780
10:10:00	27.5	24.5	28.1	28.1	27.5	24.4	21.4	22.8	20	21	69	777
10:15:00	27.9	24.4	29.9	27.3	27.8	24.4	21.3	23.4	21.5	23	68	861
10:20:00	28.3	24.6	27.5	28.3	28.2	24.3	21.4	23.5	20.8	35	68	768
10:25:00	28.4	24.9	28.8	31.3	28.2	24.3	23.4	24.8	21.4	31	65	752
10:30:00	28.4	25.2	29.6	35.7	28.4	24.4	24.6	25.8	21.8	13	66	754
10:35:00	28.5	25.5	30.9	34.3	28.5	25	23.3	25.7	21.6	23	66	817
10:40:00	29.2	25.7	33	31	29.3	25.6	22.5	24.8	20.8	14	67	802
10:45:00	30.2	25.9	31.2	29	30.1	26	21.9	24.1	21	32	66	770
10:50:00	30.4	26	30.5	30.7	30.3	26	23	25.4	22.7	39	66	311
10:55:00	30.8	26.3	30.7	32	30.5	26.1	24.1	25	21.7	31	65	223
11:00:00	31	26.5	30.9	33	30.7	26.2	24.8	26	21.4	14	66	301
11:05:00	31.5	26.6	30.1	26.6	30.8	26.3	23.2	24.2	21	13	65	302
11:10:00	31.6	26.7	30.2	27	30.9	26.2	23.3	23.9	20.9	13	65	919
11:15:00	31.5	27.2	36.3	32.9	31.2	25.9	25.8	27.4	22.4	26	64	831
11:20:00	31.9	27.6	37	36.6	32	26.5	27	28.9	23	19	64	135
11:25:00	32.6	28.1	37.8	37.4	33	27.4	27.4	28.6	21.9	42	65	246
11:30:00	33.5	28.2	32.7	31.1	33.4	28.4	24.9	25.8	20.7	26	66	895
11:35:00	33.9	28.9	38.2	37.5	33.9	28.6	27.4	29.3	22.9	24	65	524
11:40:00	34.8	29.2	34.3	34.2	34.8	29.2	26.2	27.2	21.3	34	65	554
11:45:00	35.5	29.4	32.9	31.3	35	29.6	24.8	25.8	20.9	21	61	918
11:50:00	35.5	29.8	39	41.3	35.2	29.4	27.7	29.4	23.3	19	61	1072
11:55:00	36.2	30.5	41.2	44.1	36.3	29.7	29.8	30.9	23.8	34	59	1072
12:00:00	37.1	31	40.1	42.3	37.3	30.5	30.1	30.9	23.8	24	56	1039
12:05:00	38	31.2	40.6	41.5	37.6	31.2	30.4	31.5	24.1	31	56	1046
12:10:00	38.4	31.9	43.3	45.8	38.6	31.5	31.7	32.9	24.5	32	57	1067

Time	Water Temperature (°C)		Vapour Temperature (°C)		Basin Temperature (°C)		Cover Temperature (°C)		Ambient Temperature (°C)	Wind speed (km/hr)	Relative Humidity (%)	Solar intensity (W/m2)
	MSD	NSD	MSD	NSD	MSD	NSD	MSD	NSD				
12:15:00	39.6	32.2	38.8	38.3	39.6	32.3	29.4	29.8	22.7	34	57	1046
12:20:00	40	32.8	44.7	47.5	39.9	32.5	32.1	33.3	24.4	29	56	888
12:25:00	41.1	33.5	44.8	47.1	41	33.1	32.9	33.7	24.4	11	56	870
12:30:00	41.8	33.9	45.3	46.4	41.9	33.8	32.2	33.2	23.7	26	55	988
12:35:00	42.8	34.7	46.3	46.3	42.6	34.4	32	33.1	23.7	32	55	281
12:40:00	43.7	35	42.4	41.2	43.4	35	30.6	31.6	23.7	34	55	826
12:45:00	44.2	35.4	43.1	41	43.4	35.1	30.2	31.5	23.8	21	55	823
12:50:00	44.7	35.9	45.7	44.9	43.9	34.9	31.8	33.6	24.9	31	54	197
12:55:00	45.2	36.2	46.8	45.8	44.6	35	32.5	34.1	25.3	18	53	833
13:00:00	45.7	36.5	44.8	42.2	44.7	35.5	30.6	31.8	23.4	29	53	884
13:05:00	46.1	36.9	47	45.3	45.2	35.5	31.6	33	24.4	8	53	237
13:10:00	46.8	37.2	43	38.5	45.7	35.9	29.2	30.5	23.2	14	54	253
13:15:00	46.9	37.4	44.2	39.5	45.5	35.8	29.6	31	23.8	29	52	793
13:20:00	46.9	37.5	44.2	39.9	45.1	35.5	29.4	30.6	23.3	14	54	795
13:25:00	46.6	37.5	46.7	44	45.3	34.9	31.4	32.6	25.3	26	51	842
13:30:00	46.7	37.6	47.6	45.6	45.8	34.9	32.7	34.1	25.3	29	50	861
13:35:00	47.1	37.9	48.3	47	46.4	35.5	33.6	35.1	25.7	24	49	942
13:40:00	47.5	38.4	49.3	48.9	47	36.1	34.6	35.7	25.9	16	49	362
13:45:00	48.4	38.8	47.2	44.1	47.7	37	32.7	33.4	24.5	23	51	311
13:50:00	48.9	39.2	45.6	40.5	47.6	37.6	30.8	31.5	23.8	19	50	269
13:55:00	49	39.3	46.5	42.6	47.6	37.3	31.3	32	24.5	21	50	691
14:00:00	48.9	39.4	47.2	43.2	47.6	37	31.8	33.1	24.9	23	51	701
14:05:00	49	39.6	48	44.6	47.8	36.8	32.1	33.3	24.4	35	51	694
14:10:00	49.2	39.7	47.8	44.2	47.8	36.9	31.9	33	24.3	26	51	728
14:15:00	49.5	39.9	48	45.1	48.2	37.1	32.5	34.2	25.5	24	50	158
14:20:00	50.1	40.3	46.1	40.4	48.7	37.8	30.7	32.3	23.9	21	52	652
14:25:00	49.6	40.3	47.3	43.9	48.3	37.5	32	33.4	25.2	18	52	643
14:30:00	49.8	40.4	47.4	43.5	48.5	37.6	31.8	33.3	25.1	23	52	626
14:35:00	49.9	40.5	47.3	43.7	48.6	37.6	32.1	33.1	24.1	16	53	677
14:40:00	49.9	40.7	47.4	43.8	48.7	37.8	32.1	33.3	24.8	26	52	642
14:45:00	50.2	41	47.7	44	49.1	38.1	32.7	33.5	25.2	27	52	659
14:50:00	50.1	41.1	48.2	45.6	49	38.3	33	33.8	24.8	24	54	668
14:55:00	50.4	41.4	48.8	47	49.3	38.5	33.6	34.1	24.9	11	54	243
15:00:00	50.5	41.6	49	47.3	49.5	38.7	33.4	33.9	24.3	29	54	123
15:05:00	50.8	41.9	48.1	45.1	49.3	38.9	32.1	33.2	24.6	16	54	592
15:10:00	50.9	42.1	45.6	39.4	49.3	38.9	29.7	31.1	23.3	21	54	114
15:15:00	50.5	42	46.2	41.9	48.7	38.5	30.7	31.3	24.2	8	56	237
15:20:00	50.3	41.9	45.7	40.6	48.2	38.1	30	30.9	23.3	37	57	190
15:25:00	49.6	41.7	47.8	44.6	48	37.6	32.8	33.4	25.2	35	58	86
15:30:00	49.8	41.7	44.8	39.2	47.9	37.6	30.6	31.3	23.9	32	60	406
15:35:00	49.2	41.5	43.4	37	47.2	37.4	28.8	30.1	23.2	29	59	485
15:40:00	48.3	40.9	45.2	43.3	46.5	36.8	30.2	31	23.9	23	59	283
15:45:00	47.6	40.6	46.2	45.1	46.5	36.6	31.8	32.1	24.8	13	59	90
15:50:00	48.3	41.2	43.5	39	46.8	37.1	30.2	31.1	23.9	21	60	46
15:55:00	48	41.1	42.4	36.9	46.2	37.2	29.3	30	22.9	23	61	332
16:00:00	47.5	40.9	41.3	35.7	45.4	36.9	27.8	28.9	22.4	13	61	329
16:05:00	46.3	39.8	43.5	42.5	44.8	36	29.2	30.3	23.5	32	62	60
16:10:00	46.1	39.8	41.5	38	44.7	36	28.9	29.2	23	23	62	49
16:15:00	46.1	40.3	39.9	35.4	44.3	36.1	27.5	28.6	22.3	24	62	232
16:20:00	45.4	39.7	41	38.6	43.6	35.7	27.6	29	22.5	27	61	214
16:25:00	44.9	39.5	41.9	37.6	43.4	35.3	27	28.4	22.4	24	61	200
16:30:00	44.6	39.6	39.5	37.9	43.1	35.2	27.8	28.8	22.7	24	60	190
16:35:00	44.4	39.4	39.9	35.5	42.7	34.9	27.6	28.7	22.9	29	60	190
16:40:00	43.8	39.1	38.3	34.7	42.2	34.6	26.8	28.2	22.5	31	59	162
16:45:00	43	38.7	37.2	34.3	41.4	34.2	26.5	28	22.5	24	59	130
16:50:00	42.5	38.4	37	33.9	40.8	34	26.1	27.8	22.4	23	59	63
16:55:00	41.9	38.1	36.1	33.2	40.3	33.6	25.8	27.7	22.6	18	60	83
17:00:00	41.3	37.8	35.3	32.8	39.7	33.4	25.4	27.1	22	19	60	67
17:05:00	40.7	37.5	34.8	32.4	39.1	33.1	25.1	26.5	21.7	24	60	51
17:10:00	40.2	37.2	34.3	31.9	38.5	32.8	24.7	26.2	21.5	19	60	39
17:15:00	39.6	36.9	33.9	31.4	38.1	32.6	24.6	26.1	21.4	24	60	30
17:20:00	39.1	36.6	33.4	31.3	37.6	32.4	24.2	26	21.4	29	60	28
17:25:00	38.5	36.3	32.9	31.1	37	32	23.9	25.5	21.2	23	61	26
17:30:00	37.9	35.9	32.3	30.8	36.5	31.6	24	25.5	21.1	21	60	16
17:35:00	37.5	35.7	31.8	30.5	36	31.4	23.9	25.1	20.9	26	61	11
17:40:00	37	35.4	31.1	29.8	35.6	31.2	23.3	24.9	20.8	19	61	5
17:45:00	36.5	35.1	30.9	29.7	35.1	31	23	24.6	20.6	31	62	0
17:50:00	36	34.9	30.6	29.9	34.7	30.8	22.9	24.6	20.6	18	63	0
17:55:00	35.7	34.6	30.2	29	34.2	30.5	22.8	24.1	20.3	31	63	0
18:00:00	35.2	34.3	29.6	28.9	33.9	30.3	22.6	24.2	20.3	13	64	0
18:05:00	34.7	34.1	29.4	28.9	33.3	30	22.3	23.8	20.1	13	64	0
18:10:00	34.3	33.8	29.1	28.5	32.9	29.9	22.1	23.7	20	24	65	0
18:15:00	33.9	33.5	28.6	28.3	32.6	29.6	22	23.4	19.7	24	66	0
18:20:00	33.5	33.3	28.3	28.2	32.2	29.4	21.8	23.3	19.6	26	67	0
18:25:00	33	33	27.9	27.8	31.8	29.1	21.4	23.1	19.6	21	67	0
18:30:00	32.6	32.8	27.6	27.4	31.4	29	21.3	22.8	19.4	16	68	0
18:35:00	32.2	32.5	27.1	27.1	31	28.7	21	22.4	19.1	23	68	0
18:40:00	31.8	32.3	26.6	27	30.7	28.5	20.8	22.4	19.1	23	68	0
18:45:00	31.4	32.1	26.6	26.8	30.3	28.3	20.6	22.1	19	14	68	0

Time	Water Temperature (°C)		Vapour Temperature (°C)		Basin Temperature (°C)		Cover Temperature (°C)		Ambient Temperature (°C)	Wind speed (km/hr)	Relative Humidity (%)	Solar intensity (W/m2)
	MSD	NSD	MSD	NSD	MSD	NSD	MSD	NSD				
18:50:00	31.1	31.9	26.3	26.2	29.9	28.1	20.5	22.1	19	27	68	0
18:55:00	30.7	31.7	25.8	26.6	29.6	27.9	20.3	21.8	18.7	16	68	0
19:00:00	30.3	31.4	25.4	26.1	29.3	27.6	20.1	21.6	18.6	29	68	0
19:05:00	29.9	31.2	25.4	25.8	28.9	27.5	20	21.2	18.5	19	68	0
19:10:00	29.7	31	25.1	25.9	28.7	27.3	19.8	21.3	18.6	21	68	0
19:15:00	29.4	30.8	24.8	25.6	28.3	27.1	19.7	21.2	18.5	26	70	0
19:20:00	29	30.6	24.6	25.3	28	27	19.6	21	18.4	37	71	0
19:25:00	28.7	30.3	24.1	24.9	27.7	26.7	19.4	20.9	18.3	16	72	0
19:30:00	28.5	30.1	23.6	24.8	27.4	26.6	19.3	20.6	18	19	72	0
19:35:00	28.1	30	23.9	24.9	27.2	26.4	19.2	20.6	18.1	14	72	0
19:40:00	27.8	29.7	23.6	24.7	26.9	26.2	19	20.4	17.9	18	72	0
19:45:00	27.5	29.6	23.1	24	26.6	26.1	18.9	20.2	17.8	21	72	0
19:50:00	27.2	29.3	22.9	24.5	26.4	25.9	18.6	20	17.7	24	71	0
19:55:00	26.9	29.1	22.5	24.2	26	25.6	18.4	20	17.7	13	71	0
20:00:00	26.7	28.9	22.5	23.9	25.7	25.5	18.3	19.9	17.6	13	71	0
20:05:00	26.4	28.7	22.3	23.7	25.5	25.4	18.3	19.9	17.5	13	71	0
20:10:00	26.2	28.6	22	23.7	25.3	25.2	18.1	19.8	17.6	19	71	0
20:15:00	25.9	28.3	21.9	23.2	25	25	18	19.6	17.3	11	70	0
20:20:00	25.7	28.2	21.8	23.5	24.8	24.9	17.9	19.6	17.5	11	70	0
20:25:00	25.4	28	21.3	23	24.6	24.9	17.7	19.4	17.3	18	70	0
20:30:00	25.2	27.9	21.2	23.2	24.4	24.7	17.7	19.3	17.1	21	69	0
20:35:00	24.9	27.7	20.9	23.1	24.1	24.5	17.5	19	17.1	10	69	0
20:40:00	24.7	27.5	20.9	22.7	23.9	24.3	17.3	18.9	17	23	69	0
20:45:00	24.4	27.3	20.6	22.5	23.7	24.2	17.2	18.9	17	16	69	0
20:50:00	24.3	27.1	20.5	22.3	23.5	24	17.1	18.7	16.9	32	68	0
20:55:00	24	27	20.3	22.2	23.3	23.9	17	18.6	16.9	29	68	0
21:00:00	23.7	26.7	20.2	22	23.1	23.8	16.9	18.5	16.9	24	68	0
21:05:00	23.6	26.6	20	21.9	22.8	23.6	16.8	18.4	16.7	27	68	0
21:10:00	23.4	26.5	19.7	22	22.8	23.5	16.8	18.4	16.7	21	68	0
21:15:00	23.2	26.4	19.7	21.9	22.5	23.4	16.7	18.3	16.7	26	68	0
21:20:00	23	26.1	19.4	21.4	22.3	23.2	16.6	18.2	16.7	29	68	0
21:25:00	22.8	26	19.4	21.2	22.1	23.1	16.5	18	16.7	18	67	0
21:30:00	22.6	25.8	19.4	21.3	22	23	16.5	17.9	16.5	26	66	0
21:35:00	22.4	25.7	19	21.1	21.8	22.9	16.4	17.8	16.6	21	66	0
21:40:00	22.2	25.4	18.5	21	21.6	22.7	16.3	17.8	16.5	26	65	0
21:45:00	22	25.4	18.8	20.9	21.4	22.6	16.3	17.7	16.5	32	64	0
21:50:00	21.8	25.2	18.5	20.7	21.2	22.4	16	17.6	16.4	27	63	0
21:55:00	21.6	25	18.4	20.6	21.1	22.4	16	17.5	16.2	24	62	0
22:00:00	21.5	24.9	18.1	20.6	20.9	22.1	15.9	17.4	16.3	21	62	0
22:05:00	21.3	24.7	18.2	20.2	20.8	22.1	15.8	17.4	16.4	26	61	0
22:10:00	21.1	24.6	17.9	19.9	20.6	22	15.7	17.2	16.2	29	61	0
22:15:00	21	24.4	17.9	20.2	20.5	21.8	15.7	17.1	16.1	16	60	0
22:20:00	20.7	24.3	17.7	19.8	20.3	21.7	15.6	17	16.1	19	60	0
22:25:00	20.7	24.1	17.7	19.9	20.1	21.6	15.6	16.9	16.1	13	59	0
22:30:00	20.5	24	17.5	19.7	20.1	21.6	15.4	17	16.1	16	59	0
22:35:00	20.3	23.9	17.4	19.7	19.8	21.4	15.4	16.8	15.9	13	58	0
22:40:00	20.3	23.8	17.2	19.5	19.8	21.3	15.3	16.8	16	16	57	0
22:45:00	20	23.6	17	19.4	19.6	21.2	15.2	16.7	15.9	27	56	0
22:50:00	19.9	23.5	17	19.3	19.5	21.1	15	16.7	15.9	23	56	0
22:55:00	19.8	23.4	16.8	19.3	19.4	21.1	15.1	16.5	15.8	19	55	0
23:00:00	19.7	23.3	16.8	19.1	19.2	20.9	14.9	16.5	15.8	32	54	0
23:05:00	19.6	23.1	16.9	19.2	19.1	20.9	14.9	16.4	15.9	18	54	0
23:10:00	19.3	23	16.6	18.7	18.9	20.7	14.7	16.3	15.7	29	53	0
23:15:00	19.3	22.9	16.4	18.9	18.8	20.6	14.8	16.3	15.7	21	53	0
23:20:00	19.1	22.8	16.3	18.6	18.7	20.5	14.5	16.1	15.5	24	53	0
23:25:00	19	22.6	16.2	18.7	18.6	20.4	14.5	16.1	15.6	13	52	0
23:30:00	18.8	22.5	16.1	18.4	18.4	20.3	14.3	16	15.6	23	51	0
23:35:00	18.7	22.4	15.9	18.3	18.3	20.3	14.4	16	15.5	18	50	0
23:40:00	18.5	22.2	15.9	18.2	18.1	20	14.1	15.8	15.4	11	49	0
23:45:00	18.4	22.2	15.9	18.1	18.1	20	14.1	15.8	15.4	18	48	0
23:50:00	18.3	21.9	15.6	17.8	17.9	19.9	14	15.7	15.2	26	47	0
23:55:00	18.2	21.9	15.6	18	17.9	19.9	14	15.6	15.2	27	50	0
0:00:00	18.1	21.9	15.6	18	17.8	19.8	14	15.6	15.3	28	49	0

2. The daily data of the whole experiment period

Days	Daily Solar Exposure (MJ/m^2)	Max. Ambient Temperature (°C)	Mean Wind Speed (km/hr)	Mean Relative Humidity (%)	Mean Cloud Amount (oktas)	Max Water Temperature (°C)		Max Vapour Temperature (°C)		Max Basin Temperature (°C)		Max Cover Temperature (°C)		Productivity (ml/day)		Efficiency (%)		Productivity Enhancement (%)	Efficiency Enhancement (%)
						MSD	NSD	MSD	NSD	MSD	NSD	MSD	NSD	MSD	NSD	MSD	NSD		
4/10/2017	20.9	26	6.5	62	3	53.3	50.4	54.3	48.7	50.3	45.1	42.2	37.7	874	515	19	12.3	69.7	53.8
5/10/2017	22.4	28	9	60	5	57	54.5	55	52	56	50	45	42	952	557	19.4	12.4	70.9	55.9
6/10/2017	21.2	29.3	22.5	45	1	52	49.3	51	48	50	48	43	40	880	519	18.8	12.2	69.6	53.9
7/10/2017	10.6	18.8	25	88	1	35	33	34	32	34	32	30	29	332	200	13	9.4	66	37.9
8/10/2017	16.3	22.6	14	73	1	50	48	49	47	48	45	40	38	638	388	17.3	11.9	64.4	45.2
9/10/2017	22	28.9	22	63	1	54.9	53.3	56.4	55.3	54.4	52.1	44.6	43.6	862	503	17.8	11.4	71.4	56.1
10/10/2017	20.1	30	6.5	44	2	59.4	56.5	55.2	54.6	57.4	55	42.5	41.2	834	482	18.7	12	73	56.2
11/10/2017	20.2	26	17.5	74	2	57.1	56.8	59.7	57.1	55	54.7	39.9	38.6	764	459	17.1	11.4	66.4	50.4
12/10/2017	7.8	22.9	23	91	8	32.4	31.4	31.6	29.7	31.7	30.7	25	23.7	276	166	13.9	10.6	66.3	30.2
13/10/2017	24.7	27.5	16	56	2	59.5	56.8	57.1	55.8	56	54.4	41	40.2	1045	610	19.5	12.3	71.3	57.5
14/10/2017	9.4	22	14	87	7	28.7	26.6	26.1	26.1	27.4	26.3	20.9	19.9	356	209	15.4	11.1	70.3	38.5
15/10/2017	6.6	17.2	23	99	8	20.3	18.9	20.5	19.1	19.5	18.8	15.9	15.5	204	128	11.6	9.7	59.4	20.1
1/11/2017	28.7	23	16	34	1	60.9	55.1	59.5	52.9	60.2	48.3	44.6	40.9	1246	729	20.2	12.7	70.9	59
2/11/2017	28.8	24.8	9	28	1	64.9	58.9	64.3	54	63.9	50.2	50	42.6	1272	730	20.5	12.7	74.2	62.1
3/11/2017	27.8	26.8	9	42	3	60.5	51.1	61.2	50	60.2	44.6	50	40.2	1204	694	20.1	12.5	73.5	61
4/11/2017	28.8	28.6	15	37	3	57	50.9	55.8	50	56.9	45.9	47.9	40.7	1272	730	20.5	12.7	74.2	62.1
5/11/2017	26.9	26.9	16	58	1	62.3	51.8	61.1	50.5	61.8	45.7	48.3	40.2	1162	683	20	12.7	70.1	57.5
6/11/2017	24.2	26.8	20	60	1	58.9	59.1	56.1	56	58	50.1	44.1	43	1036	603	19.7	12.5	71.8	57.7
7/11/2017	26.3	26.7	18.5	52	1	63.5	56.2	60.5	54	58.8	48	45.5	40.5	1126	652	19.8	12.4	72.7	59.6
8/11/2017	27.5	22.3	34	58	3	64.1	56.2	59.2	54.2	54.4	48.9	43.5	40.3	1198	690	20.2	12.5	73.6	61
9/11/2017	29.1	21.7	31.5	52	6	63.2	57.9	58.9	53.9	54.8	48.6	42.7	41.7	1278	734	20.4	12.6	74.1	62.1
10/11/2017	22.3	20.3	30.5	79	8	48.5	43.8	42.8	40	39.3	38.3	32.1	31.3	926	532	18.9	11.9	74.1	58.7
11/11/2017	27.9	21.1	31.5	68	2	59.9	54	56.1	47	52.2	45.5	40.2	39.3	1206	695	20.1	12.5	73.5	61.1

Days	Daily Solar Exposure (MJ/m^2)	Max. Ambient Temperature (°C)	Mean Wind Speed (km/hr)	Mean Relative Humidity (%)	Mean Cloud Amount (oktas)	Max Water Temperature (°C)		Max Vapour Temperature (°C)		Max Basin Temperature (°C)		Max Cover Temperature (°C)		Productivity (ml/day)		Efficiency (%)		Productivity Enhancement (%)	Efficiency Enhancement (%)
						MSD	NSD	MSD	NSD	MSD	NSD	MSD	NSD	MSD	NSD	MSD	NSD		
12/11/2017	28.7	22.5	27.5	53	1	61.2	55.3	57.2	48.7	54.9	46.6	42.2	41.2	1246	729	20.2	12.7	70.9	59
13/11/2017	29.1	22.3	27.5	50	1	57.6	52.8	55	45.3	51	43.3	41	40.3	1278	734	20.4	12.6	74.1	62.1
14/11/2017	29.8	23.5	26	50	1	65.3	58.8	61.2	53.4	56.4	49.3	45.7	45.2	1316	766	20.6	12.9	71.8	60.2
15/11/2017	29.9	24.8	21	48	2	65.6	63.5	63.5	58.4	58.5	52.8	47.5	47.4	1318	767	20.6	12.8	71.8	60.3
16/11/2017	25.3	25.8	17.5	54	4	57	53.3	54.6	50.4	50.7	48.6	42.7	42.3	1154	664	21	13.1	73.8	60.1
17/11/2017	24.2	24	25.5	64	6	57.6	52.4	53.6	48.4	48.9	47.3	39.6	39.3	988	579	18.7	12	70.6	56.7
18/11/2017	10.1	18.4	27.5	88	8	27.6	24.1	22.8	20.1	24.2	18.2	17.1	17.1	322	194	13.1	9.6	66	36.7
19/11/2017	26.9	22.1	31.5	81	5	54.2	46.3	50.8	41.3	48.9	34.4	37.7	30.7	1090	635	18.8	11.8	71.7	58.9
20/11/2017	29.8	23.3	26	52	1	62.9	54.8	58.7	55	54.9	48.2	44.8	39.3	1292	742	20.2	12.4	74.1	62.4
21/11/2017	29.1	23	35	61	4	55.4	51.1	54.6	50.9	52.8	46.5	38.6	39	1278	734	20.4	12.6	74.1	62.1
22/11/2017	26.2	22.5	31	59	5	52.6	49.1	51.9	48.2	50.8	42.8	38.6	37.3	1148	675	20.2	12.9	70.1	57.1
23/11/2017	30.4	24.3	23.5	56	1	63.9	58.6	60.3	55.4	58.9	52.4	43.6	41.7	1352	773	20.8	12.7	74.9	63.3
24/11/2017	29.8	26.2	20.5	56	2	67.5	63.5	65.1	61.1	62.6	53.6	49.8	48.2	1316	766	20.6	12.9	71.8	60.2
25/11/2017	29.6	26.9	23.5	54	1	67.9	65	66.4	62.7	63.4	55	52.4	49.1	1312	764	20.7	12.9	71.7	60
26/11/2017	30	27.2	30	53	1	67.5	64.6	65.6	62.4	63.5	54.8	51.3	48.7	1344	768	20.9	12.8	75	63.2
27/11/2017	28.2	27.5	22.5	58	3	65.1	63.1	64.5	61.7	62.3	53.5	50.1	47.4	1236	723	20.4	12.8	71	58.8
28/11/2017	26.1	27.1	27.5	58	5	59.3	57.4	59.3	55.7	57.1	49	44.5	43.1	1146	674	20.3	12.9	70	57
29/11/2017	10.8	21.6	26	98	8	32.3	30.3	28.7	28.7	31.3	26.1	21	21	396	238	15.3	11	66.4	38.7
30/11/2017	17.9	23.2	28.5	98	8	49.7	43.1	49.3	48.4	47.2	37.8	35.8	33.7	646	383	16.1	10.7	68.7	50.5
1/12/2017	26.5	25.5	26	69	5	53.7	46	54.2	50.1	52	40.8	39.2	35.5	1010	582	17.6	11	73.5	60.5
2/12/2017	18	26.6	18	73	6	48.5	43	43	41.8	46.7	39.4	36	33.9	664	384	16.5	10.7	72.9	54.4
3/12/2017	19.6	25.5	15	67	7	48.6	42.7	47	45.1	46.5	37.7	36.3	33.3	824	476	18.9	12.1	73.1	55.9
4/12/2017	5.4	20.1	12	75	8	24.5	24.9	26.3	29.6	24.7	22.5	18.9	19.1	147	89	9.7	8.2	65.2	18
5/12/2017	25.3	26	19.5	53	5	56.8	50.8	57.6	56.1	53.7	43.7	43.6	40.4	1106	640	20.1	12.6	72.8	59.2
6/12/2017	30.8	26.7	23.5	31	2	65.4	59.3	65.7	62.4	62.4	50.7	47.4	45.2	1360	778	20.6	12.6	74.8	63.4

Days	Daily Solar Exposure (MJ/m^2)	Max. Ambient Temperature (°C)	Mean Wind Speed (km/hr)	Mean Relative Humidity (%)	Mean Cloud Amount (oktas)	Max Water Temperature (°C)		Max Vapour Temperature (°C)		Max Basin Temperature (°C)		Max Cover Temperature (°C)		Productivity (ml/day)		Efficiency (%)		Productivity Enhancement (%)	Efficiency Enhancement (%)
						MSD	NSD	MSD	NSD	MSD	NSD	MSD	NSD	MSD	NSD	MSD	NSD		
7/12/2017	30.3	29.9	9	26	1	69.8	62.3	69.9	66.5	66.6	54.4	53.8	50	1349	774	20.8	12.8	74.3	62.7
8/12/2017	10.6	27.1	20	59	8	33	32	32.1	34.3	32.1	28.9	26.2	26.5	368	224	14.4	10.6	64.3	36.5
9/12/2017	30.3	28.7	16	52	2	70	60.4	71	66.3	62.9	52.8	54.6	48.7	1326	772	20.4	12.7	71.8	60.3
10/12/2017	28.8	25.3	22	59	3	66.1	56.8	62.6	54.8	62.2	50.2	45.2	41	1272	730	20.5	12.7	74.2	62.1
11/12/2017	30.3	25.8	24	56	1	65.3	58.7	65.3	62.9	62.6	51.6	48.7	45.9	1326	772	20.4	12.7	71.8	60.3
12/12/2017	31.4	25.6	27	52	1	63.5	57.1	63.5	59.2	60.7	49.4	47.3	44.3	1396	809	20.8	12.9	72.6	61.5
13/12/2017	30.8	26.5	24	56	1	65	58	63.8	60.8	61.5	50.4	46.9	43.9	1360	778	20.6	12.6	74.8	63.4
14/12/2017	30.9	28	18.5	50	1	68.4	62.1	70.1	65.9	65.7	54.9	52.8	49.1	1362	779	20.6	12.6	74.8	63.4
15/12/2017	31.4	30.3	19.5	53	1	68.6	62.4	68.2	65.3	65.8	54.9	52.5	49.5	1396	809	20.8	12.9	72.6	61.5
16/12/2017	28.9	29.3	20	55	1	66.5	60.2	67.9	64.7	64.5	53.5	49.1	46.5	1274	731	20.5	12.6	74.3	62.2
17/12/2017	30.6	29.2	20.5	52	1	67	62	65	64.5	64.6	54	51.8	48.5	1356	776	20.7	12.7	74.7	63.2
18/12/2017	30.3	29.1	19.5	53	2	65	61	67	63.5	63.8	52.8	50	47.5	1326	772	20.4	12.7	71.8	60.3
19/12/2017	30.9	31.8	13	46	1	67	64	70	66.1	66.9	56.8	54	51.1	1362	779	20.6	12.6	74.8	63.4
20/12/2017	30.1	34.4	7	47	1	69	65	73.4	70.5	69.1	58.9	56.8	55.2	1322	770	20.5	12.8	71.7	60.2
21/12/2017	26.3	30.7	19.5	50	5	59.6	54.7	60	60.1	58	49.3	46.9	44.5	1150	676	20.2	12.9	70.1	57.2
22/12/2017	20.2	29.3	13	65	7	58	52	58	52.8	53.5	48	43	40	836	483	18.7	12	73.1	56.4
23/12/2017	25.4	29.3	9	55	2	59	49.1	61	51.8	52.5	44.3	42.2	40.3	1108	641	20.1	12.6	72.9	59.3
24/12/2017	31.2	32.5	13	45	1	69	65.1	72.5	69.6	68.6	57	56.5	53.2	1392	807	20.9	12.9	72.5	61.3
25/12/2017	25	32	15	53	4	68	62	69	65	64.6	54.5	52.4	49.3	1100	636	20.3	12.7	73	59.2
26/12/2017	25.3	28.4	25	72	4	68	58.2	62.3	60.7	62.2	51.3	47.3	44.2	1082	640	19.7	12.6	69.1	55.8
27/12/2017	29.4	26.9	23	68	2	60	55	62	59	58.6	48.8	46.6	42.7	1284	737	20.3	12.5	74.2	62.3
28/12/2017	29.3	27.9	17	62	1	67.6	61.1	63	65.6	65	53.8	51.9	48.2	1282	760	20.4	13	68.7	57.1
29/12/2017	27.1	28.9	17	64	6	65	60.4	66	63.7	64.2	53.3	51.3	47.5	1190	686	20.3	12.7	73.5	60.7
30/12/2017	20.9	30.2	16.5	59	8	52	50	56	53	54.1	46	45	42.8	874	515	19	12.3	69.7	53.8
31/12/2017	22	30.2	19.5	70	7	58.3	52.4	55	52.3	56	47.5	44	41.8	920	528	19	12	74.2	58.7

Days	Daily Solar Exposure (MJ/m^2)	Max. Ambient Temperature (°C)	Mean Wind Speed (km/hr)	Mean Relative Humidity (%)	Mean Cloud Amount (oktas)	Max Water Temperature (°C)		Max Vapour Temperature (°C)		Max Basin Temperature (°C)		Max Cover Temperature (°C)		Productivity (ml/day)		Efficiency (%)		Productivity Enhancement (%)	Efficiency Enhancement (%)
						MSD	NSD	MSD	NSD	MSD	NSD	MSD	NSD	MSD	NSD	MSD	NSD		
1/01/2018	20.9	30.6	15	70	6	58.1	49.7	57	55.8	52.8	44.7	45.2	42.5	874	515	19	12.3	69.7	53.8
2/01/2018	17.4	29.1	12	71	1	55	46.3	52	55	50.2	42.4	40	37.3	780	449	19.9	12.9	73.7	54.5
3/01/2018	29.5	32.5	19.5	46	3	63	58	60	63	61.2	50.5	46.6	44.2	1286	738	20.3	12.5	74.3	62.4
4/01/2018	29.7	28.3	23	58	4	67	58	65.4	62.9	63.9	52.4	49.9	46.5	1314	765	20.6	12.9	71.8	60.1
5/01/2018	20	28	17	68	6	51	46.1	54	52.1	48.8	39.9	31.5	31.3	832	480	18.8	12	73.3	56.4
6/01/2018	31.1	29.5	16	53	3	63	60.3	63.8	61	65.3	53.5	50.3	46.5	1366	782	20.5	12.6	74.7	63.3
7/01/2018	31.3	31.4	13	47	1	69	62.4	70.6	66.5	67.1	55.6	53.5	49.6	1394	808	20.8	12.9	72.5	61.4
8/01/2018	31.3	32.1	16	33	1	69	63.7	70.5	68.4	68	56.1	54.9	51	1394	808	20.8	12.9	72.5	61.4
9/01/2018	30.7	32.3	13	44	1	69.1	62.5	70.5	67.9	67.3	56.2	54.5	51.1	1358	777	20.7	12.7	74.8	63.3
10/01/2018	29.9	30.5	21.5	54	3	65	58.8	65	62.7	63.3	52.5	48.8	45.8	1318	767	20.6	12.8	71.8	60.3
11/01/2018	27.8	30.5	20.5	51	1	63.4	56.7	62.9	59.8	61.9	51.4	49	45.7	1228	718	20.5	12.9	71	58.7
12/01/2018	28.6	32.7	11	52	3	61.5	56.6	61.6	59.3	60.1	51.6	49.7	46.9	1244	728	20.2	12.7	70.9	58.9
13/01/2018	28	37	25	36	1	69.8	63.6	70.2	67.2	68	57.4	56.3	52.7	1192	692	19.8	12.4	72.3	59.9
14/01/2018	28.4	31.7	35	29	1	61.4	55.1	57.5	53.5	58.9	49.2	43.2	41.1	1264	725	20.7	12.8	74.3	62
15/01/2018	30.5	29.7	12	32	1	66.2	59.7	67.4	64.4	64	52.3	50.7	47.2	1354	774	20.7	12.7	74.9	63.4
16/01/2018	30.5	28.3	14	35	1	66.8	60.3	67.7	64.5	64.7	54.2	50	47.4	1354	774	20.7	12.7	74.9	63.4
17/01/2018	28.9	29.8	13	35	1	64.6	57.9	65.5	62.6	62.6	51.9	50.4	46.8	1274	731	20.5	12.6	74.3	62.2
18/01/2018	29.8	30.4	9	42	1	67.7	61.2	69.5	66.1	65.7	54.8	54.1	50.1	1316	766	20.6	12.9	71.8	60.2
19/01/2018	30.1	33.3	17.5	26	1	68.7	62.5	69.7	67.1	66.9	57	52.8	49.7	1322	770	20.5	12.8	71.7	60.2
20/01/2018	30.1	30.6	18.5	33	1	67.5	61.4	68.3	66.4	65.7	56.2	51	48.2	1322	770	20.5	12.8	71.7	60.2
21/01/2018	20	28.1	20.5	53	5	53.6	47.8	53.3	54.2	52.4	44.6	41.3	39.6	832	480	18.8	12	73.3	56.4
22/01/2018	29.4	30.5	20.5	46	1	66.7	60.3	66.9	61.3	64.8	54.8	51.7	48	1284	737	20.3	12.5	74.2	62.3
23/01/2018	29.3	30.6	19.5	50	1	68.2	61.9	69.1	66.5	66.1	56.6	53	49.4	1282	736	20.4	12.6	74.2	62.2
24/01/2018	27.3	31.6	17	50	3	63.3	56.8	59.9	62.3	61.5	52.2	50.5	47.1	1194	688	20.3	12.6	73.5	60.8
25/01/2018	27.3	32.5	14	53	4	58.4	52.8	55.5	62.1	57.3	49.7	47.9	45.1	1194	688	20.3	12.6	73.5	60.8

Days	Daily Solar Exposure (MJ/m^2)	Max. Ambient Temperature (°C)	Mean Wind Speed (km/hr)	Mean Relative Humidity (%)	Mean Cloud Amount (oktas)	Max Water Temperature (°C)		Max Vapour Temperature (°C)		Max Basin Temperature (°C)		Max Cover Temperature (°C)		Productivity (ml/day)		Efficiency (%)		Productivity Enhancement (%)	Efficiency Enhancement (%)
						MSD	NSD	MSD	NSD	MSD	NSD	MSD	NSD	MSD	NSD	MSD	NSD		
26/01/2018	28.1	31.7	21.5	54	1	65.5	59.5	63.7	60.2	63.8	54.6	49.6	46.6	1234	722	20.4	12.8	70.9	58.7
27/01/2018	24.1	31	28.5	64	6	53.2	46.7	46.5	43.1	50.1	38.7	28	28.4	1034	602	19.7	12.5	71.8	57.6
28/01/2018	23.8	29.1	27.5	80	7	55.1	48.9	47.9	44.3	52.5	41.9	29.5	29.2	956	550	18.4	11.6	73.8	59.4
29/01/2018	18.9	26.6	23	66	8	45.5	39.8	39.7	38.4	43.5	35.5	25.8	25.1	786	467	18.7	12.4	68.3	51
30/01/2018	28.3	30.1	17.5	55	1	66.1	58.4	66.6	63.1	62.5	52.7	50.9	46.6	1238	724	20.3	12.8	71	58.9
31/01/2018	25.6	35.3	15.5	42	3	68.9	61.4	68.4	63.4	67	55.5	54.4	49.6	1112	644	20	12.6	72.7	59.2
1/02/2018	5.1	18.7	32	86	8	25.4	23.5	23	22.1	24.5	21.5	17.1	17.1	154	98	10.6	9.6	57.1	10.4
2/02/2018	4.5	16.4	34	99	8	20.6	18.2	18.5	18.4	20.1	16.8	15	15	138	88	10.4	9.8	56.8	6
3/02/2018	6.1	20.4	25.5	90	8	22.6	20	20.2	20	22.3	18.6	15.8	15.5	194	122	11.7	10	59	17.4
4/02/2018	27.3	25.5	31.5	50	5	56.8	49.3	57.1	55.9	54.4	42.7	42.7	38.6	1194	688	20.3	12.6	73.5	60.8
5/02/2018	28.5	26	25	54	1	60	52.8	59.9	56.5	57.7	46.4	43.8	39.9	1242	726	20.3	12.7	71.1	59
6/02/2018	27.7	26.5	28.5	50	2	60.3	53.5	61.4	58.9	58.4	47.6	45.9	41.9	1226	717	20.5	12.9	71	58.6
7/02/2018	28.6	26.2	27.5	47	1	58.9	53	59.8	59.1	56.9	46	44.2	40.9	1268	728	20.6	12.7	74.2	61.9
8/02/2018	27.5	26.2	26	54	1	58.1	51.1	57.3	53.8	56.6	46.1	43.7	40	1198	690	20.2	12.5	73.6	61
9/02/2018	28.8	30.3	14	42	1	66.2	59.2	66.6	63.2	64.1	52.1	51.1	47	1272	730	20.5	12.7	74.2	62.1
10/02/2018	27.9	34	15.5	46	1	67.2	60.2	68.5	64.8	65.3	53.5	53	48.5	1230	719	20.5	12.9	71.1	58.8
11/02/2018	25.1	38.4	34	36	4	70.1	63.5	72.2	69.7	68.1	56.6	57.8	53.4	1078	638	19.8	12.7	69	55.6
12/02/2018	23.2	36.3	11.5	38	3	65.2	59.7	62.8	59.2	63.8	55.1	52.2	48.7	992	567	19.6	12.2	75	60.1
13/02/2018	25.1	33.8	28	66	2	66	58.9	66.7	63.6	64.3	53.9	52.5	48.4	1078	638	19.8	12.7	69	55.6
14/02/2018	24.6	37.5	19.5	39	1	69.1	62.3	70.9	68.2	67	56.1	56.4	52.5	1044	608	19.5	12.4	71.7	57.9
15/02/2018	20.3	36.6	14	43	6	55.5	51.1	54.2	53.1	54.4	46.9	45	42.9	862	508	19.2	12.5	69.7	53.4
16/02/2018	20.3	35.5	28	63	1	66	59	69.6	67.5	64.6	53.7	55.7	51.9	838	484	18.7	11.9	73.1	56.5
17/02/2018	23.7	28.7	30.5	71	5	60.6	53.9	59.2	55.7	58.9	48.6	46.2	42.5	954	549	18.4	11.6	73.8	59.3
18/02/2018	27.1	30.4	19.5	53	3	66.2	58.8	66.4	63.1	64.4	53.5	51.3	46.9	1166	686	19.9	12.7	70	57.4
19/02/2018	23.4	33	16.5	45	2	67.1	59.4	68.7	65.1	65.3	53.5	53.9	49.4	996	593	19.5	12.7	68	53.8

Days	Daily Solar Exposure (MJ/m^2)	Max. Ambient Temperature (°C)	Mean Wind Speed (km/hr)	Mean Relative Humidity (%)	Mean Cloud Amount (oktas)	Max Water Temperature (°C)		Max Vapour Temperature (°C)		Max Basin Temperature (°C)		Max Cover Temperature (°C)		Productivity (ml/day)		Efficiency (%)		Productivity Enhancement (%)	Efficiency Enhancement (%)
						MSD	NSD	MSD	NSD	MSD	NSD	MSD	NSD	MSD	NSD	MSD	NSD		
20/02/2018	13.2	24.4	25	70	6	42.6	35.2	41.5	39.3	41.3	32.7	31.7	29.4	504	303	16.4	11.5	66.3	42.9
21/02/2018	14.1	23.1	36.5	67	7	43.4	37.4	41	39.7	42.2	33.9	30.4	28.5	538	331	16.5	11.7	62.5	40.9
22/02/2018	11.9	21.4	36.5	97	8	33.7	29.8	30.9	29.9	32.7	26.8	24.4	23.1	382	239	13.6	10	59.8	35.3
23/02/2018	12.2	22.6	24	99	8	30.7	28	29.5	30.1	30.3	26.3	22.9	22.8	316	195	11	8	62.1	37.7
24/02/2018	17.5	27.4	21.5	87	4	55.1	46.6	53.1	49.1	53.1	42.6	40.8	36.7	710	426	18.1	12.2	66.7	48.4
25/02/2018	22.1	29.7	18	65	2	62.9	53.5	63.1	59.2	61.4	48.5	48.8	44.2	922	554	19	12.5	66.4	51.6
26/02/2018	20.9	31.1	16	67	2	61.2	52.4	62.8	59.7	60.1	48.3	49.7	44.9	874	515	19	12.3	69.7	53.8
27/02/2018	15.1	23.1	31	82	8	44.5	37.5	41.2	38.6	42.4	34.6	31.4	29.2	566	326	16.4	10.8	73.6	51.9
28/02/2018	26.4	26.8	19.5	60	2	64.6	54.7	65.1	59.7	62.9	49	50.6	44.1	1152	677	20.2	12.8	70.2	57.3
1/03/2018	22.5	30.9	17	61	3	57.5	49.8	53.9	48.3	55.7	46.1	43.8	39.8	954	558	19.3	12.4	71	56
2/03/2018	21.8	27.5	24	75	2	59.5	50.1	60.5	56.4	58.2	46.5	45.4	41.2	868	502	18.1	11.5	72.9	57.3
3/03/2018	16	28.8	15	72	8	45.1	38	45.4	43.3	45	36.4	37.4	34.8	632	384	17.4	12	64.6	45
4/03/2018	19.1	28.4	19.5	66	5	56.4	48.9	57.1	55.9	54.2	43.4	44.6	41.6	790	470	18.6	12.3	68.1	51
5/03/2018	12.2	25.8	15	81	8	46.2	39.5	44.8	42.5	45	37.3	35.7	33	484	291	16.9	11.9	66.3	41.3
6/03/2018	5.4	18.9	29.5	99	8	25.1	22.8	22.2	21.4	24.3	21.4	18.2	18	180	113	11.9	10.5	59.3	13.8
7/03/2018	12	21.5	27	87	8	34.8	28.6	33.4	33	33.2	25.5	25.7	24.2	432	264	15.3	11	63.6	38.7
8/03/2018	22.3	23.7	35	62	2	53.6	44.2	50.5	45.8	51.6	39.3	37	33	926	532	18.9	11.9	74.1	58.7
9/03/2018	20.3	22.9	33.5	69	3	48.5	41.2	45.6	42.2	46.8	36.4	34.5	30.9	838	484	18.7	11.9	73.1	56.5
10/03/2018	17	23.1	23	73	3	48.6	40.3	46.8	43.9	47.1	36.2	35.3	31.6	676	396	17.6	11.6	70.7	51.5
11/03/2018	24.5	23.7	23	66	1	60.4	49.7	56.3	48	58.3	44.9	42.6	36.4	1042	606	19.5	12.4	71.9	58
12/03/2018	24.7	24.1	26	55	1	61.1	50.8	60.7	55.5	59.4	45.8	45.5	39.6	1046	609	19.5	12.3	71.8	57.9
13/03/2018	18.3	23.9	28	71	2	51	43.8	49.2	46.2	49.6	39.3	37.6	33.7	750	436	18.3	11.9	72	53.9
14/03/2018	23.2	24.8	35	61	1	53.9	45.8	50.3	46.5	51.6	40.3	36.6	33.2	992	567	19.6	12.2	75	60.1
15/03/2018	24.3	26	24	53	1	62	51.7	61.6	56.1	60.5	47.8	47.6	42.1	1038	604	19.6	12.4	71.9	57.8
16/03/2018	24.1	28.1	16.5	52	1	63.2	53.5	62.3	57.5	61.5	49.2	47.9	42.6	1034	602	19.7	12.5	71.8	57.6

Days	Daily Solar Exposure (MJ/m^2)	Max. Ambient Temperature (°C)	Mean Wind Speed (km/hr)	Mean Relative Humidity (%)	Mean Cloud Amount (oktas)	Max Water Temperature (°C)		Max Vapour Temperature (°C)		Max Basin Temperature (°C)		Max Cover Temperature (°C)		Productivity (ml/day)		Efficiency (%)		Productivity Enhancement (%)	Efficiency Enhancement (%)
						MSD	NSD	MSD	NSD	MSD	NSD	MSD	NSD	MSD	NSD	MSD	NSD		
17/03/2018	23.9	28.1	23	54	1	62.3	53	61.7	57.1	60.8	48.5	47.9	42.2	1030	599	19.8	12.5	72	57.7
18/03/2018	23.8	27.7	19.5	54	1	63	53.5	62.8	57.8	61.4	49.1	47.4	42.2	1004	598	19.3	12.6	67.9	53.9
19/03/2018	23.3	28	17.5	65	1	63	53.8	62.6	57.6	61.6	49.7	47.9	42.5	994	568	19.5	12.2	75	60.2
20/03/2018	23.1	26.6	25	66	3	60.4	51.5	59.2	55	58.8	46.7	44.8	40.6	966	566	19.1	12.3	70.7	56.1
21/03/2018	20	25.7	29.5	73	2	52.8	44.4	46.9	40.3	50.5	40.4	35.2	32.1	832	480	18.8	12	73.3	56.4
22/03/2018	17.2	23.6	29	79	6	47.4	39.7	42.6	37.9	45.5	36	31.5	28.9	680	399	17.6	11.6	70.4	51.4
23/03/2018	16.6	23.8	28	83	7	43.2	36.8	44.5	45.3	42.3	32.8	34.6	32.1	644	392	17.2	11.8	64.3	45.4
24/03/2018	19.5	24.8	28	73	5	53	43.2	51.6	46.9	51.7	39.7	37.6	33.7	798	474	18.4	12.2	68.4	51.6
25/03/2018	22.4	25.8	23.5	65	1	57.1	47	55.9	52.5	55.8	44	42.6	37.9	952	557	19.4	12.4	70.9	55.9
26/03/2018	18.7	29.4	7.5	66	2	55	45.8	51.3	43.8	53.3	42.2	41.9	36.4	758	441	18.2	11.8	71.9	54.1
27/03/2018	18.5	26.7	23	77	1	48.3	40.9	46.8	45	47.5	38.2	36.8	34.4	706	414	17.1	11.2	70.5	52.7
28/03/2018	22.1	27.3	26.5	59	1	61	50.7	60.1	54.4	59.4	47	46.4	40.8	946	554	19.5	12.5	70.8	55.6
29/03/2018	14.3	24.7	23	85	8	41.7	35.4	40.5	38.2	40.9	33.8	32.6	30.6	526	316	16	11	66.5	44.6
30/03/2018	21.1	25.3	28.5	75	1	55	52	54	51	52	49	44	42	854	494	18.4	11.7	72.9	56.8
31/03/2018	21.6	26.4	35	65	2	57	53	56	53	53	50	45	43	912	524	19.2	12.1	74	58.2
1/04/2018	21.3	26.3	29.5	67	1	50	45	49	48	47	43	38	36	882	520	18.8	12.2	69.6	54
2/04/2018	20.2	26.9	23	71	2	48	42	46	44	45	40	36	33	836	483	18.7	12	73.1	56.4
3/04/2018	17.5	24	27	74	2	39	35	36	33	38	33	30	27	638	378	16.2	10.8	68.8	50.2
4/04/2018	15.1	24.3	29	64	8	40	36	37	34	39	35	31	28	590	350	17.1	11.6	68.6	47.5
5/04/2018	20	24.9	34.5	54	1	46	41	45	44	43	40	36	34	832	480	18.8	12	73.3	56.4
6/04/2018	19	25.6	30.5	61	2	44	38	43	41	42	38	35	33	764	444	18.1	11.7	72.1	54.5
7/04/2018	19.1	24.7	32.5	58	1	43	36	42	40	40	35	30	29	766	446	18	11.7	71.7	54.3
8/04/2018	19	25.2	26	66	4	49	43	47	45	46	40	36	35	764	444	18.1	11.7	72.1	54.5
9/04/2018	20.1	28.1	16.5	56	1	41.4	35	38	35.2	39.8	36.1	28	28.1	834	482	18.7	12	73	56.2
10/04/2018	19.9	27	16	42	1	56.3	45.8	55.9	50.5	55.2	43.3	43	38.3	830	479	18.8	12	73.3	56.3

Days	Daily Solar Exposure (MJ/m^2)	Max. Ambient Temperature (°C)	Mean Wind Speed (km/hr)	Mean Relative Humidity (%)	Mean Cloud Amount (oktas)	Max Water Temperature (°C)		Max Vapour Temperature (°C)		Max Basin Temperature (°C)		Max Cover Temperature (°C)		Productivity (ml/day)		Efficiency (%)		Productivity Enhancement (%)	Efficiency Enhancement (%)
						MSD	NSD	MSD	NSD	MSD	NSD	MSD	NSD	MSD	NSD	MSD	NSD		
11/04/2018	18.8	24.4	31.5	57	4	48.9	39.4	47.2	43.2	47.6	37	35.8	31.8	760	442	18.1	11.8	71.9	54.2
12/04/2018	16.7	23.7	19.5	62	6	43.5	34.5	40.7	36.2	42.7	33.7	31.9	28.9	670	393	17.8	11.8	70.5	51
13/04/2018	19	26.3	14	47	1	53.7	42.5	49.1	40.1	52	41.1	37.8	32	788	468	18.6	12.3	68.4	51.2
14/04/2018	9.4	24.4	17	74	7	28.6	25.4	28.5	29.3	28.6	25	24.7	24.5	356	209	15.4	11.1	70.3	38.5
15/04/2018	18	29.1	28.5	52	3	50.7	40.4	50.3	46.2	49.4	38.5	38.7	35.3	720	432	17.9	12	66.7	48.8
16/04/2018	19	28.6	18.5	34	1	54.8	43.9	53.6	49.6	53.4	41.4	41.3	36.8	788	468	18.6	12.3	68.4	51.2
17/04/2018	18.8	28.8	12	29	1	55.6	44.3	55.4	49.4	54.4	42.9	43.4	37.8	784	466	18.7	12.4	68.2	50.9
18/04/2018	10.1	20.9	23	89	8	27.7	24.7	27.2	26.8	27.4	23.9	23.2	22.3	346	218	14.1	10.8	58.7	30.8
19/04/2018	17.9	23.8	25.5	72	5	48.7	38.1	48.2	44.3	47.5	35.9	35.8	32	718	431	17.9	12	66.6	48.7
20/04/2018	8.7	23.1	10.5	86	7	31.8	28	28.2	26.8	31.3	26.5	20.8	20.6	318	201	14.6	11.6	58.2	26.7
21/04/2018	16.6	23.4	19.5	66	6	45.4	35.8	46.5	44.3	43.9	33.4	36.3	32.5	644	392	17.2	11.8	64.3	45.4
22/04/2018	16.8	23.2	18.5	62	5	43.1	33.8	44.1	43.1	42	32.5	33.5	31.2	672	394	17.7	11.7	70.6	51.1
23/04/2018	17.9	23.9	13	53	1	48.8	37.8	46.7	43.3	47.4	35.6	35.6	31.7	718	431	17.9	12	66.6	48.7

3. The hourly data of the selected days.

Date/Time	Hourly insolation (MJ/m^2)	Hourly Productivity (ml/hr)		Hourly efficiency (%)		Enhancement in the hourly productivity (%)	Enhancement in the hourly efficiency (%)
		MSD	NSD	MSD	NSD		
13-10-17							
10:00	3.04	38	22	5.9	3.6	72.7	63.1
11:00	3.6	102	58	13.5	8.1	75.9	67.5
12:00	2.99	159	92	25.1	15.4	72.8	63
13:00	3	184	108	28.9	18	70.4	60.7
14:00	2.58	190	114	34.4	22.1	66.7	55.8
15:00	2.56	172	102	31.4	19.9	68.6	57.5
16:00	2	136	78	31.2	19.5	74.4	60
17:00	1.1	64	36	25	16.4	77.8	52.8
15-11-17							
10:00	3.25	66	38	9.6	5.8	73.7	64.6
11:00	3.44	145	82	20	11.9	76.8	68
12:00	3.55	194	112	26	15.8	73.2	64.9
13:00	3.4	218	130	30.4	19.1	67.7	59.3
14:00	2.98	218	129	34.5	21.6	69	59.4
15:00	2.55	204	122	37.4	23.9	67.2	56.2
16:00	2.1	166	98	36.4	23.3	69.4	56
17:00	1.33	98	56	32.5	21.1	75	54.1
14-12-17							
10:00	3.12	56	32	8.5	5.1	75	65.5
11:00	3.46	136	78	18.7	11.3	74.4	65.7
12:00	3.69	210	120	27.1	16.3	75	66.9
13:00	3.67	242	138	31.4	18.8	75.4	67.2
14:00	3.4	240	138	33.5	20.3	73.9	65.2
15:00	2.92	218	125	35.2	21.4	74.4	64.3
16:00	2.27	168	96	34.3	21.1	75	62.1
17:00	1.51	90	52	26.6	17.2	73.1	54.6
16-01-18							
10:00	3.14	68	42	10.2	6.7	61.9	53.1
11:00	3.58	144	81	19.1	11.3	77.8	69.3
12:00	3.79	198	112	24.9	14.8	76.8	68.8
13:00	3.77	222	130	28.1	17.2	70.8	63
14:00	3.54	226	132	30.4	18.6	71.2	62.9
15:00	3.07	212	119	32.6	19.4	78.2	68.3
16:00	2.42	170	96	32.7	19.8	77.1	64.8
17:00	1.66	112	60	30.4	18.1	86.7	68.4
14-02-18							
10:00	2.63	48	28	8.5	5.3	71.4	60.4
11:00	2.99	106	62	16.7	10.4	71	61.3
12:00	3.39	152	90	21.3	13.3	68.9	60.4
13:00	3.44	178	105	24.6	15.3	69.5	61.1
14:00	3.04	180	107	28	17.6	68.2	58.8
15:00	2.6	167	98	30	18.8	70.4	59.4
16:00	2.1	136	76	29.8	18.1	78.9	64.8
17:00	1.3	75	42	25.3	16.2	78.6	56.9
16-3-18							
10:00	2.46	38	22	7.2	4.5	72.7	61
11:00	2.92	107	62	17.3	10.6	72.6	62.6
12:00	3.17	156	88	23.3	13.9	77.3	67.7

Date/Time	Hourly insolation (MJ/m^2)	Hourly Productivity (ml/hr)		Hourly efficiency (%)		Enhancement in the hourly productivity (%)	Enhancement in the hourly efficiency (%)
		MSD	NSD	MSD	NSD		
13:00	3.17	179	105	26.7	16.6	70.5	61.3
14:00	2.79	183	107	30.8	19.2	71	60.7
15:00	2.51	172	102	32	20.3	68.6	57.3
16:00	1.9	137	80	32.9	21.1	71.3	56.4
17:00	1.14	62	34	23.5	14.9	82.4	57.5
16-4-18							
10:00	2.14	36	21	7.8	4.9	71.4	58.1
11:00	2.57	83	48	15.1	9.3	72.9	61.6
12:00	2.78	121	70	20.4	12.6	72.9	62.3
13:00	2.77	137	82	23.2	14.8	67.1	56.9
14:00	2.51	136	83	25.3	16.5	63.9	52.9
15:00	2.05	120	74	26.9	18	62.2	49.1
16:00	1.6	96	56	27	17.5	71.4	54.1
17:00	1.2	59	32	21.4	13.3	84.4	60.3

Appendix C: Uncertainty Analysis Calculations

Equations (6.16) and (6.17) in chapter six were used to estimate the uncertainty in the measured productivity and the calculated efficiency as follows;

$$U_{\dot{m}_e} = \sqrt{\left(\frac{\partial \dot{m}_e}{\partial V} U_V\right)^2 + \left(\frac{\partial \dot{m}_e}{\partial t} U_t\right)^2} \tag{6.16}$$

$$U_\eta = \sqrt{\left(\frac{\partial \eta}{\partial \dot{m}_e} U_{\dot{m}_e}\right)^2 + \left(\frac{\partial \eta}{\partial G} U_{G_s}\right)^2} \tag{6.17}$$

From the above-mentioned equations, the uncertainty of measured volume U_V and the uncertainty of measured time U_t are required to estimate the uncertainty of the productivity $U_{\dot{m}_e}$. Then, the uncertainty of the productivity $U_{\dot{m}_e}$ together with the uncertainty of the measured solar energy U_{G_s} are used to estimate the uncertainty of the efficiency U_η. The following two tables 1 and 2 list the uncertainties in measured values and the experimental data from the whole experiment period, which are used in the calculation.

Table 1 Uncertainties in measured values

Measurement	*Range*	*Maximum Error*	*Uncertainty*
Volume	$5\ ml - 50\ ml$	$\pm\ 0.5\ ml$	$U_{v1} = \frac{\pm 0.5}{50} = 0.01$
	$50\ ml - 500\ ml$	$\pm\ 5\ ml$	$U_{v2} = \frac{\pm 5}{500} = 0.01$
Time	$0\ s - 3600\ s$	$\pm\ 300\ s$	$U_{t1} = \frac{\pm 300}{3600} = 0.08$
	$0\ hr - 24\ hr$	$\pm\ 0.5\ hr$	$U_{t2} = \frac{\pm 0.5}{24} = 0.02$
Solar intensity	$0\ W/m^2 - 1500\ W/m^2$	$\pm\ 75\ W/m^2$	$U_G = \frac{\pm 75}{1500} = 0.05$

Table 2 Experimental Data from the whole experiment period

	NSD			MSD		
	Minimum	*Maximum*	*Average*	*Minimum*	*Maximum*	*Average*
Daily Productivity (ml)	*88*	*809*	*562.4*	*138*	*1396*	*965.4*
Hourly Productivity (ml)	*21*	*138*	*82.2*	*36*	*242*	*141.6*
Daily Efficiency (%)	*8*	*13.1*	*12.1*	*9.7*	*21*	*18.8*
Hourly Efficiency (%)	*3.6*	*23.9*	*15.4*	*5.9*	*37.4*	*24.8*

Using the values from tables 1 and 2, the uncertainty can be calculated as follows;

1. Daily productivity uncertainty

$$U_{\dot{m}_{e\,daily}} = \sqrt{\left(\frac{\dot{m}_{e_{max}} - \dot{m}_{e_{min}}}{V_{max} - V_{min}}\, U_{v2}\right)^2 + \left(\frac{\dot{m}_{e_{max}} - \dot{m}_{e_{min}}}{t_{max} - t_{min}}\, U_{t2}\right)^2}$$

For MSD system$= \sqrt{\left(\frac{1396-138}{500-50}\ 0.01\right)^2 + \left(\frac{1396-138}{86400-0}\ 0.02\right)^2} = \pm 0.0279 = \pm 2.79\%$

For NSD system$= \sqrt{\left(\frac{809-88}{500-50}\ 0.01\right)^2 + \left(\frac{809-88}{86400-0}\ 0.02\right)^2} = \pm 0.0160 = \pm 1.6\%$

2. Hourly productivity uncertainty

$$U_{\dot{m}_{e\,hourly}} = \sqrt{\left(\frac{\dot{m}_{e_{max}} - \dot{m}_{e_{min}}}{V_{max} - V_{min}}\, U_{v1}\right)^2 + \left(\frac{\dot{m}_{e_{max}} - \dot{m}_{e_{min}}}{t_{max} - t_{min}}\, U_{t1}\right)^2}$$

For MSD system$= \sqrt{\left(\frac{242-36}{50-5}\ 0.01\right)^2 + \left(\frac{242-36}{3600-0}\ 0.08\right)^2} = \pm 0.0460 = \pm 4.6\%$

For NSD system$= \sqrt{\left(\frac{138-21}{50-5}\ 0.01\right)^2 + \left(\frac{138-21}{3600-0}\ 0.08\right)^2} = \pm 0.0261 = \pm 2.61\%$

3. Daily efficiency uncertainty

$$U_{\eta\,daily} = \sqrt{\left(\frac{\eta_{max} - \eta_{min}}{\dot{m}_{e_{max}} - \dot{m}_{e_{min}}}\, U_{\dot{m}_e}\right)^2_{daily} + \left(\frac{\eta_{max} - \eta_{min}}{G_{max} - G_{min}}\, U_G\right)^2_{daily}}$$

For MSD system$= \sqrt{\left(\frac{21-9.7}{1396-138}\ 0.03\right)^2 + \left(\frac{21-9.7}{31.4-4.5}\ 0.05\right)^2} = \pm 0.0210 = \pm 2.1\%$

For NSD system= $\sqrt{\left(\frac{13.1-8}{1396-138}\ 0.03\right)^2 + \left(\frac{13.1-8}{31.4-4.5}\ 0.05\right)^2} = \pm 0.0095 = \pm 0.95\%$

4. Hourly efficiency uncertainty

$$U_{\eta_{hourly}} = \sqrt{\left(\frac{\eta_{max}-\eta_{min}}{\dot{m}_{e_{max}}-\dot{m}_{e_{min}}} U_{\dot{m}_e}\right)^2_{hourly} + \left(\frac{\eta_{max}-\eta_{min}}{G_{max}-G_{min}}\ U_G\right)^2_{hourly}}$$

For MSD system= $\sqrt{\left(\frac{37.4-5.9}{242-36}\ 0.05\right)^2 + \left(\frac{37.4-5.9}{31.4-1.1}\ 0.05\right)^2} = \pm 0.0346 = \pm 3.46\%$

For NSD system= $\sqrt{\left(\frac{23.9-3.6}{138-21}\ 0.05\right)^2 + \left(\frac{23.9-3.6}{31.4-1.1}\ 0.05\right)^2} = \pm 0.0525 = \pm 5.25\%$